Dissecting the signaling pathways controlling inflammation during Gram-negative bacterial infections : the role of ALPK1, TIFA and TRAF6 during Shigella flexneri infection

Milica Milivojevic

UNIVERSITÉ PARIS DESCARTES

MEMBRE DE
USPC
Université Sorbonne Paris Cité

Université Paris Descartes

Ecole doctorale BioSPC

Equipe « Signalisation Cellulaire et Infections Bactériennes »
Institut Cochin - INSERM U1016, CNRS UMR8104, Université Paris Descartes

Dissecting the signaling pathways controlling inflammation during Gram-negative bacterial infections:

The role of ALPK1, TIFA and TRAF6 during *Shigella flexneri* infection

Par Milica Milivojevic

Thèse de doctorat d'Infectiologie

Dirigée par Dr. Cécile Arrieumerlou

Présentée et soutenue publiquement le 16 Novembre 2017

Devant un jury composé de :
Dr. Agathe SUBTIL – Rapporteur
Dr. Thomas HENRY – Rapporteur
Dr. Laurence ARBIBE – Examinatrice
Pr. Olivier DUSSURGET – Examinateur
Dr. Emmanuel LAPLANTINE – Examinateur
Dr. Cécile ARRIEUMERLOU – Directrice de thèse

Contents

Resume

Epithelial cells represent the first line of defense against pathogens and play an active role in innate immunity. Via local secretion of cytokines, they are able to orchestrate the immune response against invading pathogens. The activation of both intracellular and extracellular pathogen recognition receptors leads to a complex signaling cascade, resulting in the activation of the transcription factor nuclear factor κB (NF-κB) and the subsequent production of pro-inflammatory cytokines. However, the molecular mechanisms governing this process have not been fully elucidated. The Gram-negative bacterium *Shigella flexneri* is an important human pathogen and the causative agent of bacillary dysentery. This disease is characterized by acute inflammation of the colon resulting in the destruction of the intestinal tissue and, in severe cases, death. *S. flexneri* can invade and replicate within colonic epithelial cells. Following detection of the bacteria, both infected and uninfected bystander cells initiate inflammatory signaling pathways, which result in massive interleukin-8 (IL-8) production by the latter.

Using *S. flexneri* as a model of infection, we have identified a novel signaling pathway, which is central to the activation of NF-κB and the subsequent production of IL-8 during Gram-negative bacterial infections. Following the cytosolic detection of bacteria, the protein TRAF-interacting factor with forkhead-associated domain (TIFA) forms oligomers, a process dependent on its threonine at position 9 and the forkhead-associated domain. These oligomers interact with TNF receptor associated factor (TRAF) 6, leading to its oligomerization and the subsequent activation of NF-κB . In addition, we show that oligomerization of TIFA is dependent on the kinase alpha-kinase (ALPK)1 and that this pathway is activated in response to the detection of the bacterial metabolite heptose-1, 7-bisphosphate (HBP). These observations could be extended to the enteroinvasive pathogen *Salmonella typhimurium* as well as the extracellular bacteria *Neisseria meningitidis*. Our results therefore demonstrate the central role of the ALPK1-TIFA-TRAF6 signaling pathway in response to HBP of both intracellular and extracellular Gram-negative bacterial pathogens, and offer a better understanding of the molecular mechanisms governing the epithelial cell immune response to pathogenic bacteria.

Abbreviations

AHNAK:	Neuroblast differentiation-associated protein
ALPK1:	Alpha kinase 1
ANXA2:	Annexin 2
AP-1:	Activator protein 1
ASC:	Apoptosis-associated speck-like protein containing a CARD
ATP:	Adenosine triphosphate
BAG2:	BCL2 associated athanogene 2
BCV:	Bacteria-containing vacuole
CARD:	Caspase activation and recruitment domain
CBM:	CARD-MALT-BCL
cGAMP :	cyclic guanosine monophosphate–adenosine monophosphate
cGAS:	cyclic GMP–AMP synthase
CLR:	C-type lectin receptor
DAG:	Diacylglycerol
DAMP:	Danger associated molecular pattern
EPEC:	Enteropathogenic *Escherichia Coli*
ERK:	Extracellular signal-regulated kinase
FAE:	Follicle associated epithelium
FHA:	Forkhead-associated
GBP:	Guanylate binding protein
GEF:	Guanine nucleotide exchange factor
GTP:	Guanosine-5'-triphosphate
HBP:	Heptose-1, 7-bisphosphate
HGMB:	High-mobility group protein B
HP1:	Hetrochromatin protein 1
HSP:	Heat shock protein
IBD:	Inflammatory bowel disease
IEC:	Intestinal epithelial cell
ie-DAP:	γ-d-glutamyl-*meso*-diaminopimelic acid
IFN:	Interferon
IKK:	Inhibitor of κB Kinase

IL-	Interleukin
IRAK:	IL-1 receptor associated kinase
IκB:	Inhibitor of κB
JNK:	Jun N-terminal kinase
KD:	Knock-down
Kdo:	Ketodeoxyoctonic acid
KO:	Knock-out
LAMP:	Lysosome-associated protein
LPS:	Lipopolysaccharide
LTA:	Lipoteichoic acid
M cell:	Microfold cell
MAL:	MYD88 adaptor-like protein
MAPK:	Mitogen activated protein kinases
MD-2:	Myeloid differentiation factor 2
MDP:	Muramyl dipeptide
MOI:	Multiplicity of infection
mRNA:	messenger RNA
MSK:	Mitogen and stress activated protein kinase
MSU:	Monosodium urate
Myd88:	Myeloid differentiation primary response gene 88
NAG:	N-acetylglucosamine
NBD:	N-terminal protein binding domain
NEMO:	NF-κB Essential Modulator
NF-κB :	Nuclear factor κB
NK:	Natural Killer
NLR:	NOD-like receptor
NOD:	Nucleotide-binding oligomerization domain
PAMP:	Pathogen associated molecular pattern
PGN:	Peptidoglycan
$PI(4,5)P_2$:	Phosphatidylinositol 4,5-bisphosphate
PKC:	Protein kinase C
PMA:	phorbol 12-myristate 13-acetate
PMN:	Polymorphonuclear cell

PRR: Pathogen recognition receptor

RING: Really interesting new gene

RIP2: Receptor-interacting serine/threonine-protein kinase 2

RISC: RNA-induced silencing complex

RLR: RIG-like receptor

RNAi: RNA interference

ROCK: Rho-associated protein kinase

SARM: Sterile α- and armadillo-motif

SCV: *Salmonella*-containing vacuole

STING: Stimulator of IFN genes

T3SS: Type 3 secretion system

T4SS: Type 4 secretion system

TAB: TAK1-binding protein

TAK1: Transforming growth factor-β activated kinase-1

Th: T helper

TIFA: TRAF interacting forkhead associated

TIR: Toll-interleukin 1 receptor

TLR: Toll-like receptor

TNFα: Tumor necrosis factor α

TRAF: TNF receptor associated factor

TRAM: TRIF-related adaptor molecule

TRIF: TIR domain containing adaptor protein inducing IFNβ

WT: Wild-type

INTRODUCTION

*A*n organism's ability to detect and respond quickly and efficiently to invading pathogens is paramount to its survival. The innate immune system is charged with the task of recognising microbes and initiating the primary immune response. This is crucial in orchestrating the adaptive immune response which follows and shaping the outcome of infection. The cells of the innate immune system are equipped with an array of extracellular and intracellular receptors capable of recognising conserved microbial components. This results in a complex downstream signalling cascade, which ultimately leads to the production of pro-inflammatory cytokines and chemokines. Epithelial cells represent the first line of defence and play a central role in the establishment of this primary response.

Bacteria of the *Shigella* genus are important human pathogens, which cause the disease bacillary dysentery. This disease is characterized by acute inflammation and destruction of the intestinal epithelium. *Shigella* have adapted to an intracellular lifestyle and employ a number of mechanisms to interfere with host cell signalling processes and to ensure their survival, replication and spread within epithelial cells. Understanding the molecular mechanisms involved in bacterial sensing and the establishment of the innate immune response has been the aim of my thesis.

The first part of this introduction is aimed at reminding the reader of the different mechanisms employed by epithelial cells to sense bacterial pathogens, with a focus on Gram-negative bacteria. I will then go on to describe the different signalling pathways implicated in this process. The second part will be focused on the Gram-negative bacteria *S. flexneri*, the model pathogen used in this work. The third and final part is aimed at introducing the reader to the three proteins which we have identified as playing an important role during Gram-negative bacterial infections.

1 Epithelial cells in immunity

Epithelial cells line the cavities of organisms. Due to their exposure to the external environment, they are continuously faced with the challenge of protecting the organism from incoming pathogens. For this reason, they are often referred to as the sentinels, representing the first line of defense. They provide both a physical barrier, due to the presence of intercellular tight junctions, as well as a chemical one, via the secretion of antimicrobial peptides. Whilst they themselves are not considered immune cells, they are equipped with a number of innate mechanisms for sensing and responding to infection.

Intestinal epithelial cells (IECs) are of particular interest since they are continually exposed to residing microorganisms, termed the microbiota (Sansonetti, 2004). Whilst they must manage this constant contact with a huge number of commensals, they must also respond effectively and appropriately to potential breaches of this homeostasis from invasive pathogenic bacteria. Their ability to do so is paramount in orchestrating the adaptive immune response which follows.

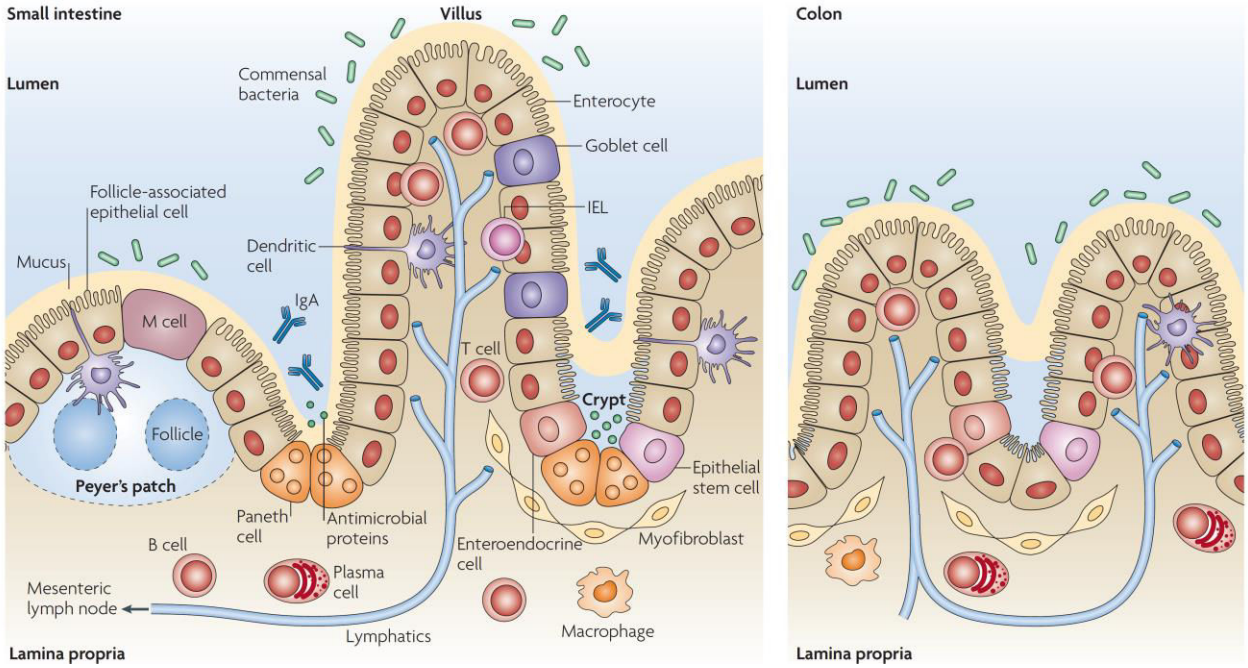

Figure 1. Anatomy of the small intestine and colon (Abreu, 2010). Intestinal epithelial cells (IECs), linked via tight-junctions, form a single cell barrier separating the lumen from the lamina propria. The vast majority of this layer is made up of enterocytes. Goblet cells secrete mucus, which forms a gel-like protective layer, separating IECs from the commensals. Microfold (M) cells, overlying the Peyer's patches, transport luminal antigens and microorganisms to the immune cells in the lamina propria. Resident macrophages, dendritic cells, and both B and T lymphocytes are all found in the lamina propria.

IECs are polarized cells with an apical pole on the luminal side of the intestine and a basolateral pole. They are composed of five cell types. The enterocytes are the most abundant in both the small and large intestine (Figure 1) and are the ones that I will be referring to when using the term IECs. They form tight junctions between them, creating an impermeable barrier. They also actively secrete antimicrobial peptides capable of directly killing bacteria, and secrete cytokines, which coordinate the action of both innate and adaptive immune cells. There are three secretory cell types: goblet cells, Paneth cells and enteroendocrine cells. The main function of goblet cells is to secrete mucus, which forms a protective layer and separates the microbiota from the rest of the

IECs (Kim and Ho, 2010). Paneth cells are mainly found in the small intestine and are capable of secreting granules filled with microbicidal proteins (Ayabe et al., 2000). The enteroendocrine cells are important for sensing nutrients and releasing peptide hormones, which mediate digestion but also participate in the inflammatory response (Worthington et al., 2017). Finally, there are the microfold (M) cells. They are generally in specialized regions called the follicle associated epithelium and overlie the Peyer's patches. They serve to "sample" the environment by transepithelially transporting antigens and microorganisms to the underlying immune cells, which include resident macrophages, dendritic cells as well as B and T lymphocytes (Kraehenbuhl and Neutra, 2000).

1.1 Immune sensing

Innate immune recognition, unlike adaptive, relies on a limited number of germline-encoded receptors termed Pathogen Recognition Receptors (PRRs). They are mainly expressed in cells of the innate immune system such as dendritic cells and macrophages but IECs possess them as well. Whilst the repertoire and spatial distribution of these PRRs may differ between these cell types, PRRs allow IECs to sense and respond to infection. PRRs sense infection either by directly binding to exogenous Pathogen Associated Molecular Patterns (PAMPs), or indirectly through endogenous danger signals termed Danger Associated Molecular Patterns (DAMPs).

1.1.1 PAMPs

The concept of PAMPs was first introduced by Charles Janeway Jr in 1989 (Janeway, 1989). PAMPs are characteristic molecular motifs conserved between groups of pathogens including fungi, viruses and bacteria. These motifs are highly evolutionarily conserved since they are usually central to the microbes physiology (Medzhitov and Janeway, 1997). PAMPs can be both intracellular as well as present on the surface of the microorganisms. They vary in their composition and can be composed of lipids, proteins, lipoproteins, monosaccharides or nucleic acids. Since they are absent in the host, they provide an exogenous signal to the cell of a pathogenic presence and promote an immune response. Bacteria have a number of PAMPs, which can be recognized by the host. Some PAMPs, such as DNA, are present in all bacteria. Indeed, bacterial DNA, like that of viruses, is recognized as a PAMP since they have unmethylated CpG-DNA whereas, in mammals, it tends to be methylated (Häcker et al., 2002). Other PAMPs are only present in certain subsets of bacteria. Bacteria such as *Salmonella typhimurium, Escherichia coli* and *Listeria monocytogenes* possess a flagellum, an organelle which provides the bacterium with motility. The main protein component of flagella, flagellin, is a PAMP which elicits an immune response following recognition (Ciacci-Woolwine et al., 1998). Bacteria, such

as the pathogens *Shigella flexneri*, *S. typhimurium, pseudomonas aeruginosa,* and enteropathogenic *E*scherichia *coli* (EPEC) have a type 3 secretion system (T3SS), which is structurally related to flagella (Blocker et al., 2003) and can also be recognized as PAMP (Miao et al., 2010).

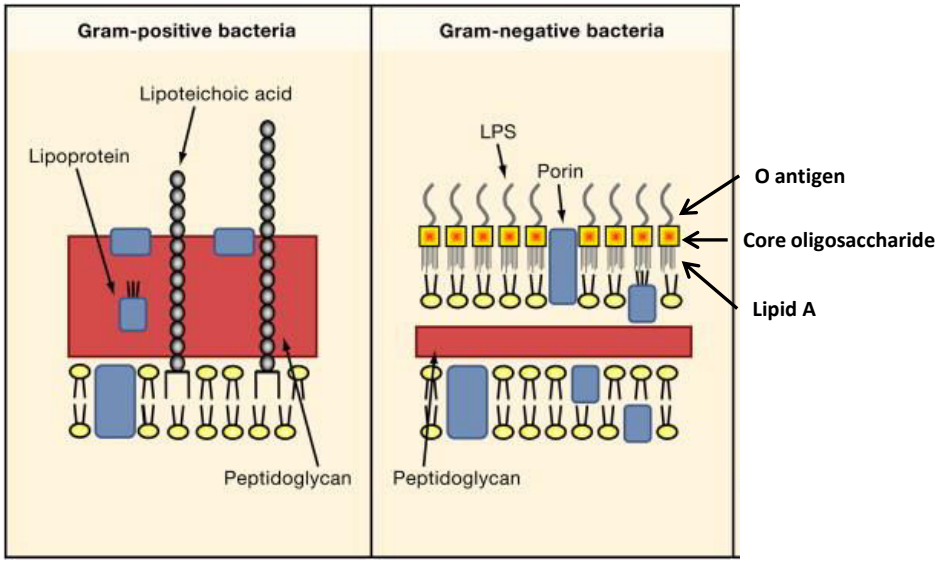

Figure 2. Schematic representation of the cell walls of Gram-positive and Gram-negative bacteria. (Adapted from Akira et al., 2006). The cytoplasmic lipid membrane of Gram-positive bacteria is covered by a thick wall made up of peptidoglycan and containing lipoproteins and lipoteichoic acids. In Gram-negative bacteria this peptidoglycan wall is much thinner and lacks lipoteichoic acid. In addition, it is covered by an outer membrane made up of lipopolysaccharide (LPS). The LPS is made up of the Lipid A anchor, a core oligosaccharide unit and the variable outer O antigen.

Bacteria can be divided into two large groups based on their surface composition: Gram-positive and Gram-negative bacteria (Figure 2). They both possess a cytoplasmic lipid membrane surrounded by the cell wall, which is made up of peptidoglycan (PGN). This is a polymer of N-acetylglucosamine and N-acetylmuramic acid, crosslinked by short peptides (Dziarski, 2003). In Gram-positive bacteria, this cell wall is thick and contains teichoic acids, both lipoteichoic acids (LTA) and wall teichoic acids. Peptidoglycan and LTA both constitute bacterial PAMPs, which can be recognized by the host. Gram-negative bacteria, on the other hand, have a much thinner PGN wall lacking teichoic acids. This wall is covered by an outer lipid membrane made up of lipopolysaccharide (LPS). The LPS is composed of 3 domains; a hydrophobic lipid moiety embedded in the outer membrane, termed lipid A; a relatively conserved oligosaccharide core attached to the lipid A *via* ketodeoxyoctonic acid (Kdo), which influences permeation properties of the outer membrane; and the variable O-antigen, containing a variable number of repeating saccharide units which contributes to bacterial antigenicity and serospecificity (Wang and Quinn, 2010). Lipid A, also known as the endotoxin, is the immunogenic component of LPS and is

responsible for LPS-induced sepsis (Raetz and Whitfield, 2002). Recently, it has also been shown that heptose-1,7-bisphosphate (HBP), a cytosolic intermediate of the LPS biosynthetic pathway, represents a potent new PAMP (Gaudet et al., 2017). This will be discussed in further detail later on.

1.1.2 DAMPs

It has become increasingly clear that cells do not only respond following the recognition of pathogen associated molecules, but can also respond to endogenous danger signals termed DAMPs. This concept was first proposed by Polly Matzinger who suggested that cells were less concerned with non-self and more so with the presence of danger (Matzinger, 1994, 2002). It now seems that inflammation and the immune response is triggered by a combination of the two. Unlike PAMPs, DAMPs are endogenous molecules, which are released following tissue stress or damage. Their production is not limited to the presence of infection and can be induced through sterile injury and disease. To date, many DAMPs have been identified. DAMPs can be either intracellular or extracellular in origin and vary enormously in their size and composition (Schaefer, 2014). These include small molecules like uric acid (Kono et al., 2010) or ATP (McDonald et al., 2010), to whole proteins such as high-mobility group protein B1 (HMGB1) and heat shock proteins (HSP) (Wheeler et al., 2009). They are sensed largely by the same PRRs responsible for the sensing of PAMPs, which will be discussed in the next section. The result of DAMP recognition can lead to a number of different outcomes such as autophagy and inflammation, and is associated with a number of diseases including sepsis (Kung et al., 2012), Crohn's disease (Pastorelli et al., 2011), autoimmune diseases such as systemic lupus erythematosus (Urbonaviciute et al., 2008) and cancer (Huang et al., 2015).

1.1.3 PRRs

A number of different PRRs have been described to date. They can be divided into four groups: RIG-like-receptors (RLRs), Nucleotide Oligomerization Domain (NOD)-like receptors (NLRs), C-type lectin receptors (CLRs) and Toll-like receptors (TLRs). The former two are cytoplasmic while the latter two are membrane-associated receptors present either at the cellular surface or in intracellular compartments such as endosomes. RLRs are mainly associated with the recognition of double- and single-stranded RNA from viruses whilst CLRs recognize carbohydrates and are mainly involved in fungal recognition. I will focus on TLRs and NLRs which, amongst other triggers, can be activated by bacteria.

1.1.3.1 TLRs

The discovery of TLRs revolutionized the field of innate immunity. The protein Toll was first identified in the anti-fungal response in *Drosophila* (Lemaitre et al., 1996). A year later, a human homologue of Toll, TLR4, was shown to lead to the production of inflammatory cytokines when constitutively active (Medzhitov et al., 1997). Since then, much work has gone into the characterization of this family of proteins. Currently, there are 10 functional TLRs in humans and 12 in mice, with TLRs 1-9 conserved between the two species (Figure 3). They are type I transmembrane proteins with an ectodomain comprised of leucine rich repeats (LRRs) important in the recognition of PAMPs, a transmembrane domain and an intracellular tail required for downstream signaling called the Toll-Interleukin 1 receptor (TIR) domain (Kawai and Akira, 2010). They can be located either at the plasma membrane or in intracellular compartments and are expressed in cells both of immune origin and non-immune origin such as epithelial cells. They recognize diverse molecules including lipids, proteins, lipoproteins and nucleic acids from bacteria, viruses, parasites and fungi, with each TLR having a distinct PAMP recognition specificity (Akira et al., 2006). Ligand binding to the ectodomain is accompanied by receptor dimerization. Adaptor proteins, which themselves possess a TIR domain, are recruited via TIR-TIR interactions. This serves as a platform for the formation of higher order complexes, which will set off a signaling cascade resulting in the production of cytokines (Gay et al., 2014).

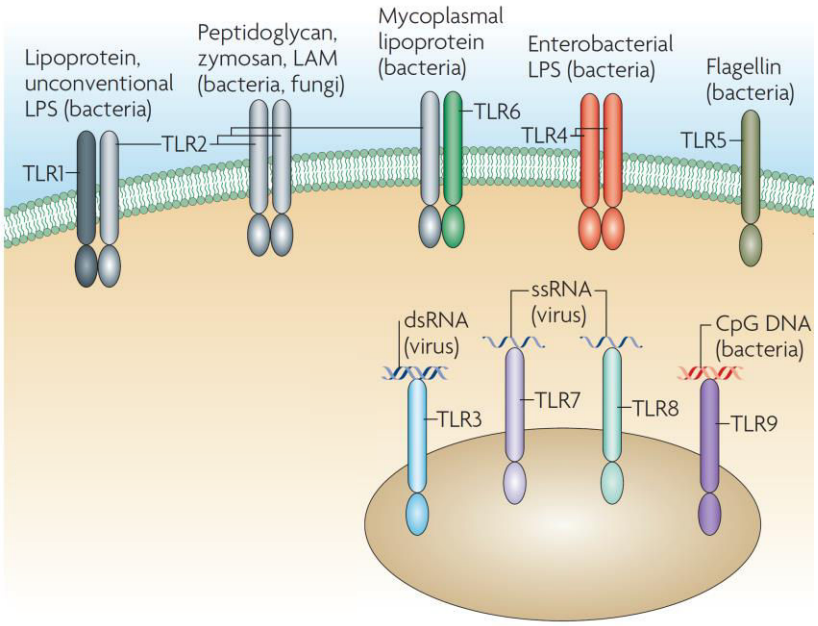

Figure 3. Toll-like receptors (TLRs) and their ligands. (Adapted from Kaufmann, 2007). TLRs 1, 2 and 4-6 are located at the plasma membrane whilst TLRs 3 and 7-9 are associated with membranes of intracellular compartments.

The TLRs most associated with the recognition of bacterial PAMPs are TLR2, TLR4, TLR5 and TLR9. TLR9 is located in the endosomes and recognizes unmethylated CpG DNA, which is present in bacteria but rarely in mammalian cells (Häcker et al., 2002). TLR5 is expressed at the cell surface and is responsible for the recognition of flagellin of both Gram-positive and Gram-negative bacteria such as *L. monocytogenes* and *S. typhimurium,* respectively (Hayashi et al., 2001). The founding member and, by far, the most-well studied is TLR4. It is particularly important in Gram-negative bacterial infections due to its central role in LPS recognition (Poltorak et al., 1998). Indeed mice, which do not possess a functional TLR4 receptor, are much more susceptible to infections with Gram-negative bacteria such as *Haemophilus influenza* and *Klebsiella pneumoniae* (Branger et al., 2004; Wang et al., 2002). Interestingly, TLR4 does not function alone since the myeloid differentiation factor 2 (MD-2) was found to be indispensable in response to LPS challenge both *in vitro* and *in vivo* (Nagai et al., 2002; Shimazu et al., 1999) MD-2 associates with the extracellular domain of TLR4 and structural studies have shown that five of the six lipid chains of lipid A, the immunogenic unit of LPS, bind to the MD-2 hydrophobic pocket with the sixth binding to TLR4 (Park et al., 2009). In addition, the glycosylphosphatidylinositol-linked protein CD14 acts as a co-receptor (Poltorak et al., 1998). LPS released from certain Gram-negative bacteria associates with LPS binding protein (LBP), an acute-phase protein present in the bloodstream. This LPS-LBP complex can then bind to CD14, expressed on the cell surface of phagocytes, which transfers the LPS to MD-2 and TLR4 (Poltorak et al., 1998; Shimazu et al., 1999; Ulevitch and Tobias, 1995). Whilst TLR4 confers protection to Gram-negative bacterial infections by its recognition of LPS, it also exacerbates endotoxic shock. Indeed, mice with mutations in TLR4 or MD-2 are hyporesponsive to LPS (Hoshino et al., 1999; Nagai et al., 2002; Qureshi et al., 1999) and TLR4 Knock Out (KO) mice are protected from *E.coli*-induced lethal septic shock (Roger et al., 2009).

TLR2, like TLR4, is located at the plasma membrane. It recognizes a variety of PAMPs from a wide range of microorganisms including bacterial lipoproteins and PGN and LTA from Gram-positive bacteria. TLR2 generally forms heterodimers with TLR1 or 6, which confers the specificity of recognition (Takeuchi et al., 2001, 2002). The TLR2-TLR1 heterodimer recognizes triacetylated lipopeptides, which bind hydrophobic pockets of both TLR1 and TLR2 (Jin et al., 2007). TLR6 lacks this hydrophobic pocket, therefore the TLR2-6 heterodimer is associated with the recognition of diacetylated lipopeptides (Kang et al., 2009). In addition, TLR2 can interact with the co-receptors CD36 and CD14 (Hoebe et al., 2005; Janot et al., 2008; Jimenez-Dalmaroni et al., 2009). TLR2 has been implicated in a number of bacterial infections, and most Gram-positive bacteria activate it to some extent (Oliveira-Nascimento et al., 2012). TLR2-deficient mice are much more susceptible to infections with bacteria such as *Staphylococcus aureus* (Takeuchi et

al., 2000) or *L. monocytogenes* (Torres et al., 2004). Its role in Gram-negative bacterial infections is less pronounced although some have been described. For example, TLR2 KO mice have higher bacterial burdens during *S. typhimurium* infection; however bacterial resolution and mortality rates are not altered compared to wild-type (WT) mice (Seibert et al., 2010). In the context of Gram negative bacterial infections, TLR4 has the defining role, with TLR2 playing more of a synergistic role. Indeed, double KO mice have increased susceptibility to *Leptospira* and *Klebsiella* infection compared to single TLR4 KO mice (Chassin et al., 2009; Spiller et al., 2007). This is also true during septic shock since a double KO of TLR4 and TLR2 results in 100% survival rates in mice in a model of sepsis using *E. Coli* or *S. typhimurium* (Spiller et al., 2008).

As previously mentioned, PRRs are not only involved in the sensing of PAMPs but DAMPs as well. TLR9 can sense mitochondrial DNA released into the circulation following injury (Zhang et al., 2010). TLR2 and TLR4 have been particularly implicated in the sensing of a wide range of DAMPs. Due to their presence at the extracellular surface, they are involved in sensing soluble proteoglycans of the extracellular matrix (Frey et al., 2013) as well as the normally intracellular molecules HGMB1, HSP and histones, which have been released from dying cells (Schaefer, 2014). Exactly how these structurally varied DAMPs are capable of activating the same PRRs is not completely clear.

1.1.3.1.1 TLRs in epithelial cells

Whilst TLRs are largely associated with sensing of pathogens by immune cells such as macrophages and dendritic cells, they are also present in epithelial cells where they play an important role. Expression of human TLRs 1-9 have all been detected in IECs, at least at RNA level, particularly in the colon (Abreu, 2010). However, unlike immune cells, IECs are constantly exposed to predominantly unharmful bacteria. They therefore regulate the expression of their TLRs both quantitatively as well as spatially to avoid constant activation, which would be deleterious for the host. TLR3 is abundantly expressed throughout the intestine whilst TLR2 and TLR4 are thought to only be expressed at low levels (Cario and Podolsky, 2000). Looking closer at TLR4, IECs, for example, do not express the CD14 co-receptor. In addition, TLR4 and MD-2 are expressed at low levels under steady state conditions (Abreu et al., 2001) but can be upregulated under inflammatory conditions such as following Interferon (IFN)γ and Tumor Necrosis Factor (TNF)α stimulation (Abreu et al., 2002; Suzuki et al., 2003). Indeed, an increase of TLR4 and MD-2 expression is observed in inflammatory bowel disease (IBD), a disease characterized by chronic inflammation (Vamadevan et al., 2010).

In addition to regulation of expression levels, TLR localization is also controlled. TLR5 localizes exclusively to the basolateral pole of polarized IECs in order to only detect bacteria, which have breached the intestinal barrier (Gewirtz et al., 2001). Similarly, the expression of TLR4 and MD-2, whilst low, is localized to the basolateral pole (Fusunyan et al., 2001; Vamadevan et al., 2010) although they were found to be highly expressed on the apical side during Crohn's disease (Cario and Podolsky, 2000). Another study found TLR4 to be localized intracellularly at the Golgi apparatus, requiring LPS internalization for its activation, thus avoiding activation by extracellular LPS (Hornef et al., 2003). TLR9 may also be differently distributed in IECs than immune cells. Studies on mouse colonic epithelial cells showed that TLR9 was expressed both apically and basolaterally but not in endosomes (Lee et al., 2006). Stimulation of apical TLR9 leads to inhibition of Nuclear Factor -κB (NF-κB) activation whilst basolateral stimulation leads to its activation.

1.1.3.2 NLRs

Unlike TLRs, which are membrane bound receptors, NLRs are cytosolic PRRs and recognize both PAMPs and DAMPs. The downstream signaling cascades triggered following NLR activation promote a number of cellular processes such as inflammasome assembly, immune signaling and autophagy (Motta et al., 2015). NLRs share an N-terminal protein binding domain (NBD), C-terminal leucine rich repeats and a central Nucleotide NOD domain. The NOD domain is also known as the NACHT domain and consists of seven conserved motifs. The family can be subdivided into four families NLRA, NLRB, NLRC and NLRP (Ting et al., 2008). In humans, only one member of each the NLRA and NLRB families is expressed; CIITA and NAIP respectively. The NLRC subfamily consists of six members: NLRC1 (NOD1), NLRC2 (NOD2), NLRC3 (NOD3), NLRC4 (IPAF), NLRC5, and NLRX1 and is characterized by the presence of a Caspase Recruitment Domain (CARD) domain, at least in NOD1, NOD2 and NLRC4. The NLRP family is characterized by the presence of an N-terminal pyrin domain. Whilst the expression of NLRs is found largely in immune cells, not all of them have been found to be expressed in epithelial cells (Pott and Hornef, 2012). Those found in IECs are NAIP (Maier et al., 2007), the NLRCs NOD1 and NOD2 (Philpott and Girardin, 2004) as well as NLRC4 (Nordlander et al., 2014; Sellin et al., 2014) and the NLRPs 1, 3, 6 and 12 (Allen et al., 2012; Elinav et al., 2011; Song-Zhao et al., 2014; Williams et al., 2015) (Figure 4).

Family	Structure	Gene	Stimuli	Function	Epithelial cells
NLRA		CTIIA	IFNγ	MHC-II expresiion	No
NLRB	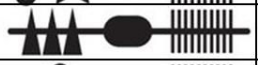	NAIP	T3SS, Flagellin	Inflammasome	**Yes (Maier et al,sellin et al 2014)**
NLRC	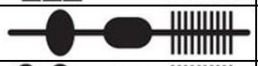	NOD1 NLRC4	PGN – iE-DAP NAIP	NFkB/MAPK Inflammasome	**Yes (Girardin et al 2001)** **Yes (Nordlander etal 2014)**
		NOD2	PGN-MDP	NFkB/MAPK	**Yes (Girardin and Philpott 2004)**
	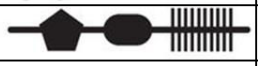	NLRC3 NLRC5	Unknown IFN	Negative regulator T-cells MHC-I expression	No
NLRP		NLRP1	MDP/ anthrax lethal toxin	Inflammasome	**Yes (Williams et al, 2015)**
		NLRP10	Unknown	DC migration	No
		NLRP2-9, 11-14	Various/unknown	Inflammasome – 3,6,7,12 Other/Unknown	**Yes- NLRP3, 6, 12 (Song-Zhao et al 2013,Elinav et al, 2011, Allen et al 2012**

Figure 4. NOD-Like Receptors (NLRs) structure and function. (Adapted from (Motta et al., 2015). LLR, leucine-rich repeats; TA, transactivation; CARD, caspase recruitment domain; BIR, baculoviral inhibition of apoptosis protein repeat; PYD, pyrin domain.

1.1.3.2.1 NOD1 and NOD2

NOD1 was the first NLR family member to be identified (Bertin et al., 1999). NOD2, which is closely related to NOD1 but has an extra CARD domain, was described shortly thereafter (Ogura et al., 2001). The two proteins were shown to be able to activate NF-κB and mitogen activated protein kinases (MAPKs) in response to infection with intracellular Gram-negative bacteria. This observation was first attributed to the recognition of LPS (Girardin et al., 2001; Inohara et al., 2001). However, further studies showed that it was, in fact, PGN that was recognized by these two proteins. NOD2 recognizes muramyl dipeptide (MDP), a component common to both Gram-negative and Gram-positive bacteria (Girardin et al., 2003a) whereas NOD1 recognizes γ-d-glutamyl-*meso*-diaminopimelic acid (iE-DAP) mainly present in Gram-negative bacteria (Chamaillard et al., 2003; Girardin et al., 2003b). It has been suggested that both NOD1 and NOD2 interact directly with their cognate ligands via the LRR region (Grimes et al., 2012; Laroui et al., 2011). Without stimulation, NOD1 and NOD2 exist in a monomeric auto-inhibited states in the cytosol (Caruso et al., 2014). Upon ligand binding, a conformational change occurs leading to their homo-oligomerization and the recruitment of the receptor-interacting serine/threonine-protein kinase 2 (RIP2) through homotypic CARD-CARD interactions. This process is necessary for the downstream activation of NF-κB and the MAPK (Hasegawa et al., 2008).

How PGN enters the cytosol depends on the bacterial model. Certain bacteria invade the cell making peptidoglycan fragments available in the cytosol. This is the case for the sensing of the Gram-negative bacteria *S. flexneri* (Girardin et al., 2001), enteroinvasive *E. coli* (Kim et al 2004) as well as by the Gram-positive bacteria *L. monocytogenes* (Opitz et al., 2006) by NOD1. Other modes of delivery include direct injection into the cytosol by the Gram-negative bacteria *Helicobacter pylori* (Viala et al., 2004) as well as outer membrane vesicles from *H. pylori*, *Neisseria gonorrhoeae* and *P. aeruginosa* (Kaparakis et al., 2010). Others have found that PGN can enter cells through endocytosis (Lee et al., 2009; Marina-García et al., 2009). Whilst NOD1 is important for sensing of PGN, *in vivo* studies have only shown moderate effects of NOD1 KO in mice (Philpott et al., 2014). This is likely due to the presence of other receptors such as TLRs, which activate the same downstream signaling pathways thus conferring a certain level of redundancy (Park et al., 2009). Consistently, the importance of NOD1 signaling is enhanced in TLR unresponsive cells (Kim et al., 2004).

1.1.3.2.2 NLRs and the inflammasome

The other NLRs expressed by epithelial cells; NAIP, NLRC4, and NLRPs 1, 3, 6 and 12 are all involved with inflammasome assembly. The inflammasome is a multimeric protein complex, which activates caspase-1 (Martinon et al., 2002). This is a necessary step in the maturation of the pro-inflammatory cytokines IL-1β and IL-18, which are expressed as inactive precursors in the cytoplasm. It also leads to a caspase-1-dependent inflammatory cell death termed pyroptosis characterized by IL-1β release (Bergsbaken et al., 2009). Activation is triggered by the recognition of PAMPs or DAMPs by specific NLRs. Upon activation, NLRs oligomerize via their NBD. They then recruit pro-caspase-1 either directly via the CARD domain, as is the case for NLRC4, or through the CARD-pyrin containing adaptor associated speck-like protein (ASC). This results in caspase-1 activation and the subsequent cleavage of pro-IL1β and pro-IL-18. Since the inflammasome is mainly associated with cells of hematopoietic origin, most studies into its activation and function have been performed in these cells. However, a growing number of evidence has brought to light the importance of the inflammasome in epithelial cells (Sellin et al., 2015).

In IECs NLRP6 and NLRP12 are thought to play a regulatory role and to be involved in the maintenance of intestinal homeostasis (Chen, 2014). NLRP6, for example, seems to be particularly important in goblet cells for the production of mucus (Wlodarska et al., 2014). NLRP3 is one of the most well studied NLRs and is activated by a large number of stimuli including bacteria, viruses, fungi as well as DAMPs such as ATP and hyaluronan (Menu and Vince, 2011). It is therefore thought that it does not directly recognize a specific ligand *per se* but rather that it

senses changes within the cell such as potassium efflux (Muñoz-Planillo et al., 2013) or mitochondrial factors such as the production of ROS (Zhou et al., 2011). A unique characteristic of NLRP3 is that it requires a two-step activation. The first priming step following TLR stimulation leads to NF-κB activation and results in the transcription of the *caspase-1* and *IL-1β* genes as well as NLRP3 itself (Bauernfeind et al., 2009) although more recently, studies have shown that there is also transcription independent priming which is rather dependent of post-translational modifications such as deubiquitination (Juliana et al., 2012) and phosphorylation (Song et al., 2017). The second step is induced by the NLRP3 activating agent and leads to its oligomerization and inflammasome activation. A number of bacterial pathogens have been shown to activate NLRP3 in macrophages. These include both Gram-positive bacteria including *S. pneumoniae, L. monocytogenes*, and *S. aureus*, as well as the Gram-negative bacteria *N. gonorrhea*, *P. aeruginosa and S. typhimurium* (Menu and Vince, 2011). In epithelial cells, its role is less clear although one study has suggested that NLRP3 may protect against *Citobacter rodentium* colonization and spread (Song-Zhao et al., 2014).

In mice, the NAIP/NLRC4 inflammasome is activated in macrophages in response to a number of Gram-negative bacterial pathogens including *S. typhimurium*, *P. aeruginosa* and *S. flexneri* (Miao et al., 2006; Suzuki et al., 2007). The mouse NAIP5 and NAIP 1/2 recognize flagellin and the T3SS respectively (Zhao et al., 2011). The only NAIP in humans was thought to recognize proteins present in the T3SS of certain bacteria but not flagella (Yang et al., 2013). However, another recent study has shown that an isoform present in primary macrophages, but not in certain cell lines, was able of detecting flagellin (Kortmann et al., 2015). Recognition of the ligand by NAIP leads to its association with the downstream NLR, NLRC4. NLRC4 is responsible for the downstream recruitment of caspase via direct CARD-CARD domain interactions. In epithelial cells, NAIP and NLRC4 have been shown to have a protective role during *S. typhimurium* and *C. rodentium* infection with *Nlrc4* KO mice showing increased bacterial loads compared to wild-type mice, especially early on in infection (Nordlander et al., 2014; Sellin et al., 2014). The activation of the NAIP/NLRC4 inflammasome is thought to control *S. typhimurium* infection by leading to the cell death of infected cells, thus favoring their extrusion from the epithelial lining and limiting infection (Sellin et al., 2014).

1.1.3.2.3 Non-canonical inflammasome

In addition to the NLR-mediated inflammasome assembly, the inflammasome can also be activated independently of NLRs. This non-canonical inflammasome is based on the direct activation of caspase-11 in mice or the human counterparts, caspases 4/5. These caspases have been shown to directly bind LPS and are thus thought to be the intracellular receptors of LPS

(Hagar et al., 2013; Kayagaki et al., 2013; Meunier et al., 2014; Shi et al., 2014). The non-canonical inflammasome has been shown to play an important role in the restriction of a number of bacterial infections. In murine macrophages, caspase-11 activation can induce pyroptosis, which increases clearance of *S. typhimurium* (Aachoui et al., 2013). In epithelial cells, the non-canonical inflammasome is required for IL-18 but not IL-1β secretion in IECs of both mice and humans (Knodler et al., 2014a). In human epithelial cells, the bacteria *S. flexneri, S. typhimurium* and *E. Coli* all cause caspase-4-dependent cell death favoring expulsion of infected cells from the intestinal epithelium (Knodler et al., 2014a; Kobayashi et al., 2013).

1.1.4 Downstream signaling and NF-κB activation

Whilst different PRRs exist, many of the downstream signaling pathways converge. The signaling pathways, apart from those activated following inflammasome assembly which results in IL-1β and IL-18 production, lead to the activation of the NF-κB and the MAPKs extracellular signal-regulated kinase (ERK), p38 and Jun N-terminal kinase (JNK). This results in the production of pro-inflammatory cytokines, which are responsible for the inflammatory response associated with infection.

NF-κB was first identified in B cells as a nuclear factor that binds the enhancer element of the immunoglobulin (Ig)κ light-chain gene (Sen and Baltimore, 1986). It is now known that NF-κB proteins are ubiquitously expressed and are a family of transcription factors that control the transcription of many different genes in the cell ranging from its own regulation, to cell survival and apoptosis and, of course, immune signaling and inflammation (Vallabhapurapu and Karin, 2009). The family consists of five proteins, which can form homo- or heterodimers and all possess a Rel homology domain responsible for dimerization and DNA binding (Ghosh et al., 1998). The most abundant and the most ubiquitously expressed of these dimers is the p65/p50 heterodimer. Due to its central role in gene transcription, NF-κB activation is tightly regulated. In steady state, it is present in an inactive form in the cytoplasm. The inhibitor of κB (IκB) protein ensures this by occluding its nuclear localization site (Verma et al., 1995). In order for NF-κB to be released, IκB must be phosphorylated and ubiquitinated, tagging it for degradation by the proteasome (Chen et al., 1995; Henkel et al., 1993). Two pathways of NF-κB activation exist, the canonical and the non-canonical pathways, of which I will only discuss the former. In the canonical pathway, the complex responsible for IκB phosphorylation is IκB Kinase (IKK). This multimeric complex is composed of 2 catalytic subunits IKKα and IKKβ as well as a non-catalytic regulatory subunit NF-κB Essential Modulator NEMO (DiDonato et al., 1997; Rothwarf et al., 1998; Yamaoka et al., 1998). Activation of the IKK complex requires the phosphorylation of the IKKα and IKKβ subunits

(Mercurio et al., 1997). Transforming growth factor-β activated kinase-1 (TAK1) is central to this process (Wang et al., 2001).

Following TLR recognition of a ligand and dimerization, TIR-containing adaptor proteins are recruited via TIR-TIR domain interactions. Five have been described to date in the literature; Myd88, Myd88 adaptor-like protein (MAL), TIR domain containing adaptor protein inducing IFNβ (TRIF), TRIF-related adaptor molecule (TRAM) and sterile α- and armadillo-motif-containing protein (SARM) (O'Neill and Bowie, 2007). Myd88 is the most common and is utilized by all of the TLRs apart from TLR3. Its recruitment is followed by the recruitment of the IL-1 receptor associated kinase (IRAK) 4, which subsequently interacts with IRAK1 and IRAK 2 (Lin et al., 2010; Motshwene et al., 2009). IRAK1 and 2 possess motifs, which interact with the E3 ubiquitin ligase Tumor necrosis factor Receptor Associated Factor (TRAF) 6. Ubiquitination, although well characterized as a process targeting proteins for proteasomal degradation, is emerging as highly important in immune signaling events (Hu and Sun, 2016). It is a sequential three-step process involving ubiquitin-activating (E1), ubiquitin-conjugating (E2), and ubiquitin-ligating (E3) enzymes, which can conjugate either single ubiquitin molecules or ubiquitin chains to a lysine residue on target protein. These modifications can be "read" by ubiquitin binding proteins and lead to downstream signaling events (Husnjak and Dikic, 2012).

Following its recruitment, TRAF6 undergoes autoubiquitination. TAK1 forms a complex with the regulatory proteins TAK1-binding protein (TAB)1, TAB2 and/or TAB3. Whilst TAB1 enhances TAK1 kinase activity (Shibuya et al., 1996), TAB2 and TAB3 are capable of binding to the ubiquitin chains of TRAF6 (Kanayama et al., 2004). This is an essential step in the activation of TAK1 since mutants of TAB, which do not bind these ubiquitin chains, are unable to activate the kinase (Kanayama et al., 2004; Xia et al., 2009). TAK1 is a serine/threonine kinase and plays a central role in the activation of NF-κB since it is the kinase responsible for the phosphorylation and activation of the IKK complex (Wang et al., 2001). It is not completely clear how this is achieved but NEMOs capacity to bind K63 polyubiquitinated chains may play a part in this by bringing the two complexes into proximity (Wu et al., 2006). Signaling via the NLRs NOD1 and NOD2 also leads to the activation of TAK1. However, this does not happen through the recruitment of the IRAK kinases but rather through RIP2. RIP2 is recruited to NOD via CARD-CARD interactions (Inohara et al., 1999). It undergoes K63-linked ubiquitination and interacts with TAB2/TAB3 leading to the activation of TAK1 and subsequent activation of IKK and NF-κB (Hasegawa et al., 2008) (figure 5).

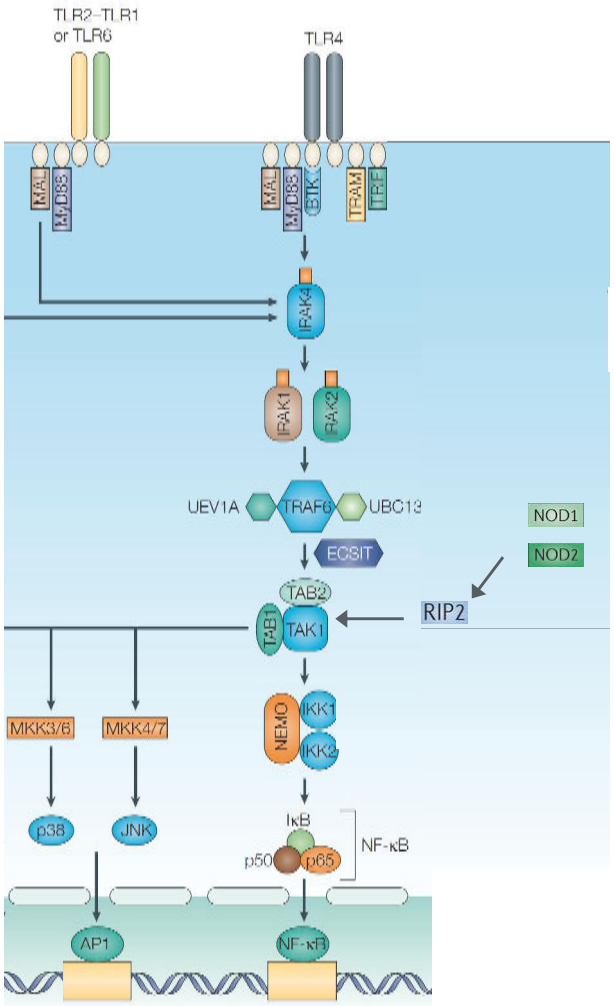

Figure 5. Signalling cascade activated following TLR and NOD 1/2 activation. (Adapted from Liew et al., 2005). TLR dimerization following ligand recognition leads to the recruitment of adaptor proteins such as MAL and Myd88. This is followed by the activation of IRAK4, IRAK1 and IRAK2. IRAKs 1 and 2 interact with the ubiquitin ligase TRAF6, which activates TAK1. TAK1 can also be activated following NOD1 and NOD2 stimulation, resulting in the activation of the kinase RIP2 and subsequently TAK1. TAK1 in turn activates the IKK complex, which tags IκB for proteasomal activation thus releasing NF-κB, which then translocates to the nucleus and exerts its activity as a transcription factor. TAK1 also phosphorylates MAPKKs (MKK), which activate the MAPKs such as p38 and ERK. This step is necessary for the activation of the transcription factor AP-1 which, like NF-κB, induces transcription of proinflammatory cytokines.

In addition to its role in phosphorylating IKK, TAK1 is also central in the activation of the MAPKs JNK, ERK and p38. These proteins are involved with the regulation of transcriptional responses mediated by external signals (Whitmarsh, 2007). The MAPK signaling cascade is a three-step process whereby a MAPK kinase kinase (MAPKKK) phosphorylates and activates a MAPK Kinase (MAPKK), which subsequently activates the aforementioned MAPKs by dual phosphorylation of the Thr–X–Tyr activation motif. TAK1 is itself a MAPKKK, and is responsible for the activation of p38 and JNK whilst also participating indirectly to the activation of ERK via IKK-induced proteolysis

of the NF-κB subunit precursor protein p105 (Beinke et al., 2004). Activated MAPKs have many targets and functions and can phosphorylate their substrates either in the cytoplasm or translocate to the nucleus to exert this function (Yang et al., 2003). JNK and p38, for example, are important for the activation of another transcription factor called activator protein 1 (AP-1). This transcription factor is a dimeric complex most commonly formed by JUN and Fos proteins in mammals (Eferl and Wagner, 2003). It plays a key role in regulation of cell proliferation, differentiation and inflammatory processes and controls the expression of a number of cytokines. p38 and ERK activate Mitogen and stress activated protein kinases 1 and 2 (MSK1/2), which, among many other roles, phosphorylate histone H3, making DNA more accessible to transcription factors (Arthur, 2008).

1.1.5 Cytokines

Upon infection, the result of the activation of the transcription factors is ultimately the production of pro-inflammatory cytokines, which are necessary for the immune response that follows. Whilst IECs can produce a number of different cytokines, by far the most abundantly produced during bacterial infections is interleukin-8 (IL-8). The IL-8 promoter possesses both AP-1 and NF-κB DNA binding sites (Roebuck, 1999). It is, in fact, a chemokine and a strong chemoattractant for polymorphonuclear cells (PMNs), which express the chemokine receptors CXCR1 and CXCR2. This leads to their recruitment to the infected tissue. These cells are the first to be recruited and play a key role in bacterial clearance. Indeed, strong IL-8 production and neutrophil influx is observed following infection with invasive bacteria such as *S. typhimurim*, *S. flexneri* and *L. monocytogenes* (Eckmann et al., 1993; Sansonetti et al., 1999). Other cytokines, which are also produced by epithelial cells include interleukin-6 (IL-6) and TNFα. IL-6 participates in neutrophil recruitment (Fielding et al., 2008) as well as other inflammatory processes such as the acute phase response. It also plays a role in both T and B lymphocyte activation (Ataie-Kachoie et al., 2014). TNFα has many roles both in inflammation as well as normal physiological processes. It is an activator of NF-κB via the TNF receptor promoting the further production of cytokines including IL-6 (Shalaby et al., 1989), IL-8 (Kolios et al., 1996) and TNFα itself (Philip and Epstein, 1986). TNFα, along with IL-1β, which is also capable of activating NF-κB , is one of the key mediators of endotoxic shock (Dinarello, 1991).

As previously mentioned, the two cytokines IL-1β and IL-18 are produced following inflammasome activation. Both of these cytokines belong to the IL-1 family of cytokines. The family is particularly associated with the effects of acute inflammation such as fever, vasodilation and hypertension (Dinarello, 2009). Whilst the main producers of IL-1β are macrophages, epithelial cells do produce

it as well (Franchi et al., 2012; Knodler et al., 2014a). IL-1β has many roles both in inflammation and beyond. It is capable of stimulating NF-κB activation through signaling via the IL-1 receptor and thus all the associated downstream effects. IL-1β also leads to the increased expression of adhesion molecules favoring infiltration of inflammatory cells (Beck-Schimmer et al., 1997; Smith et al., 1988). It functions as a co-stimulator for T cells along with an antigen or mitogen and is important for polarizing T helper 17 (Th17) cells (Acosta-Rodriguez et al 2007). Unlike pro-IL-1β, pro-IL-18 is constitutively expressed throughout the gastrointestinal tract under steady state conditions (Puren et al 1999). IL-18 is particularly important for inducing the production of IFNγ by T lymphocytes in conjunction with IL-12 (Tominaga et al., 2000). IFNγ is important in restricting pathogen intracellular replication as is seen during *Francisella tularensis* and *S. flexneri* infections (Le-Barillec et al., 2005; Lindgren et al., 2007; Way et al., 1998). Similarly, IL-18 is also important for Natural Killer (NK)-derived IFNγ as well as attracting and activating NK cell granule secretion during *S. typhimurium* infection (Müller et al., 2016).

2 Intracellular Pathogens and Immunity

In spite of all the defense mechanisms developed by the host to protect the organism from pathogens, certain bacteria manage to establish infection. Some cause disease by colonizing the extracellular surface of epithelial cells such as *H. pylori* and EPEC, whilst others have opted for an intracellular lifestyle. Enteroinvasive pathogens that target IECs include both Gram-negative and Gram-positive bacteria. These bacteria use different mechanisms in order to gain access to the IEC cytoplasm where they can survive and replicate. The result of such infections is acute inflammation of the gut although specific symptoms and severity vary depending on the pathogen. An important Gram-positive intestinal pathogen is *L. monocytogenes,* which causes the disease listeriosis. This disease has a variety of symptoms depending on the infected individual, from gastroenteritis in healthy individuals to meningitis in immunocompromised patients and abortions in pregnant women (Cossart, 2011). *Salmonella* are Gram-negative enteroinvasive bacteria causing a range of diseases, including gastroenteritis, bacteremia, enteric fever and focal infections. There are over 2500 serovars in the *Salmonella enterica* species, defined on the basis of their flagella and LPS (LaRock et al., 2015). The most commonly studied is *Salmonella typhimurim*, a non typhoidal strain, which generally causes acute gastroenteritis in humans. In our work, we have used the Gram-negative bacterial pathogen *S. flexneri* as a model.

2.1 *Shigella flexneri*: A model pathogen

2.1.1 Epidemiology

Bacteria of the genus *Shigella* are Gram-negative bacteria belonging to the family *Enterobacteriacae* and are the cause of the disease shigellosis, otherwise known as bacillary dysentery. This disease can vary in severity from watery diarrhea to severe inflammatory dysentery characterized by blood and mucus in the stool, and accompanied by abdominal cramps and fever (Schroeder and Hilbi, 2008). It is the most prevalent cause of bloody diarrhea in developing countries, accounting for anywhere between 80 - 165 million cases of infection per year (Bowen, 2017). It is thought to be associated with around 600 000 deaths per year, mainly in children under the age of 5, although these estimates vary (Mani et al., 2016). It is spread via the faeco-oral route, either by direct contact or through contaminated food and water. As few as 10-100 microorganisms are thought to be enough to cause disease (DuPont et al., 1989). The current treatment for shigellosis is antibiotic treatment; however multi-drug resistance has become a growing concern (Phalipon and Sansonetti, 2007). A vaccine is highly desirable but current efforts thus far have been unsuccessful (Mani et al., 2016).

The genus *Shigella* is divided into 4 subgroups *S. boddyi*, *S. sonnei*, *S. dysenteriae* and *S. flexneri* which, apart from *S. sonnei*, can be further divided into several serotypes. The serotypes are defined by the O-antigen, the outer most part of the LPS (Lindberg et al., 1991). The first 2 species are generally associated with the milder form of the disease whilst *S. dysenteria* is the cause of the most devastating epidemic outbreaks and represents the most severe form of dysentery largely due to the presence of the Shiga toxin (Phalipon and Sansonetti, 2007). *S. flexneri* is the principal cause of endemic shigellosis in developing countries and is the most studied and well characterized. It is the strain used in this work.

2.1.2 Virulence plasmid and T3SS

Genetic studies have shown that there is only 1.5% divergence between *Shigella* and non-invasive *E. coli* (Lan and reeves, 2002). *Shigella* have acquired a 213 kb virulence plasmid allowing them to adapt to a facultative intracellular lifestyle (Sansonetti 1982, Sasakawa 1986). This plasmid, pWR100, encodes around 100 genes (Buchrieser et al., 2000). A 31 kb region is of particular importance for bacterial entry into host cells (Maurelli et al., 1985; Sasakawa et al., 1989). It encodes the Mxi/spa proteins, which form the T3SS, a syringe like complex extending a needle into the external milieu. It spans both the outer and inner bacterial membranes and is necessary for bacterial entry into host cells (Blocker et al., 2001; Tamano et al., 2000). Around 25 Gram-negative bacterial species possess such an apparatus including *Chlamydia, pseudomonas, Yersinia* and *Salmonella* (Cornelis 2006). Whilst architectural differences are observed between species, they all possess a conserved core related to the flagellar T3SS (Diepold and Armitage, 2015).

The T3SS is capable of penetrating the host cell and translocating proteins from the bacterial cytoplasm into the host cytoplasm. These proteins, called effectors, are able to interfere with a number of cellular processes to facilitate bacterial entry, survival and spread, and regulate inflammation (Figure 6). In *S. flexneri,* the expression of these genes is under tight regulation with the key trigger being the temperature switch to 37°C (Tobe et al., 1991). This leads to the increased expression of the transcription activator VirF, which in turn leads to the production of VirB (Tobe et al., 1993). VirB controls the expression of the entry region (Le Gall et al., 2005). Whilst the needle complex is assembled at 37°C, it is only weakly active (Allaoui et al., 1993) with the effectors stored in the cytoplasm associated to chaperone proteins (Ménard et al., 1994). Contact of bacteria with host cells, or the dye Congo red, constitutes a secretion signal leading to a rapid burst of protein secretion (Ménard et al., 1994; Parsot et al., 1995). This activation signal leads to the production of a second set of genes necessary for the intracellular phase of the life cycle and regulated by the transcriptional activator MixE (Mavris et al., 2002).

Shigella effector	Host targets	Effect on host process
OspE1	Bind to exterior of polarized cells	Increase adherence to polarized cells
OspE2	Bind to exterior of polarized cells	Increase adherence to polarized cells
IpgB1	Act as GEF for Rac	Induce actin remodeling to facilitate invasion
IpgB2	Act as GEF for RhoA	Induce actin remodeling to facilitate invasion
IpgD	Act as phosphatase to generate PI5P	Induce actin remodeling to facilitate invasion
IpaB	Bind to filopodia and cholesterol on the host cell surface Insert into vacuole membrane Reduce and disrupt balanced levels of cholesterol and lipids	Insert into eukaryotic membrane to form a pore Facilitate invasion Form T3SS complex Promote vacuole breakdown Interfere with proper Golgi function
IpaD	Bind to filopodia on the host cell surface	Facilitate interaction and invasion Form T3SS complex
IpaC	Activate Src Kinase and Cdc42 Insert into vacuole membrane	Facilitate invasion Form T3SS complex Promote vacuole breakdown
IpaA	Host-cell focal adhesion component vinculin	Functions as an anchor to the site of membrane ruffling
OspB	Induce mTOR signaling through IQGAP1	Inhibit autophagy
VirA	Catalyze GTP hydrolysis in Rab1 Induce p53 degradation	Disrupt ER-to-Golgi trafficking and autophagy Block apoptosis
IpgD	Host cell recycling endosome machinery Increase levels of PI5P leading to p53 degradation	Rapid escape from the entry vacuole Induce PI3K/Akt-dependent survival pathways
IpaJ	Cleave N-myristoylated glycine from ARF1 to disrupt its localization	Disrupt autophagosome maturation and host membrane trafficking
IpaH9.8	Target and degrade NEMO/IKKγ	Disrupt NF-κB signaling
IpaH4.5	Target and degrade p65 subunit of NF- κB	Disrupt NF- κB signaling
IpaH0722	Target and degrade TRAF2	Disrupt NF- κB signaling
OspZ	Prevent nuclear translocation of p65	Disrupt NF- κB signaling
OspI	Deamidate UBC13 E2 enzyme needed for activation of TRAF6	Disrupt NF- κB signaling
OspG	Interfere with ubiquitin proteasomal degradation of IκB-α	Disrupt NF- κB signaling
OspF	Inactivate MAPK signaling components like ERK and p38 by epigenetic modifications using its phosphothreonine lyase activity	Disrupt MAPK signaling
OspC3	Interact with caspase-4-p19 subunit and inhibit its heterodimerization and activation	Inhibit pyroptosis within epithelial cells
IcsB	Block autophagy targeting by binding Atg5 Bind cholesterol	Reduce autophagy Escape from the vacuole following cell-to-cell spread

Figure 6. List of S*higella* effectors and their function (Killackey et al., 2016).

Over 25 proteins are involved in the needle complex assembly, which consists of 2 pairs of rings joined together and spanning the inner and outer bacterial membrane, and the needle, which protrudes out (Cornelis, 2006) (Figure 7). Electron microscopy studies on the needle complex of both *S. typhimurium* and *S. flexneri*, which share structural similarities, have revealed much about its architecture (Blocker et al., 1999, 2001; Kubori et al., 1998; Sani et al., 2007; Tamano et al., 2000). The basal body has a length of around 32 nm and a width of 20-40 nm whilst the needle is around 45 nm in length and 7 nm in width (Tamano et al., 2000). An internal 2-3 nm channel spans

the complex (Blocker et al., 2001). The first step in assembly is the formation of the basal body, which consists of the periplasmic and inner membrane rings made up of the proteins MxiJ and MxiG. These proteins interact with MixD and MixM, which form the outer membrane ring (Blocker et al., 1999; Schuch and Maurelli, 2001; Tamano et al., 2000). Once assembled, the rest of the needle structure can be formed. It is composed of a major subunit MxiH and a minor subunit MxiI, which form an extracellular helical polymer (Blocker et al., 2001; Cordes et al., 2003; Tamano et al., 2000).

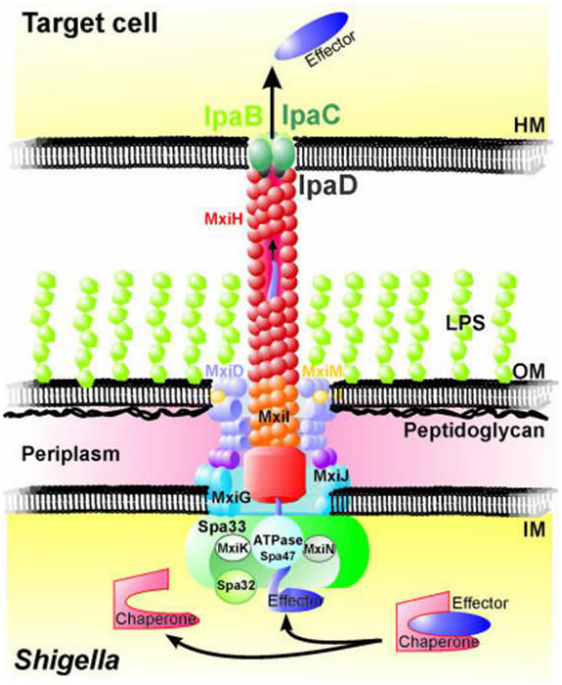

Figure 7. The *S. flexneri* Mxi-Spa T3SS (Schroeder and Hilbi, 2008). The basal body spans the bacterial inner-membrane and outer-membrane with the hollow needle protruding into the extracellular medium. Upon contact with the host cell, IpaB and IpaC insert into the membrane forming a pore, stabilized by IpaD. Effectors, which are stored in the cytoplasm linked to chaperone proteins, can then be unfolded and translocated into the host cell.

The whole process is tightly controlled by a number of proteins, which are associated with the basal body. Spa33 is central to the recruitment and export of T3SS-associated proteins (Morita-Ishihara et al., 2006). It interacts with the proteins MxiK, MxiN, Spa32 and the ATPase spa47. MxiK and MxiN are necessary for MxiH transport to the needle complex (Jouihri et al., 2003). Spa32 controls the length of the needle (Magdalena et al., 2002). Spa47 is thought to provide the energy required for the unfolding of T3SS substrates, chaperone release, and transmembrane transport as is the case with *the Salmonella* ATPase InvC (Akeda and Galán, 2005) since the translocation of proteins is an energetically unfavorable process and fully folded proteins cannot pass through the channel.

2.1.3 Infection Cycle

The T3SS allows *Shigella* to invade and survive within the cellular cytoplasm, but to understand the symptoms of the disease, one must look at the whole infection cycle. Much of *Shigella's* life cycle was established in the 80s and 90s using *S. flexneri* and has been very well studied since, although many of the molecular mechanisms still remain to be determined. One challenge with studying *S. flexneri* infection has been the lack of appropriate animal models since it is a human and primate only pathogen. A ligated ileal loop model in rabbits has been used for much of the phenotypical characterization as it leads to invasion and an acute inflammation with the associated symptoms. However, limited availability of the necessary immunological tools and practical issues make this model more difficult to use (Phalipon and Sansonetti, 2007). In mice, *S. flexneri* does not cause disease that resembles that of the human disease in the intestine although a pulmonary model following intranasal inoculation has proved useful (van de Verg et al., 1995) as well as infection as in newborn mice (Fernandez et al., 2003). Other organisms, which have been used as models for *S. flexneri* infection are guinea pigs (Barman et al., 2011; Shim et al., 2007), piglets (Jeong et al., 2010) and, recently, zebrafish larvae (Mostowy et al., 2013). The latter may hold promise due to the ever-growing availability of molecular tools and the possibility of *in vivo* imaging of the transparent larvae (Lieschke and Currie, 2007). More work will be needed to establish the relevance of this model in terms of human disease.

The general infection cycle is as follows (Figure 8). Following ingestion, *S. flexneri* travels through the intestine to the colon where it infects colonic epithelial cells. Whilst invasion is possible at the apical pole of polarized IECs (Carayol and Tran Van Nhieu, 2013), the majority occurs via the basolateral pole (Mounier et al., 1992). In order to get access to the underside, *S. flexneri* uses transcytosis via M cells (Wassef et al., 1989), and is quickly engulfed by the resident macrophages. *S. flexneri* is able to escape from the macrophage and induces its own uptake into epithelial cells. Once inside the cell, bacteria can replicate and perform intracellular and intercellular movement, infecting cells along the epithelium. Epithelial cells are capable of sensing infection and respond by producing the chemokine IL-8. PMNs migrate to the site of infection in response, a key step in bacterial clearance. However, in the process, PMNs also destabilize the integrity of the epithelium, resulting in the symptoms associated with bacillary dysentery. Each step of this process involves a complex interlay of bacterial and host factors, which will now be discussed in further detail.

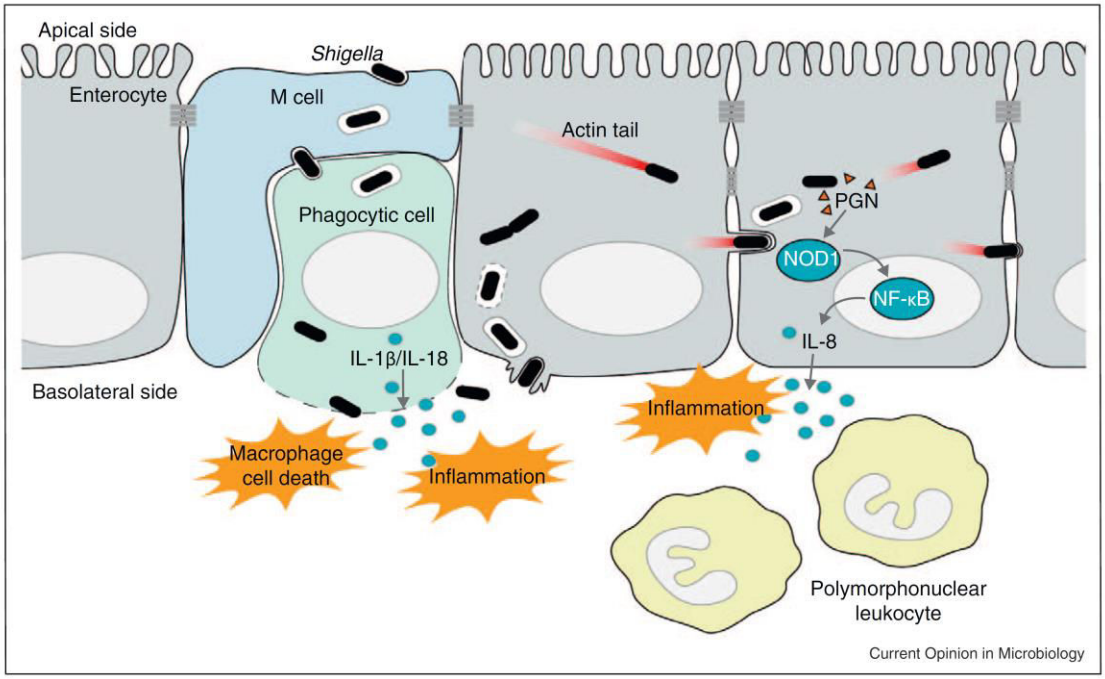

Figure 8. *S. flexneri* infection cycle (Ashida et al., 2011).

2.1.3.1 Macrophage escape

Shigella's first challenge in avoiding an untimely end is escaping destruction by macrophages. *S. flexneri* is capable of escaping the phagocytic vacuole and inducing what was thought to be apoptosis in the infected macrophage (Zychlinsky et al., 1992). It has since been shown that it is in fact pyroptotic cell death, dependent on the activation of caspase-1 (Hilbi et al., 1998) and accompanied by the release of the pro-inflammatory cytokines IL-1β and IL-18. The bacterial effector IpaB is central to this process. It co-localizes with activated caspase-1 on the bacterial surface, in the cytoplasm and on vesicular membranes of infected macrophages (Schroeder et al., 2007). The spontaneous formation of IpaB oligomers, which can insert into the vacuolar membrane causes an ion flux and subsequent disintegration of the vacuolar membrane (Senerovic et al., 2012). This event leads to the activation of caspase-1 via a NLRC4-dependent mechanism (Senerovic et al., 2012; Suzuki et al., 2007). Although this inflammatory cell death serves as a danger signal, it, in fact, seems to be beneficial for the bacteria by facilitating entry. Indeed, blocking IL-1 activity in a rabbit ligated ileal loop model of infection led to a decrease in bacterial invasion (Sansonetti et al., 2000). Furthermore, in a IL-1β KO model of lung infection, the inflammatory response was reduced but with similar bacterial clearance (Arondel et al., 1999).

2.1.3.2 Epithelial cell entry

Once escaped from the dying macrophage, the bacterium enters into epithelial cells. Unlike macrophages, which are phagocytic by nature, epithelial cells are not. Whilst *S. flexneri* has no identified cognate receptor, it adheres to epithelial cells by binding the hyaluronan receptor CD44 and $\alpha_5\beta_1$ integrin (Skoudy et al., 2000; Watarai et al., 1996). Recent evidence suggest that prior to this, the bacteria interact with cellular filopodia, which facilitate their contact with the cellular body (Romero et al., 2011). Once in contact with the host cell, *S. flexneri* is able to induce its own uptake in a T3SS-dependent manner. The effectors IpaB, IpaC and IpaD, whose expression is under control of VirB, are necessary for this process (Ménard et al., 1993). IpaB and IpaC associate separately with the chaperone protein IpgC in the bacterial cytoplasm but can form a complex together once secreted by the bacterium (Ménard et al., 1994). IpaD has self-chaperoning activity and locates at the tip of the needle where it acts as a plug to avoid premature secretion (Espina et al., 2006; Johnson et al., 2007). Exposure to bile salts is thought to lead to the recruitment of IpaB to the tip where it associates with IpaD (Olive et al., 2007; Sani et al., 2007; Veenendaal et al., 2007). From this position, it can sense the host cell membrane components and recruit IpaC (Epler et al., 2009). IpaB then inserts into the host cell membrane and, along with IpaC, forms the 2.5 nm wide pore (Blocker et al., 1999). The efficiency of insertion is increased by IpaD (Picking et al., 2005). The formation of this translocon is necessary for the translocation of other bacterial effectors into the host cytoplasm and entry via macropinocytosis. A number of bacterial effectors including IpgB1, IpgB2 and IpaC as well as host components such as Rho GTPases and kinases lead to the induction of complex cytoskeletal rearrangements, which results in the formation of lamelipodia or “ruffles”, enveloping and engulfing the bacterium (Carayol and Tran Van Nhieu, 2013). Another effector, IpgD, is also important for the formation of the ruffles with deletion mutants causing much smaller entry foci but not showing a defect in invasion. This is attributed to its hydrolytic activity on Phosphatidylinositol 4,5-bisphosphate ($PI(4,5)P_2$), which destabilizes cortical actin, leaving more monomers free to polymerize at the invasion site (Niebuhr et al., 2002).

2.1.3.3 Vacuolar escape and cellular dissemination

Once inside the cell, the bacteria find themselves within a vacuole from which they must escape in order to gain access to the cytoplasm, their replicative niche. This vacuolar rupture is induced as soon as 10-15 min post infection and can be visualized in real time using galectin-3 as a marker of disassembled membranes (High et al., 1992; Paz et al., 2010; Ray et al., 2010; Sansonetti et al., 1986). Unlike the IpaB-dependent rupture, which has been suggested in macrophages, efficient vacuolar rupture was dependent on the recruitment of host Rab-GTPase Rab11 to the

bacterial entry site (Mellouk et al., 2014). This is mediated by IpgD since the deletion mutant did not recruit Rab11 and showed delayed and incomplete vacuolar rupture (Mellouk et al., 2014). It has recently been shown that macropinosomes other than the bacteria containing vacuole (BCV) are formed during this internalization process (Weiner et al., 2016) (Figure 9). Their formation is dependent on the presence of IpgD. The availability of the macropinosomes is correlated to the efficiency of vacuolar rupture; the fewer the macropinosomes, the slower the rupture. It is, in fact, to these macropinosomes that Rab11 is recruited and they interact directly with the BCV during vacuolar lysis (Weiner et al., 2016).

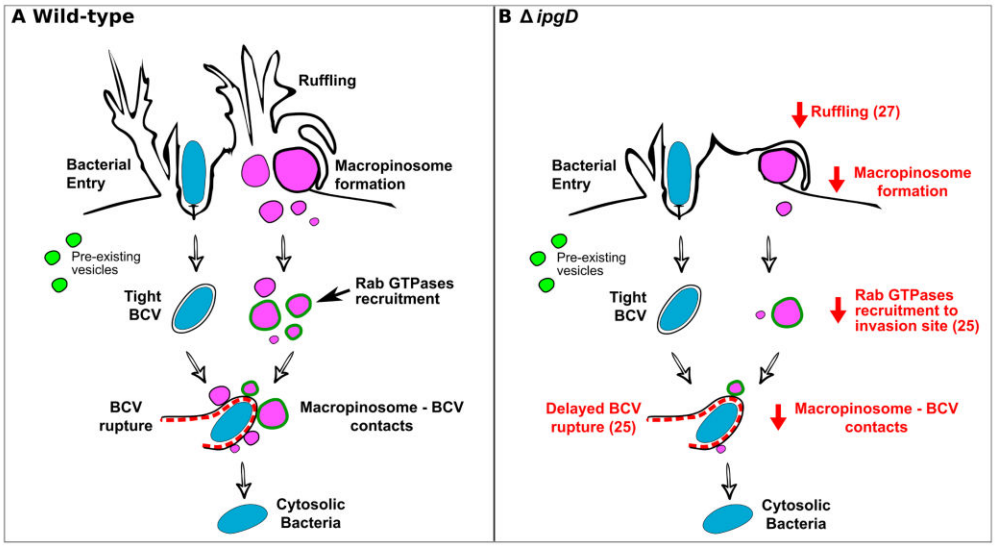

Figure 9. Role of IpgD during bacterial entry and vacuolar rupture. (Weiner et al., 2016). During WT *S. flexneri* infection, macropinosomes are formed along with the BCV. They recruit Rab GTPases and participate in vacuolar rupture. The Δ*ipgD S. flexneri* mutant causes less membrane ruffling and less macropinosome formation. This results in delayed vacuolar rupture.

Once in the cytoplasm, *S. flexneri* can move both intracellularly and intercellularly (Bernardini et al., 1989; Monack and Theriot, 2001). This is achieved through the action of the bacterial protein IcsA/ VirG. It localizes to one pole of the bacterium and can interact with host cell factors, including the neuronal Wiskott-Aldrich syndrome protein (N-WASP) and the Arp2/Arp3 complex. This serves as an actin nucleator and catalyzes the directed elongation of an actin tail, propelling the bacteria through the cytoplasm (Egile et al., 1999). This intracellular movement is also necessary for the intercellular spread. Bacteria target tricellular junctions where bacteria-containing pseudopodia are engulfed by neighboring cells via clathrin-mediated endocytosis (Fukumatsu et al., 2012). The *virG* deletion mutant is not compromised in its ability to invade epithelial cells. However, it is unable of cell-cell spread and thus forms a microcolony in the cell, which it invades.

2.1.3.4 Intracellular detection of bacteria

Whilst the intracellular IEC niche allows *Shigella* to avoid detection by other immune cells lurking outside, it is not without its dangers. Epithelial cells dispose of a number of mechanisms for detecting and responding to infection, as previously described. Indeed, following detection of *S. flexneri*, NF-κB and MAPKs are activated leading to the production of pro-inflammatory cytokines, notably IL-8 (Philpott et al., 2000). Since IECs have low expression of TLR4 and MD-2 as well as lacking the CD14 co-receptor, detection of bacteria mostly happens in the cytoplasm (Abreu et al., 2001) (Figure 10). The main receptor thought to be responsible for *S. flexneri* detection is NOD1 which recognizes cytosolic PGN, specifically iE-DAP (Chamaillard et al., 2003; Girardin et al., 2003b). NOD1, although cytosolic, is associated with the cellular membrane and is recruited to the bacterial entry site (Kufer et al., 2008). It was shown that NEMO also localizes to these structures, suggesting that the downstream signaling cascade is triggered directly at the entry site (Kufer et al., 2008). Additionally, the host factor guanine nucleotide exchange factor (GEF)-H1 has a role to play (Fukazawa et al., 2008). It is required for NF-κB activation following bacterial invasion via a dual mechanism. Firstly, it is recruited away from the tight junctions to the entry site where it activates the Rho GTPase, RhoA. This is not only required for invasion, but RhoA also activates the kinase ROCK, which subsequently leads to the activation of NF-κB. Secondly, GEF-H1 was shown to interact with NOD1 and be involved in the PGN-mediated NF-κB activation via RIP2 activation. Furthermore, the *S. flexneri* effectors OspB and IpgB2 lead to the activation of NF-κB (Fukazawa et al., 2008). This is dependent on both GEF-H1 and NOD1 suggesting that NOD1 may be more broadly involved in sensing of infection, independently of PGN sensing (Fukazawa et al., 2008).

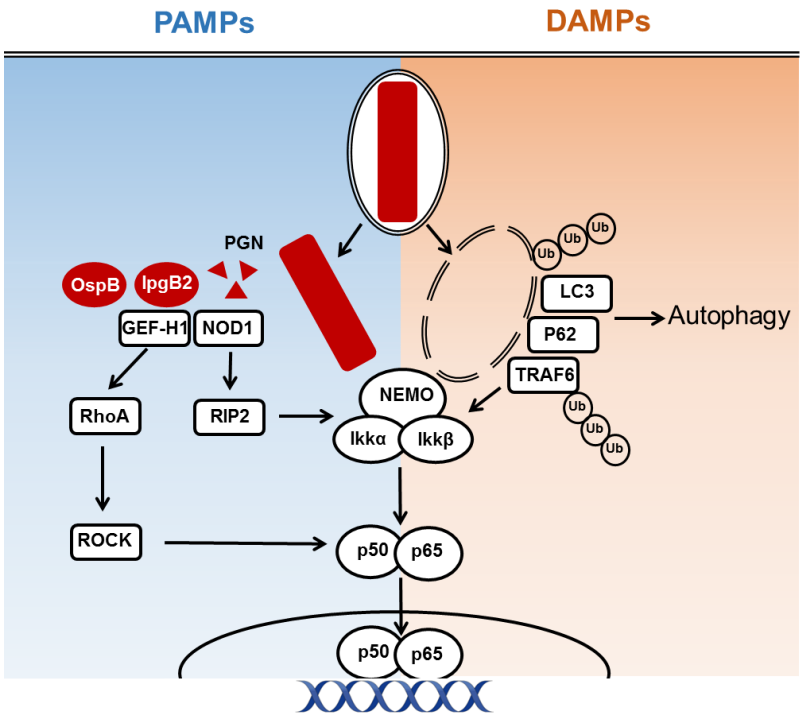

Figure 10. **Intracellular detection of *S. flexneri*.** *S. flexneri* is recognized via both PAMPs and DAMPs. NOD1 and GEF-H1 lead to NF-κB activation in response to bacterial peptidoglycan recognition and the secretion of the bacterial effectors OspB and IpgB2. Vacuolar remnants produced following vacuolar rupture are sensed as DAMPs. They are targeted for degradation by autophagy but also act as signalling platforms recruiting proteins such as TRAF6, which lead to the downstream activation of NF-κB.

In addition to the direct recognition of PAMPs, the bacteria are also recognized through the DAMPs they produce during infection such as the vacuolar membrane remnants (Dupont et al., 2009; Sanada et al., 2012). The vacuolar remnants produced following BCV rupture have been shown to act as a signaling platform to which a number of proteins are recruited (Dupont et al., 2009). The remnants are poly-ubiquitinated and recruit TRAF6, which is itself poly-ubiquitinated following infection (Dupont et al., 2009). NEMO is also found localized at these remnants suggesting that downstream signaling is initiated at these platforms. In accordance, a study by Sanada et al. also found TRAF6 to be involved in the NF-κB activation associated with the recognition of vacuolar remnants as DAMPs (Sanada et al., 2012). The remnants were also found to recruit the autophagy marker LC3 as well as the scaffold protein P62. This results in targeting these structures to degradation by autophagy, potentially a way of limiting the inflammation (Dupont et al., 2009). Consistent with this, components of the inflammasome such as NLRP3, NLRC4, ASC and caspase-1 are also recruited but instead of having a pro-death/pro-inflammatory effect, it seems that they are sequestered to be targeted for degradation by autophagy, thus attenuating inflammation and being a pro-survival signal (Dupont et al., 2009).

Following the recognition of bacterial PAMPs and DAMPs, the downstream signaling cascade leads to the activation of NF-κB and subsequently, the production of inflammatory cytokines. As previously described, the most abundantly produced by epithelial cells following *S. flexneri* infection is IL-8. Since IL-8 is a strong chemoattractant for PMN cells, they migrate to the site of infection in their masses. Blocking IL-8 in a rabbit ileal loop model of infection leads to a decrease of PMN influx as well as attenuating the destruction of the epithelium (Sansonetti et al., 1999). However, the bacteria, which are normally limited to the epithelium, were found to disseminate deeply into the lamina propria (Sansonetti et al., 1999). The destruction of the epithelial integrity caused by PMNs is further exacerbated by the bacteria themselves. *S. flexneri* is able to alter the tight-junction protein composition (Sakaguchi et al., 2002), which leads to integrity deterioration. This allows PMNs to form transepithelial protrusions to entrap luminal bacteria. In the process, PMNs further destabilize the epithelium, which can promote more bacterial entry, independently of M cells. Therefore, whilst PMNs are necessary for the resolution of the infection, they are a double-edged sword since it is at the cost of the integrity of the epithelium. The combined effects of the bacteria as well as the acute immune response exacerbate infection and lead to the tissue destruction, which is responsible for the symptoms of the disease. Therefore, whilst inflammation is a necessary part of the infection process, if it is uncontrolled it can be detrimental to both the host and the bacteria.

2.1.4 Effectors interfering with immunity

Whilst a certain level of inflammation may promote bacterial entry and dissemination, an excessive immune response would not necessarily be beneficial for the bacteria since it results in an increase of bactericidal activity and a loss of replicative niche through destruction of the epithelial cell lining (Kim et al 2010). For this reason, a number of their effector proteins are involved with the manipulation of the host immune signaling pathways (Figure 11). Bacterial effectors particularly, but not exclusively, target the NF-κB pathway.

2.1.4.1 Osp genes

The Osp family of genes is involved in the control of immune signaling. The effectors OspG, OspZ and OspI all interfere with the NF-κB signaling pathway. OspG, for example, dampens NF-κB signaling by preventing the proteasome-dependent degradation of IκB (Kim et al., 2005). It has sequence similarity to serine/threonine kinases, and is capable of binding ubiquitin as well as ubiquitinated E2 ubiquitin conjugating enzymes (Grishin et al., 2014; Kim et al., 2005; Pruneda et al., 2014; Zhou et al., 2013). OspG binds to the E2 site, which is also required for the recruitment

of E3 ubiquitin ligases, a process necessary for ubiquitination of IκB (Grishin et al., 2014). In addition, the binding of ubiquitin or ubiquitinated E2s enhances the effectors kinase activity, which is required for its attenuation of the NF-κB pathway although the targets of phosphorylation remain unclear (Grishin et al., 2014; Kim et al., 2005; Pruneda et al., 2014; Zhou et al., 2013). OspZ too is capable of blocking p65 nuclear translocation as well as inhibiting the degradation of IκB (Newton et al., 2010), the exact mechanisms of which still remain to be determined. OspI affects the NF-κB signaling pathway in an indirect way. Diacylglycerol (DAG) accumulates at the site of bacterial infection and stays associated with the membrane remnants (Sanada et al., 2012). DAG activates the CARD-Bcl10-MALT1 (CBM) complex, which recruits TRAF6. TRAF6 is then responsible for the activation of the TAK1-IKK- NF-κB pathway. OspI is a glutamine deamidase that affects this pathway by selectively deamidating the glutamine of UBC13, an E2 ubiquitin ligase, to a glutamic acid residue (Sanada et al., 2012). This inhibits its E2 ubiquitin-conjugating function, which is necessary for TRAF6 activation and downstream signaling, thus attenuating NF-κB activation.

Other Osp proteins target different pathways. OspC3 is thought to counteract inflammatory cell death of intestinal epithelial cells (Kobayashi et al., 2013). An OspC3 deletion mutant was found to increase inflammatory cell death, which corresponded to a decrease in bacterial burden in a guinea pig model of infection. The authors found that this effector was capable of interacting with caspase-4, inhibiting its activation by preventing heterodimerisation and thus, inhibiting activation of the non-canonical inflammasome (Kobayashi et al., 2013). OspF has a unique phosphothreonine lyase activity and interferes with MAPK signaling (Li et al., 2007). It translocates to the nucleus where it is capable of irreversibly dephosphorylating and inactivating ERK and p38 (Arbibe et al., 2007; Li et al., 2007). This blocks the downstream MSK1-mediated phosphorylation of histone H3 at serine-10, promoting chromatin condensation and masking the NF-κB binding site. This results in the repression of transcription of genes such as IL-8 (Arbibe et al., 2007). MSK1 is also important for the phosphorylation of the transcriptional regulator HP1γ.This phosphorylation recruits HP1γ to sites of transcriptional elongation. OspF is able to modulate the phosphorylation state of HP1γ mainly through its inactivation of MAPK signaling and the subsequent lack of MSK1 activation. OspF also binds to chromatin of target genes such as IL-8 and modulates decreases HP1γ binding at these sites leading to an attenuation of the inflammatory response (Harouz et al., 2014). OspF indirectly potentiates activation of JNK and NF-κB, an effect dependent on its phosphothreonine lyase activity on p38 and the result of the disruption of the p38 and TAK1 negative feedback loop (Reiterer et al., 2011). The potentiated JNK activation, however, was not associated with enhanced c-jun signaling as its expression at the transcriptional level is also inhibited by OspF (Reiterer et al., 2011).

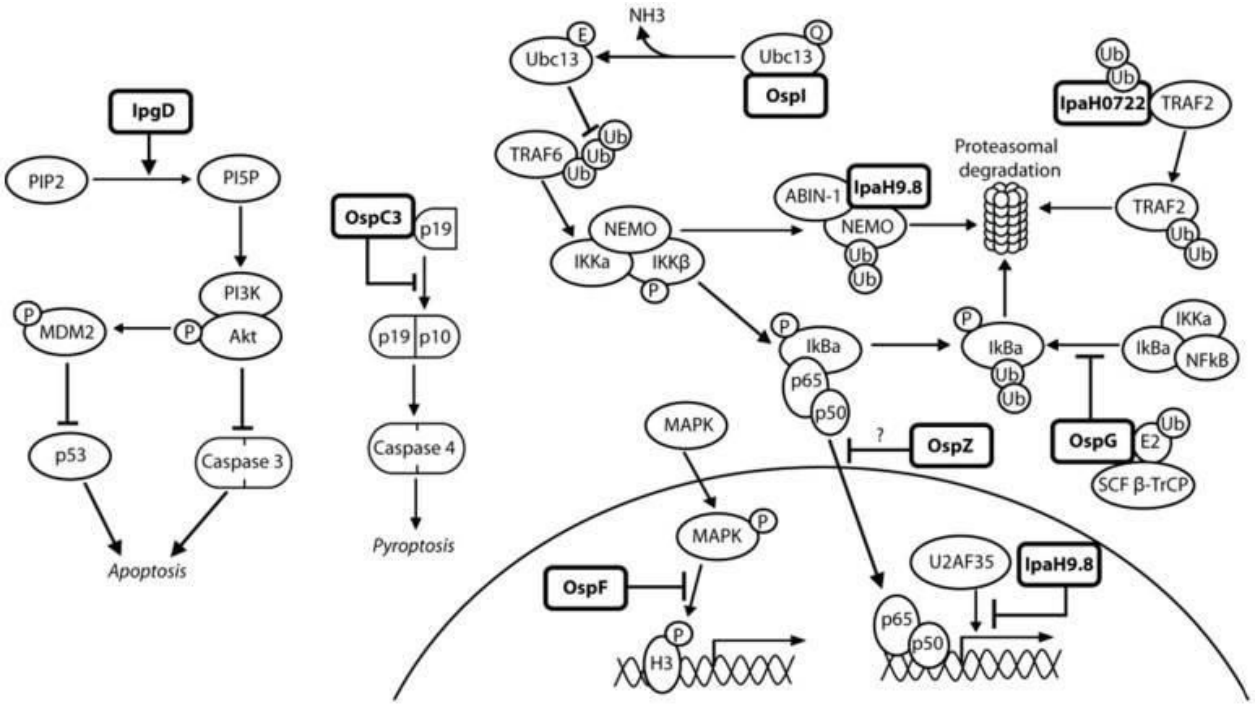

Figure 11. *S. flexneri* effectors interefering with host cell inflammatory signaling pathways. (Mattock and Blocker, 2017). Bacterial effectors are denoted in bold. OspI, OspZ, OspG, Ipa9.8 and IpaH0722 all target the NF-κB signaling pathway. OspF targets MAPK signaling and OspC3 promotes non-canonical inflammasome activation.

2.1.4.2 IpaH

The IpaH proteins are a family of effectors, which are encoded by 12 genes residing both on the virulence plasmid and on the chromosome (Ashida and Sasakawa, 2016). They have a conserved LRR region and E3 ubiquitin ligase activity in their C-terminal region (Rohde et al., 2007). They mainly target the NF-κB signaling pathway although this is not the case for IpaH7.8, which targets the NLRP3/NLRC4 inflammasome in macrophages (Suzuki et al., 2014). Unlike the other IpaH proteins, which dampen the immune response, IpaH7.8 promotes pyroptotic cell death accompanied by release of IL-1β. However, this benefits the bacteria since it promotes bacterial invasion (Sansonetti et al., 2000). In epithelial cells, three particular IpaH effectors are of importance for the dampening of the immune response. IpaH 9.8 binds to NEMO and a ubiquitin binding adaptor protein thus promoting NEMOs ubiquitination and tagging it for proteasomal degradation (Ashida et al., 2010). IpaH0722 is capable of binding TRAF2 and promoting its ubiquitination, tagging it for proteasomal degradation (Ashida et al., 2013). TRAF2 is a protein, which acts downstream of protein kinase C (PKC) to activate NF-κB. PKC has been shown to be activated during *S. flexneri* infection (Ashida et al., 2013). Since DAG activates PKC and is found to accumulate at the bacterial entry site (Sanada et al., 2012), IpaH0722 dampens the vacuolar

remnants DAMP-induced NF-κB signaling but independently of the DAG-CBM-TRAF6 pathway (Ashida et al., 2013). Another IpaH protein, IpaH4.5, interferes with NF-κB signaling by targeting p65 for degradation although the mechanism is unclear (Wang et al., 2013).

2.2 Mechanism of bystander cell activation

With so many mechanisms developed by the bacteria in order to attenuate immune signaling within the infected cell, it seems paradoxical that the devastating symptoms of the disease are due to an excessive inflammatory response. Kasper and colleagues showed that it was not the infected cells which were producing pro-inflammatory cytokines, but the non-infected cells surrounding them, termed bystander cells (Kasper et al., 2010) (Figure 12). Using *a virG* deletion mutant, unable to perform cell-cell spread, and an image-based assay allowed them to visualize the spatial distribution of IL-8 producing cells after infection. NF-κB was activated in infected and bystander cells as early as 15 min post-infection. The same was observed for the MAPKs JNK, ERK and p38. However, IL-8 was only produced by bystander cells in spite of the nuclear translocation of NF-κB in infected cells. They showed that this process was not mediated by paracrine signaling via the release of TNFα following infection, and that it was dependent on cell-to-cell contact and gap junctions. Gap junctions are made up of connexin hemichannels from both donor and recipient cells forming a pore, and permit direct cell-to-cell transfer of small molecules and ions of up to 1-2 kDa (Yeager and Nicholson, 1996). They therefore proposed that there exists a gap junction-mediated cell-to-cell communication, which allows the circumvention of bacterial effectors, too big to pass through the channel, and the amplification of the inflammatory response. A similar result was obtained during *L. monocytogenes* and *S. typhimurium* infection, showing that this seems to be a common mechanism during enteroinvasive bacterial infections. However, whether the same mechanisms are at play and which are the specific mediators of this communication remain to be determined.

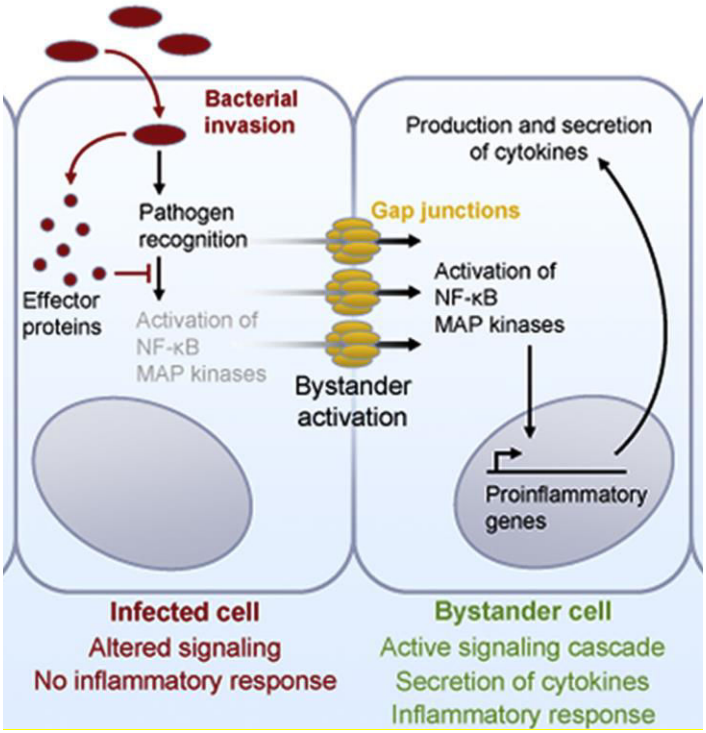

Figure 12. Mechanism of bystander cell activation during enteroinvasive bacterial infections (Kasper et al., 2010). Bacteria invade host cell. This leads to induction of inflammatory signaling pathways following bacterial recognition. However, certain pathogens such as *S.flexneri* or *S.typhimurium* have effector proteins capable of blocking these pathways thus blocking production of pro-inflammatory cytokines. A gap-junction mediated cell-cell communication exists which allows activation of uninfected bystander cells. This leads to the successful production of pro-inflammatory cytokines.

The existence of the bystander phenomenon has begun to be more and more appreciated in the context of viral, bacterial or protozoan infections. Multiple studies have shown that there exists a cell-cell communication, either through direct contact or through soluble mediators, which allows the infected cell to signal to other cells the presence of infection (Holmgren et al., 2017). In accordance with the study by Kasper et al., Dolowschiak and colleagues also observed the bystander effect following *L. monocytogenes* infection (Dolowschiak et al., 2010). They, however, did not find this to be dependent on gap junctions, rather attributed it to the NADPH oxidase (Nox) 4-dependent oxygen radical formation, which mediated paracrine activation of bystanders. ATP has also been proposed as a stimulator in support of cell contact-independent bystander cell activation (Van Nhieu et al., 2003). *S. flexneri* infection leads to the opening of hemichannels and the release of ATP in the extracellular medium. This extracellular ATP was shown to be a potent inducer of pro-inflammatory cytokines in the ileal loops of infected rabbits (Puhar et al., 2013).

The presence of a gap junction mediated cell-to-cell communication has been observed during viral infections. The sensing of viral DNA in the cytoplasm of cells was enough to induce the

production of pro-inflammatory cytokines such as TNFα in uninfected bystander cells, a process dependent on contact via gap junctions (Patel et al., 2009). Cytosolic viral DNA is sensed by cyclic GMP–AMP synthase (cGAS), which upon binding of the foreign DNA, produces cyclic guanosine monophosphate–adenosine monophosphate (cGAMP). cGAMP acts as a second messenger and can pass through gap junctions to uninfected cells where it binds to stimulator of IFN genes (STING), inducing Interferon regulatory factor 3 and the subsequent transcription of interferon-dependent genes (Ablasser et al., 2013).

The basis of my thesis was to understand the molecular mechanisms governing bystander cell activation and to identify the key players involved using *S. flexneri* as a model pathogen.

3 RNAi screen and Identification of candidates

In order to identify potential players in bystander cell activation, the group of Dr Arrieumerlou performed a genome wide RNAi screen. The technology is based on the endogenous cellular process whereby messenger RNAs (mRNAs) are targeted for degradation following recognition via a short double stranded (ds) RNA of identical sequence. In the cell, dsRNAs are processed by an RNase III type enzyme called Dicer, which cleaves them into 21-28 nucleotide siRNA duplexes. A single siRNA strand is incorporated into the RNA-induced silencing complex (RISC), which can then cleave perfectly complementary mRNAs thus leading to their degradation and ensuing gene (Dorsett and Tuschl, 2004). The discovery of the process has earnt Andrew Fire and Craig Mello the Nobel Prize in Physiology or Medicine in 2006 and opened the way to perform loss-of-function genetic screens in mammalian cells.

Hundreds of RNAi screens have been performed to date either on cells from Drosophila, mice or humans, as well as a growing number of in-vivo screens in whole organisms such as *Drosophila*, *C. elegans* and even mice (Mohr et al., 2014). These screens have allowed the identification of many important proteins involved in processes such as cell survival, drug susceptibility, development, and cancer and host pathogen interactions. In relation to the latter, genome-wide screens in *Drosophila* cells have helped to identify human orthologues, which are key factors in the replication of influenza viruses (Hao et al., 2008). Screens performed in mammalian cells have been used to identify key cellular factors important for entry of both viral and bacterial pathogens (Rämö et al., 2014).

Whilst RNAi screens offer the opportunity to systematically silence each gene from the whole genome, they are not without their disadvantages. The most important issue with RNAi remains the off-target effects whereby a siRNA recognizes sequences of mRNAs other than the intended target. Using bioinformatic tools in reagent design and the use of multiple siRNAs targeting the same gene reduces these effects. However, potential candidates must still be extensively characterized and verified experimentally.

The genome wide RNAi screen to identify the molecular players involved in bystander cell activation was performed using a mammalian epithelial cell line. HeLa cells were infected with *S. flexneri ΔvirG* mutants at a low multiplicity of infection (MOI) in order to be able to observe bystander cell activation. The production of IL-8 by bystander cells was detected using a high-throughput image-based assay and analyzed using bioinformatic image analysis. A number of hits were identified, which led to a decrease in IL-8 production following infection. During my thesis, I focused on 3 proteins in particular; TRAF6, TRAF-interacting protein with forhead-associated domain (TIFA) and alpha kinase 1 (ALPK1), which I will now discuss in further detail.

3.1 TRAF6

TRAF6 is no stranger when it comes to immune signaling pathways. Extensive literature is available on the role of TRAF6 in the development, regulation and homeostasis of the immune system (Walsh et al., 2015). It belongs to the TRAF family of proteins, which were first identified as signaling adaptors, binding directly to the cytoplasmic regions of TNF superfamily receptors. The TRAF family consists of six members with a controversial seventh member, which does not share the distinctive TRAF domain (Xie, 2013). The C-terminal TRAF domain mediates protein interactions as well as TRAF oligomerization whilst the N-terminal domain is important for downstream signaling and consists of a varying number of zinc fingers and a RING domain, with the exception of TRAF1 (Wajant et al., 2001). The RING domain makes up the core of the catalytic ubiquitin ligase domain and is found in many E3 ubiquitin ligases. In accordance with this, TRAF2, 3, 5 and 6 have all been found to act as E3 ubiquitin ligases along with their role as adaptor molecules in signaling pathways (Xie, 2013).

TRAF6 is well conserved between species and broadly expressed in mammalian tissues (Walsh et al., 2015). It was first identified as a downstream adaptor of the TNF family receptor CD40 (Ishida et al, 1996) as well as being a signal transducer of the IL-1 receptor (Cao et al., 1996). Since the IL-1R shares the cytoplasmic TIR domain with TLRs, TRAF6 is also involved in this pathway (Aderem and Ulevitch, 2000). It is a non-conventional E3 ubiquitin ligase, which links polyubiquitin through lysine K63 instead of the K48 linkage associated with proteasomal degradation. This is in conjunction with the E2 ubiquitin conjugating enzymes Ubc13 and Uev1a (Deng et al., 2000). As previously described, following TLR signaling, Myd88 is recruited to the TIR domain subsequently recruiting the downstream IRAK 1, 2 and 4 (Lin et al., 2010; Motshwene et al., 2009). Phosphorylated IRAK1 is thought to recruit TRAF6 to the complex followed by their dissociation from the rest of the complex (Takaesu et al., 2000). This is followed by the oligomerization of TRAF6 and its autoubiquitination (Lamothe et al., 2007). TAB2 and/or TAB3 are able to recognize and bind the K63 linked ubiquitin chains of TRAF6 (Kanayama et al., 2004). This is required for the activation of TAK1 (Wang et al., 2001), which subsequently activates IKK and the MAPK. The exact mechanisms involved in this process have not been fully elucidated. The specific role of TRAF6, relies on its E3 ubiquitin ligase activity. A number of targets have been identified. It has been suggested that IRAK1 may be a target of TRAF6 K63 polyubiquitination, which leads to the recruitment of NEMO (Conze et al., 2008; Lamothe et al., 2007). NEMO itself has also been proposed as ubiquitination target of TRAF6 (Abbott et al., 2007). Whether TRAF6 is involved in the NOD-mediated NF-κB activation is less clear. Whilst RIP2 K63 linked ubiquitination is important for TAK1 activation and TRAF6 is capable of catalyzing this, it seems

that it is not the only E3 ubiquitin ligase able to fulfill this role and thus may not be indispensable (Hasegawa et al., 2008).

Due to the central role of TRAF6 in the Myd88 dependent downstream signaling cascade, it is implicated in a number of infections following TLR recognition. However, in terms of *S. flexneri* infection there are few reports on the exact role of TRAF6. The two studies specifically showing a role of TRAF6 in this infection have both linked it to the recognition of vacuolar remnants as DAMPs (Dupont et al., 2009; Sanada et al., 2012). As previously mentioned, Dupont et al. found that it was recruited to the membrane remnants where it was found to be ubiquitinated, thus activated (Dupont et al., 2009). A recent study by Sanada and colleagues found that DAG accumulated at the site of bacterial entry, and is therefore present at the vacuolar membrane remnants (Sanada et al., 2012). This leads to the activation of the NF-κB pathway via the CBM signalosome, which through TRAF6, activates IKK and the downstream cascade.

3.2 TIFA

One of the strongest hits identified through the screen was the protein TIFA. Up until very recently, relatively little was known about the function of this protein. TIFA is a 20 kDa protein that is encoded on Ch4q25 (Hillier et al., 2005). It is found expressed in all tissues with a cellular localization both in the nucleus and the cytoplasm (Uhlén et al., 2015). It is the smallest known protein to contain a Forkhead-associated (FHA) domain. The FHA domain, first described in 1995 (Hofmann and Bucher, 1995), is a domain known to specifically recognize phosphothreonine residues (Pennell et al., 2010). This interaction can regulate biological functions, ranging from DNA damage repair to signal transduction (Mahajan et al., 2008). TIFA was first identified as a TRAF2 binding protein (and referred to as T2BP) in a mammalian two-hybrid screen, able to activate NF-κB and AP1 in response to TNFα, as well as in the absence of TNFα when overexpressed (Kanamori et al., 2002). Later, it was shown to interact with TRAF6 in a yeast-two hybrid screen (Ye et al., 2002). The study showed that TIFA contained a consensus TRAF6 binding motif *XX*P*X*E*XX*-(aromatic/acidic residue) (Ye et al., 2002) with the critical binding site being an alanine at position 178 (Takatsuna et al., 2003). When this was substituted for a glutamine, the interaction was abolished (Takatsuna et al., 2003). This suggests a different mechanism of TIFA-TRAF6 and TIFA-TRAF2 interaction, in which the latter requires an almost fully intact protein (Kanamori et al., 2002). TIFA was shown to be constitutively linked to TRAF6 but could also interact with IRAK1 (Takatsuna et al., 2003). The latter was shown to be an inducible interaction following IL-1 stimulation, thus suggesting that TIFA acted as adaptor protein for the IRAK1-TRAF6 interaction and the downstream activation of NF-κB in the Myd88-dependent signaling pathway following IL-1R or TLR4 stimulation (Takatsuna et al., 2003). TIFA is capable

of homo-oligomerization (Takatsuna et al., 2003), a process necessary for the downstream activation of IKK and thus NF-κB (Ea et al., 2004). The activation of downstream signalling is also dependent on TIFA's ability to bind TRAF6. The oligomerization of TIFA promotes the oligomerization of TRAF6 and thus, its E3 ubiquitin ligase activity (Ea et al., 2004). TIFA oligomerization is dependent on the phosphorylation of a threonine at position 9 (T9) and the FHA domain (Huang et al., 2012). Unphosphorylated TIFA is thought to exist as an intrinsic dimer constitutively linked to TRAF6. Upon TNFα stimulation, an unknown kinase phosphorylates T9. This is recognized by the FHA domain of other TIFA dimers leading to its oligomerization thus the oligomerization of TRAF6, enhancing its E3 ubiquitin ligase activity and thus, leading to the activation of the TAK1-IKK-NF-κB pathway (Figure 13).

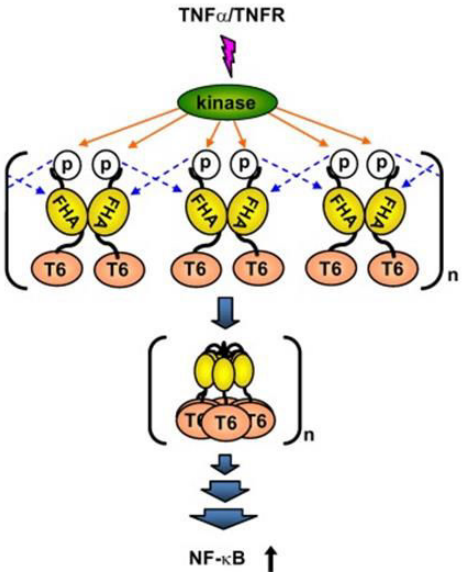

Figure 13. Proposed mechanism for TIFA oligomerization (adapted from Huang et al., 2012). Upon TNFα stimulation, an kinase phosphorylates T9 of TIFA dimers. This pT9 is recognized by the FHA domain leading to its oligomerization. Since TIFA is constitutively linked to TRAF6, this leads to the oligomerization of TRAF6 and the subsequent activation of NF-κB.

Functional roles of TIFA are now beginning to come to light. A recent study found that oxidative stress leads to TIFA expression in endothelial cells by activating an oxidative stress-induced transcription factor Sterol regulatory element binding protein 2 (SREBP2) (Lin et al., 2016). TIFA, through its activation of NF-κB acts as signal 1 for the NLRP3 inflammasome by inducing caspase-1 and pro-IL-1β transcription as well as signal 2, dependent on its oligomerization. The group attributed the phosphorylation necessary for TIFA oligomerization to the kinase Akt, which is capable of phosphorylating TIFA, and could be activated following TLR recognition of oxidative stress components (Lin et al., 2016). Another report shows that TIFA supports acute myeloid

leukemia (AML) progression by promoting NF-κB-mediated cell survival, a process controlled by Aurora-A, a serine/threonine kinase involved in the regulation of chromosome alignment, segregation, and cytokinesis during mitosis (Wei et al., 2017). They found that both TIFA and Aurora-A were upregulated in AML patients and that Aurora-A could phosphorylate TIFA leading to NF-κB activation and pro-survival signals (Wei et al., 2017). In contrast, Shen et al. found that TIFA was tumor suppressive in liver cancer (Shen et al., 2015). The study does not offer any mechanistic explanation but found that TIFA was decreased in these patients. They found that reconstituting TIFA leads to p53-mediated cell cycle arrest as well as activation of caspases-8 and 3, thus promoting apoptosis and having a protective role in this cancer (Shen et al., 2015).

3.2.1 HBP

In the course of our study on the role of TIFA in *S. flexneri* infection, a report implicating TIFA in innate immunity during Gram-negative bacterial infection was published in *Science* (Gaudet et al., 2015). The authors identified the novel PAMP HBP to be the activator of this pathway. HBP is a small bacterial metabolite, which is an intermediate in the biosynthetic pathway of the LPS core (Figure 14). The LPS inner core is composed of two 3-deoxy-D-*manno*-oct-2-ulosonic acids (Kdo) and three L-*glycero*-D-*manno*-heptose (Hep): HepI, HepII, and HepIII and these are conserved across Gram-negative bacterial species (Nakao et al 2012). The genes necessary for the biosynthesis of the core are found on the waa (rfa) locus, which is encoded by 3 operons. Sedoheptulose-7-phosphate is transformed into d-*glycero*-D-*manno*-heptose-7-phosphate by the ketose-aldose isomerase GmhA. This is then phosphorylated by the bifunctional enzyme HldE to form d-*glycero*-β-D-*manno*-heptose-1-7-bisphosphate also known as HBP. A dephosphorylation at position 7 is carried out by GmhB forming d-*glycero*-β-D-*manno*-heptose-1-phosphate. HldE subsequently exerts its second function and catalyzes the adenylyl transfer to the phosphate group at position 1 making ADP-d-*glycero*-β-d-*manno*-heptose. HldD transfers it into ADP-l-*glycero*-β-d-*manno*-heptose, which is then incorporated into LPS by the heptosyltransferase WaaC (Kneidinger et al., 2002).

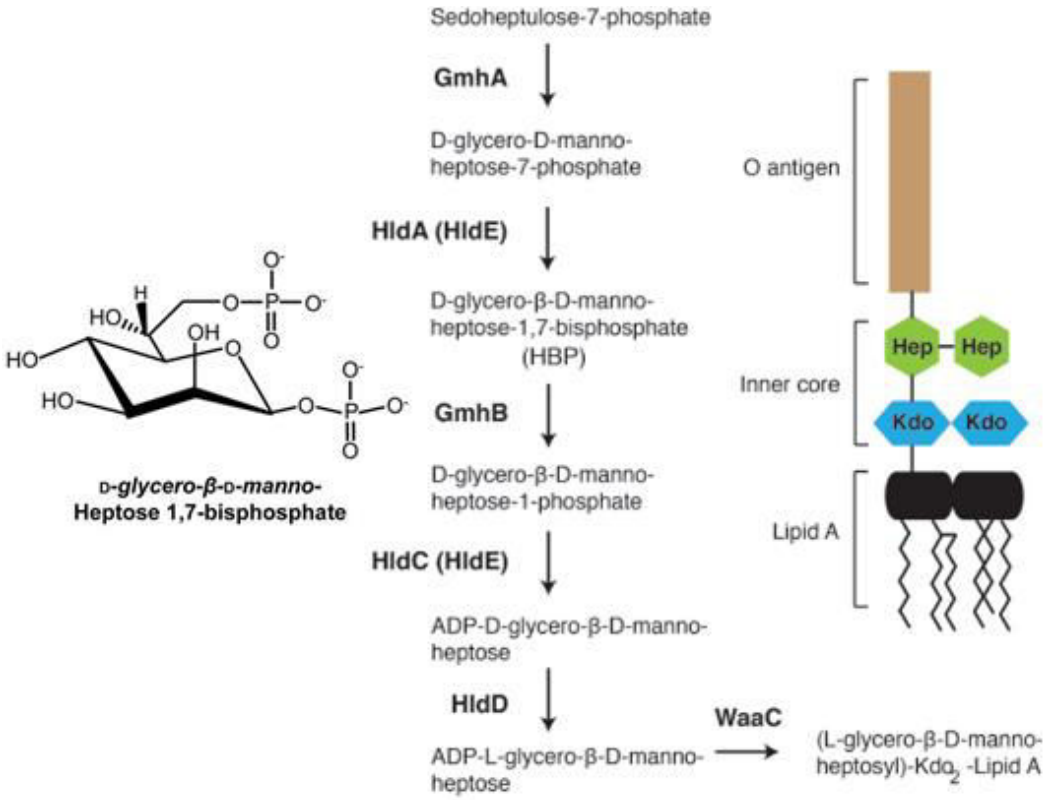

Figure 14. Synthetic pathway of the heptose inner core of LPS. (Adated from Gaudet et al., 2017). Heptose -1, 7-bisphosphate (structure shown) is an intermediate formed by the phosphorylation of heptose-7-phosphate by the enzyme HldA in *Neisseria* or the bifunctional HldE enzyme in most other Gram-negative bacteria.

This pathway is conserved in most Gram-negative bacteria. However, some exceptions exist. For example in *Neisseria*, there are 2 independent enzymes that play the bifunctional role of HldE; HldA and HldC. Other bacteria do not possess this pathway such as *Moraxella*. Bacteria which harbor mutations in this pathway and thus do not possess the heptose core are referred to as deep rough LPS mutants. They are still viable, however, due to the altered composition of the outer membrane, they are more sensitive to external factors *in vivo* such as bile and antibiotics. These mutants have also been shown to have attenuated virulence (Kanipes et al., 2004; Raetz and Whitfield, 2002; Sisti et al., 2002; Stojiljkovic et al., 1997). Deep rough *S. flexneri* mutants are much more adhesive and invasive *in vitro* albeit with undermined fitness since they are incapable of infection *in vivo* (Xue et al., 2016). For this reason, efforts have already been made to target this biosynthetic pathway. The HldE kinase, due to its low similarity with human enzymes (40%) and its conservation between species, has been of particular interest (Desroy et al., 2009, 2013).

Gaudet and colleagues recently showed that the product of the enzyme HldE, HBP, was a PAMP in its own right (Gaudet et al., 2015). This 370 Da monosaccharide is capable of inducing NF-κB

activation and cytokine production. Using *N. gonorrheae* which, unlike other bacteria, releases HBP into the extracellular medium, they showed that bacterial supernatants were sufficient to stimulate cells. Lysates from HBP proficient Gram-negative were enough to activate NF-κB, whereas HldE deletion mutant lysates were not. The phenotype of activation was restored when stimulating cells with lysates of a mutant of the downstream enzyme WaaC. They were able to purify HBP and showed that it was sufficient for NF-κB and downstream cytokine production. HBP requires internalization to activate NF-κB via clathrin-dependent endocytosis, at least in macrophages and Jurkat cells. The activation of NF-κB and subsequent cytokine production was shown to be dependent on the TIFA-TRAF6 pathway and independent of TLR and NOD signaling (Figure 15).

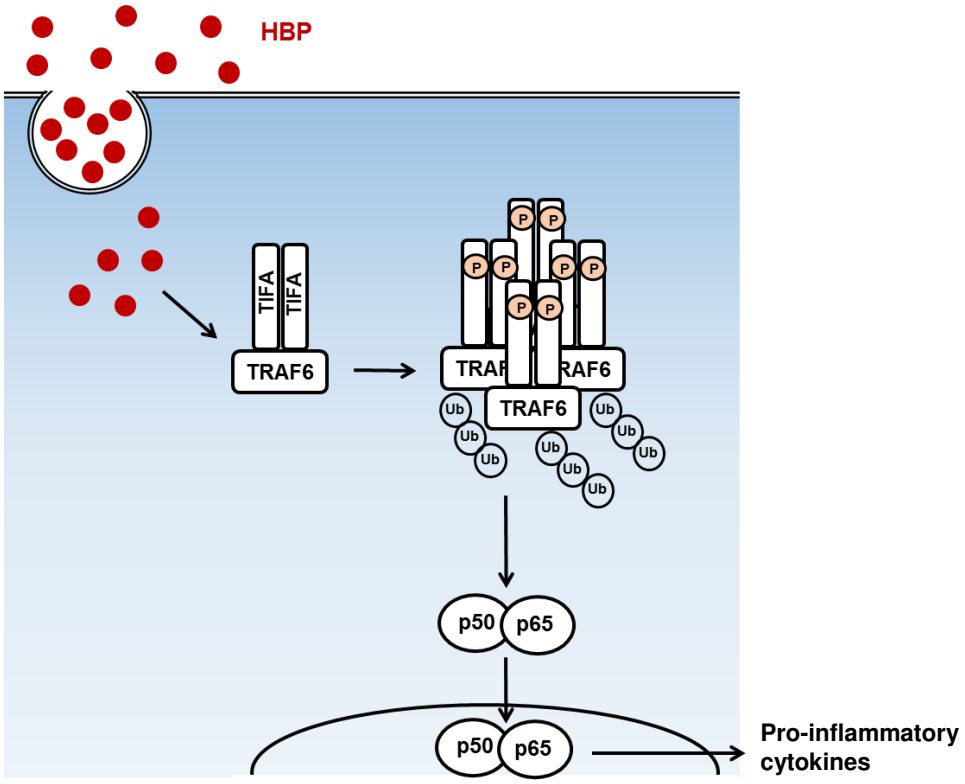

Figure 15. HBP-induced NF-κB activation via the TIFA-TRAF6 pathway. Extracellular HBP is internalized via clathrin-mediated endocytosis. Cytosolic HBP leads to the phosphorylation of TIFA and its oligomerization, thus the oligomerization of TRAF6 and its ubiquitination. This results in the activation and nuclear translocation of NF-κB and the subsequent production of pro-inflammatory cytokines.

ALPK1

Another of the proteins identified in the screen was ALPK1. Once again, not much literature is available surrounding this protein. It belongs to the class of alpha kinases (Ryazanov et al., 1999), which fall into the family of atypical protein kinases, representing 10% of all protein kinases (Middelbeek et al., 2010). This class of kinases shares very little homology to other kinases but the catalytic domain bears resemblance to the myosin heavy chain kinases of *Dictyostelium.* There are 6 members within this family in humans and they show little homology between them. Alpha kinases were given their name as they were thought to recognize phosphorylation targets within an alpha helical context. However, certain members of the family have been found to phosphorylate targets outside of this confirmation (Clark et al., 2008; Jørgensen et al., 2003).

Most studies on ALPK1 have been population-based genetic studies and have associated polymorphisms with a number of diseases including heart disease (Fujimaki et al., 2014; Yamada et al., 2015a), type 2 diabetes (Shimokata et al., 2013; Yamada et al., 2015b), kidney disease (Yamada et al., 2013, 2015c) and cancers including breast cancer (Strietz et al., 2016) and colorectal cancer (Liao et al., 2016). ALPK1 has been most often associated with gout (Kuo et al., 2017; Lee et al., 2016; Wang et al., 2011) although this has been contested (Chiba et al., 2015). Of the few functional studies, which have been published so far, ALPK1 has been implicated in the apical protein transport pathway (Heine et al 2005). ALPK1 was found to be present on vesicles destined for the apical membrane of epithelial cells that had left the Golgi apparatus. Myosin IA was also associated with these vesicles and ALPK1 was shown to be able to catalyze its phosphorylation. Knock-down of ALPK1 led to a reduction in the delivery of apical cargo but did not lead to a change in targeting (Heine et al., 2005). In relation to this, ALPK1 has also been implicated in the traffic of Golgi-derived TNFα trafficking through the phosphorylation of the motor protein myosin IIa in gout-induced inflammation (Lee et al., 2016). Gout is characterized by the deposit of monosodium urate (MSU) crystals in joints leading to the production of pro-inflammatory cytokines, pain and swelling. ALPK1 is upregulated following stimulation of cells with MSU as well as in gouty patients (Lee et al., 2016; Wang et al., 2011) and is thought to promote TNFα, IL-1β and IL-8 production in a MAPK-dependent pathway (Wang et al., 2011). Another hypothesis is that ALPK1 interacts with myosin IIa, calmodulin and F-actin via its N-terminal and that it is necessary for myosin IIa phosphorylation. Whilst this phosphorylation has not been shown directly, the authors base themselves on the theory that another member of the alpha kinase family TRMP7 is able to do so (Lee et al., 2016). This phosphorylated myosin would then be involved in the transport of Golgi-derived vesicles containing TNFα but not involved in the process of non-Golgi-dependent IL-1β secretion (Lee et al 2016). ALPK1 has also been shown to be involved in a negative feedback loop with testosterone, which is anti-inflammatory, leading to a higher

production of pro-inflammatory cytokines (Kuo et al., 2017). The ALPK1-testosterone negative feedback loop could have a link with gout since testosterone regulates the expression of URAT1, a protein responsible for renal urate reabsorption (Hosoyamada et al., 2010). Increased ALPK1 expression may lower testosterone levels leading to lower expression of URAT1. This results in lower urate reabsorption, thus more uric acid in the bloodstream and a higher chance of developing gout (Kuo et al., 2017). So whilst roles for ALPK1 are emerging in the literature, there has not yet been a link described between ALPK1 and infection.

RESULTS

Article summary

The aim of this study was to elucidate the molecular mechanisms underlying the activation of the inflammatory response in epithelial cells to the enteronvasive pathogen *S. flexneri*. Epithelial cells represent the organism's first line of defense and are capable of sensing and responding to invading pathogens. In addition, they can communicate with their un-infected neighbors via gap-junctions, resulting in the local secretion of pro-inflammatory cytokines and chemokines, namely IL-8. However, the signaling pathways involved in this process remain poorly understood.

A genome-wide RNAi screen using the human HeLa epithelial cell line allowed us to identify several proteins important for the production of IL-8 following *S. flexneri* infection. Using a high-throughput image based assay, and a *S. flexneri* mutant incapable of performing cell-cell spread, we were able to identify the proteins TIFA and TRAF6 as being necessary for bystander cell IL-8 production. In this work we show that following sensing of intracellular *S. flexneri*, TIFA forms oligomeric structures. Their formation is dependent on the threonine 9 and Forkhead-associated domain of TIFA. These oligomers allow the oligomerization of TRAF6 leading to its activation and the subsequent activation of NF-κB both in infected and bystander cells. This was confirmed in a colonic epithelial cell line. The same phenomenon was observed with the enteroinvasive Gram-negative bacteria *Salmonella typhimurium* but not the Gram-positive bacteria *Listeria monocytogenes*. We show that the specificity of the TIFA-TRAF6 pathway is mediated by the bacterial metabolite heptose-1, 7-bisphosphate (HBP), an intermediate in the LPS synthesis pathway in Gram-negative bacteria. Bacteria lacking the HldE enzyme, necessary for HBP synthesis, did not elicit an immune response.

In addition, a kinome screen allowed us to identify ALPK1 as the upstream kinase necessary for TIFA oligomerization. The kinase domain of ALPK1 was necessary to activate the TIFA-TRAF6-NF-κB pathway in a HBP-dependent manner. We show that this pathway is triggered in response to intracellular bacteria *S. flexneri* and *S. typhimurium*, as well as the extracellular pathogen *Neisseria meningitidis*. Our work therefore identifies the novel ALPK1-TIFA-TRAF6 signaling pathway which is specifically triggered by HBP from both intracellular and extracellular Gram-negative bacteria and plays a central role in the activation of an inflammatory response in epithelial cells.

PLOS | PATHOGENS

RESEARCH ARTICLE

ALPK1 controls TIFA/TRAF6-dependent innate immunity against heptose-1,7-bisphosphate of gram-negative bacteria

Milica Milivojevic[1], Anne-Sophie Dangeard[1], Christoph Alexander Kasper[2], Therese Tschon[2], Mario Emmenlauer[2], Claudine Pique[1], Pamela Schnupf[3], Julie Guignot[1], Cécile Arrieumerlou[1]*

1 INSERM, U1016, Institut Cochin, Paris, France, CNRS, UMR8104, Paris, France, Université Paris Descartes, Sorbonne Paris Cité, France, **2** Biozentrum, University of Basel, Basel, Switzerland, **3** Institut Imagine, UMR_S1163, Paris, France

* cecile.arrieumerlou@inserm.fr

Citation: Milivojevic M, Dangeard A-S, Kasper CA, Tschon T, Emmenlauer M, Pique C, et al. (2017) ALPK1 controls TIFA/TRAF6-dependent innate immunity against heptose-1,7-bisphosphate of gram-negative bacteria. PLoS Pathog 13(2): e1006224. doi:10.1371/journal.ppat.1006224

Editor: Dana J. Philpott, University of Toronto, CANADA

Received: August 16, 2016

Accepted: February 7, 2017

Published: February 21, 2017

Data Availability Statement: All relevant data are within the paper and its Supporting Information files.

Funding: This work was supported by the Swiss National Science Foundation (http://www.snf.ch/fr/Pages/default.aspx) with the grant 310030_138377 to CA and by the Agence Nationale de la Recherche (http://www.agence-nationale-recherche.fr/) with the Project ANR-14-ACHN-HostTarget to CA. The funders had no role in study design, data collection

Abstract

During infection by invasive bacteria, epithelial cells contribute to innate immunity via the local secretion of inflammatory cytokines. These are directly produced by infected cells or by uninfected bystanders via connexin-dependent cell-cell communication. However, the cellular pathways underlying this process remain largely unknown. Here we perform a genome-wide RNA interference screen and identify TIFA and TRAF6 as central players of *Shigella flexneri* and *Salmonella typhimurium*-induced interleukin-8 expression. We show that threonine 9 and the forkhead-associated domain of TIFA are necessary for the oligomerization of TIFA in both infected and bystander cells. Subsequently, this process triggers TRAF6 oligomerization and NF-κB activation. We demonstrate that TIFA/TRAF6-dependent cytokine expression is induced by the bacterial metabolite heptose-1,7-bisphosphate (HBP). In addition, we identify alpha-kinase 1 (ALPK1) as the critical kinase responsible for TIFA oligomerization and IL-8 expression in response to infection with *S. flexneri* and *S. typhimurium* but also to *Neisseria meningitidis*. Altogether, these results clearly show that ALPK1 is a master regulator of innate immunity against both invasive and extracellular gram-negative bacteria.

Author summary

Epithelial cells line internal body cavities of multicellular organisms. They represent the first line of defense against various pathogens including bacteria and viruses. They can sense the presence of invasive pathogens and initiate the recruitment of immune cells to infected tissues via the local secretion of soluble factors, called chemokines. Although this phenomenon is essential for the development of an efficient immune response, the molecular mechanism underlying this process remains largely unknown. Here we demonstrate that the host proteins ALPK1, TIFA and TRAF6 act sequentially to activate the transcription factor NF-κB and regulate the production of chemokines in response to infection by

and analysis, decision to publish, or preparation of the manuscript.

Competing interests: The authors have declared that no competing interests exist."

the pathogens *Shigella flexneri*, *Salmonella typhimurium* and *Neisseria meningitidis*. In addition, we show that the production of chemokines is triggered after detection of the bacterial monosaccharide heptose-1,7-bisphosphate, found in gram-negative bacteria. In conclusion, our study uncovers a new molecular mechanism controlling inflammation during infection by gram-negative bacteria and identifies potential targets for treatments aiming at modulating inflammation during infection.

Introduction

Intestinal epithelial cells (IECs) are not considered to be professional immune cells. However, they play an important role in immuno-surveillance and contribute to the initial phase of inflammation after infection by invasive bacteria or viruses. They can sense the presence of pathogens and orchestrate, together with resident macrophages, the recruitment of immune cells to sites of infection. IECs sense highly conserved pathogen-associated molecular patterns (PAMPs) via pathogen recognition receptors (PRRs) including Toll-like (TLRs) and NOD-like receptors (NLRs). They also detect cellular stress-induced danger-associated molecular patterns (DAMPs) produced during infection. All these sensing mechanisms result in complex signal transduction cascades regulating the expression of proinflammatory genes coding for cytokines, chemokines and antimicrobial peptides.

Shigella flexneri is an enteroinvasive bacterium responsible for shigellosis, an acute intestinal inflammation in humans [1]. After ingestion of contaminated food or water, bacteria reach the large intestine and cross the intestinal barrier by transcytosis through M-cells. Once in the submucosal area, they utilize a type III secretion (T3S) apparatus to induce apoptosis in macrophages and invade IECs from their basolateral side. A T3S apparatus is a syringe-like nanodevice enabling the injection of bacterial effector proteins into target cells [2]. Once effectors have translocated into cells, they can subvert the cellular activities of central host factors to favor bacterial internalization. *Shigella* bacteria then escape the internalization vacuole, multiply within the cytoplasm and use actin-based motility to spread from cell-to-cell within the intestinal epithelium. It has been proposed that the main PRR involved in the direct recognition of *S. flexneri* is the NLR NOD1 [3]. This receptor recognizes a component of the peptidoglycan called D-glutamyl-meso-diaminopimelic acid that is part of the gram-negative bacterial cell wall [4]. Upon recognition, NOD1 oligomerises and interacts with the receptor-interacting serine/threonine-protein kinase 2 (RIP2) [5]. This protein associates with the transforming growth factor (TGF)-β-activated kinase 1 (TAK1), and the TAK1 binding protein 1 and 2 (TAB1 and 2) complex. This process leads to the phosphorylation, ubiquitination and degradation of the inhibitory κB (IκB), the nuclear translocation of the NF-κB transcription factor and the transcription of pro-inflammatory genes including the gene coding for interleukin-8 (IL-8). TAK1 is also involved in the activation of the MAPKs JNK, p38 and ERK, which are important for the activation of the transcription factor AP1 [6] and histone H3 phosphorylation. In addition, *S. flexneri* infection can also be sensed indirectly via the production of DAMPs. For instance, Dupont *et al*. found that the membrane vacuolar remnants produced after vacuolar lysis are detected by host cells and that the signals produced contribute to inflammation [7]. In particular, the accumulation of diacylglycerol around the bacterial entry site and within membrane remnants activates NF-κB via a mechanism dependent on the CARD–BCL10–MALT1 complex and TRAF6 [8]. Interestingly, *S. flexneri* possesses a number of tools downregulating the immune response of infected cells. In particular, several type III effectors interfere with the NF-κB and MAPK pathways to reduce IL-8 expression. For instance, OspG reduces the

nuclear translocation of NF-κB by preventing IκB ubiquitination and degradation [9]. OspF reduces transcription via its phosphothreonine lyase activity towards p38 and ERK1/2 and its subsequent impact on chromatin remodeling [10].

Although bacteria manipulate the inflammatory response of infected cells, a massive influx of polymorphonuclear cells is observed in tissues infected with *S. flexneri* [11]. ATP, released by intestinal epithelial cells after infection by *S. flexneri*, contributes to this inflammation [12]. In addition, a previous study by our laboratory showed that innate immunity during *S. flexneri* infection is potentiated by a gap junction-mediated mechanism of cell-cell communication between adjacent epithelial cells [13]. We observed NF-κB and MAP kinase activation in uninfected cells located in the proximity of cells containing bacteria and showed that these bystander cells produced large amounts of inflammatory cytokines including IL-8 and tumor necrosis factor alpha (TNFα). IL-8 was also largely produced in bystander cells after infection with *Salmonella typhimurium* and *Listeria monocytogenes* [13, 14], suggesting that potentiation of innate immunity by cell-cell communication is a common host response to different bacterial infections. This phenomenon also occurs during viral infections. First, Patel *et al*. found that recognition of viral double stranded DNA leads to type I interferon expression in bystander cells via a gap junction-mediated mechanism [15]. More recently, it has been shown that anti-viral immunity can spread via the diffusion of cGMP-AMP through gap junctions; cGMP-AMP then binds to the receptor STING localized at the endoplasmic reticulum, which subsequently induces anti-viral gene expression [16].

Although the control of innate immunity has important physiological consequences during bacterial infection, the molecular basis of its regulation remains poorly understood. Here we performed a genome-wide RNAi screen and identified the proteins TIFA and TRAF6 as critical factors for the control of IL-8 expression during *S. flexneri* infection. We show that threonine 9 (T9) and the forkhead-associated domain (FHA domain) of TIFA are both important for the oligomerization of TIFA occurring in infected and bystander cells. This process is required for the subsequent oligomerization of TRAF6 and the activation of NF-κB. We demonstrate that TIFA/TRAF6-dependent IL-8 expression is triggered by the bacterial metabolite heptose-1,7-bisphosphate (HBP). In addition, we identify alpha-kinase 1 (ALPK1) as the critical kinase controlling TIFA oligomerization and show that ALPK1 controls innate immunity in response to the invasive bacteria *S. flexneri* and *S. typhimurium* as well as to the extracellular pathogen *Neisseria meningitidis*.

Results

TIFA and TRAF6 are critical players of innate immunity in *S. flexneri* infection

In order to characterize the signaling pathways controlling inflammation during infection of epithelial cells by enteroinvasive bacteria, we systematically searched for proteins regulating IL-8 expression following *S. flexneri* infection. For this purpose, we developed a high throughput assay that monitors IL-8 expression at the single-cell level using fluorescence microscopy (Fig 1A) and performed a genome-wide RNAi screen. HeLa cells, an epithelial cell line commonly used in *S. flexneri* infection assays, were infected for 3.5 hours with the Δ*virG* mutant of *S. flexneri* as previously described [17]. This mutant is unable to perform actin-based motility [18] and forms large intracellular microcolonies, which are easily detectable by automated image analysis (Fig 1B and S1 Fig). Background signals from remaining extracellular bacteria were minimized by engineering *S. flexneri* to express the dsRed protein only once it is intracellular [19]. dsRed expression was restricted to cytosolic bacteria by placing dsRed under the transcriptional control of the glucose 6-phosphate transporter *uhpt* promoter, which is only

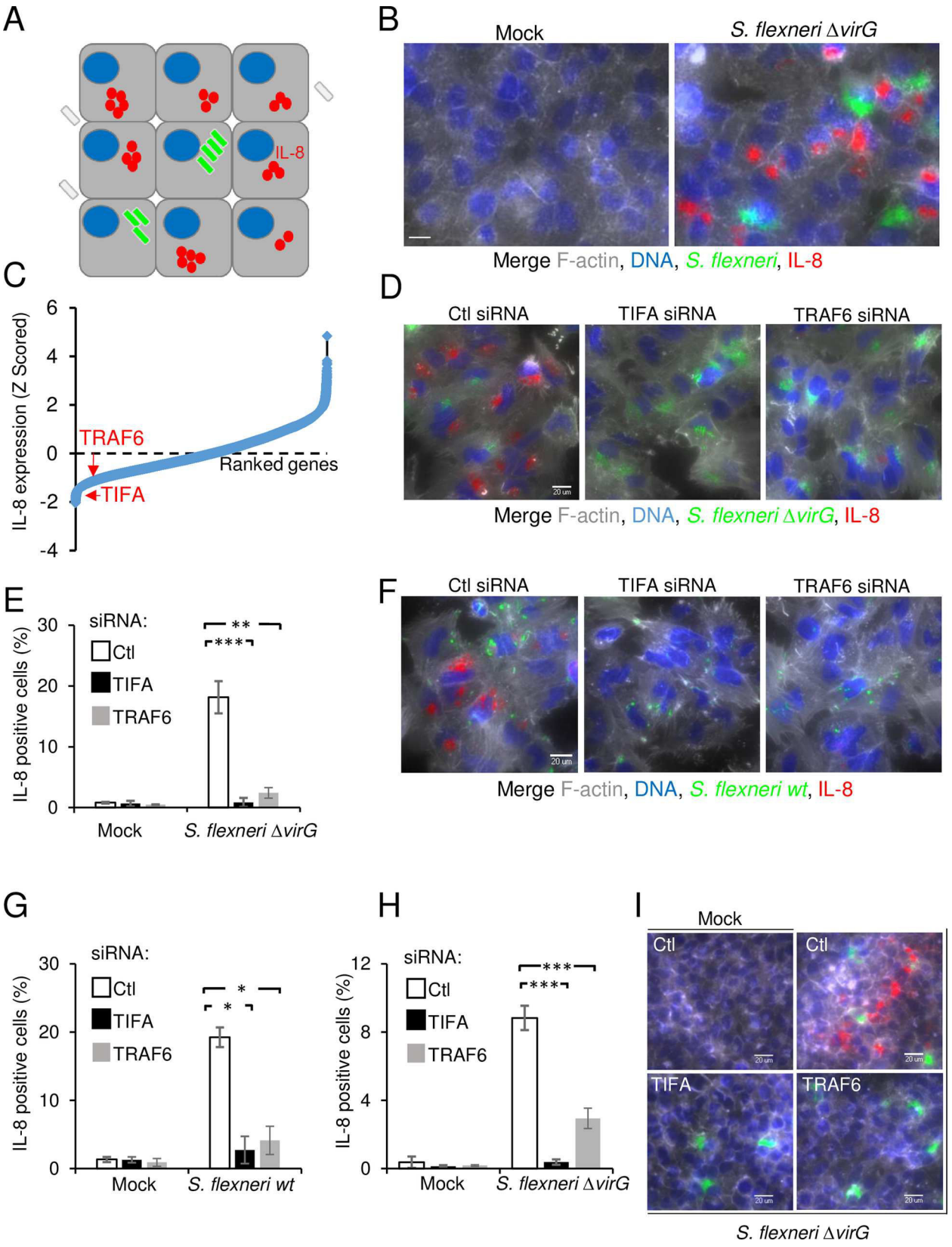
A
IL-8
B
Mock
S. flexneri ΔvirG
Merge F-actin, DNA, S. flexneri, IL-8
C
IL-8 expression (Z Scored)
6
4
2
0
-2
-4
TRAF6
TIFA
Ranked genes
D
Ctl siRNA
TIFA siRNA
TRAF6 siRNA
Merge F-actin, DNA, S. flexneri ΔvirG, IL-8
E
IL-8 positive cells (%)
30
20
10
0
siRNA:
Ctl
TIFA
TRAF6
**
***
Mock
S. flexneri ΔvirG
F
Ctl siRNA
TIFA siRNA
TRAF6 siRNA
Merge F-actin, DNA, S. flexneri wt, IL-8
G
IL-8 positive cells (%)
30
20
10
0
siRNA:
Ctl
TIFA
TRAF6
*
*
Mock
S. flexneri wt
H
IL-8 positive cells (%)
12
8
4
0
siRNA:
Ctl
TIFA
TRAF6
***
***
Mock
S. flexneri ΔvirG
I
Mock
Ctl
Ctl
TIFA
TRAF6
S. flexneri ΔvirG

Fig 1. RNAi screen reveals the roles of TIFA and TRAF6 in *S. flexneri* infection-induced IL-8 expression. A) Schematic representation of the assay used to monitor IL-8 expression in the *S. flexneri* infection assay. **B**) Illustration of the image-based assay developed for the screen. HeLa cells were infected for 3.5 hours with *S. flexneri* Δ*virG* expressing dsRed under the control of the *uhpT* promoter (green). Cells were stained for F-actin (grey), DNA (blue) and IL-8 (red). Scale bars, 20 μm. **C**) Genome-wide RNAi screening data of IL-8 expression after *S. flexneri* infection in HeLa cells. IL-8 measurements were extracted with CellProfiler, Z-scored and ranked. **D**) Validation of the role of TIFA and TRAF6 in *S. flexneri* infection-induced IL-8. HeLa cells were transfected with control, TIFA- or TRAF6-targeting siRNAs and infected with *S. flexneri* Δ*virG* for 3.5 hours. Cells were stained as in B. **E**) Impact of TIFA and TRAF6 depletion on IL-8 expression. Quantification of cells producing IL-8 as shown in D by automated image analysis (see Methods). Data show the mean +/- SD of 3 independent experiments, p**<0.005, p***<0.0005. **F)** TIFA and TRAF6 control inflammation after wild-type *S. flexneri* infection of HeLa cells. Cells were treated as in D and infected with wild-type *S. flexneri* for 3.5 hours. **G)** Impact of TIFA and TRAF6 depletion on IL-8 expression. Quantification of cells producing IL-8 as shown in F. Data show the mean +/- SD of 3 independent experiments, p*<0.05. **H)** TIFA and TRAF6 regulate IL-8 expression in HEK293 cells. HEK293 cells were transfected and infected as in D. IL-8 was measured by image analysis. Data correspond to the mean +/- SD of 3 independent experiments, p***<0.0005. **I)** Images showing the implication of TIFA and TRAF6 in HEK293 cells after infection as quantified in H.

doi:10.1371/journal.ppat.1006224.g001

upregulated once bacteria are in the presence of glucose 6-phosphate [20]. Cells were then treated with monensin to trap IL-8 in intracellular compartments. After fixation, cells were stained for DNA, F-actin and IL-8 and visualized by immunofluorescence. In agreement with previous work [13], IL-8 expression was largely restricted to uninfected cells located in the proximity of infected cells (Fig 1B and S1 Fig), confirming the importance of bystander cell activation in the control of inflammation during *S. flexneri* infection [13, 21]. In order to identify proteins involved in the control of IL-8 expression, the assay was run in a high throughput setup to screen a commercially available genome-wide library made up of pools of 4 siRNAs per gene. Total cell number, infection rates and IL-8 measurements were extracted for all targeted genes using CellProfiler (see Materials and Methods, S1 Table). As expected from previous work [22] [23], pools targeting NF-κB p65 and TAK1 had strong inhibitory effects on IL-8 expression (S1 Table), validating the approach and the experimental setup of the screen. TIFA and TRAF6 were found amongst proteins whose depletion strongly inhibited IL-8 expression after *S. flexneri* infection, and were thus selected for further validation and molecular characterization (Fig 1C, S1 Table). TRAF6 mediates signaling from members of the TNF receptor superfamily as well as the Toll/IL-1 family [24]. Interestingly, a previous publication had already reported that TRAF6 was involved in the activation of NF-κB in *S. flexneri*-infected cells [8]. TIFA is a 20-kDa protein that was first identified as a TRAF6-interacting protein in a yeast two-hybrid screen [25]. It contains a FHA domain, known to bind phosphothreonines and phosphoserines, and a consensus TRAF6-binding motif [26]. In TNFα signaling, it is involved in the oligomerization of TRAF6, which is required for downstream activation of NF-κB [27]. Very recently, it has been reported that TIFA is involved in the inflammatory response triggered following the detection of heptose-1,7-bisphosphate (HBP), a metabolite present in gram-negative bacteria [28]. HBP can be secreted or released upon bacterial lysis and internalized by eukaryotic cells via endocytosis. In order to exclude possible off-target effects in the RNAi screening data and confirm the specific implication of TIFA and TRAF6 during *S. flexneri* infection, silencing of these two genes was repeated with an independent set of siRNA sequences. While infection remained comparable (S2 Fig), this independent approach confirmed a dramatic inhibition of IL-8 after *S. flexneri* Δ*virG* infection of cells depleted for TIFA and TRAF6 (Fig 1D and 1E). Similar results were obtained upon infection with wild-type bacteria (Fig 1F and 1G) as well as in HEK293 cells (Fig 1H and 1I), showing that the contribution of TIFA and TRAF6 was not restricted to infections with the Δ*virG* mutant or with HeLa cells. Altogether, these data show that TIFA and TRAF6 play an essential role in the control of inflammation in *S. flexneri* infection of epithelial cells and confirm that RNAi screens are valuable tools to identify new players in a given cellular pathway.

TIFA and TRAF6 control *S. flexneri*-induced NF-κB activation

Since a published report indicated that TRAF6 was involved in the activation of NF-κB in *S. flexneri*-infected cells [8], we tested whether TIFA was also required for this process. The activation of NF-κB was monitored by following the nuclear translocation of the p65 subunit in conditions where nearly all cells were infected with *S. flexneri*. Interestingly, p65 translocation was reduced both in TRAF6 and TIFA-depleted cells (Fig 2A and 2B), showing that these proteins were required to activate NF-κB in infected cells. When cells were infected at a lower MOI (Fig 2C and 2D), a reduction of NF-κB translocation was also found in bystander cells, showing that the depletion of TIFA and TRAF6 had an impact on NF-κB activation in both cell types. The role of TIFA in NF-κB activation was more broadly tested using stimuli other than *S. flexneri* infection. In contrast to TRAF6, depletion of TIFA failed to inhibit NF-κB activation induced by phorbol 12-myristate 13-acetate (PMA) (Fig 2E), showing that TIFA is not systematically involved in pathways activating NF-κB and that TRAF6 can also function independently of TIFA. Depleting TIFA and TRAF6 had no significant effect on TNFα-induced NF-κB activation (Fig 2F) but partially inhibited activation induced by the NOD1 ligand C12-iE-DAP (Fig 2G). Together, these results show that TIFA is not involved in the intrinsic machinery of NF-κB activation. Instead, we found TIFA to be implicated in at least two signaling pathways that link bacterial infection to inflammation.

T9-FHA domain interaction and binding to TRAF6 are required for IL-8 expression

TIFA contains a FHA domain (Fig 3A), a widespread signaling unit that recognizes phosphorylated threonine and serine residues and binds proteins intra- and inter-molecularly [29]. Huang *et al*. showed that when TIFA is unphosphorylated at the threonine 9 position, it exists as an intrinsic dimer [27]. Upon TNFα stimulation, T9 is phosphorylated by an unknown kinase and FHA-pT9 binding occurs between different dimers forming large TIFA oligomers. This mechanism leads to the subsequent oligomerization of TRAF6 and activation of NF-κB. In order to characterize the mode of action of TIFA during *S. flexneri* infection, we investigated the contribution of T9 and the FHA domain. For this purpose, we measured IL-8 expression after infection of cells that were first depleted for TIFA by RNAi and then transfected with siRNA-resistant wild-type or mutated TIFA cDNA constructs. As expected, we found that wild-type TIFA was able to significantly rescue IL-8 expression (Fig 3B and 3C). In contrast, TIFA mutated at T9 (T9A mutant) or within the FHA domain (RKN mutant) failed to restore IL-8 expression. The same result was observed with the TIFA E178A mutant [27], which is unable to bind TRAF6 (Fig 3B and 3C). Altogether, these results show that T9, the FHA domain and E178 are all essential for TIFA activity suggesting that, as in TNFα signaling, the pT9-FHA interaction and the ability to bind TRAF6 are necessary to induce IL-8 expression during *S. flexneri* infection.

TIFA and TRAF6 form co-localizing oligomers in infected and bystander cells

In order to better characterize the role of TIFA in *S. flexneri* infection of epithelial cells, we monitored its subcellular localization. For this, cells were transfected with a TIFA cDNA construct and TIFA was visualized after infection by immunofluorescence using a TIFA-specific antibody. In the absence of infection, the protein was uniformly distributed in the cytoplasm and the nucleus (Fig 4A). Following infection with *S. flexneri*, punctate structures, likely corresponding to large TIFA protein oligomers [27], were formed. These structures were still visible

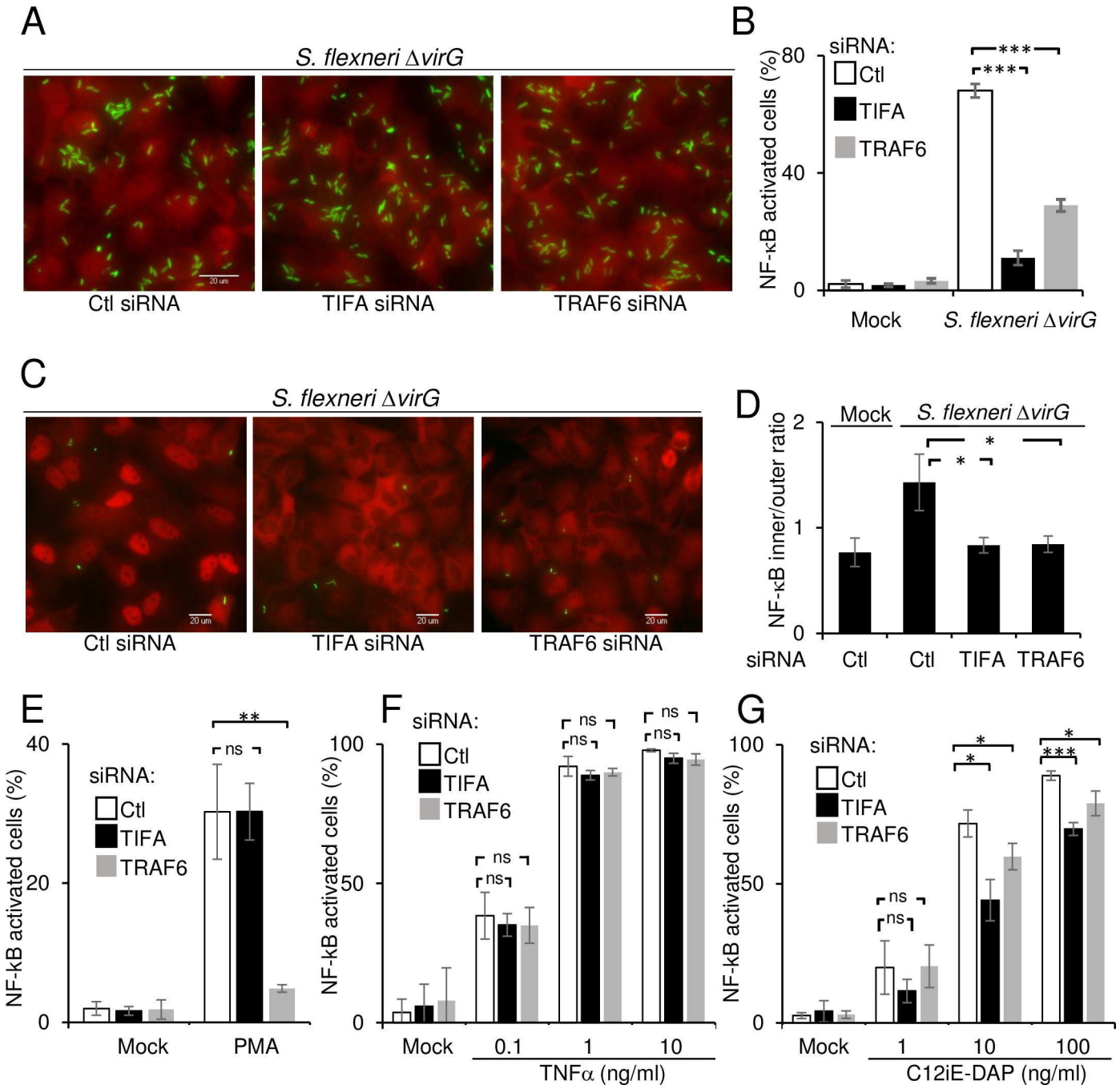

Fig 2. TIFA and TRAF6 control *S. flexneri*-induced NF-κB activation. A) TIFA and TRAF6 control *S. flexneri*-induced NF-κB activation in infected cells. HeLa cells were transfected with control, TIFA- or TRAF6-targeting siRNAs and infected with *S. flexneri* Δ*virG* (green) at MOI 20 for 60 minutes. After fixation, cells were stained for NF-κB p65 (red). **B**) Quantification of NF-κB translocation in infected cells after depletion of TIFA and TRAF6. NF-κB translocation was quantified by measuring the intensity ratio between the nucleus and the cytoplasm by automated image analysis, defining a threshold ratio and quantifying the fraction of NF-κB positive cells. Data correspond to the mean +/- SD of triplicate wells from a representative of 3 independent experiments, p***<0.0005. **C**) TIFA and TRAF6 control NF-κB activation both in infected and bystander cells. HeLa cells were treated as in A and infected at a MOI 0.5 (bacteria in green) for 60 minutes. After fixation, cells were stained for NF-κB p65 (red). **D**) Quantification of NF-κB translocation in bystander cells. The fluorescence intensity ratio between the cytoplasm and the nucleus was measured in bystander cells. Data correspond to the mean +/- SD of 3 independent experiments, p*<0.05. **E**) Impact of TIFA and TRAF6 depletion on PMA-induced NF-κB activation. After siRNA transfection, HeLa cells were stimulated with PMA (100 ng/ml) for 60 minutes. Data correspond to the mean +/- SD of 3 independent experiments, p**<0.005, ns: non-significant p>0.05. **F**) Impact of TIFA and TRAF6 depletion on TNFα-induced NF-κB activation. After siRNA transfection, HeLa cells were stimulated for 30 minutes with TNFα at the indicated concentrations. Data correspond to the mean +/- SD of 3 independent experiments, ns: non-significant p>0.05. **G**) Impact of TIFA and TRAF6 depletion on C12-iE-DAP-induced NF-κB activation. After siRNA transfection, HeLa cells were

stimulated for 60 minutes with C12-iE-DAP at the indicated concentrations. Data correspond to the mean +/- SD of 3 independent experiments, non-significant p>0.05, p*<0.05, p***<0.0005.

doi:10.1371/journal.ppat.1006224.g002

in *S. flexneri*-challenged cells after several hours (Fig 4A and 4B). TIFA oligomers were found in both infected and bystander cells, suggesting that TIFA was functionally active in both cell types during infection. A co-staining between TIFA and NF-κB p65 showed that TIFA oligomers formed as early as 15 minutes post-infection and seemed to even precede NF-κB activation as visible in some cells (Fig 4C). TIFA oligomerization was also observed following infection of the Caco-2 cell line (S3 Fig), revealing that this process is also a relevant host response to *S. flexneri* infection in human colonic cells.

The role of the FHA-pT9 interaction and TRAF6 binding in the mechanism of TIFA oligomerization was investigated in cells transfected with the different TIFA mutants. Neither the T9A nor the RKN mutant was able to form oligomers (Fig 4D), indicating that the FHA-pT9 interaction was necessary. In contrast, the E178A mutant formed oligomers (Fig 4D), demonstrating that binding to TRAF6 was not required for TIFA oligomerization. Extrapolating these data to the IL-8 rescue experiment (Fig 3B and 3C) suggests that TIFA oligomerization

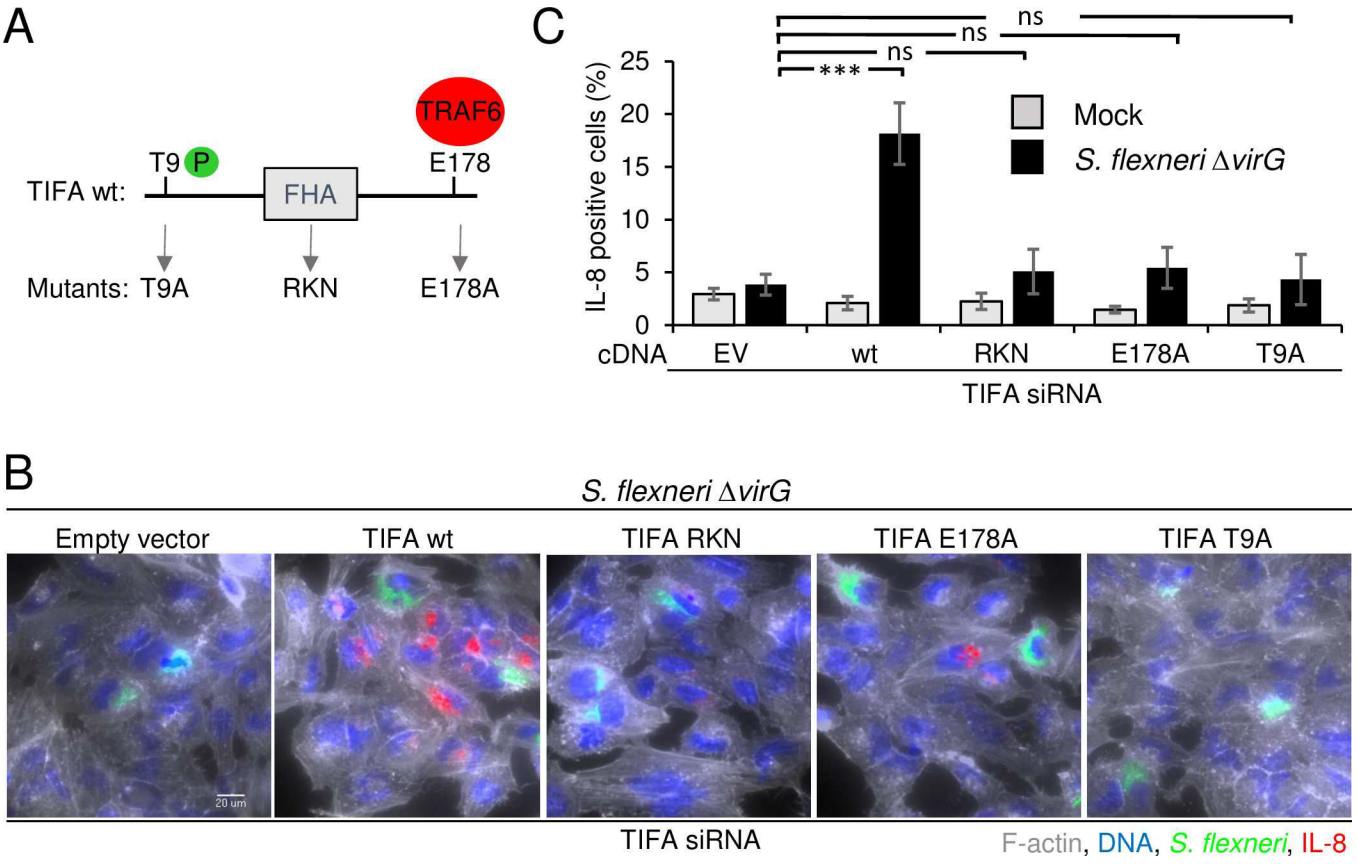

Fig 3. Residue T9, the FHA domain and residue E178 of TIFA are necessary for IL-8 expression. A) Schematic representation of wild-type TIFA and the T9, RKN and E178A TIFA mutants. **B**) Only wild-type TIFA rescues IL-8 expression after siRNA-mediated depletion of TIFA. HeLa cells were transfected for 72 hours with TIFA-targeting siRNA. 24 hours prior infection, cells were transfected with empty vector, wild-type or mutated TIFA cDNA constructs. All TIFA cDNA constructs are TIFA siRNA-resistant. Cells were infected with *S. flexneri* Δ*virG* (green) for 3.5 hours. After fixation, cells were stained for F-actin (grey), DNA (blue) and IL-8 (red). Scale bars, 20 μm. **C**) Quantification of IL-8 as shown in B. Data correspond to the mean +/- SD of 3 independent experiments, p***<0.0005, ns: non-significant p>0.05.

doi:10.1371/journal.ppat.1006224.g003

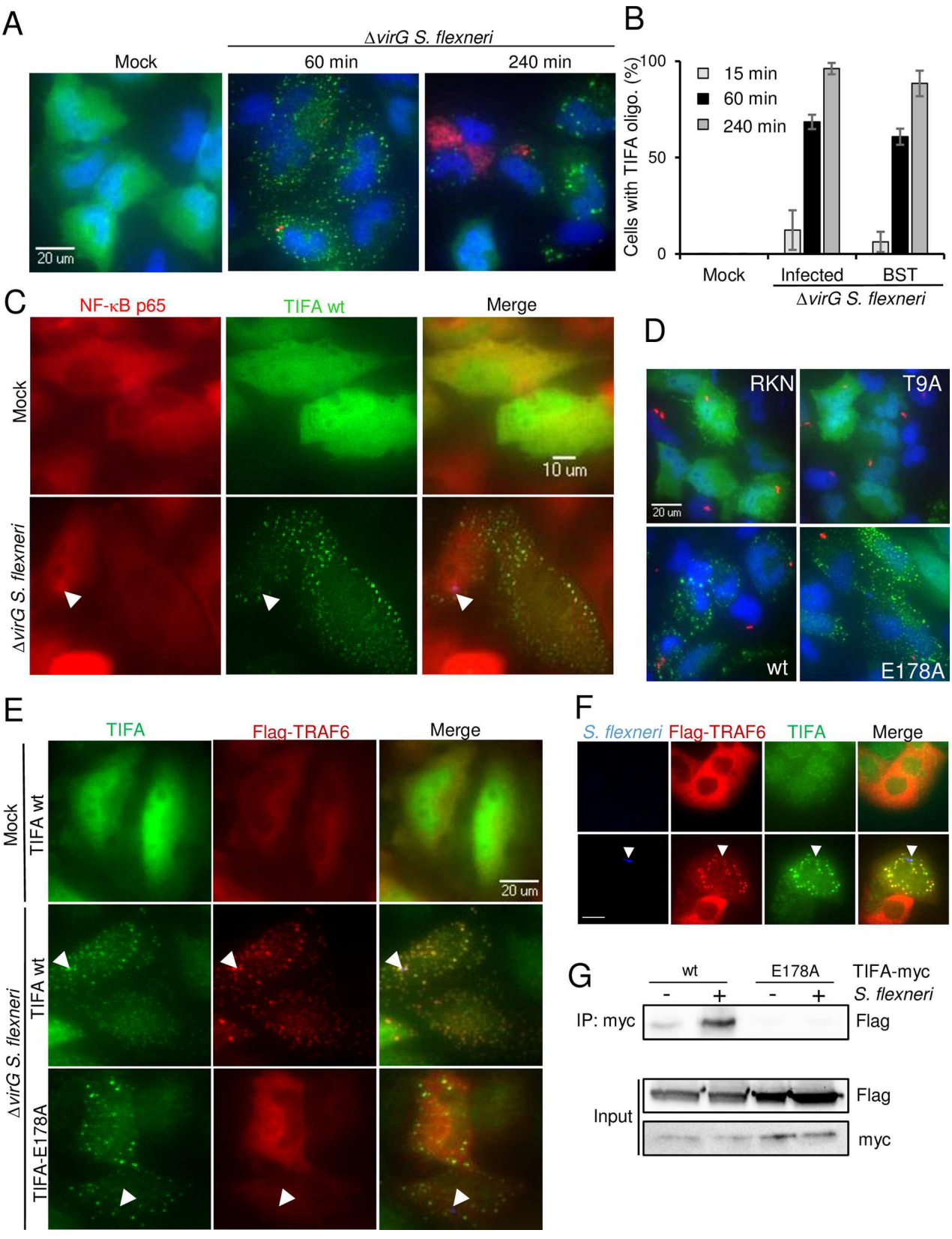
A
ΔvirG S. flexneri
Mock
60 min
240 min
20 um
B
Cells with TIFA oligo. (%)
100
50
0
15 min
60 min
240 min
Mock
Infected
BST
ΔvirG S. flexneri
C
NF-κB p65
TIFA wt
Merge
Mock
ΔvirG S. flexneri
10 um
D
RKN
T9A
20 um
wt
E178A
E
TIFA
Flag-TRAF6
Merge
Mock
TIFA wt
ΔvirG S. flexneri
TIFA wt
TIFA-E178A
20 um
F
S. flexneri Flag-TRAF6
TIFA
Merge
G
wt
E178A
TIFA-myc
S. flexneri
- + - +
IP: myc
Flag
Input
Flag
myc

Fig 4. TIFA and TRAF6 form co-localizing oligomers in infected and bystander cells. A) TIFA forms large oligomers in infected and bystander cells. HeLa cells were transfected with wild-type TIFA cDNA and infected or not with *S. flexneri* Δ*virG* (red) at MOI 0.5. Cells were stained for TIFA (green) and DNA (blue). **B**) Quantification of cells showing TIFA oligomers post infection. Cells were treated as in A. Cells showing TIFA punctuates were manually quantified for infected and bystander cells. Graph shows the mean of triplicate wells with a total of n = 130 cells per condition, data representative of 3 experiments. **C**) TIFA oligomerization occurs within minutes of infection in infected and bystander cells. HeLa cells were transfected with wt TIFA cDNA, infected or not for 15 minutes and co-stained for TIFA (green) and NF-κB p65 (red). Arrows indicate bacteria. **D**) Localization of wt, T9A, RKN and E178A TIFA mutants. Cells were transfected with wt TIFA or the different mutants, infected for 1 hour and stained as in A. Images are representative of three independent experiments. **E**) TRAF6 oligomerization is TIFA-dependent. HeLa cells were co-transfected with wild-type TIFA or E178A TIFA and Flag-TRAF6. After infection, cells were stained for TIFA (green) and Flag (red). Arrows indicate *S. flexneri*. **F**) Co-localizing TIFA and TRAF6 oligomers after *S. flexneri* infection in Caco-2 cells. Arrows indicate *S. flexneri*. Scale bars, 20 μm **G**) Co-immunoprecipitation of TIFA and TRAF6 after *S. flexneri* infection. HeLa cells were co-transfected with wt or E178A myc-TIFA and Flag-TRAF6 and infected for 1 hour at MOI 10. Myc IP was blotted with an anti-Flag antibody and the input lysate with anti-Flag and anti-myc antibodies. Data representative of two independent experiments.

doi:10.1371/journal.ppat.1006224.g004

and binding to TRAF6 are both required to induce IL-8 expression after *S. flexneri* infection. These results further suggested that, in line with published data on TNFα signaling [27], TIFA also induces the oligomerization of TRAF6 and the subsequent activation of NF-κB following *S. flexneri* infection. This hypothesis was tested by determining whether TIFA and TRAF6 co-localized after infection. The localization of both proteins was first visualized in *S. flexneri*-infected HeLa cells co-transfected with TIFA-myc and TRAF6-Flag cDNA constructs. As shown in Fig 4E, TRAF6 was also found in punctate structures both in infected and bystander cells. Furthermore, these structures were perfectly co-localized with TIFA oligomers. The same result was obtained upon infection of Caco-2 cells (Fig 4F). Interestingly, the E178A TIFA mutant that is unable to bind TRAF6 did not co-localize with TRAF6 (Fig 4E). The absence of TRAF6 oligomers in these cells showed that the formation of these structures was dependent on the ability of TIFA to bind TRAF6. The interaction between TIFA and TRAF6 was further addressed by co-immunoprecipitation in cells transfected with TIFA-myc and TRAF6-Flag (Fig 4G). A weak signal was detected in uninfected cells showing some TIFA-TRAF6 interaction under basal conditions whereas their interaction was strongly enhanced upon *S. flexneri* infection. As expected, this interaction was not observed when cells were transfected with the E178A TIFA mutant (Fig 4G), confirming that TIFA and TRAF6 interact in a TIFA E178-dependent manner. Altogether, these results show that *S. flexneri* infection induces the formation of co-localizing TIFA and TRAF6 oligomers and that the TIFA-TRAF6 interaction depends on E178 of TIFA.

TIFA/TRAF6-dependent innate immunity is triggered by HBP in *S. flexneri* and S. *typhimurium* infection

To elucidate the mechanism triggering the activation of the TIFA/TRAF6 pathway, we tested whether TIFA was also involved in the induction of the IL-8 response observed after *Listeria monocytogenes* and *Salmonella typhimurium* infections. Like *S. flexneri*, these two enteroinvasive bacteria induce the secretion of the inflammatory cytokine IL-8. In both cases, IL-8 expression is potentiated via cell-cell communication between adjacent epithelial cells [13]. Depletion of neither TIFA nor TRAF6 had an impact on *L. monocytogenes*-induced IL-8 production (Fig 5A) and TIFA failed to form oligomers after infection (Fig 5B). In contrast, the depletion of either TIFA or TRAF6 abolished IL-8 expression after *S. typhimurium* infection (Fig 5C), while TIFA formed oligomers in both infected and bystander cells (Fig 5B). Since *S. flexneri* and *S. typhimurium* are both gram-negative, these results suggested that TIFA/TRAF6-dependent IL-8 expression was specifically triggered during gram-negative bacterial infections. We hypothesized that this innate immune response was induced by the recognition of HBP, a recently identified PAMP present in gram-negative bacteria [28]. HBP is a phosphorylated metabolic intermediate of lipopolysaccharide biosynthesis, produced from D-glycero-D-manno-heptose-7-phosphate

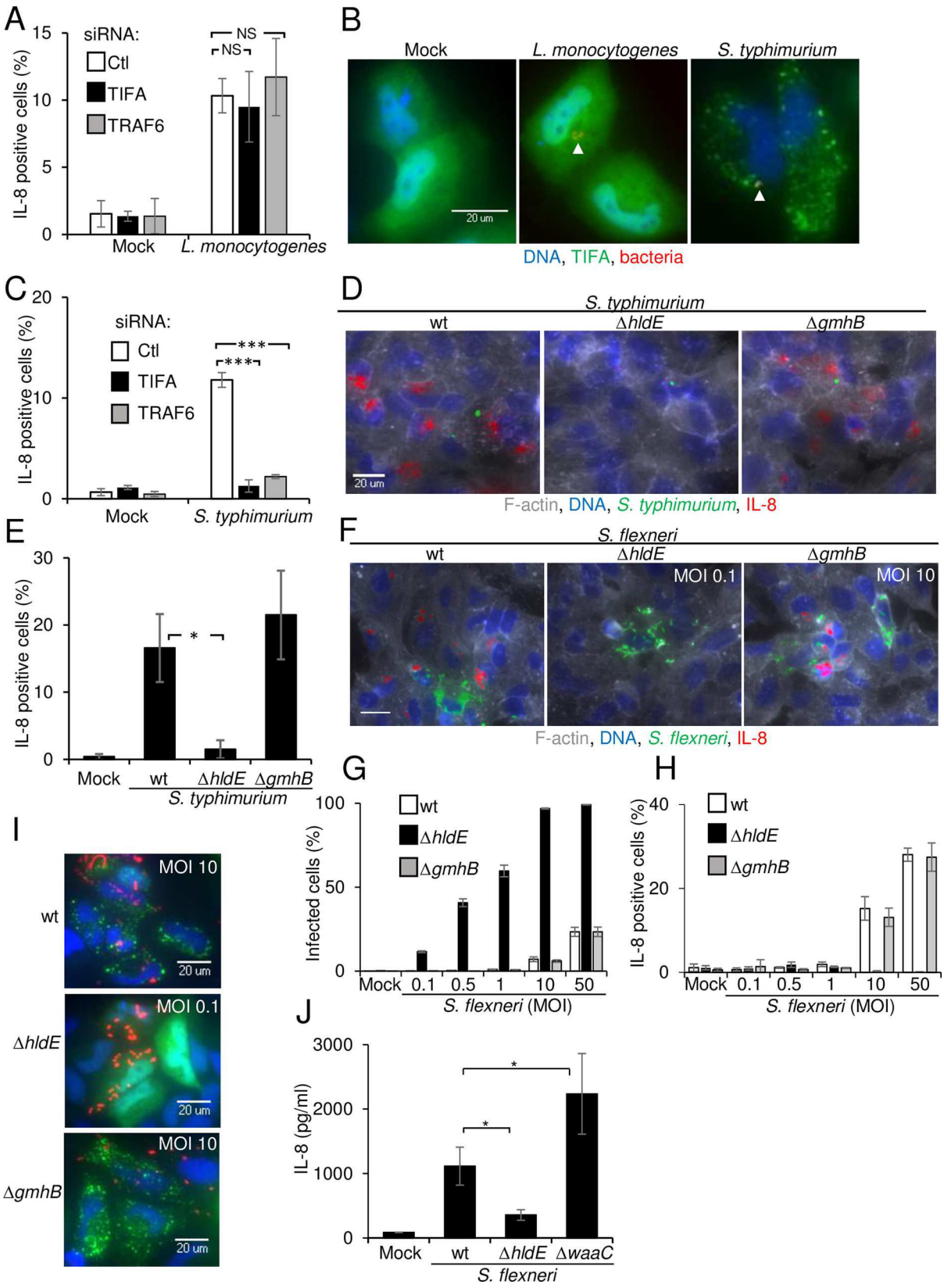
A
siRNA:
Ctl
TIFA
TRAF6
IL-8 positive cells (%)
NS
NS
Mock
L. monocytogenes
B
Mock
L. monocytogenes
S. typhimurium
20 um
DNA, TIFA, bacteria
C
siRNA:
Ctl
TIFA
TRAF6
IL-8 positive cells (%)
***
***
Mock
S. typhimurium
D
S. typhimurium
wt
ΔhldE
ΔgmhB
20 um
F-actin, DNA, S. typhimurium, IL-8
E
IL-8 positive cells (%)
*
Mock
wt
ΔhldE
ΔgmhB
S. typhimurium
F
S. flexneri
wt
ΔhldE
ΔgmhB
MOI 0.1
MOI 10
F-actin, DNA, S. flexneri, IL-8
G
wt
ΔhldE
ΔgmhB
Infected cells (%)
Mock
0.1
0.5
1
10
50
S. flexneri (MOI)
H
wt
ΔhldE
ΔgmhB
IL-8 positive cells (%)
Mock
0.1
0.5
1
10
50
S. flexneri (MOI)
I
wt
ΔhldE
ΔgmhB
MOI 10
MOI 0.1
MOI 10
20 um
J
IL-8 (pg/ml)
*
*
Mock
wt
ΔhldE
ΔwaaC
S. flexneri

Fig 5. Sensing of HBP triggers TIFA/TRAF6-dependent innate immunity. A) TIFA and TRAF6 are not involved in *L. monocytogenes*-induced IL-8 production. Cells were transfected with control, TIFA- or TRAF6-targeting siRNAs, infected with *L. monocytogenes* for 3.5 hours and stained for IL-8. Data show the mean +/- SD of 3 independent experiments, ns: p>0.05. **B**) *S. typhimurium* infection induces TIFA oligomers. Hela cells were transfected with wild-type TIFA cDNA, infected with *L. monocytogenes* or *S. typhimurium* for 45 minutes and stained for TIFA (green) and DNA (blue). Arrows indicate bacteria (red). **C**) TIFA and TRAF6 are involved in IL-8 expression after *S. typhimurium* infection. Cells were transfected as in A, infected with *S. typhimurium* for 3.5 hours and stained for IL-8. Data show the mean +/- SD of 3 independent experiments, p***<0.0005. **D**) HBP is required for IL-8 induction after *S. typhimurium* infection. Cells were infected with wt, Δ*hldE* or Δ*gmhB S. typhimurium* (green) and stained for IL-8 (red), F-actin (grey) and DNA (blue). **E**) Quantification of IL-8 after infection with wt, Δ*hldE* or Δ*gmhB S. typhimurium*. Data show the mean +/- SD of 3 independent experiments, p*<0.05. **F**) HBP is required for IL-8 expression after *S. flexneri* infection. Cells were infected with wt, Δ*hldE* or Δ*gmhB S. flexneri* (green) and stained as in D. Scale bars, 20 μm. **G**) Comparison of the infection rates after infection with wt, Δ*hldE* or Δ*gmhB S. flexneri* at multiple MOIs. Data show the mean +/- SD of triplicate wells, graph representative of 3 independent experiments. **H**) Quantification of IL-8 after infection with wt, Δ*hldE* or Δ*gmhB S. flexneri*. Data show the mean +/- SD of triplicate wells, graph representative of 3 independent experiments. **I**) TIFA oligomerization is HBP-dependent. Cells were transfected with TIFA cDNA and infected with wt, Δ*hldE* or Δ*gmhB S. flexneri* (red). Cells were stained for TIFA (green) and DNA (blue). **J**) IL-8 secretion of *S. flexneri*-infected Caco-2 cells is largely HBP-dependent. ELISA assay measuring the secretion of IL-8 after infection of Caco-2 cells. Cells were infected for 6 hours with wt (MOI 400), Δ*hldE* (MOI 4) or Δ*waaC* (MOI 4) *S. flexneri*. Data correspond to the mean +/- SD of 3 independent experiments, p*<0.05.

doi:10.1371/journal.ppat.1006224.g005

by the HldE enzyme [28] (S4A Fig). The role of HBP in the induction of IL-8 expression was directly tested by measuring IL-8 production in response to infection with a *S. typhimurium* mutant deleted for the *hldE* gene (Δ*hldE*) and which expressed the dsRed protein under the *uhpT* promoter. Data showed that infection with the Δ*hldE* mutant, which is unable to synthesize HBP, failed to induce IL-8 production both in infected and bystander cells (Fig 5D and 5E). As expected, infection with bacteria deficient for the enzymes GmhB (Δ*gmhB*) or WaaC (Δ*waaC*), which act downstream of HldE in the ADP heptose biosynthetic pathway [30] (S4A Fig), induced strong IL-8 expression (Fig 5D and 5E, S4B Fig). The same experiment was repeated with *S. flexneri* mutants. Interestingly, the Δ*hldE* and Δ*waaC* mutants were dramatically more invasive than wild-type or Δ*gmhB* bacteria (Fig 5G and S4C Fig). However, at all multiplicities of infection tested, the absence of HBP led to a complete inhibition of IL-8 expression (Fig 5F and 5H). As with *S. typhimurium*, the Δ*gmhB* and Δ*waac* mutants induced massive IL-8 expression, indicating that the expression of IL-8 was dependent on bacterial synthesis of HBP (Fig 5F and 5H, S4D Fig). In addition, infection with the *S. flexneri* and *S. typhimurium* Δ*hldE* mutants failed to induce the oligomerization of TIFA (Fig 5I, S5A and S5B Fig). Finally, multiplex cytokine analysis showed that *S. flexneri* infection of HeLa cells induced the secretion of IL-6, IL-1β, IFNγ, IL-8 and TNFα in an HBP-dependent manner (S6A Fig). Furthermore, the induction of IL-8 and TNFα observed in Caco-2 cells after *S. flexneri* infection was also largely dependent on HBP (Fig 5J and S6B Fig). Altogether, these results show a causal link between HBP, the oligomerization of TIFA/TRAF6, the activation of NF-κB and inflammatory cytokine expression. They also show for the first time, that HBP is a critical PAMP that triggers inflammation in epithelial cells during infection by at least two invasive gram-negative pathogens, S. *typhimurium* and *S. flexneri*.

ALPK1 controls *S. flexneri* infection-induced cytokine expression and TIFA oligomerization

The observation that TIFA oligomerization was dependent on T9 and the FHA domain of TIFA suggested that at least one kinase was involved upstream of TIFA to control IL-8 expression. In order to identify kinase candidates, an RNAi screen targeting each gene of the human kinome with three individual siRNAs, was performed. TAK1, known to be involved in *S. flexneri*-induced NF-κB activation downstream of TRAF6 and RIPK2 [8], was the strongest negative hit (S2 Table, Fig 6A). We tested whether this kinase could also control TIFA oligomerization during infection. Although depleting TAK1 completely abrogated IL-8 production (Fig 6A and 6B, S2 Table),

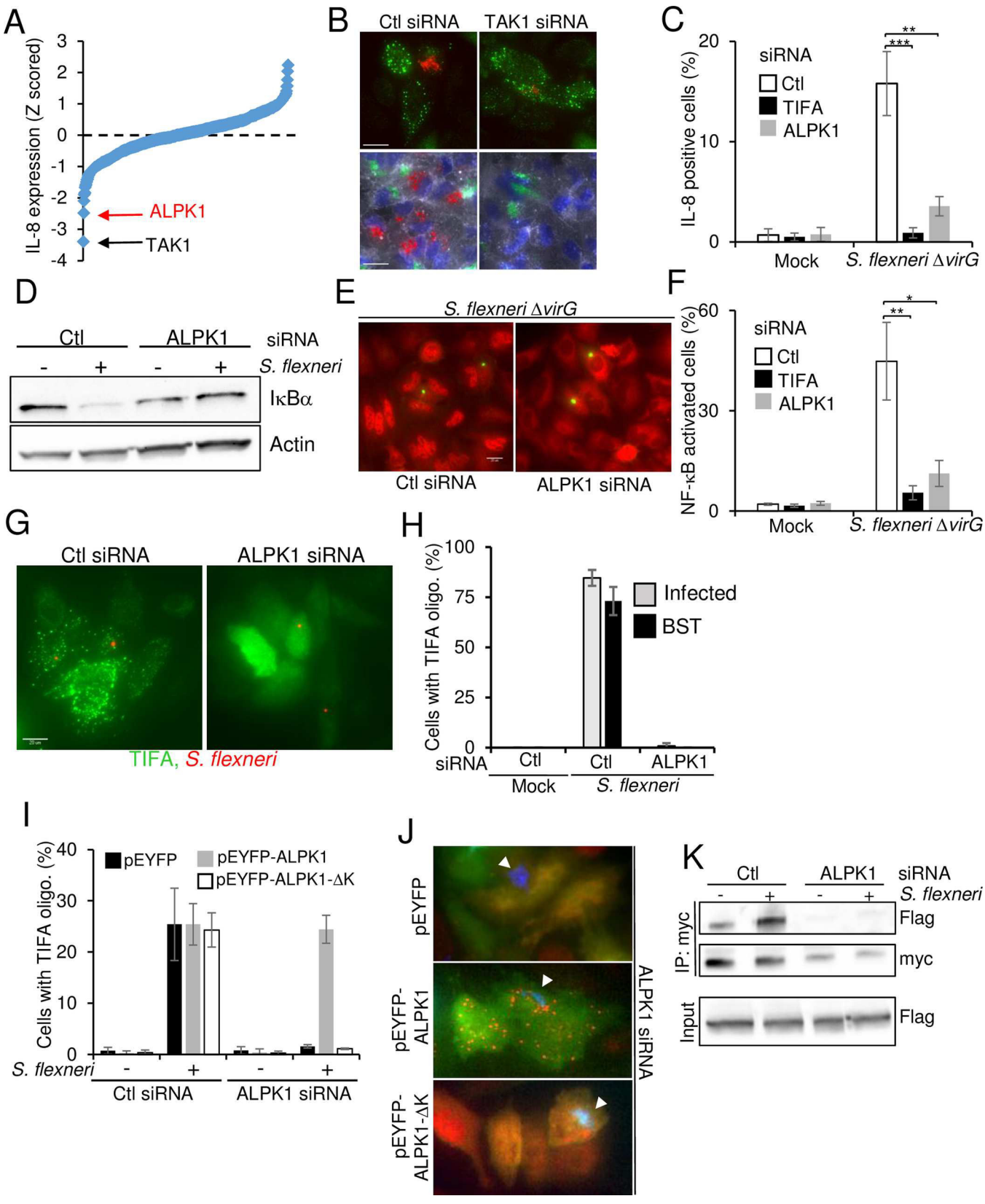
A
IL-8 expression (Z scored)
ALPK1
TAK1
B
Ctl siRNA
TAK1 siRNA
C
IL-8 positive cells (%)
siRNA
Ctl
TIFA
ALPK1
Mock
S. flexneri ΔvirG
D
Ctl
ALPK1
siRNA
S. flexneri
IκBα
Actin
E
S. flexneri ΔvirG
Ctl siRNA
ALPK1 siRNA
F
NF-κB activated cells (%)
G
Ctl siRNA
ALPK1 siRNA
TIFA, S. flexneri
H
Cells with TIFA oligo. (%)
Infected
BST
siRNA
Ctl
ALPK1
Mock
S. flexneri
I
Cells with TIFA oligo. (%)
pEYFP
pEYFP-ALPK1
pEYFP-ALPK1-ΔK
S. flexneri
Ctl siRNA
ALPK1 siRNA
J
pEYFP
pEYFP-ALPK1
pEYFP-ALPK1-ΔK
ALPK1 siRNA
K
Ctl
ALPK1
siRNA
S. flexneri
IP: myc
Flag
myc
Input
Flag

Fig 6. ALPK1 controls TIFA-mediated innate immunity during infection with invasive bacteria. A) Kinome RNAi screening data of IL-8 expression after *S. flexneri* infection in HeLa cells. IL-8 measurements were extracted with CellProfiler, Z-scored and ranked. **B**) Silencing TAK1 prevents *S. flexneri*-induced IL-8 expression but not TIFA oligomerization. Top panels show TIFA in green and *S. flexneri* in red. Bottom panels show F-actin in grey, DNA in blue, IL-8 in red and *S. flexneri* in green. Scale bars, 20 μm. **C**) Silencing ALPK1 inhibits IL-8 expression induced by *S. flexneri* infection. Cells were transfected with control, TIFA and ALPK1-targeting siRNAs, infected and stained for IL-8. Data correspond to the mean +/- SD of three independent experiments, p**<0.005, p***<0.0005. **D**) Silencing ALPK1 inhibits *S. flexneri*-induced IκBα degradation. Lysates of control or infected cells were blotted with IκBα or actin antibodies. **E**) ALPK1 depletion inhibits *S. flexneri*-induced NF-κB activation. Cells were transfected with control and ALPK1-targeting siRNAs, infected with *S. flexneri* Δ*virG* (green) and stained for NF-κB p65 (red). Scale bars, 20 μm. **F**) Silencing ALPK1 inhibits NF-κB activation induced by *S. flexneri* infection. Cells were transfected as in E, infected for 1h and stained for NF-κB p65. Cells showing NF-κB nuclear translocation were quantified. Data show the mean +/- SD of 3 independent experiments, p**<0.005, p*<0.05. **G**) Silencing ALPK1 prevents the formation of TIFA oligomers. Cells were transfected as in E and with wt TIFA cDNA. After infection (*S. flexneri* in red) for 45 minutes, cells were stained for TIFA (green). **H**) Impact of ALPK1 depletion on the formation of TIFA oligomers. Cells were treated as in G. Cells showing TIFA punctuates were manually quantified (n = 130 cells per condition), BST: bystander. Data show the mean +/- SD of triplicate wells, graph representative of 3 independent experiments. **I**) Only full length ALPK1 rescues TIFA oligomerization in ALPK1-depleted cells. Cells were transfected with control or ALPK1 siRNAs and then with pEYFP, pEYFP-ALPK1 or pEYFP-ALPK1-ΔK cDNA constructs. The fraction of cells showing TIFA oligomers was manually quantified (n>180 cells). Data show the mean +/- SD of three independent experiments. **J**) Images illustrating the oligomerization of TIFA in the rescue experiment as described in I. TIFA is show in red, YFP-ALPK1 in green and *S. flexneri* in blue. Arrows indicate bacteria. **K**) ALPK1 controls the TIFA-TRAF6 interaction. Co-immunoprecipitation of TIFA-myc after *S. flexneri* infection. HeLa cells were transfected with control or ALPK1 siRNAs and with myc-TIFA and Flag-TRAF6. They were then infected for 1 hour at MOI 10. Myc IPs were blotted with anti-Flag and anti-myc antibodies and input lysates with an anti-Flag antibody.

doi:10.1371/journal.ppat.1006224.g006

TIFA oligomers were still visible in infected and bystander cells (Fig 6B), confirming that TAK1 was implicated downstream of TIFA. The second strongest hit was ALPK1. ALPK1 belongs to the atypical kinase group [31] and is poorly characterized. It is a component in apical transport of epithelial cells [32]. Furthermore, polymorphism in the *alpk1* gene is associated with type 2 diabetes, dyslipidemia, gout and chronic kidney disease [33–36]. Strikingly, the *alpk1* and *tifa* genes are direct neighbors on human chromosome 4 [37], suggesting that they may be co-regulated and part of a common cellular pathway. ALPK1 was thus further investigated for its implication in *S. flexneri* infection and TIFA-dependent innate immunity. First, the role of ALPK1 in IL-8 production after *S. flexneri* infection was confirmed by intracellular IL-8 staining (Fig 6C) and ELISA (S7A Fig). The secretion of IL-6, IL-1β, IFNγ and TNFα was reduced in ALPK1-depleted cells (S7B Fig), showing that ALPK1 is a master regulator of *S. flexneri*-induced inflammatory cytokine expression, a process largely triggered in response to HBP (S6A Fig). Since TIFA and TRAF6 regulated *S. flexneri*-induced NF-κB activation, we investigated the role of ALPK1 in this process. Western blot experiments performed on uninfected and infected cells revealed that depleting ALPK1 reduced the degradation of the inhibitor of NF-κB, IκBα, in infected cells (Fig 6D). In agreement, ALPK1 depletion also impaired the nuclear translocation of NF-κB after *S. flexneri* infection without significantly affecting bacterial entry (Fig 6E and 6F and S2 Fig). Altogether, these results suggested that ALPK1 was a promising candidate for the control of TIFA-dependent innate immunity. The role of ALPK1 in this process was directly addressed by several means. First, depletion of ALPK1 prevented the formation of TIFA oligomers both in infected and bystander cells during *S. flexneri* infection (Fig 6G and 6H). Second, in rescue experiments, whereby cells were transfected with control or ALPK1 siRNA and then transfected with the empty vector pEYFP or a siRNA-resistant full-length ALPK1-YFP cDNA construct (Fig 6I and 6J), overexpression of YFP-ALPK1 did not induce the formation of TIFA oligomers in the absence of infection, indicating that this process was tightly regulated. Notably, when ALPK1-depleted cells were transfected with full-length YFP-ALPK1, TIFA oligomerization was restored in a large fraction of infected and bystander cells. This result excluded the possible contribution of RNAi off target effects and unambiguously established the role of ALPK1 in *S. flexneri*-induced TIFA oligomerization. Interestingly, transfection of a siRNA-resistant cDNA construct deleted for the kinase domain of ALPK1 (YFP-ALPK1-ΔK) failed to rescue TIFA oligomerization (Fig 6I and 6J), showing that the kinase domain of ALPK1 was necessary for the induction of TIFA oligomerization after *S. flexneri* infection. Finally, the role of ALPK1 on the TIFA-TRAF6 interaction

was investigated by co-immunoprecipitation experiments. Data showed that the TIFA-TRAF6 interaction induced upon *S. flexneri* infection was strongly reduced in ALPK1-depleted cells, demonstrating that this interaction was ALPK1-dependant (Fig 6K). Altogether, these results showed that ALPK1 is a master regulator of cytokine expression during *S. flexneri* infection and that TIFA oligomerization depends on the kinase domain of ALPK1.

ALPK1 is a master regulator of HBP-induced innate immunity

As *S. flexneri*-induced TIFA oligomerization occurred in response to HBP (Fig 5I), we tested whether ALPK1 was involved in this process. Cells were stimulated with lysates from *S. flexneri* containing an empty pUC19 vector or expressing the HBP-synthesizing enzyme HldA from *N. meningitidis* [28]. As expected, the lysate from HldA-overexpressing bacteria was more potent at inducing IL-8 expression than those of wild-type bacteria (Fig 7A and 7B). Interestingly, depletion of ALPK1 prevented the oligomerization of TIFA (Fig 7C) as well as IL-8 production (Fig 7A and 7B) in response to both lysates, showing that ALPK1 controlled the oligomerization of TIFA following HBP recognition. As with TIFA, depletion of ALPK1 failed to inhibit IL-8 expression and NF-κB activation observed after *L. monocytogenes* infection (S8A and S8B Fig), suggesting a specific implication in infection by invasive gram-negative bacteria. Furthermore, ALPK1 was not required to activate NF-κB in response to PMA (S9A Fig) or TNFα (S9B Fig). As with TIFA and TRAF6, depleting ALPK1 had a moderate but significant effect on C12-iE-DAP-induced NF-κB activation (S9C Fig). The role of ALPK1 was further characterized in the inflammatory response triggered by *Neisseria meningitidis*, an important gram-negative extracellular human pathogen. This bacterium is responsible for meningitis and other forms of meningococcal diseases including meningococcemia, a case of life-threatening sepsis [38]. Upon infection with this pathogen, HBP can be secreted or released by lysing bacteria [28]. We confirmed that treating HeLa cells with *N. meningitidis* lysate induced TIFA oligomerization (Fig 7D and 7E) and IL-8 expression (Fig 7F). Furthermore, depleting either TIFA or TRAF6 prevented IL-8 expression (Fig F). Interestingly, we found that TIFA oligomerization and IL-8 expression were both completely abrogated in ALPK1-depleted cells (Fig 7D, 7E and 7F), showing that ALPK1 also controls the innate immune response to *N. meningitidis* infection (Fig 7G). Altogether, these results show that HBP is a key bacterial PAMP sensed by epithelial cells during infection by both invasive and extracellular gram-negative bacteria and that TIFA/TRAF6-dependent innate immunity against HBP is controlled by ALPK1.

Discussion

An RNAi screen implicated TIFA and TRAF6 in the control of IL-8 expression after *S. flexneri* infection. We show that these two proteins act upstream of NF-κB p65 activation in infected and bystander cells. In particular, we provide evidence demonstrating that *S. flexneri* induces the oligomerization of TIFA and TRAF6 in infected and bystander cells in a FHA/T9-dependent manner. In cells expressing a TIFA mutant unable to bind TRAF6, the formation of TRAF6 oligomers was not observed, showing that the TIFA-TRAF6 interaction is necessary to trigger TRAF6 oligomerization. Given that TRAF6 oligomerization has been shown to increase its E3 ubiquitin ligase activity [39], our data suggest that TIFA works as an adaptor protein promoting TRAF6 oligomerization and thereby NF-κB activation and inflammatory gene expression (Fig 7G). In infected and bystander cells, TIFA oligomers are distributed evenly throughout the cytoplasm. They appear within minutes of infection and are still visible four hours post infection. Co-staining of TIFA and lysosomal-associated membrane protein 1 (LAMP1) in *S. flexneri*-infected cells revealed that TIFA/TRAF6 oligomers are not localized to

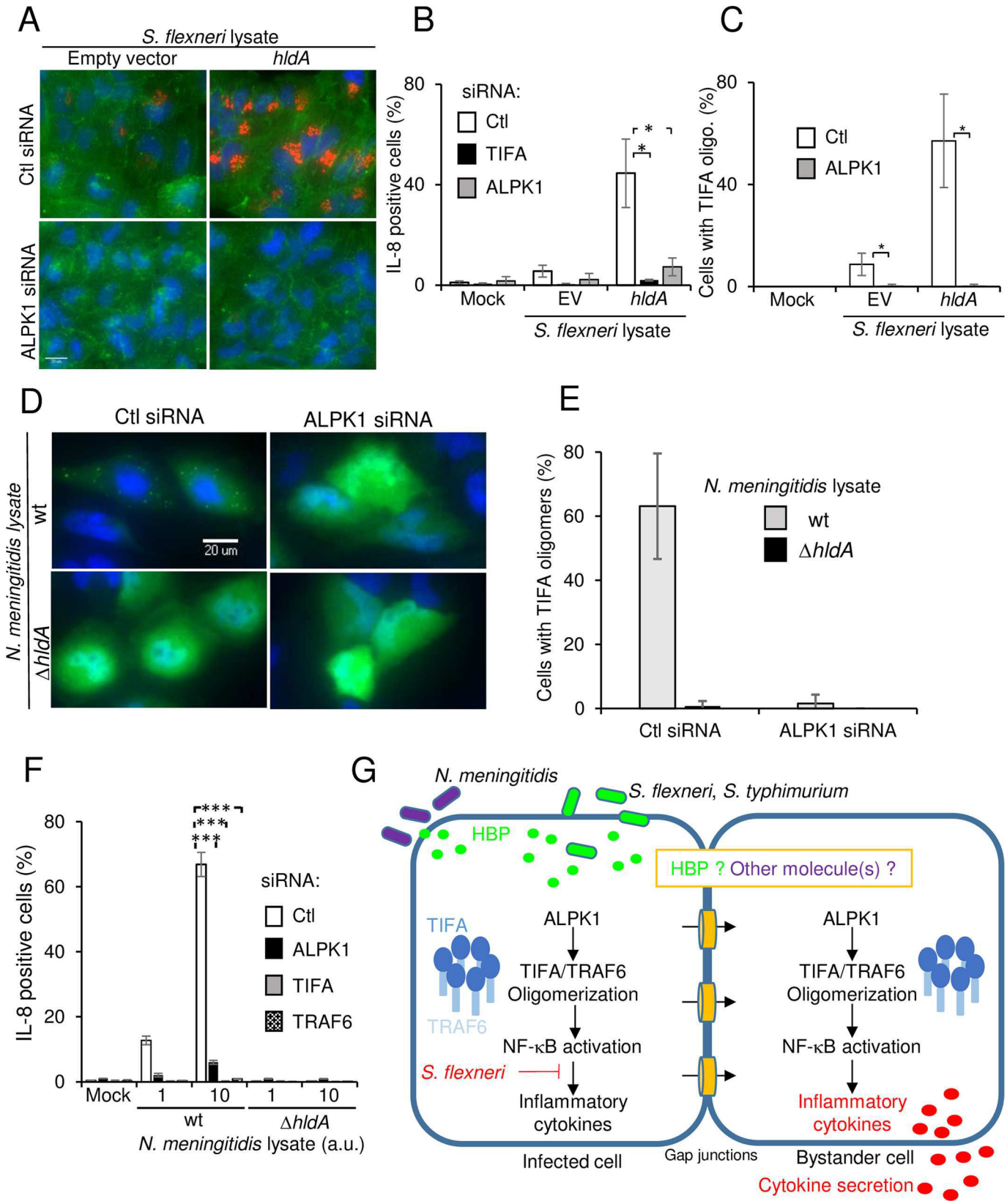
A
S. flexneri lysate
Empty vector
hldA
Ctl siRNA
ALPK1 siRNA
B
IL-8 positive cells (%)
siRNA:
Ctl
TIFA
ALPK1
Mock
EV
hldA
S. flexneri lysate
C
Cells with TIFA oligo. (%)
Ctl
ALPK1
Mock
EV
hldA
S. flexneri lysate
D
Ctl siRNA
ALPK1 siRNA
N. meningitidis lysate
wt
ΔhldA
20 um
E
Cells with TIFA oligomers (%)
N. meningitidis lysate
wt
ΔhldA
Ctl siRNA
ALPK1 siRNA
F
IL-8 positive cells (%)
siRNA:
Ctl
ALPK1
TIFA
TRAF6
Mock
1
10
1
10
wt
ΔhldA
N. meningitidis lysate (a.u.)
G
N. meningitidis
S. flexneri, S. typhimurium
HBP
HBP ? Other molecule(s) ?
TIFA
TRAF6
ALPK1
TIFA/TRAF6
Oligomerization
NF-κB activation
S. flexneri
Inflammatory
cytokines
Infected cell
Gap junctions
Bystander cell
Cytokine secretion

Fig 7. ALPK1 is a master regulator of HBP-induced innate immunity. A) ALPK1 controls IL-8 expression and the formation of TIFA oligomers induced by HBP. Cells were transfected with control or ALPK1 siRNAs and incubated with lysates from *S. flexneri* containing pUC19 empty vector (EV) or expressing *hldA* from pUC19. They were stained for IL-8 (red), F-actin (green) and DNA (blue). Scale bars, 20 μm. **B**) Quantification of data shown in F. Data show the mean +/- SD of 3 independent experiments, p*<0.05. **C**) Silencing ALPK1 prevents HBP-induced TIFA oligomerization. Cells were transfected as in A and with wt TIFA. After incubation with lysates from *S. flexneri* containing pUC19 or pUC19-*hldA*, cells were stained for TIFA. Cells showing TIFA punctuates were manually quantitated (n = 105 cells per condition). Data show the mean +/- SD of 3 independent experiments, p*<0.05. **D**) Silencing ALPK1 abrogates the formation of TIFA oligomers induced by *N. meningitidis* HBP. HeLa cells were transfected with control or ALPK1-targeting siRNA and then with wt TIFA cDNA. After incubation with lysates from wt or Δ*hldA N. meningitidis*, cells were stained for TIFA (green) and DNA (blue). **E**) Impact of ALPK1 depletion on TIFA oligomerization. Cells were treated as in D. The fraction of cells showing TIFA punctuates was manually quantitated with n = 130 cells per condition. Data show the mean +/- SD of triplicate wells and the graph is a representative of 3 independent experiments. **F**) Silencing ALPK1 abrogates the production of IL-8 induced by *N. meningitidis* lysates. Cells were transfected with control, TIFA, TRAF6 or ALPK1-targeting siRNA. Cells were then incubated with lysates from wt or Δ*hldA N. meningitidis* and stained for IL-8. Data show the mean +/- SD of triplicate well and the graph is a representative of 3 independent experiments, p***<0.0005. **G**) Schematic illustration of the ALPK1/TIFA/TRAF6 pathway controlling IL-8 expression after infection by gram-negative bacteria.

doi:10.1371/journal.ppat.1006224.g007

lysosomes (S10 Fig). More work is needed to determine whether these aggregation platforms are associated with other subcellular structures or whether they freely diffuse in cells.

We show that during *S. flexneri* and *S. typhimurium* infection, the TIFA/TRAF6 pathway is activated in response to the bacterial monosaccharide HBP, present in gram-negative bacteria. Indeed, we found that the Δ*hldE* mutants of *S. flexneri* and *S. typhimurium*, which are unable to synthesize HBP, fail to induce the oligomerization of TIFA and the production of IL-8. These results open up a new avenue to understand the molecular processes controlling inflammation in bacterial infection and highlight the central role of HBP during infection by invasive bacteria. In contrast to the study by Gaudet *et al.* [28], the production of IL-8 in response to *S. flexneri* and *S. typhimurium* infection is unlikely due to the simple mechanism of HBP endocytosis. Indeed, we previously demonstrated that noninvasive *S. flexneri* bacteria failed to induce IL-8 expression [13]. This point was further confirmed by Lippmann *et al.* who showed that the expression of IL-8 in bystander cells requires bacterial internalization [21]. Mechanisms explaining how HBP could therefore be detected within minutes of bacterial invasion have to be envisioned. Although there is, to our knowledge, no evidence in the literature for the release of metabolites via type III secretion, we cannot exclude the possibility that HBP may be directly secreted into the host cytoplasm via the injectisome. An alternative mechanism would consist in the cellular uptake of HBP during the process of bacterial internalization. A study using dynamic imaging and advanced large volume correlative light electron microscopy recently reported that two distinct compartments are formed during the first step of bacterial invasion: the bacterial containing vacuole (BCV) and surrounding macropinosomes [40]. Whereas the membrane of the BCV tightly surrounds the bacterium, macropinosomes are heterogeneous in size and contain significant volumes of extracellular fluid [40]. HBP, released from residual secretion or bacterial lysis, may be engulfed by infected cells via the BCV or macropinosomes and released into the cytoplasm shortly after membrane rupture. The small molecular size of HBP (370 Da) should allow its diffusion to adjacent cells via gap junctions leading to TIFA oligomerization and IL-8 expression in bystander cells (Fig 7G). Alternatively, HBP sensing in infected cells may lead to the production of a second messenger that could diffuse to bystander cells and activate the ALPK1/TIFA/TRAF6 pathway. In the case of *S. typhimurium*, the complete rupture of the internalization vacuole is a rare event. In most cases, bacteria remain inside *Salmonella*-containing compartments. Interestingly, a recent study shows that early *Salmonella*-containing compartments are leaky and that autophagy proteins promote the repair of endosomal membranes damaged by the type III secretion system 1 [41]. In this context, HBP may leak out of these early compartments, be released into the cytoplasm of infected cells and induce IL-8 expression both in infected and bystander cells, as observed previously [13]. We showed that secretion of inflammatory cytokines after *S. flexneri* infection of epithelial cells *in*

vitro is largely HBP-dependent, which supports a central role of HBP in the control of innate immunity in *S. flexneri* infection. More work is needed to determine the exact contribution of HBP in *in vivo* infection where other PAMPs, including peptidoglycan-derived peptides and LPS, have previously been shown to play a role [4, 42].

Our results show that TIFA's activity in *S. flexneri*-induced IL-8 expression is dependent on residue T9 and the FHA domain of TIFA. As the interaction between these two features occurs once T9 is phosphorylated and is required to trigger TIFA oligomerization, we searched for a kinase acting upstream of TIFA oligomerization in bacterial infection. We identified the kinase ALPK1 in a human kinome RNAi screen. Strikingly, the genes coding for ALPK1 and TIFA are immediate neighbors on human chromosome 4 [37]. Gene neighborhood is conserved across several species including coelacanth, xenopus, chicken and mouse, suggesting that both genes may be co-regulated and the encoded proteins part of a same cellular pathway. We show that depleting ALPK1 strongly reduced NF-κB activation and the production of several cytokines including IL-8, TNFα, IL-1β, IFNγ and IL-6 after *S. flexneri* infection. IL-8 production was also reduced after *S. typhimurium* infection. ALPK1 depletion completely prevented the formation of TIFA oligomers after *S. flexneri* infection, a process triggered in response to HBP sensing. TIFA oligomerization was restored by overexpressing a siRNA-resistant full length ALPK1 construct. In contrast, overexpressing a construct deleted of the kinase domain of ALPK1 failed to do so, showing that the kinase domain of ALPK1 is essential for the regulation of TIFA oligomerization. In addition, co-immunoprecipitation experiments revealed that the TIFA-TRAF6 interaction is dependent on ALPK1. All these results demonstrate that ALPK1 is involved in the early signaling cascade controlling inflammation following cellular invasion by gram-negative bacterial pathogens. Furthermore, we show that ALPK1 is also implicated in the control of inflammation after stimulation with *N. meningitidis* lysates, indicating that this kinase acts as a master regulator of innate immunity to both invasive and extracellular gram-negative bacteria. ALPK1 is an atypical kinase belonging to the α-kinase family that recognizes phosphorylation sites in the context of an alpha-helical conformation [31]. The fact that T9 is not in this environment is not sufficient to exclude that ALPK1 can directly phosphorylate TIFA. Indeed, it has been shown that members of this protein family can also phosphorylate substrates independently of a helical conformation [31]. More experiments are required to elucidate the mode of action of ALPK1 in the activation of the TIFA/TRAF6 pathway. In addition, it will be informative to determine whether HBP can directly bind to ALPK1 or whether this new bacterial PAMP binds to a yet unknown pathogen recognition receptor able to activate ALPK1 and trigger TIFA oligomerization. Interestingly, by sensing the presence of HBP, a metabolite of the LPS biosynthetic pathway, such a receptor would constitute a new specific sensor for the presence of gram-negative bacteria.

In conclusion, we show that ALPK1 is a master regulator of innate immunity against both invasive and extracellular gram-negative bacteria. This kinase acts in response to the detection of HBP to activate the TIFA/TRAF6 pathway. By regulating the expression of inflammatory cytokines, this new signaling pathway is critical to orchestrate the initial host immune response and limit bacterial dissemination within infected tissues. It may also contribute to the control of intestinal homeostasis by regulating the molecular cross-talk taking place between gram-negative bacteria of the microbiota, the intestinal epithelium and the immune system.

Materials and methods

Cell culture, transfections and cDNA constructs

HeLa (American Type Culture Collection) and HEK293 (American Type Culture Collection) cells were cultured in Dulbecco's modified Eagle's (DMEM) medium supplemented with 10%

FCS and 2 mM Glutamax-1. Caco-2 cells (American Type Culture Collection) were cultured in MEM, 20% FCS and 1% non-essential amino acids. Transfection of siRNAs was carried out using RNAiMAX (Invitrogen). HeLa cells, seeded in 96-well plates (6,000 cells/well), were reverse transfected with 20 nM siRNA according to the manufacturer's instruction. Cells were used 72 hours after transfection. siRNAs against TIFA (s40984), TRAF6 (s14389) and ALPK1 (s37074) were from Ambion and TAK1 from Dharmacon. For cDNA transfection, HeLa cells were seeded in a 96-well plate at a density of 12,500 cells/well. The next day, cells were transfected with 80 ng of plasmid using Fugene 6 (Roche) according to the manufacturer's instruction. Wild-type, T9A, E178A and the RKN TIFA cDNA constructs [27] were kindly provided by Prof. M.D. Tsai (Institute of Biological Chemistry, Academia Sinica, Taiwan). They were made TIFA siRNA (s40984) resistant by the introduction of 3 silent point mutations within the recognition site of the siRNA. Point mutations were introduced by overlapping PCR using primers TIFA_BamHI_F, TIFA_R2, TIFA_F2, TIFA_XbaI_R and TIFA_EA_XbaI_R (listed in S3 Table). The resulting PCR products were digested with BamHI and XbaI and ligated into pcDNA3. A YFP-ALPK1 construct was kindly provided by Pr R. Jacob (Marburg University, Germany). It was made siRNA (s37074)-resistant by the introduction of 5 silent point mutations at positions 761-762-763-767-768 by directed mutagenesis (Agilent Technology). A mutant deleted for the kinase domain of ALPK1 was generated by introducing a stop codon at position 3059 before the kinase domain by directed mutagenesis. All primers used in directed mutagenesis are listed in S3 Table.

For TIFA and ALPK1 rescue experiments, Hela cells were first reverse transfected with TIFA or ALPK1 siRNAs (s40984, s37074 respectively). After 48 hours, they were transfected with the different siRNA-resistant TIFA cDNA constructs or siRNA-resistant full length or kinase domain-deleted YFP-ALPK1. As a negative control, cells were transfected with the empty vectors pcDNA or pEYFP. Wild-type Flag-TRAF6 cDNA was a gift from John Kyriakis (Addgene plasmid # 21624) [43].

Bacterial strains

The M90T wild-type *Shigella flexneri* strain and the *icsA* (*virG*) deletion mutant have been previously described [44]. The *Salmonella typhimurium* 12023 strain expressing pKD46 was provided by J. Guignot (Institut Cochin, Paris, France) and the EGDe.PrfA *Listeria monocytogenes* strain stably expressing GFP [45] was provided by Prof. P. Cossart (Institut Pasteur, Paris, France). All *Shigella* and *Salmonella* strains were transformed with the pMW211 plasmid and constitutively express the dsRed protein [13]. When specifically mentioned, bacteria were alternatively transformed with a variant of pMW211 expressing dsRed under the control of the *uhpT* promoter (P*uhpT*::dsRed) [17]. For *Neisseria meningitidis*, a piliated capsulated Opc$^-$ Opa$^-$ variant of serogroup C strain 8013 named 2C43 was used. The *hldA* deficient mutant was obtained as previously described in [46].

Deletion mutants and overexpressing strains

S. flexneri M90T and *S. typhimurium* 12023 deletion mutants were generated by allelic exchange using a modified protocol of lambda red-mediated gene deletion [47]. Briefly, to obtain the *S. flexneri* M90T and *S. typhimurium hldE* (Δ*hldE*), *gmhB (*Δ*gmhB)* and *waaC* (Δ*waaC)* deletion mutants, the kanamycin cassette of the pkD4 plasmid was amplified by PCR with the primers listed in S3 Table. The purified PCR product was electroporated into the wild-type strains expressing the genes for lambda red recombination from the pKM208 (for *S. flexneri* mutants) or pKD46 (for *S. typhimurium* mutants) plasmids [48]. Recombinants were

selected on TSB or LB plates containing 50 μg ml-1 of kanamycin. Single colonies were screened by PCR.

S. flexneri M90T overexpressing the *hldA* gene from *Neisseria meningitidis* was generated as follows. The *hldA* gene was amplified by PCR from a bacterial lysate with the primers listed in S3 Table. After gel purification (Macherey-Nagel), the PCR product was digested with EcoRI and HindIII, and ligated into EcoRI/HindIII-digested pUC19 (Life Technology). The ligation product was used to transform Top10 *E. Coli*. pUC19-HldA was purified and used to electroporate *S. flexneri* M90T. As a control, *S. flexneri* M90T was also electroporated with the pUC19 empty vector.

Preparation of bacterial lysates

Bacterial lysates were prepared as described in Gaudet *et al*. [28]. Briefly, 1 OD_{600} unit of bacteria from an overnight culture was centrifuged, resuspended in 100 μl PBS and boiled for 15 mins. Bacterial debris were removed by centrifugation at 13 000 rpm for 10 mins. Supernatants were collected and protein concentration was measured by BCA assay (Interchim) for normalization. Lysates were then treated with RNAse A (10 μg/ml), DNAse I (20U) (both Roche) and proteinase K (100 μg/ml) (Sigma-Aldrich). Samples were boiled for a further 5 minutes, centrifuged and the supernatant passed through a 0.22 μm filter. Lysates were stored at -20˚C.

Infection assays and stimulations

S. flexneri, *S. typhimurium* and *L. monocytogenes* were used in exponential growth phase. *Shigella* and *Salmonella* were coated, or not, with poly-L-lysine prior to infection. Cells seeded in 96-well plates, were infected at indicated MOIs in DMEM supplemented with 10 mM Hepes and 2 mM glutamax-1. After adding bacteria, plates were centrifuged for 5 minutes and placed at 37˚C for indicated time periods. Extracellular bacteria were killed by gentamicin (100 μg/ml). For stimulation experiments, cells were incubated with PMA (Sigma), C12-iEDAP (Invivogen) and TNFα (R&D Systems) at indicated concentrations. For intracellular IL-8 measurements, monensin (50 μM) was added together with gentamycin to block IL-8 secretion. Infection and stimulation assays were stopped by 4% PFA fixation.

RNAi screens

The screening methodology has already been described [17]. Briefly, RNA interference (RNAi) directed against the human genome was achieved using the commercially available genome-wide siRNA library from Dharmacon (pools of 4 siRNAs/gene). The human kinome RNAi screen was performed with the Ambion library made of three individual siRNAs per gene. All experiments were conducted in a 384-well plate format. In addition to gene-specific siRNAs, all plates contained general siRNA controls for transfection efficiency (e.g. Kif11), positive control siRNAs known to affect inflammation after *S. flexneri* infection (TAK1, p65 NF-κB) and non-targeting siRNAs. In each experiment, 25 μl of RNAiMAX/DMEM (0.1 μl/24.9 μl) mixture was added to each well of the screening plates containing 1.6 pmol siRNA diluted in 5 μl RNase-free ddH2O. Screening plates were incubated at room temperature (RT) for 1 hour. Following incubation, 600 HeLa CCL-2 cells were added per well in a volume of 50 μl DMEM/16% FCS, resulting in a final FCS concentration of 10%. Plates were incubated at 37˚C and 5% CO2 for 72 h prior to infection. For infection, *S. flexneri* M90T Δ*virG* pCK100 (PuhpT::dsRed) were harvested in exponential growth phase and coated with 0.005% poly-L-lysine (Sigma-Aldrich). Afterwards, bacteria were washed with PBS and resuspended in assay medium (DMEM, 2 mM L-Glutamine, 10 mM HEPES). 20 μl of bacterial suspension was added to each well with a final MOI of 15. Plates were then centrifuged for 1 min at 37˚C and

incubated at 37˚C and 5% CO_2. After 30 min of infection, 75 μl were aspirated from each well and monensin (Sigma) and gentamicin (Gibco) were added to a final concentration of 66.7 μM and 66.7 μg/ml, respectively. After a total infection time of 3.5 hours, cells were fixed with 4% PFA for 10 minutes. Liquid handling was performed using the Multidrop 384 (Thermo Scientific) for dispension steps and a plate washer (ELx50-16, BioTek) for aspiration steps. For immunofluorescent staining, cells were washed with PBS using the Power Washer 384 (Tecan). Subsequently, cells were incubated with a mouse anti-human IL-8 antibody (1:300, BD Biosciences) in staining solution (0.2% saponin in PBS) for 2 hours at RT. After washing the cells with PBS, Hoechst (5 μg/ml, Invitrogen), DY-495-phalloidin (1.2 U/ml, Dyomics) and Alexa Fluor 647-coupled goat anti-mouse IgG (1:400, Invitrogen) were added and incubated for 1 hour at RT. The staining procedure was performed using the Biomek NXP Laboratory Automation Workstation (Beckman Coulter).

Microscopy was performed with Molecular Devices ImageXpress microscopes. MetaXpress plate acquisition wizard with no gain, 12 bit dynamic range, 9 sites per well in a 3×3 grid with no spacing and no overlap and laser-based focusing was used. Robotic plate handling was used to load and unload plates (Thermo Scientific). A 10X S Fluor objective with 0.45NA was used.

Data analysis was performed using the computational infrastructure described in [17]. Cell counts, rates of infection and IL-8 positive cells were quantified as described in [17]. In brief, intensity and texture features were extracted from bacterial and IL-8 images. Based on these features, cells were scored for infection and IL-8 expression using CellClassifier and supervised machine learning using a Support Vector Machine based binary classifier [49]. Measurements were normalized for plate-to-plate variations and population context dependency as described in [17].

Immunofluorescence

After fixation, cells were permeabilized in 0.1% Triton X-100 for 10 minutes, incubated in PBS supplemented with 0.5% BSA for 2 hours and then overnight at 4˚C with different combinations of primary antibodies. NF-κB p65 localization was visualized by using a mouse monoclonal anti-p65 antibody (Santa Cruz Biotechnology, USA), TIFA was visualized with a polyclonal rabbit anti-TIFA primary antibody (Sigma-Aldrich), and LAMP1 was visualized with an anti-mouse anti-LAMP1 (Abcam). Cells were then stained with Alexa 647- or Alexa 488-conjugated secondary antibodies (Invitrogen, Carlsbad, USA). DNA and F-actin were stained with Hoechst and FITC-phalloidin, respectively. The production of IL-8 was measured by immunofluorescence using an anti-human IL-8 antibody in 0.2% saponin in PBS (BD Pharmingen, San Jose, USA) 4 hours post infection.

Automated microscopy and image analysis

Images were automatically acquired with an ImageXpress Micro (Molecular devices, Sunnyvale, USA). Image analysis was performed using the custom module editor (CME) of MetaXpress. Briefly, cell nuclei were identified by the "autofind blobs" function of the CME. Nuclei were then extended by 6 pixels to define the cellular mask of each cell that was used to measure bacteria and IL-8 signals. Bacteria and IL-8 signals were both detected with the "keep marked object" function of the CME based on minimal/maximal size requirements and intensity threshold. Cells showing IL-8 signals above threshold were defined as IL-8 positive. Quantification of NF-κB activation was performed with the "translocation enhanced" module of MetaXpress (Molecular Devices, USA) that automatically identifies the nuclei and cytoplasmic compartments from a Hoechst image. Quantification was done by measuring the intensity ratio of p65 in the nucleus and the cytoplasm in several thousand cells per well and in three

wells per condition. Cells showing nuclear/cytoplasmic p65 intensity ratio above a threshold ratio were defined as NF-κB positive cells.

Cell lysis, immunoprecipitation and immunoblotting

Cells were plated in 6-well plates (180 000 cells/well), transfected or not with 20 nM siRNA and/or 2.4 μg cDNA and infected according to the experiment. After infection, cells were washed twice in ice cold PBS with gentamicin (100 μg/ml), lysed in RIPA buffer supplemented with inhibitors of proteases (Promega) and phosphatases (Thermofisher Scientific), incubated on ice for 30 minutes and subsequently centrifuged at 4˚C for 30 minutes at 16,000g. The BCA Protein Assay kit (Interchim) was used to determine protein concentration. 15–20 ug of protein was subjected to SDS-polyacrylamide gels and electroblotted onto nitrocellulose membranes. For immunoprecipitation (IP), cell lysates were incubated with an anti-myc antibody (9E10, Santa Cruz) overnight. Protein A/G-coated beads (ThermoFisher) were then added for 2 hours and washed six times in Mac Dougall buffer. Cell lysates and IPs were diluted in Laemmli buffer containing SDS and β-mercaptoethanol, boiled for 6 minutes and subjected to SDS-PAGE. Immunoblotting was performed using primary antibodies diluted in phosphate buffered saline containing 0.1% Tween and 5% nonfat dry milk. HRP-conjugated secondary antibodies were purchased from GE Healthcare or Cell signaling technology or ThermoFisher Scientific. The blots were developed with an enhanced chemiluminescence method (Super-Signal West Pico Chemiluminescent substrate, Thermofisher Scientific).

ELISA and cytokine multiplex assays

IL-8 secretion was measured by ELISA in the supernatant of HeLa and Caco-2 cells infected with *S. flexneri* for 6 hours. The cell-free supernatants from triplicate wells were analyzed for their IL-8 content using the commercial ELISA kit (eBioscience). The secretion of additional cytokines including TNFα, IL-1β, IL-6 and IFNγ was measured using the Cytokine Human Magnetic 10-plex Panel for Luminex Platform (Life Technologies).

Statistical analysis

Data are expressed as mean ± standard deviation of triplicates samples as indicated. p values were calculated with a two-tailed two-sample equal variance t-test.

Supporting information

S1 Fig. Images illustrating the RNAi screen assay. HeLa cells were infected for 3.5 hours with *S. flexneri* Δ*virG* expressing dsRed under the control of the *uhpT* promoter (in green). After fixation, cells were stained for F-actin (in grey), DNA (in blue) and IL-8 (in red). Scale bars, 20 μm.
(PDF)

S2 Fig. Silencing TIFA or ALPK1 has no significant effect on *S. flexneri* entry. HeLa cells were transfected for 72 hours with control, TIFA- or ALPK1-targeting siRNAs. HeLa cells were infected for 3.5 hours with Δ*virG S. flexneri* expressing dsRed. After fixation, cells were stained for F-actin and DNA. Infection rate was evaluated by automated image analysis. Data correspond to the mean +/- SD of 3 independent experiments, NS = non-significant $p>0.05$.
(PDF)

S3 Fig. TIFA oligomerization after *S. flexneri* infection of Caco-2 cells. Caco-2 cells were transfected with a wild-type TIFA cDNA construct and infected for 3 hours with Δ*virG S.*

flexneri expressing dsRed (in blue). After fixation, cells were co-stained for TIFA (in green) and NF-κB p65 (in red). Scale bars, 20 μm.
(PDF)

S4 Fig. *S. typhimurium* and *S. flexneri*-induced IL-8 production is largely HBP-dependent. **A**) ADP-Heptose biosynthetic pathway. **B**) *S. typhimurium*-induced IL-8 production is largely HBP-dependent. HeLa cells were infected with *S. typhimurium* for 4 hours, fixed and stained for intracellular IL-8. Data correspond to the mean +/- SD of three independent experiments, $p^{**}<0.005$. **C**) Infectivity of wt, Δ*hldE* and Δ*waaC S. flexneri*. HeLa cells were infected with wt (MOI 100), Δ*hldE* (MOI 1) and Δ*waaC* (MOI 1) *S. flexneri* expressing dsRed. The rate of infection was quantified automatically. Data correspond to the mean +/- SD of three independent experiments, non-significant $p>0.05$. **D**) *S. flexneri*-induced IL-8 production is largely HBP-dependent. HeLa cells were infected with *S. flexneri* for 4 hours, fixed and stained for intracellular IL-8. Data correspond to the mean +/- SD of three independent experiments, $p^{**}<0.005$.
(PDF)

S5 Fig. TIFA oligomerization is HBP-dependent. A) HeLa cells were transfected with a wild-type TIFA cDNA construct. After 24 hours, they were infected with wild-type, Δ*hldE* or Δ*gmhB S. typhimurium* expressing dsRed under the control of the *uhpT* promoter. The fraction of infected cells showing TIFA punctuates was manually evaluated. Data correspond to the mean +/- SD of 3 independent experiments. **B**) HeLa cells were transfected with a wild-type TIFA cDNA construct. After 24 hours, they were infected with wild-type, Δ*hldE* or Δ*gmhB S. flexneri* expressing dsRed. The fraction of infected cells showing TIFA punctuates was manually evaluated. Data correspond to the mean +/- SD 3 independent experiments.
(PDF)

S6 Fig. The production of cytokines induced by *S. flexneri* infection is largely HBP-dependent. A) HeLa cells were infected or not with *S. flexneri* for 6 hours with wt (MOI 10), Δ*hldE* (MOI 0.1) and Δ*waaC* (MOI 0.1) *S. flexneri*. Cytokine secretion was measured in the supernatant of infected cells by a multiplex cytokine assay. Data correspond to the mean +/- SD of triplicates, $p^{**}<0.005$, $p^{***}<0.0005$. # indicates not detected. **B**) Caco-2 cells were infected or not with *S. flexneri* for 6 hours with wt (MOI 10), Δ*hldE* (MOI 0.1) and Δ*waaC* (MOI 0.1) *S. flexneri*. Cytokine secretion was measured in the supernatant of infected cells by a multiplex cytokine assay. Data correspond to the mean +/- SD of triplicates, $p^{**}<0.005$. IL-1β, IFNγ and IL-6 were not detected in Caco-2 cells.
(PDF)

S7 Fig. The production of cytokines induced by *S. flexneri* infection depends on ALPK1. A) ELISA assay showing that *S. flexneri*-induced IL-8 expression is ALPK1-dependent. HeLa cells were transfected with control or ALPK1 siRNA, and infected, or not, with *S. flexneri* for 6 hours. IL-8 secretion was measured in the supernatant of infected cells by ELISA. Data correspond to the mean +/- SD of three independent experiments, $p^{*}<0.05$. **B**) HeLa cells were transfected with control or ALPK1 siRNA, and infected or not with *S. flexneri* for 6 hours. Cytokine secretion was measured in the supernatant of infected cells by a multiplex cytokine assay. Data correspond to the mean +/- SD of triplicates, $p^{**}<0.005$, $p^{***}<0.0005$. # indicates not detected.
(PDF)

S8 Fig. ALPK1 is not involved in *L. monocytogenes*-induced inflammation. A) ALPK1 is not involved in *L. monocytogenes*-induced IL-8 expression. HeLa cells were transfected for 72 hours with control or ALPK1-targeting siRNAs and infected for 3.5 hours with *L. monocytogenes* expressing GFP. After fixation, cells were stained for F-actin, DNA, and IL-8. IL-8 was

quantified by automated image analysis. Data correspond to the mean +/- SD of triplicate wells and the graph is representative of 3 independent experiments, ns: non-significant $p>0.05$. **B**) ALPK1 is not involved in *L. monocytogenes*-induced NF-κB activation. Cells were treated as in A but stained for NF-κB p65 after one hour of infection. Quantification of the NF-κB p65 nuclear/cytoplasmic fluorescence intensity ratio. Data show the mean +/- SD of three independent experiments, ns: non-significant $p>0.05$.
(PDF)

S9 Fig. Roles of ALPK1 in different pathways activating NF-κB. A) ALPK1 depletion has no effect on PMA-induced NF-κB activation. Cells were transfected with control or ALPK1 siRNAs, stimulated with PMA (100 ng/ml) for 1 hour and stained for NF-κB p65. Data show the mean +/- SD of three independent experiments, ns: non-significant $p>0.05$. **B**) ALPK1 depletion has no effect on TNFα-induced NF-κB activation. Cells were treated as in A and stimulated with indicated concentrations of TNFα for 30 min. Data show the mean +/- SD of three independent experiments, ns: non-significant $p>0.05$. **C**) ALPK1 depletion has a moderate inhibitory effect on C12-iE-DAP-induced NF-κB activation. Cells were treated as in A and stimulated with indicated concentrations of C12-iE-DAP for 1 hour. Data show the mean +/- SD of three independent experiments, ns: non-significant $p>0.05$, $p^{*}<0.05$.
(PDF)

S10 Fig. TIFA oligomers are not co-localized with Lysosomal-associated membrane protein 1 (LAMP-1). HeLa cells were left uninfected or infected for 1 hour with *S. flexneri* expressing dsRed at MOI 0.5. Cells were stained for TIFA and LAMP1. Scale bar, 10 μm.
(PDF)

S1 Table. Results of the genome wide RNAi screen. Z-scored values of total cell counts, infection rates and IL-8 measurements obtained with CellProfiler for all genes targeted by the siRNA library (see Materials and Methods). Data correspond to the mean of duplicate screening data. TIFA, TRAF6 and ALPK1 are shown in red. The positive controls RelA (NF-κB p65) and MAP3K7 (TAK1) are shown in blue.
(XLSX)

S2 Table. Results of the human kinome screen. Data show Z-scored values of total cell counts, infection rates and IL-8 measurements obtained with CellProfiler for all genes targeted by the human kinome library (see Materials and Methods). Data are shown for all 3 individual sequences/gene or pooled.
(XLSX)

S3 Table. Primers used in this study.
(PDF)

Acknowledgments

We thank Prof. X. Nassif (INEM, Paris, France) for the generous gift of *Neisseria meningitidis* bacteria (wt and Δ*hldA*), Prof. P. Cossart (Institut Pasteur, Paris, France) for *Listeria monocytogenes* expressing GFP, Prof. M.D. Tsai (Institute of Biological Chemistry, Academia Sinica, Taiwan) for the TIFA cDNA constructs and Prof. R. Jacob for the YFP-ALPK1 cDNA. We also thank K. Bailly from the Cochin Cytometry and Immunobiology Facility for her technical help.

Author Contributions

Conceptualization: CA.

Data curation: ME.

Formal analysis: CAK MM CA.

Funding acquisition: CA.

Investigation: MM ASD CAK TT CA PS CP JG.

Methodology: MM ASD CAK TT.

Project administration: CA.

Software: ME CAK MM.

Supervision: CA.

Visualization: MM ASD CA.

Writing – original draft: CA.

Writing – review & editing: MM ASD CAK CA JG.

References

1. Schroeder GN, Hilbi H. Molecular pathogenesis of Shigella spp.: controlling host cell signaling, invasion, and death by type III secretion. Clin Microbiol Rev. 2008; 21(1):134–56. Epub 2008/01/19. PubMed Central PMCID: PMC2223840. doi: 10.1128/CMR.00032-07 PMID: 18202440
2. Cornelis GR. The type III secretion injectisome. Nat Rev Microbiol. 2006; 4(11):811–25. Epub 2006/10/17. doi: 10.1038/nrmicro1526 PMID: 17041629
3. Girardin SE, Tournebize R, Mavris M, Page AL, Li X, Stark GR, et al. CARD4/Nod1 mediates NF-kappaB and JNK activation by invasive Shigella flexneri. EMBO Rep. 2001; 2(8):736–42. Epub 2001/07/21. PubMed Central PMCID: PMC1083992. doi: 10.1093/embo-reports/kve155 PMID: 11463746
4. Girardin SE, Boneca IG, Carneiro LA, Antignac A, Jehanno M, Viala J, et al. Nod1 detects a unique muropeptide from gram-negative bacterial peptidoglycan. Science. 2003; 300(5625):1584–7. Epub 2003/06/07. doi: 10.1126/science.1084677 PMID: 12791997
5. Hasegawa M, Fujimoto Y, Lucas PC, Nakano H, Fukase K, Nunez G, et al. A critical role of RICK/RIP2 polyubiquitination in Nod-induced NF-kappaB activation. EMBO J. 2008; 27(2):373–83. Epub 2007/12/15. PubMed Central PMCID: PMC2234345. doi: 10.1038/sj.emboj.7601962 PMID: 18079694
6. Wang C, Deng L, Hong M, Akkaraju GR, Inoue J, Chen ZJ. TAK1 is a ubiquitin-dependent kinase of MKK and IKK. Nature. 2001; 412(6844):346–51. Epub 2001/07/19. doi: 10.1038/35085597 PMID: 11460167
7. Dupont N, Lacas-Gervais S, Bertout J, Paz I, Freche B, Van Nhieu GT, et al. Shigella phagocytic vacuolar membrane remnants participate in the cellular response to pathogen invasion and are regulated by autophagy. Cell Host Microbe. 2009; 6(2):137–49. Epub 2009/08/18. doi: 10.1016/j.chom.2009.07.005 PMID: 19683680
8. Sanada T, Kim M, Mimuro H, Suzuki M, Ogawa M, Oyama A, et al. The Shigella flexneri effector OspI deamidates UBC13 to dampen the inflammatory response. Nature. 2012; 483(7391):623–6. Epub 2012/03/13. doi: 10.1038/nature10894 PMID: 22407319
9. Kim DW, Lenzen G, Page AL, Legrain P, Sansonetti PJ, Parsot C. The Shigella flexneri effector OspG interferes with innate immune responses by targeting ubiquitin-conjugating enzymes. Proc Natl Acad Sci U S A. 2005; 102(39):14046–51. Epub 2005/09/16. PubMed Central PMCID: PMC1236552. doi: 10.1073/pnas.0504466102 PMID: 16162672
10. Li H, Xu H, Zhou Y, Zhang J, Long C, Li S, et al. The phosphothreonine lyase activity of a bacterial type III effector family. Science. 2007; 315(5814):1000–3. Epub 2007/02/17. doi: 10.1126/science.1138960 PMID: 17303758
11. Sansonetti PJ, Arondel J, Huerre M, Harada A, Matsushima K. Interleukin-8 controls bacterial transepithelial translocation at the cost of epithelial destruction in experimental shigellosis. Infect Immun. 1999; 67(3):1471–80. Epub 1999/02/20. PubMed Central PMCID: PMC96483. PMID: 10024597
12. Puhar A, Tronchere H, Payrastre B, Nhieu GT, Sansonetti PJ. A Shigella effector dampens inflammation by regulating epithelial release of danger signal ATP through production of the lipid mediator

PtdIns5P. Immunity. 2013; 39(6):1121–31. Epub 2013/12/18. doi: 10.1016/j.immuni.2013.11.013 PMID: 24332032

13. Kasper CA, Sorg I, Schmutz C, Tschon T, Wischnewski H, Kim ML, et al. Cell-cell propagation of NF-kappaB transcription factor and MAP kinase activation amplifies innate immunity against bacterial infection. Immunity. 2010; 33(5):804–16. Epub 2010/11/26. doi: 10.1016/j.immuni.2010.10.015 PMID: 21093316

14. Dolowschiak T, Chassin C, Ben Mkaddem S, Fuchs TM, Weiss S, Vandewalle A, et al. Potentiation of epithelial innate host responses by intercellular communication. PLoS Pathog. 2010; 6(11):e1001194. Epub 2010/12/03. PubMed Central PMCID: PMC2987820. doi: 10.1371/journal.ppat.1001194 PMID: 21124989

15. Patel SJ, King KR, Casali M, Yarmush ML. DNA-triggered innate immune responses are propagated by gap junction communication. Proc Natl Acad Sci U S A. 2009; 106(31):12867–72. Epub 2009/07/21. PubMed Central PMCID: PMC2722330. doi: 10.1073/pnas.0809292106 PMID: 19617563

16. Ablasser A, Schmid-Burgk JL, Hemmerling I, Horvath GL, Schmidt T, Latz E, et al. Cell intrinsic immunity spreads to bystander cells via the intercellular transfer of cGAMP. Nature. 2013; 503(7477):530–4. Epub 2013/10/01. doi: 10.1038/nature12640 PMID: 24077100

17. Ramo P, Drewek A, Arrieumerlou C, Beerenwinkel N, Ben-Tekaya H, Cardel B, et al. Simultaneous analysis of large-scale RNAi screens for pathogen entry. BMC Genomics. 2014; 15:1162. Epub 2014/12/24. PubMed Central PMCID: PMC4326433. doi: 10.1186/1471-2164-15-1162 PMID: 25534632

18. Makino S, Sasakawa C, Kamata K, Kurata T, Yoshikawa M. A genetic determinant required for continuous reinfection of adjacent cells on large plasmid in S. flexneri 2a. Cell. 1986; 46(4):551–5. Epub 1986/08/15. PMID: 3524856

19. Schmutz C, Ahrne E, Kasper CA, Tschon T, Sorg I, Dreier RF, et al. Systems-level overview of host protein phosphorylation during Shigella flexneri infection revealed by phosphoproteomics. Mol Cell Proteomics. 2013; 12(10):2952–68. Epub 2013/07/06. PubMed Central PMCID: PMC3790303. doi: 10.1074/mcp.M113.029918 PMID: 23828894

20. Runyen-Janecky LJ, Payne SM. Identification of chromosomal Shigella flexneri genes induced by the eukaryotic intracellular environment. Infect Immun. 2002; 70(8):4379–88. Epub 2002/07/16. PubMed Central PMCID: PMC128171. doi: 10.1128/IAI.70.8.4379-4388.2002 PMID: 12117948

21. Lippmann J, Gwinner F, Rey C, Tamir U, Law HK, Schwikowski B, et al. Bacterial Internalization, Localization, and Effectors Shape the Epithelial Immune Response during Shigella flexneri Infection. Infect Immun. 2015; 83(9):3624–37. Epub 2015/07/01. PubMed Central PMCID: PMC4534675. doi: 10.1128/IAI.00574-15 PMID: 26123804

22. Kim ML, Jeong HG, Kasper CA, Arrieumerlou C. IKKalpha contributes to canonical NF-kappaB activation downstream of Nod1-mediated peptidoglycan recognition. PLoS One. 2010; 5(10):e15371. Epub 2010/10/27. PubMed Central PMCID: PMC2955547. doi: 10.1371/journal.pone.0015371 PMID: 20976174

23. Reiterer V, Grossniklaus L, Tschon T, Kasper CA, Sorg I, Arrieumerlou C. Shigella flexneri type III secreted effector OspF reveals new crosstalks of proinflammatory signaling pathways during bacterial infection. Cell Signal. 2011; 23(7):1188–96. Epub 2011/03/16. doi: 10.1016/j.cellsig.2011.03.006 PMID: 21402152

24. Kobayashi T, Walsh MC, Choi Y. The role of TRAF6 in signal transduction and the immune response. Microbes Infect. 2004; 6(14):1333–8. Epub 2004/11/24. doi: 10.1016/j.micinf.2004.09.001 PMID: 15555541

25. Takatsuna H, Kato H, Gohda J, Akiyama T, Moriya A, Okamoto Y, et al. Identification of TIFA as an adapter protein that links tumor necrosis factor receptor-associated factor 6 (TRAF6) to interleukin-1 (IL-1) receptor-associated kinase-1 (IRAK-1) in IL-1 receptor signaling. J Biol Chem. 2003; 278(14):12144–50. Epub 2003/02/05. doi: 10.1074/jbc.M300720200 PMID: 12566447

26. Li J, Lee GI, Van Doren SR, Walker JC. The FHA domain mediates phosphoprotein interactions. J Cell Sci. 2000; 113 Pt 23:4143–9. Epub 2000/11/09.

27. Huang CC, Weng JH, Wei TY, Wu PY, Hsu PH, Chen YH, et al. Intermolecular binding between TIFA-FHA and TIFA-pT mediates tumor necrosis factor alpha stimulation and NF-kappaB activation. Mol Cell Biol. 2012; 32(14):2664–73. Epub 2012/05/09. PubMed Central PMCID: PMC3416184. doi: 10.1128/MCB.00438-12 PMID: 22566686

28. Gaudet RG, Sintsova A, Buckwalter CM, Leung N, Cochrane A, Li J, et al. INNATE IMMUNITY. Cytosolic detection of the bacterial metabolite HBP activates TIFA-dependent innate immunity. Science. 2015; 348(6240):1251–5. Epub 2015/06/13. doi: 10.1126/science.aaa4921 PMID: 26068852

29. Mahajan A, Yuan C, Lee H, Chen ES, Wu PY, Tsai MD. Structure and function of the phosphothreonine-specific FHA domain. Sci Signal. 2008; 1(51):re12. Epub 2008/12/26. doi: 10.1126/scisignal.151re12 PMID: 19109241

30. Kneidinger B, Marolda C, Graninger M, Zamyatina A, McArthur F, Kosma P, et al. Biosynthesis pathway of ADP-L-glycero-beta-D-manno-heptose in Escherichia coli. J Bacteriol. 2002; 184(2):363–9. Epub 2001/12/26. PubMed Central PMCID: PMC139585. doi: 10.1128/JB.184.2.363-369.2002 PMID: 11751812

31. Middelbeek J, Clark K, Venselaar H, Huynen MA, van Leeuwen FN. The alpha-kinase family: an exceptional branch on the protein kinase tree. Cell Mol Life Sci. 2010; 67(6):875–90. Epub 2009/12/17. PubMed Central PMCID: PMC2827801. doi: 10.1007/s00018-009-0215-z PMID: 20012461

32. Heine M, Cramm-Behrens CI, Ansari A, Chu HP, Ryazanov AG, Naim HY, et al. Alpha-kinase 1, a new component in apical protein transport. J Biol Chem. 2005; 280(27):25637–43. Epub 2005/05/11. doi: 10.1074/jbc.M502265200 PMID: 15883161

33. Ko AM, Tu HP, Liu TT, Chang JG, Yuo CY, Chiang SL, et al. ALPK1 genetic regulation and risk in relation to gout. Int J Epidemiol. 2013; 42(2):466–74. Epub 2013/04/10. PubMed Central PMCID: PMC3695596. doi: 10.1093/ije/dyt028 PMID: 23569188

34. Shimokata S, Oguri M, Fujimaki T, Horibe H, Kato K, Yamada Y. Association between polymorphisms of the alpha-kinase 1 gene and type 2 diabetes mellitus in community-dwelling individuals. Biomed Rep. 2013; 1(6):940–4. Epub 2014/03/22. PubMed Central PMCID: PMC3917034. doi: 10.3892/br.2013.173 PMID: 24649057

35. Yamada Y, Matsui K, Takeuchi I, Fujimaki T. Association of genetic variants with coronary artery disease and ischemic stroke in a longitudinal population-based genetic epidemiological study. Biomed Rep. 2015; 3(3):413–9. Epub 2015/07/03. PubMed Central PMCID: PMC4461855. doi: 10.3892/br.2015.440 PMID: 26137247

36. Yamada Y, Nishida T, Ichihara S, Kato K, Fujimaki T, Oguri M, et al. Identification of chromosome 3q28 and ALPK1 as susceptibility loci for chronic kidney disease in Japanese individuals by a genome-wide association study. J Med Genet. 2013; 50(6):410–8. Epub 2013/03/30. doi: 10.1136/jmedgenet-2013-101518 PMID: 23539754

37. Hillier LW, Graves TA, Fulton RS, Fulton LA, Pepin KH, Minx P, et al. Generation and annotation of the DNA sequences of human chromosomes 2 and 4. Nature. 2005; 434(7034):724–31. Epub 2005/04/09. doi: 10.1038/nature03466 PMID: 15815621

38. Coureuil M, Join-Lambert O, Lecuyer H, Bourdoulous S, Marullo S, Nassif X. Pathogenesis of meningococcemia. Cold Spring Harb Perspect Med. 2013; 3(6). Epub 2013/06/05. PubMed Central PMCID: PMC3662350.

39. Yin Q, Lin SC, Lamothe B, Lu M, Lo YC, Hura G, et al. E2 interaction and dimerization in the crystal structure of TRAF6. Nat Struct Mol Biol. 2009; 16(6):658–66. Epub 2009/05/26. PubMed Central PMCID: PMC2834951. doi: 10.1038/nsmb.1605 PMID: 19465916

40. Weiner A, Mellouk N, Lopez-Montero N, Chang YY, Souque C, Schmitt C, et al. Macropinosomes are Key Players in Early Shigella Invasion and Vacuolar Escape in Epithelial Cells. PLoS Pathog. 2016; 12 (5):e1005602. Epub 2016/05/18. PubMed Central PMCID: PMC4868309. doi: 10.1371/journal.ppat.1005602 PMID: 27182929

41. Kreibich S, Emmenlauer M, Fredlund J, Ramo P, Munz C, Dehio C, et al. Autophagy Proteins Promote Repair of Endosomal Membranes Damaged by the Salmonella Type Three Secretion System 1. Cell Host Microbe. 2015; 18(5):527–37. Epub 2015/11/17. doi: 10.1016/j.chom.2015.10.015 PMID: 26567507

42. Paciello I, Silipo A, Lembo-Fazio L, Curcuru L, Zumsteg A, Noel G, et al. Intracellular Shigella remodels its LPS to dampen the innate immune recognition and evade inflammasome activation. Proc Natl Acad Sci U S A. 2013; 110(46):E4345–54. Epub 2013/10/30. PubMed Central PMCID: PMC3832022. doi: 10.1073/pnas.1303641110 PMID: 24167293

43. Zhong J, Kyriakis JM. Germinal center kinase is required for optimal Jun N-terminal kinase activation by Toll-like receptor agonists and is regulated by the ubiquitin proteasome system and agonist-induced, TRAF6-dependent stabilization. Mol Cell Biol. 2004; 24(20):9165–75. Epub 2004/10/01. PubMed Central PMCID: PMC517887. doi: 10.1128/MCB.24.20.9165-9175.2004 PMID: 15456887

44. Bernardini ML, Mounier J, d'Hauteville H, Coquis-Rondon M, Sansonetti PJ. Identification of icsA, a plasmid locus of Shigella flexneri that governs bacterial intra- and intercellular spread through interaction with F-actin. Proc Natl Acad Sci U S A. 1989; 86(10):3867–71. Epub 1989/05/01. PubMed Central PMCID: PMC287242. PMID: 2542950

45. Kuhbacher A, Cossart P, Pizarro-Cerda J. Internalization assays for Listeria monocytogenes. Methods Mol Biol. 2014; 1157:167–78. Epub 2014/05/06. doi: 10.1007/978-1-4939-0703-8_14 PMID: 24792557

46. Geoffroy MC, Floquet S, Metais A, Nassif X, Pelicic V. Large-scale analysis of the meningococcus genome by gene disruption: resistance to complement-mediated lysis. Genome Res. 2003; 13(3):391–8. Epub 2003/03/06. PubMed Central PMCID: PMC430250. doi: 10.1101/gr.664303 PMID: 12618369

47. Datsenko KA, Wanner BL. One-step inactivation of chromosomal genes in Escherichia coli K-12 using PCR products. Proc Natl Acad Sci U S A. 2000; 97(12):6640–5. Epub 2000/06/01. PubMed Central PMCID: PMC18686. doi: 10.1073/pnas.120163297 PMID: 10829079

48. Murphy KC, Campellone KG. Lambda Red-mediated recombinogenic engineering of enterohemorrhagic and enteropathogenic E. coli. BMC Mol Biol. 2003; 4:11. Epub 2003/12/16. PubMed Central PMCID: PMC317293. doi: 10.1186/1471-2199-4-11 PMID: 14672541

49. Ramo P, Sacher R, Snijder B, Begemann B, Pelkmans L. CellClassifier: supervised learning of cellular phenotypes. Bioinformatics. 2009; 25(22):3028–30. Epub 2009/09/05. doi: 10.1093/bioinformatics/btp524 PMID: 19729371

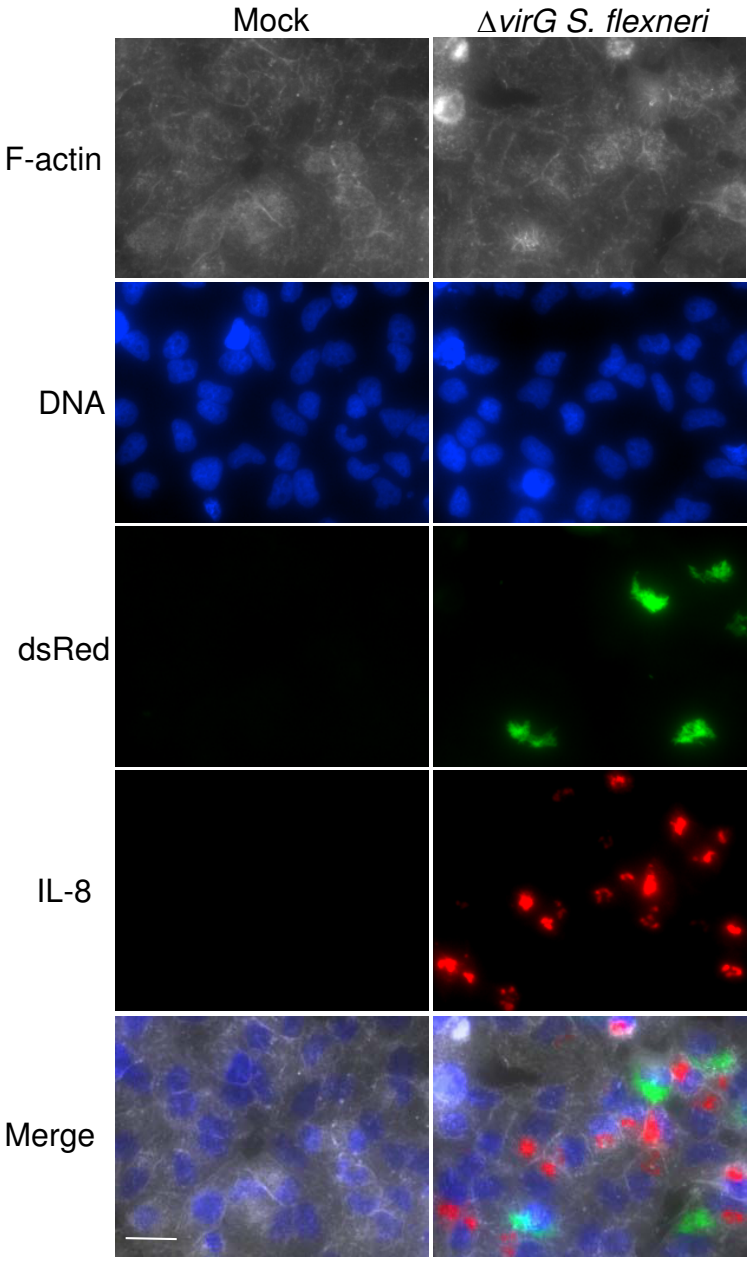

Figure S1: Images illustrating the assay of the RNAi screen.
HeLa cells were infected for 3.5 hours with *S. flexneri* Δ*virG* expressing dsRed under the control of the *uhpT* promoter (in green). After fixation, cells were stained for F-actin (in grey), DNA (in blue) and IL-8 (in red). Scale bars, 20 μm.

Figure S1

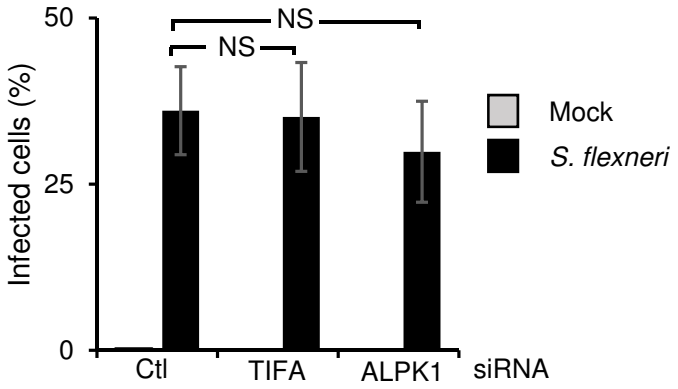

Figure S2: Silencing TIFA or ALPK1 has no significant effect on *S. flexneri* entry
HeLa cells were transfected for 72 hours with control, TIFA or ALPK1-targeting siRNAs. HeLa cells were infected for 3.5 hours with Δ*virG S. flexneri* expressing dsRed. After fixation, cells were stained for F-actin and DNA. Infection rate was evaluated by automated image analysis. Data correspond to the mean +/- SD of 3 independent experiments, NS = non-significant $p>0.05$.

Figure S2

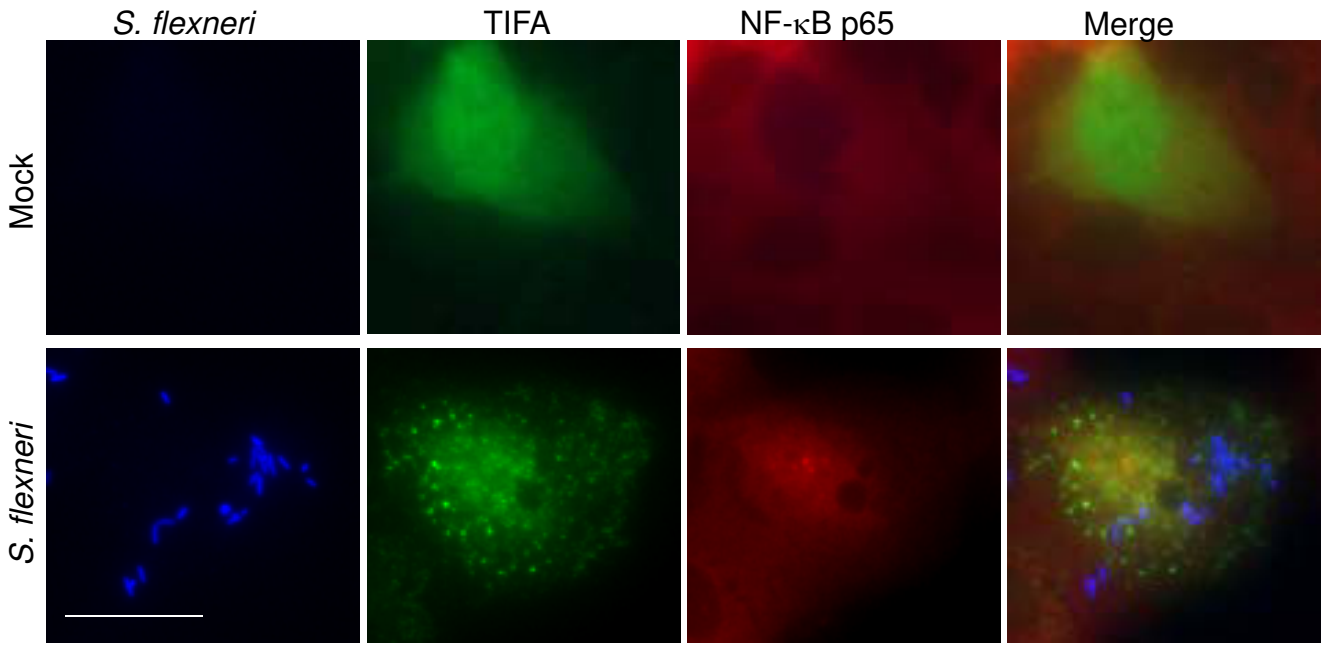

Figure S3: TIFA oligomerization after *S. flexneri* infection of Caco-2 cells.
Caco-2 cells were transfected with a wild-type TIFA cDNA construct and infected for 3 hours with Δ*virG* *S. flexneri* expressing dsRed (in blue). After fixation, they were co-stained for TIFA (in green) and NF-κB p65 (in red). Scale bars, 20 μm.

Figure S3

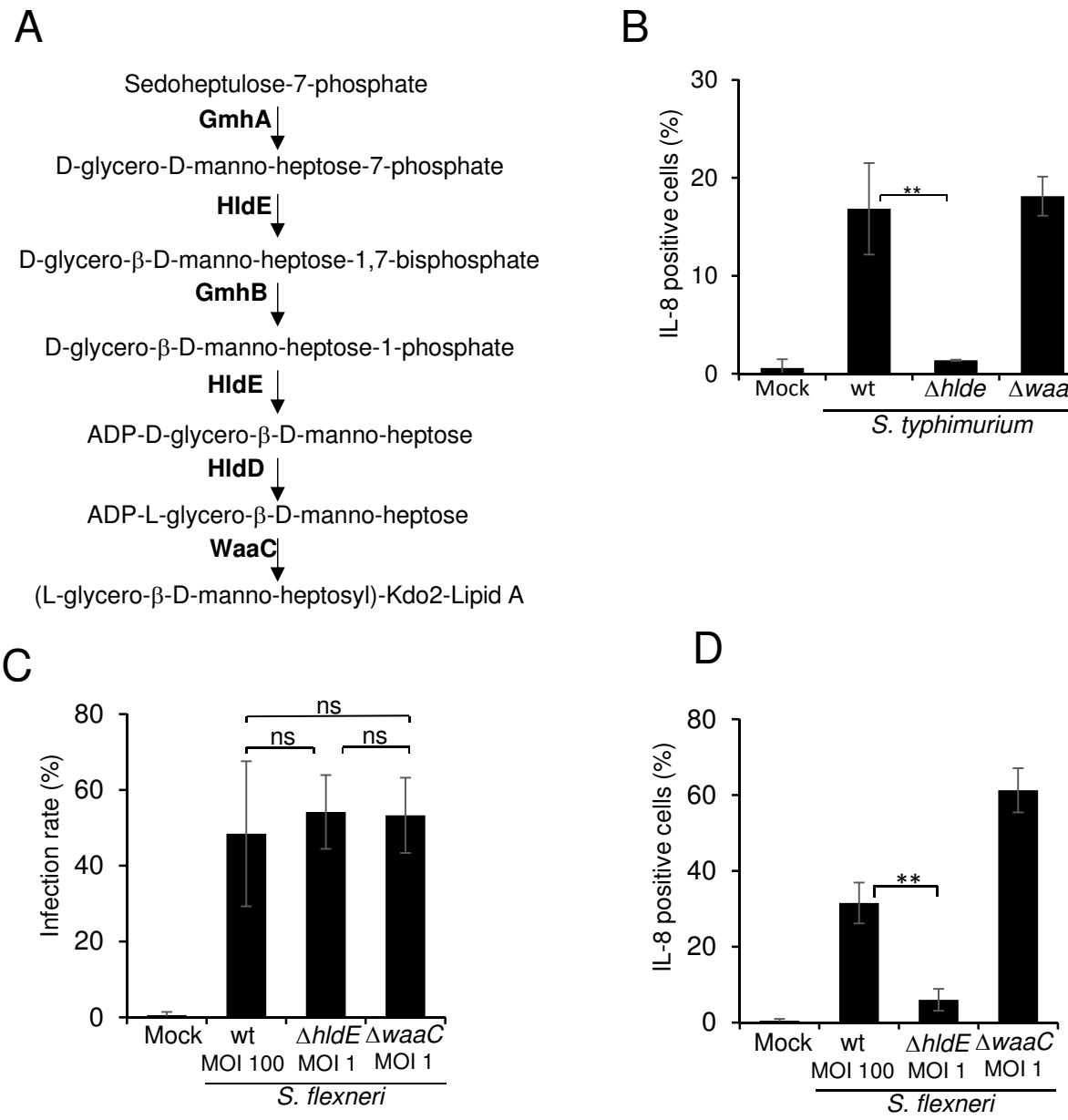

Figure S4: *S. typhimurium* and *S. flexneri*-induced IL-8 production is largely HBP-dependent.
A) ADP-Heptose biosynthetic pathway. **B**) *S. typhimurium*-induced IL-8 production is largely HBP-dependent. HeLa cells were infected with *S. typhimurium* for 4 hours, fixed and stained for intracellular IL-8. Data correspond to the mean +/- SD of three independent experiments, p**<0.005. **C**) Infectivity of wt, Δ*hldE* and Δ*waaC S. flexneri*. HeLa cells were infected with wt (MOI 100), Δ*hldE* (MOI 1) and Δ*waaC* (MOI 1) *S. flexneri* expressing dsRed. The rate of infection was quantified automatically. Data correspond to the mean +/- SD of three independent experiments, non-significant p>0.05. **D**) *S. flexneri*-induced IL-8 production is largely HBP-dependent. HeLa cells were infected with *S. flexneri* for 4 hours, fixed and stained for intracellular IL-8. Data correspond to the mean +/- SD of three independent experiments, p**<0.005.

Figure S4

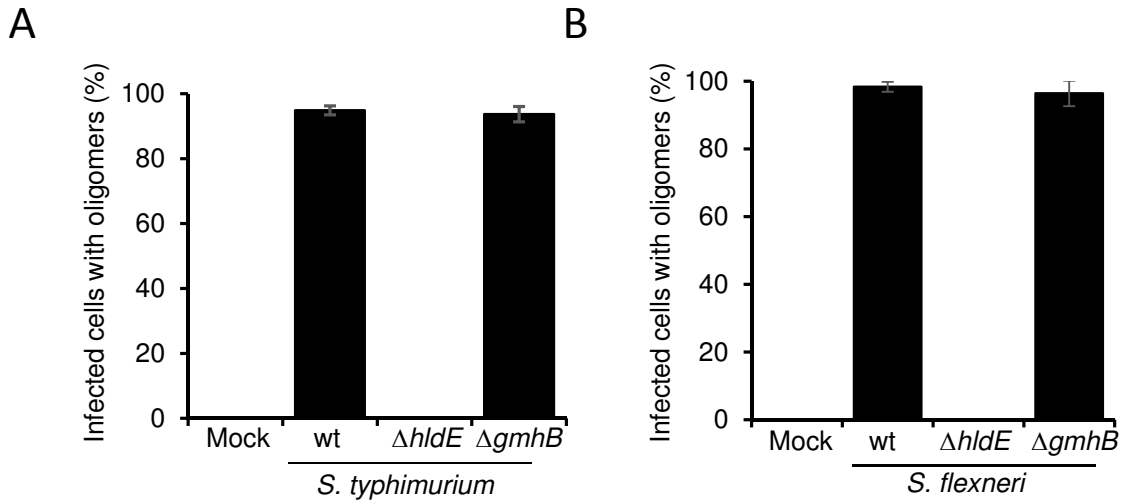

Figure S5: TIFA oligomerization is HBP-dependent.
A) HeLa cells were transfected with a wild-type TIFA cDNA construct. After 24 hours, they were infected with wild-type, Δ*hldE* or Δ*gmhB S. typhimurium* expressing dsRed under the control of the *uhpT* promoter. The fraction of infected cells showing TIFA punctuates was manually evaluated. Data correspond to the mean +/- SD of 3 independent experiments.
B) HeLa cells were transfected with a wild-type TIFA cDNA construct. After 24 hours, they were infected with wild-type, Δ*hldE* or Δ*gmhB S. flexneri* expressing dsRed. The fraction of infected cells showing TIFA punctuates was manually evaluated. Data correspond to the mean +/- SD 3 independent experiments.

Figure S5

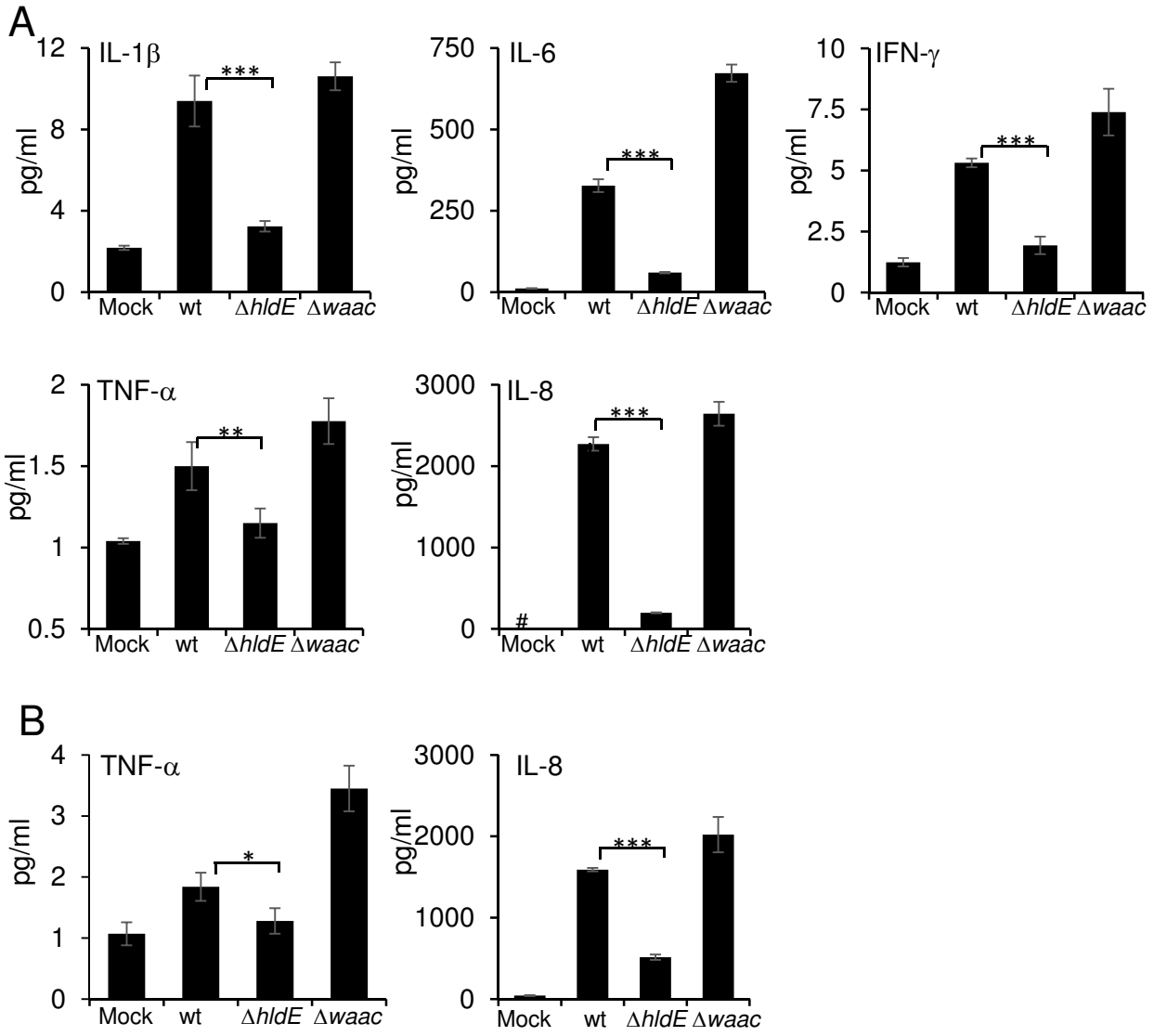

Figure S6: The production of cytokines induced by *S. flexneri* infection is largely HBP-dependent.

A) HeLa cells were infected or not with *S. flexneri* for 6 hours with wt (MOI 10), Δ*hldE* (MOI 0.1) and Δ*waaC* (MOI 0.1) *S. flexneri.* Cytokine secretion was measured in the supernatant of infected cells by a multiplex cytokine assay. Data correspond to the mean +/- SD of triplicates, p**<0.005, p***<0.0005. # indicates not detected. **B**) Caco-2 cells were infected or not with *S. flexneri* for 6 hours with wt (MOI 10), Δ*hldE* (MOI 0.1) and Δ*waaC* (MOI 0.1) *S. flexneri*. Cytokine secretion was measured in the supernatant of infected cells by a multiplex cytokine assay. Data correspond to the mean +/- SD of triplicates, p**<0.005. IL-1β, IFNγ and IL-6 were not detected in Caco-2 cells.

Figure S6

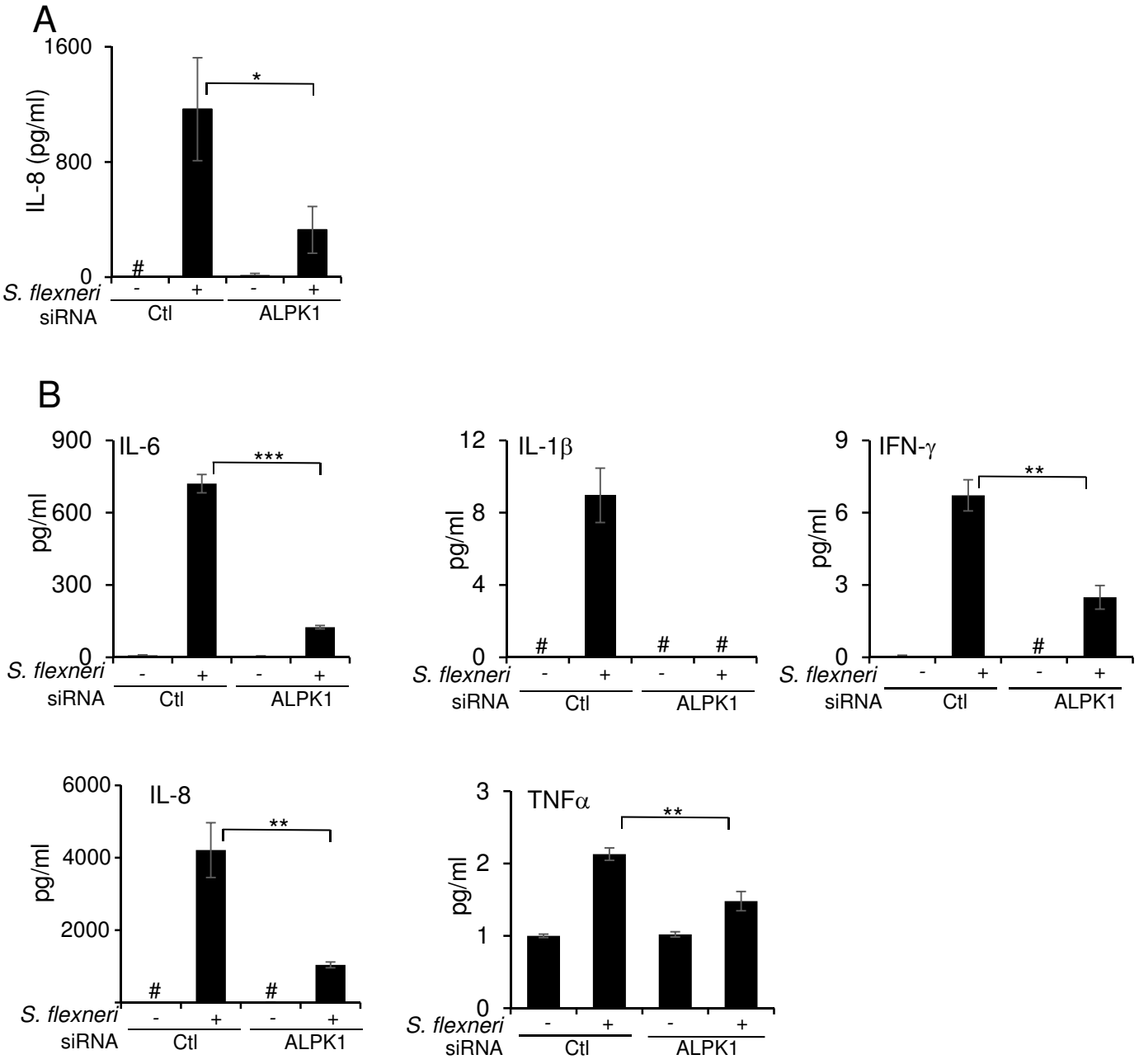

Figure S7: The production of cytokines induced by *S. flexneri* infection depends on ALPK1.
A) ELISA assay showing that *S. flexneri*-induced IL-8 expression is ALPK1-dependent. HeLa cells were transfected with control or ALPK1 siRNA, and infected or not with *S. flexneri* for 6 hours. IL-8 secretion was measured in the supernatant of infected cells by ELISA. Data correspond to the mean +/- SD of three independent experiments, p*<0.05. **B**) HeLa cells were transfected with control or ALPK1 siRNA, and infected or not with *S. flexneri* for 6 hours. Cytokine secretion was measured in the supernatant of infected cells by a multiplex cytokine assay. Data correspond to the mean +/- SD of triplicates, p**<0.005, p***<0.0005. # indicates not detected.

Figure S7

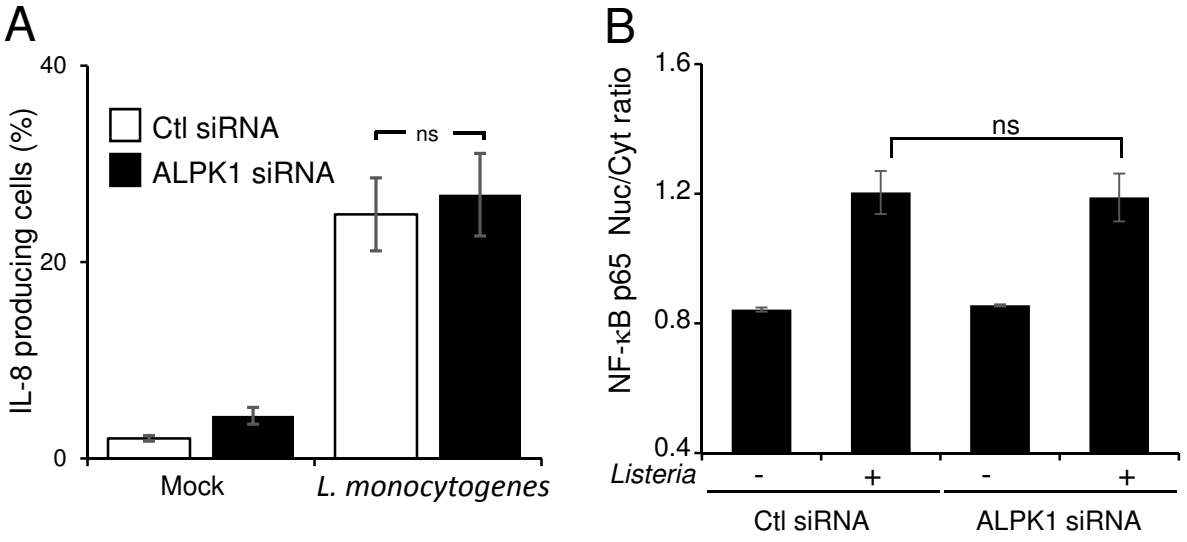

Figure S8: ALPK1 is not involved in *L. monocytogenes*-induced inflammation
A) ALPK1 is not involved in *L. monocytogenes*-induced IL-8 expression. HeLa cells were transfected for 72 hours with control or ALPK1-targeting siRNAs and infected for 3.5 hours with *L. monocytogenes* expressing GFP. After fixation, cells were stained for F-actin, DNA, and IL-8. IL-8 was quantified by automated image analysis. Data correspond to the mean +/- SD of triplicate wells, graph representative of 3 independent experiments, ns: non-significant $p>0.05$. **B**) ALPK1 is not involved in *L. monocytogenes*-induced NF-κB activation. Cells were treated as in A but stained for NF-κB p65 after one hour of infection. Quantification of the NF-κB p65 nuclear/cytoplasmic fluorescence intensity ratio. Data show the mean +/- SD of three independent experiments, ns: non-significant $p>0.05$.

Figure S8

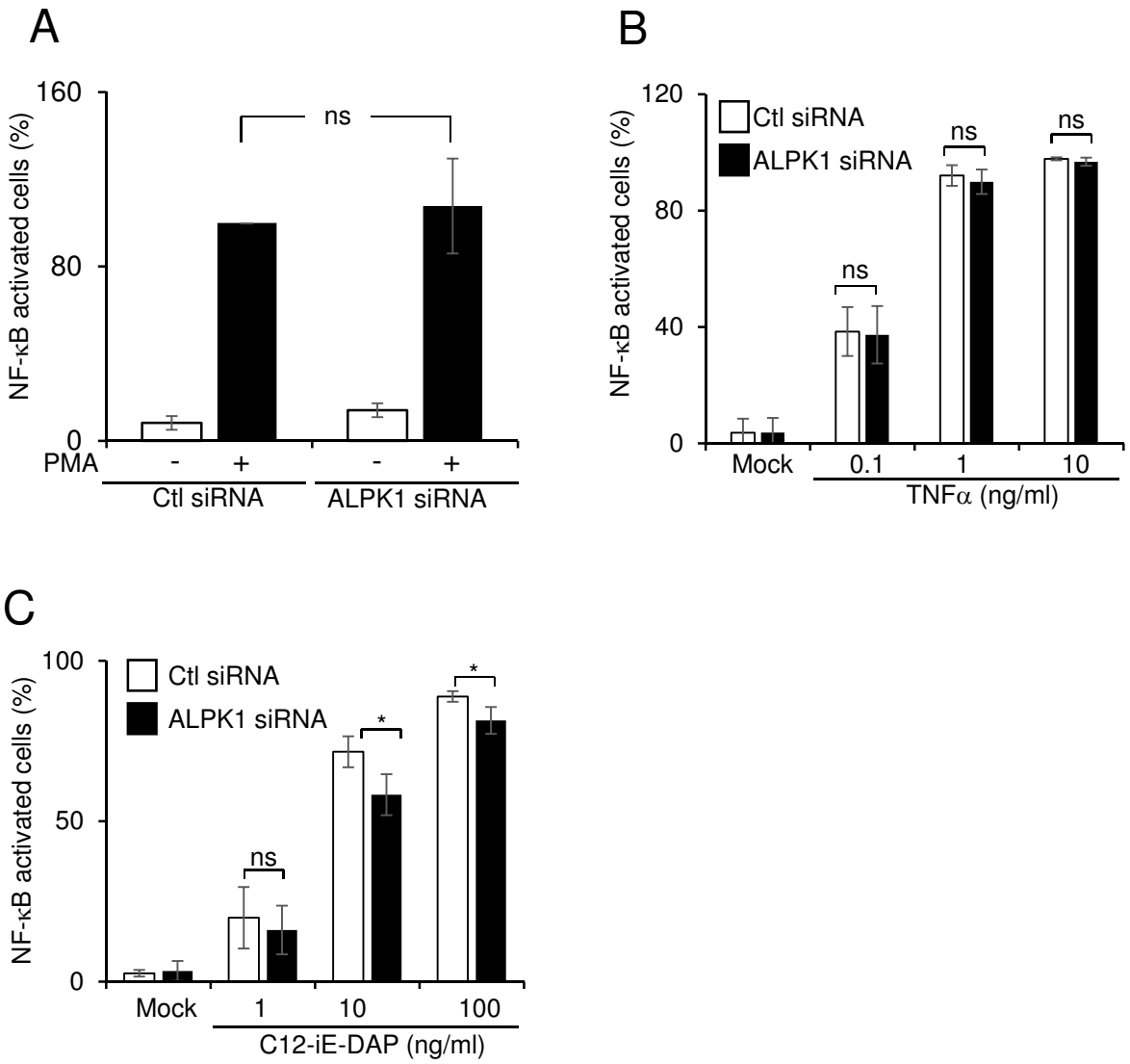

Figure S9: Roles of ALPK1 in different pathways activating NF-κB.
A) ALPK1 depletion has no effect on PMA-induced NF-κB activation. Cells were transfected with control or ALPK1 siRNAs, stimulated with PMA (100 ng/ml) for 1 hour and stained for NF-κB p65. Data show the mean +/- SD of three independent experiments, ns: non-significant $p>0.05$. **B**) ALPK1 depletion has no effect on TNFα-induced NF-κB activation. Cells were treated as in A and stimulated with indicated concentrations of TNFα for 30 min. Data show the mean +/- SD of three independent experiments, ns: non-significant $p>0.05$. **C**) ALPK1 depletion has a moderate inhibitory effect on C12-iE-DAP-induced NF-κB activation. Cells were treated as in A and stimulated with indicated concentrations of C12-iE-DAP for 1 hour. Data show the mean +/- SD of three independent experiments, ns: non-significant $p>0.05$, $p^*<0.05$.

Figure S9

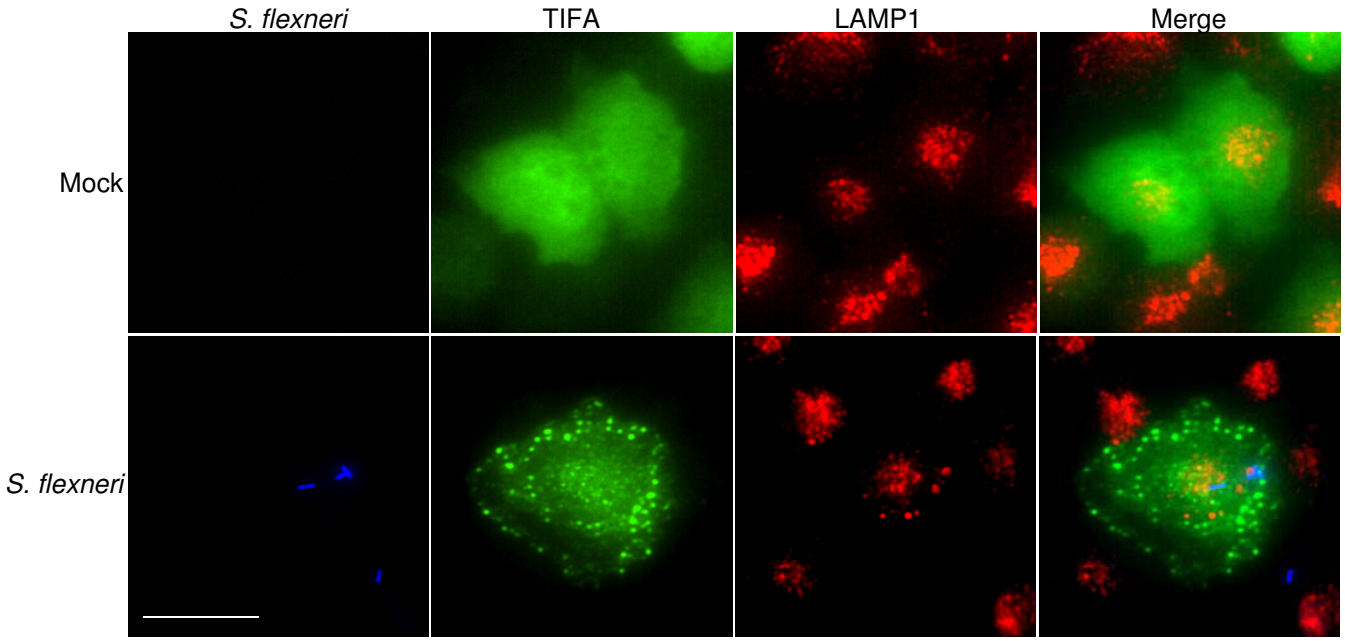

Figure S10: TIFA oligomers are not co-localized with *Lysosomal*-associated membrane protein 1 (*LAMP-1*). HeLa cells were left uninfected or infected for 1 hour with *S. flexneri* expressing dsRed at MOI 0.5. Cells were stained for TIFA and LAMP1. Bar, 10 μm.

Table S1.

GeneName	Cell counts (Z score)	Infection rate (Z score)	IL-8 (Z score)
KCNK1	-0.07839	-0.5184495	-2.0448
GNPDA1	-1.12625	0.12955	-2.02305
RAC1	0.886065	-0.77175	-1.95815
RIMS3	1.21072	-1.137325	-1.9434
TIFA	0.13651	1.6204	-1.91115
ATG16L2	0.7945	-0.918505	-1.8995
SNX32	-0.8219165	-0.398595	-1.89345
GGA3	0.490975	-1.968	-1.8614
EIF2C3	0.29043	-2.31095	-1.84755
SCAMP5	-0.027093	-1.476845	-1.84125
HNRNPR	0.91246	-1.05277	-1.82715
FKBP6	-1.19142	-0.413205	-1.81525
CCDC19	-0.800935	-3.2996	-1.8123
FBL	-0.36844	0.485605	-1.78625
OSBPL5	-0.2769	-0.174915	-1.7844
MAP2K2	0.45527	-0.93616	-1.78425
GLT8D1	0.370405	-0.84757	-1.78235
C14orf101	0.841755	-2.262	-1.7715
SH3GLB2	0.504695	0.3082156	-1.77135
SF1	0.59137	-0.966385	-1.771
ACCS	1.589435	0.702205	-1.7684
ITGB1BP2	0.5185765	-2.1711	-1.76015
NGFRAP1	0.155525	-1.113675	-1.75845
SMARCE1	1.057915	-0.90452	-1.7416
RAB3B	-0.19888	-0.780975	-1.73785
SLC25A12	0.1026135	0.53849	-1.7298
CD5	0.962275	-1.06639	-1.7266
ZNF70	0.729405	-0.93507	-1.7261
STX11	0.215055	0.496215	-1.723
LRRC66	0.555085	-0.144555	-1.72165
MAP3K7	1.0877	0.00655	-1.7088
ZNF750	0.162275	-1.4598	-1.7011
ING1	1.6608	-1.388095	-1.6968
OR11H4	1.053565	-1.8945	-1.69415
NUP85	-0.52094	0.13747	-1.69385
UBL4B	0.884935	-1.076765	-1.69055
WFIKKN1	0.3858	0.59952	-1.68925
KCNA2	0.430625	-0.89106	-1.68785
TRIB3	-0.362396	0.01634	-1.68655
DOCK8	-1.2643	-0.188807	-1.68345
CATSPER1	-0.092165	-0.524715	-1.68215

GRINA	0.36623	-1.083535	-1.67995
HCFC2	0.155361	-0.57441	-1.67215
METRN	-1.41985	-0.18403	-1.6695
LOC284009	0.71238	-2.07615	-1.66495
WT1	0.115085	-0.749765	-1.6624
C17orf78	-0.982135	-0.716785	-1.6613
CXorf1	1.090815	0.2414	-1.66105
PKHD1L1	-0.27827	-0.50391	-1.65755
LCN12	0.424575	-1.35918	-1.65635
NPM2	-0.736805	-1.614245	-1.64615
KCND3	-0.884095	-0.02365	-1.6433
FAM120A	-0.6827265	-0.438585	-1.64215
RIN2	0.816225	-1.3989	-1.64195
APOH	-1.24981	1.284935	-1.64055
SULT2A1	1.06702	-0.535195	-1.63855
ECH1	0.238	-1.099095	-1.63795
SRSF1	-0.019405	0.02264	-1.63575
GRAMD1A	-1.1286	-1.37748	-1.6317
ITM2C	-1.16722	-1.27055	-1.6296
AVL9	1.011585	-0.538865	-1.6292
ZNF474	0.508705	-0.056125	-1.62805
TFDP3	-0.79987	-0.365795	-1.62775
PSKH2	1.05545	-0.682275	-1.62705
UTP18	-0.04688	-1.16345	-1.6257
LHFP	-0.830155	-2.25845	-1.62175
CCDC144NL	0.654985	-0.18136	-1.6207
CPNE2	0.62985	0.3047945	-1.6204
SUPT16H	0.846075	0.692305	-1.61335
RXRB	-0.155105	-1.37385	-1.61305
STRN3	0.035892	-1.84145	-1.6125
KNCN	-0.7178	-0.306755	-1.6123
SAFB	0.754405	0.440595	-1.6102
ANXA4	0.76048	-2.39565	-1.6102
PPP2R5D	-0.08784	-1.3356	-1.60905
CFL2	-0.361745	-0.45516	-1.60365
RAPGEF3	0.74093	-1.38954	-1.6036
MORC2	-0.382195	-2.0293	-1.6034
UBR4	-1.01093	-0.216415	-1.6027
DCD	-0.99782	0.595655	-1.6016
IMP4	-0.548495	-0.60251	-1.60135
SLC28A2	0.33357	-2.58335	-1.5905
RELA	**0.24936**	**0.93379**	**-1.5892**
ANGPTL4	-0.678205	0.13325	-1.5871
CCDC121	-0.7464275	1.517	-1.58575

IKBKG	0.787705	-1.2764	-1.58515
ALOX15B	-1.035315	-0.1423175	-1.58475
EGFL6	0.2449345	0.903125	-1.5808
TFAP2E	0.335275	-0.682185	-1.58055
RAB2A	0.178299	-0.83123	-1.5721
CLK3	1.23255	-0.669395	-1.57175
TMEM18	0.056975	0.622775	-1.5717
G0S2	0.972905	-1.29458	-1.5694
DCLK2	0.74038	-1.54135	-1.56875
SCNN1D	0.214655	-2.58735	-1.56705
CNKSR3	-0.96963	0.031205	-1.56485
SCIN	1.00581	-0.14454605	-1.56465
PSMG2	0.72215	-1.2529	-1.56415
PLAT	-0.161655	-1.434285	-1.56285
ESPN	-1.254235	-1.065785	-1.56115
BCHE	0.881565	-1.05878	-1.5581
BNIPL	0.135323	-1.59705	-1.55795
ZMIZ2	1.083595	-1.099565	-1.55785
IGFLR1	0.458635	0.385605	-1.55755
TIPIN	0.167326	-2.30755	-1.55525
RD3	-0.29399	-1.013895	-1.55405
NHS	-0.87343	0.15683	-1.5532
IQCD	-0.103085	-1.42928	-1.55275
CHST5	-0.64759	-1.6902	-1.55115
MAPK10	-0.091375	-0.44521	-1.5488
MYOZ1	0.40245	-1.3881	-1.54495
HRH4	1.48315	-0.924815	-1.54475
MYO1B	-0.33544	-0.712015	-1.54395
TNFRSF12A	-0.771595	-1.1575	-1.542715
PVR	-0.737775	0.0433815	-1.54205
CDC40	-1.8989	0.219845	-1.5419
PEX14	1.007715	-0.1049525	-1.5418
MET	-0.862775	-0.344165	-1.53995
RPL27	-1.9649	-0.514635	-1.5386
BAMBI	0.389565	-1.208435	-1.5356
SLC25A39	0.36124	-1.12831	-1.5349
EPHB1	0.401415	-0.5126315	-1.5341
RPS4Y1	-1.6148	0.226114	-1.5339
ZNF593	0.65749	-1.130225	-1.52995
C19orf50	0.087465	-2.4992	-1.528695
KRT4	0.92566	1.03702	-1.52835

MYEOV	0.347555	-0.96787	-1.52575
SSTR1	0.85331	-2.3202	-1.5249
PDS5A	0.323828	0.40067	-1.5241
FCF1	-0.150057	-0.738895	-1.5237
SELT	1.5952	-1.176195	-1.5229
LIN9	-0.333181	-2.30255	-1.52285
SLC12A2	0.324895	-0.73205	-1.51975
DICER1	0.40693	-0.22305	-1.5193
SSX5	-0.25528985	-1.6239	-1.5191
FGF11	1.224755	-0.203535	-1.517965
C1QTNF2	-0.2055	-1.044935	-1.51755
IL31RA	-1.19942	0.8471	-1.5167
GPR107	-0.393665	-0.38016	-1.51585
SHANK1	-0.03061	-1.6159	-1.51485
PIN1	-0.74278	-0.750135	-1.51475
ZNF846	1.25915	-1.22792	-1.51405
CHTF18	0.192935	0.017695	-1.513
NCAM1	-1.0633	-0.532245	-1.51135
MYF6	0.176345	-0.442995	-1.50985
PIK3C2A	-0.160385	-0.8412	-1.50985
CACNB3	0.282265	0.507895	-1.50965
TSPAN10	1.40345	-0.583065	-1.50765
SCN9A	1.3406	-1.413085	-1.50645
SMAD6	0.11302	0.478975	-1.50505
TBC1D2B	0.609675	-0.6232945	-1.50475

Table S1: Table showing results of RNAi Screen.

Data show Z-scored values of total cell counts, infection rates and IL-8 measurements obtained with CellProfiler for all genes targeted by the siRNA library (see Material and Methods). Data correspond to the mean of duplicate screening data. TIFA, TRAF6 and ALPK1 are shown in red. The positive controls RelA (NF-κB p65) and MAP3K7 (TAK1) are shown in blue.

(Adapted from Table S1: Showing top 150 gene hits based on IL-8 Z score. TRAF6 appears at position 1930 with a Z score of -0.964055. ALPK1 appears at position 1967 with a Z score of -0.95659. Full results can be found at: https://doi.org/10.1371/journal.ppat.1006224.s011)

Table S2.

GeneName	siRNASequence	Cell count (Z score)	Infection rate (Z score)	IL-8 (Z score)	Mean 3 sequences Cell count (Z score)	Mean 3 sequences infection rate (Z score)	Mean 3 sequences IL-8 (Z score)
AAK1	AACGTGAGTAGCGGTGATGTA	-0.29874	-0.94255	1.788	-0.52015	-0.561171667	0.876208167
AAK1	CTCCTCGGACCTCTCAACAAA	-1.280505	-0.13374	0.935245			
AAK1	AGGACAAGCAATGGGATGAAA	0.018795	-0.607225	-0.0946205			
AATK	ACGGTGAAGATTGGTGACTAT	-0.28873	0.84678	-1.2853	-0.054545	-0.658505	-1.16536
AATK	CCCGGTTCCGCTGAGATCAGA	1.3748	-1.93815	-2.77565			
AATK	CTGCACCTTCATCGCAACAAT	-1.249705	-0.884145	0.56487			
ABL1	ACGAAGGGAGGGTGTACCATT	0.4156445	-1.036555	-0.246015	0.4857265	-1.312435	0.410150167
ABL1	TACGACAAGTGGGAGATGGAA	-0.581515	-1.0349	1.1859			
ABL1	AACACTCTAAGCATAACTAAA	1.62305	-1.86585	0.2905655			
ABL2	AACCCTGTCCTTAATAACTTA	0.420492	-1.09307	1.5855	0.146029	-1.003018333	1.327513333
ABL2	ATCAAGCATCCTAATCTGGTA	1.500845	-1.105615	1.10442			
ABL2	ATCCCTCAAACTCGCAACAAA	-1.48325	-0.81037	1.29262			
ACVR1	CTGAGGCATGAAAATATCTTA	1.416095	-0.55052	0.541685	0.413748333	-0.692521667	0.86382
ACVR1	TTGGATCATTCGTGTACATCA	-0.167755	-0.870315	1.3567			
ACVR1	GAGTTGCTCTCCGAAAATTTA	-0.007095	-0.65673	0.693075			
ACVR1B	GAAGTACTTGATGAAACCATT	0.47303	0.1853615	0.1765586	0.843938333	-0.132571167	0.128274867
ACVR1B	CCGAACCATCGTTTTACAAGA	0.97212	-0.55766	0.198875			
ACVR1B	GGGAAGCAGAGATATACCAGA	1.086665	-0.025415	0.009391			
ACVR1C	CCGCCTAACTGCTCTTCGTAT	0.72625	0.153895	0.934045	0.168853333	0.828728333	0.3479415
ACVR1C	AACAATGTTACCAAAACCGAA	-0.39666	1.27135	0.418425			
ACVR1C	AGGGCTCCTTATATGACTATT	0.17697	1.06094	-0.3086455			
ACVR2A	AAGCCCAGTTGCTTAACGAAT	1.20083	0.211225	0.771495	0.049648333	0.176501417	0.135725
ACVR2A	CTGGATGATATCAACTGCTAT	-0.897465	0.17919425	-0.60965			
ACVR2A	ATCAGACTTTCTTAAGGCTAA	-0.15442	0.139085	0.24533			
ACVR2B	AACATCATCACATGGAACGAA	-0.20141	-0.181344	1.08894	0.101396667	-0.014829667	0.365826667
ACVR2B	CACCATCGAGCTCGTGAAGAA	-0.135605	0.070495	-0.60391			
ACVR2B	AGGCTCCAACCTCGAAGTAGA	0.641205	0.06636	0.61245			
ACVRL1	CACCGAGTTCGTCAACCACTA	-0.33514	-0.12578	-0.721745	-0.245881335	0.18574745	0.043797667
ACVRL1	GCGGATCAAGAAGACACTACA	-0.505175	0.531855	-0.211397			
ACVRL1	CAGATCCGCACGGACTGCTTT	0.102670995	0.15116735	1.064535			
ADCK2	AGGAATTCCCGTGGACTTGAA	0.03957	-1.47575	0.925765	0.3815625	0.027718333	0.675175
ADCK2	CAGACCAGTCGTTTCTAGAAA	0.650835	1.517295	0.38561			
ADCK2	CAGATTGACCTGCGTTACGAA	0.4542825	0.04161	0.71415			
ADCK4	CGGCTTGTGCCCAGAATTTCA	0.05899	0.0416515	-0.67496	0.422218333	0.4291805	-0.118638333
ADCK4	CCTCACAGGCTTTGAAACCAA	1.41875	1.7051	0.590995			
ADCK4	CAGGACCTGCGGAACCAGATT	-0.211085	-0.45921	-0.27195			
ADCK5	AAGGCCTTTGCTGAGCAGATA	-0.43427	1.3806	-0.60438	-0.169466667	0.566044	0.154418
ADCK5	CAGTGCATGACATAGCAGAAA	-0.695255	-0.452168	1.003225			
ADCK5	TGGCAACGTTCTGGTGCGGAA	0.621125	0.7697	0.064409			
ADK	GAGCAAGGCTTTGAGACTAAA	0.50018	-0.41833	0.8924	0.318021667	-0.128819	0.601633333

ADK	ATGCATTGGGATAGATAAATT	-0.83852	0.25382	-0.309695			
ADK	ATGCCTTATGTTGATATACTT	1.292405	-0.221947	1.222195			
ADPGK	AGGGAATATCCTTCCACTTCA	-0.744315	-0.304345	0.2049755	-0.116978333	0.28269	-0.4920765
ADPGK	CAGCATTCTGCATTCAAGGAA	-0.368305	-0.351235	-0.688465			
ADPGK	CTGAATGAACAGGAGCTGTTA	0.761685	1.50365	-0.99274			
ADRBK1	GTGGAAGAATGTGGAGCTCAA	0.835965	1.32945	0.75371	0.742491667	1.264613333	-0.404186667
ADRBK1	CCGGGAGATCTTCGACTCATA	1.01512	1.298935	-1.64195			
ADRBK1	ATACATCGAAGAGATTTGTCA	0.37639	1.165455	-0.32432			
ADRBK2	TGGCAGCAAGAAGTAACGGAA	0.877	-1.39375	0.38888	1.178433333	-0.738575	0.333415
ADRBK2	AAGCAAGCTGTAGAACACGTA	1.54895	-1.11304	0.118505			
ADRBK2	AAGCTACTTGATTGCGACCAA	1.10935	0.291065	0.49286			
AGK	CTGCATTGAACCTGACACCAT	-1.8468	0.932985	0.57577	-0.848140167	0.862489167	0.585504667
AGK	GACTATTGTTAAGACAGATTA	-0.903045	0.6909625	1.14895			
AGK	GTGCACTTTGCTTATCCCGGA	0.2054245	0.96352	0.031794			
AK1	CCGAATGAAATCCGAACAGTT	-0.834815	-0.0938585	1.084	-0.101325833	-0.1469615	-0.005843333
AK1	TTCATTTCCATTGGTTATTTA	0.563785	-0.251366	0.58007			
AK1	TTGGTGCTCACGTGTCCTTAA	-0.0329475	-0.09566	-1.6816			
AK2	AAGCTTGATTCTGTGATTGAA	1.43065	-1.3098	0.4521055	0.402348333	-1.086285	-0.390604833
AK2	CAGACTCTCTGCTGATCCGAA	0.1237	-1.43505	-1.7827			
AK2	CCGTCGATCAGATGATAATGA	-0.347305	-0.514005	0.15878			
AK3	AAGGCTTATGAAGACCAAACA	0.781845	1.300385	0.2212	0.22827	0.453165	0.87045
AK3	CAGCGTGAGGATGATAAACCA	-0.79573	-0.112745	1.72795			
AK3	TTGGCCCTATGTATATGCTTT	0.698695	0.171855	0.6622			
AK5	AAGGAGACTAATGAACTTCAA	-0.95077	0.3952	0.679675	0.087316667	0.764421667	-0.145243
AK5	CTGGCTTGTGCTAATCAGAGA	0.458425	0.683945	-0.656369			
AK5	AACGATATGGATTCCAATACA	0.754295	1.21412	-0.459035			
AK7	CGGGACATCAATATCGACGAT	-0.79016	-0.37804	-0.608685	-0.230831667	-0.657506667	-0.41037
AK7	CAGAATAGACTTGCTATCAAA	0.10334	-0.475475	0.60831			
AK7	CTGGATGCTTCGGATGAGTTT	-0.005675	-1.119005	-1.230735			
AK8	CACGGTCCTGATCGAGAGAAA	1.23417	-1.052725	0.63521	0.690716667	-0.378515167	2.030858333
AK8	TCTGACCTATGTCCAAAGCAA	0.148725	0.1971195	4.047165			
AK8	CCTGGAGAACCTGATCTTAAA	0.689255	-0.27994	1.4102			
AKAP12	TCCCAGGCTAATGATATTGGA	0.824865	-0.318342	-0.175041	0.47408	-0.121970667	0.289691333
AKAP12	GACCATGACTGTTGAGGTAGA	0.188945	-0.51244	0.50145			
AKAP12	CACGAAACAGCTGTTACCGTA	0.40843	0.46487	0.542665			
AKAP14	GAGGATGAATTGACTCAAGTA	0.234465	0.069205	-1.94255	0.971031667	-0.571951667	-0.515105
AKAP14	AAACATCAAGTGGATGACTCA	1.86005	-0.87247	-0.49527			
AKAP14	TGCTGTTAAGATTGTGGAAGA	0.81858	-0.91259	0.892505			
AKAP7	CAAGTGCTAAGTTTAAAATAA	-2.234925	0.313345	0.6236075	-0.052911667	0.13702	-0.0847375
AKAP7	TGAACTAGTAAGGCTCAGTAA	1.07001	0.834185	0.202925			
AKAP7	AACCGAAGCAGCTGATCAGAA	1.00618	-0.73647	-1.080745			
AKAP8	AACGGAAGCAGTTCCAACTTT	-0.585485	0.620064	-0.72361	-0.312806333	0.041243	0.226181667
AKAP8	TTCCGTAGCTTTGATGACGAA	-0.209364	-0.741975	0.47921			
AKAP8	GGGCAGTACAGTGAATGCCGA	-0.14357	0.24564	0.922945			

AKAP8L	AAGGAACACTTTAAGTACGTA	0.2869465	-0.78643	0.6076395	0.349837167	-0.85151	0.959693167
AKAP8L	GACCATGGATCACAACCGGAA	0.456825	-0.68745	1.003825			
AKAP8L	TGCAGTCGACATACTCGGATA	0.30574	-1.08065	1.267615			
AKT1	CCGCGTGACCATGAACGAGTT	-1.64045	-0.476335	-1.05769	-1.1403	0.683715	0.060465
AKT1	CAGAACAATCCGATTCACGTA	1.16435	0.95688	-0.210715			
AKT1	CACGGTAGCACTTGACCTTTT	-2.9448	1.5706	1.4498			
AKT2	AACAACTTCTCCGTAGCAGAA	0.673985	-1.2591	0.784735	0.650081667	-1.009338333	0.22067
AKT2	CAGCAAGGCACGGGCTAAAGT	0.809485	-1.41585	-1.38595			
AKT2	AATGACTTCGACTATCTCAAA	0.466775	-0.353065	1.263225			
AKT3	AAGTAACATCTGAGACAGATA	0.331125	-0.2584475	0.0279	0.014841667	-0.8729825	0.253816667
AKT3	TTGGACTATCTACATTCCGGA	0.47205	-1.0956	0.04994			
AKT3	TGGCTCATTCATAGGATATAA	-0.75865	-1.2649	0.68361			
ALDH18A1	CAGCGTGATGAGATCCTGTTA	-2.0963	0.060975	-0.710685	-1.736921667	-0.112246667	-1.299006667
ALDH18A1	CTGGAATTATGCATTGAAGTA	-2.09415	-0.39763	-1.390535			
ALDH18A1	CACGGATGTCATCGTCACAGA	-1.020315	-8.5E-05	-1.7958			
ALK	ACCATGCTCTATTGCTCAGTA	0.69803	0.1282275	-1.043	0.118740183	0.3873725	-0.187414583
ALK	ACCTGTTTGAGAGAAACCCAA	-0.25344495	0.75001	-0.43943375			
ALK	TACAAACCAGTTAATCCAGAA	-0.0883645	0.28388	0.92019			
ALPK1	**GAGGAAGTGAATTATCACGTT**	**0.845335**	**-0.959875**	**-1.2756**	**0.885295**	**-0.891352833**	**-2.486783333**
ALPK1	**TAGAGATGTTGTGGTCGATTT**	**0.6783**	**-1.2067**	**-2.74435**			
ALPK1	**TTCCATGAGCAAGAACGATTA**	**1.13225**	**-0.5074835**	**-3.4404**			
ALPK2	TCCATCGGCCTGAGAACAATA	-0.04017	0.087185	0.684015	-0.105243333	-0.540210167	-0.531518333
ALPK2	TTCCATGACCTTCATTGATCA	0.492065	-0.6321455	-1.367915			
ALPK2	CTGGGCTGTACCTGATAGTCT	-0.767625	-1.07567	-0.910655			
ALPK3	CCGACTAGGCCTTTCAACAGA	-0.09607	0.7343555	-0.4874625	-0.41819	0.366420167	-0.049419833
ALPK3	CTGGTACAAGGATGATACGGA	-0.77255	0.089955	-0.097617			
ALPK3	ACCCATGGATATGGAAACCCA	-0.38595	0.27495	0.43682			
AMHR2	CACGACCACATTGTCCGATTT	0.788585	-1.06209	0.14222	0.586143333	-0.425053333	0.517788333
AMHR2	CAGAATGTGCTCATTCGGGAA	0.54608	0.19979	0.194995			
AMHR2	CACTGGGAGAGCTGCTAGATA	0.423765	-0.41286	1.21615			
ANKK1	TCAGCACATCGTGTCTATCTA	0.835698	0.1281	-0.316604	0.726725	0.1627985	-0.340424667
ANKK1	GGGCAAATACCTGATCTGCAA	1.56594	-0.036345	0.54373			
ANKK1	CAGGTTCCGCATCATCCATGA	-0.221463	0.3966405	-1.2484			
ARAF	ACCGAGATCTCAAGTCTAACA	1.36885	-0.0419295	-0.0709045	0.160413333	-0.4615915	-0.1419215
ARAF	CTGTGTTGACATGAGTACCAA	-1.588515	-0.46217	-0.41939			
ARAF	CATGCACAATTTTGTACGGAA	0.700905	-0.880675	0.06453			

Table S2. Results of the human kinome screen.

Data show Z-scored values of total cell counts, infection rates and IL-8 measurements obtained with CellProfiler for all genes targeted by the human kinome library (see Materials and Methods). Data are shown for all 3 individual sequences/gene or pooled.

(Adapted from Table S2. Showing first 40 proteins in alphabetical order. Full table can be found at: https://doi.org/10.1371/journal.ppat.1006224.s012)

DISCUSSION

The aim of my thesis was to dissect the cellular signalling pathways that lead to the activation of NF-κB and the production of IL-8 by bystander cells following enteroinvasive bacterial infections, using *S. flexneri* as a model pathogen. An RNAi screen enabled us to identify TIFA and TRAF6 as the potential candidates involved in this process, which we have verified and characterized. We have shown that following infection, TIFA forms oligomers. Their formation is dependent on the presence of a threonine at position 9, which can be phosphorylated and on its recognition by the FHA domain. These oligomers act as a platform for TRAF6 oligomerization and activation and the subsequent downstream activation of NF-κB in both infected and non-infected bystander cells, a process necessary for IL-8 production in the latter. In addition, we show that this is dependent on the presence of the kinase ALPK1, in the absence of which, no oligomerization of TIFA is observed. This is true for infections with the Gram-negative intracellular pathogens *S. flexneri* and *S. typhimurium* but not for the Gram-positive bacteria *L. monocytogenes* or other stimuli such as TNFα or the activator of PKC Phorbol, 12-myristate 13-acetate (PMA)

The specificity of this pathway is due to the presence of the newly identified PAMP, HBP, a cytosolic bacterial metabolite, which is an intermediate of the LPS synthetic pathway (Gaudet et al, 2015). We show that when bacteria are mutated for the enzyme which synthesises HBP, they no longer elicit TIFA oligomerization, NF-κB activation or IL-8 production. This is not due to a modified LPS since bacteria mutated for downstream enzymes of this pathway and presenting the same “deep rough” phenotype, are capable of inducing an inflammatory response like the wild-type bacteria. HBP is sensed in the cytosol of host cells (Gaudet et al., 2015) but the mechanisms by which it gains access remain unclear. The current hypotheses will be discussed in the following section. HBP is quite different to the PAMPs previously shown to be important during Gram-negative bacterial infections, particularly lipid A, ie-DAP and MDP. Firstly, it is intracellular, compared to the others, which are present on the bacterial surface. Secondly, HBP, as far as we know, is not part of a larger structure as is the case for the lipid A of LPS or ie-DAP and MDP of PGN. The relative contribution of the HBP-mediated inflammatory response in relation to that elicited by the aforementioned PAMPs still remains to be determined. It is likely that during infection, the sensing of different PAMPs leads to the independent but cumulative activation of the inflammatory response.

The results of this work show the importance of ALPK1 in the regulation of the early innate immune response to invasive Gram-negative bacteria in a HBP-dependent manner. This leads to the activation of the TIFA-TRAF6-NF-κB pathway and results in the production of inflammatory cytokines, particularly IL-8. This finding opens up a number of key questions, which still remain to

be explored: how does HBP enter into cells and how is it sensed; is ALPK1 the kinase which phosphorylates TIFA and what are the spatiotemporal dynamics of this process?

1 HBP delivery and detection

We and others have begun to unveil the role of HBP in the inflammatory response following both intracellular and extracellular Gram-negative bacterial infections (Gall et al., 2017; Gaudet et al., 2015, 2017; Milivojevic et al., 2017; Stein et al., 2017; Zimmermann et al., 2017). HBP is highly conserved among bacterial species including *E. coli*, *S. typhimurium*, S*. flexneri*, *Haemophilus influenzae, P. aeruginosa* and *H. pylori,* to name a few. It is becoming clear that for HBP to elicit a response, it must be released from the bacteria and detected in the host cell cytosol. Indeed, whole heat-killed extracellular bacteria do not activate epithelial cells, whereas transfected HBP-containing lysates do (Gaudet et al., 2015). However, how HBP is released from the bacterial cytosol and how it enters host cells during infection still remains to be defined. A number of hypotheses can be envisaged, which I will now discuss.

1.1 Endocytosis/ macropinocytosis?

In their work, Gaudet et al. proposed that HBP enters the host cell cytosol via endocytosis. In accordance, they found that blocking dynamin and thus clathrin-dependent endocytosis leads to the loss of response to HBP-containing lysates (Gaudet et al., 2015). We confirmed that HBP-containing lysates are capable of inducing NF-κB activation and IL-8 production in epithelial cells, most likely via a process of endocytosis. However, whilst host cells may be able to take up HBP via this mechanism, its significance during enteroinvasive bacterial infections remains to be determined. In the case of *N. gonorrhoeae*, which was used in the Gaudet study, HBP is released into the extracellular medium (Malott et al., 2013); however, this does not seem to be the case for other bacteria such as *E. coli* and *S. typhimurium* (Gaudet et al., 2015). One way for HBP to be liberated into the extracellular medium would be through residual lysis during growth. However, simply stimulating cells with the supernatant of cultured bacteria is not enough to induce a response (unpublished data, Gaudet et al, 2017). This may be due to a lack of HBP in the growth medium or due to a low concentration. It could be possible that although the concentration is low, it may be enhanced following the macropinocytosis induced during bacterial invasion. Weiner and colleagues showed that macropinosomes other than the BCV are formed following bacterial internalisation (Weiner et al., 2016). The lysis of these, or the BCV itself, may liberate HBP into the cytosol. We have begun to test this hypothesis by using the IpgD deletion mutant, which causes much less membrane ruffling and thus less macropinocytosis, as well as incomplete vacuolar rupture. The preliminary results show that there is no difference in the amount of IL-8

produced or in the number of cells with TIFA oligomers between WT and mutant bacteria (personal communication, unpublished data). This suggests that macropinocytosis is not the mechanism of HBP cytosolic delivery during *S. flexneri* infection. Further experiments are needed to confirm this result.

1.2 Intracellular lysis?

An alternative hypothesis proposed by Gaudet et al. is that HBP is released into the cytosol following bacterial lysis within phagocytic cells (Gaudet et al., 2015). Indeed, they found that non-invasive opsonised *E. coli* could induce the production of IL-6 in THP1 macrophages following phagocytosis and lysosomal degradation. This effect was eliminated with *ΔhldE* mutant. In addition, they found that TIFA oligomers co-localized with lysosome-associated protein (LAMP)-2 following stimulation of 293T cells with HBP, suggesting that HBP sensing is linked to the lysosome. Whilst lysosomal degradation of bacteria may be a way of liberating HBP into the host cell cytosol, its significance during enteroinvasive bacterial infections is questionable. *S. flexneri* has adapted to an intracellular life and its lysis within either macrophages or epithelial cells is rarely observed unless induced for example by treatment with antibiotics (Tattoli et al., 2008). Recently, the guanylate binding proteins(GBP) 2 and 5, which are IFN inducible genes, have been shown to promote bacteriolysis of the cytosolic bacteria *Francisella tularensis* subspecies *novicida* (Man et al., 2015; Meunier et al., 2015). This results in the liberation of bacterial DNA, which activates the AIM2 inflammasome in infected macrophages (Man et al., 2015; Meunier et al., 2015). Whether the same mechanisms could be at play during *S. flexneri* infection, either in macrophages or in epithelial cells, and whether this could, in part, contribute to the release of HBP, is not known. However, whilst this may happen in some cells, it is unlikely that it would occur at such a frequency consistent with the strong and reproducible response that we observe during infection. In addition, GBP-mediated bacteriolysis was observed 8 hours post-infection, which is incompatible with the early HBP-mediated response we observe. If GBPs could indeed be involved in the lysis of cytosolic *S. flexneri* and contribute to HBP release, it may be at later stages of infection.

1.3 Cytosolic bacterial replication?

Bacteria release a number of molecules, such as ATP (Mempin et al., 2013), quorum sensing molecules (Papenfort and Bassler, 2016) and metabolites (Sridharan et al., 2014) during replication, which can have an impact on host cell processes. Some of these molecules have been shown to activate an immune response such as the quorum-sensing molecule released by *P. aeruginosa,* which promotes neutrophil chemotaxis (Zimmermann et al., 2006), or the intracellular release of di-AMP by the invasive pathogen *Chlamydia trachomatis,* which activates the

inflammasome in infected macrophages in a STING-dependent manner (Webster et al., 2017). A further study by Gaudet et al. suggests that HBP is released by actively replicating *S. flexneri* in the host cell cytoplasm (Gaudet et al., 2017). Whilst the concentration of extracellularly released HBP may be low, it is concentrated when the bacteria are replicating in the cytosol (Gaudet et al., 2017). In addition they propose that TIFA acts as a sensor for bacterial growth, triggered by increasing cytosolic HBP concentrations (Gaudet et al., 2017). They found that NF-κB nuclear translocation within the first 60 min following infection was NOD-1-dependent but TIFA-independent. This was reversed 120 min post-infection with NF-κB activation becoming completely dependent on TIFA. These observations led them to propose a sequential model of inflammation whereby the first wave of PGN-dependent NOD1-mediated NF-κB activation may serve to upregulate TIFA expression which, independently of NOD-1, controls the later stages of infection-induced inflammation in response to HBP.

Our results do not contradict the proposal that TIFA may be involved in HBP-sensing at later stages of infection as the bacteria divide and release HBP into the host cytosol. Indeed, we see an increase in the number of cells, both infected and bystander, which possess TIFA oligomers with increasing time, whereby at 4h post-infection, it represents almost 100%. However, this model does not explain the TIFA activation that we observe as soon as 15 min post-infection. It could be due to very early bacterial replication within the infected cell. Indeed, Weiner et al. observed that some bacteria were in division in the BCV (Weiner et al., 2016). The resolution of the images used in this study does not allow us to exclude this possibility, although this may not account for every infected cell where TIFA oligomerization is observed. In addition, contrary to the study by Gaudet et al., we find that TIFA is central to early NF-κB activation following infection since there is no NF-κB nuclear translocation in the absence of TIFA from 15 min to 1 hour post infection. The discrepancies in our results likely originate from the different cellular models used during infection since different cell lines are known to have distinctive expression profiles and regulation of certain genes. Consistently, Gall et al. found that the IL-8 response to *H. pylori* was partially dependent on NOD1 in a gastric cell line, whereas it was solely TIFA-dependent in a colonic epithelial cell line (Gall et al., 2017).

In addition to the observation that HBP was released during bacterial replication and that TIFA acted as an intracellular sensor of bacterial growth, Gaudet et al. also showed that there was no potent NF-κB response if the bacteria remained in the vacuole as is this case with *S. typhimurium* (Gaudet et al., 2017). NF-κB activation increased when a Δ*sifA* mutant that escapes the vacuole was used but abrogated in the absence of TIFA suggesting that HBP was the activator. Previous studies have shown that a small proportion of *S. typhimurium* escape the *Salmonella* containing

vacuole (SCV) as soon as 15 min post-infection (Knodler et al., 2014b). This cytosolic population represents around 20% of bacteria within 90 min of infection, going up to 50% at later time points due to the increased rate of replication in the cytosol (Knodler et al., 2014b). GBPs have been shown to contribute to vacuolar rupture during *Salmonella* infection in mouse macrophages (Meunier et al., 2014), but this does not seem to be the case in human epithelial cells, since the human orthologue of mouse GBP2, hGBP1, did not co-localize with the SCV (Johnston et al., 2016). Vacuolar escape may, in part, explain the response we observe during *S. typhimurium* infection. However, it does not account for the observation that almost all *S. typhimurium* infected cells present TIFA oligomers. A recent publication showed that the SCV was leaky at early time points and later repaired by autophagy machinery (Kreibich et al., 2015). If HBP is released within the vacuole, the leakiness of the SCV along with vacuolar escape, could explain the early release of HBP into the cytosol during *Salmonella* infection.

1.4 T3SS-dependent delivery

A tempting hypothesis to explain the early TIFA-mediated response is that HBP could be delivered directly to the cytoplasm via the T3SS owing to its small size. HBP is predicted to have a size of around 10 Å (unpublished data), which would be sufficiently small to pass through the 20–30 Å needle structure. Although, to date, the T3SS has solely been associated with the delivery of proteins in a highly regulated manner, other bacterial secretion systems are known to deliver substrates other than proteins. The type IV secretion system present in many Gram-negative bacteria such as *H. pylori* is able to deliver DNA (Varga et al., 2016) and PGN fragments (Viala et al., 2004) into host cells. Interestingly, three recent publications have shown that HBP was necessary for the activation of TIFA-mediated IL-8 production during *H. pylori* infection and this, in a T4SS-dependent manner (Gall et al., 2017; Stein et al., 2017; Zimmermann et al., 2017). All three groups found that *H. pylori*'s ability to elicit a cellular response was dependent on the presence of the cag pathogenicity island, which encodes the T4SS. *ΔhldE* mutants of *H.pylori*, unlike *ΔgmhB* or *ΔwaaC* mutants, were unable to elicit a cellular response following infection. This was independent of the translocation of the oncogenic effector CagA (Stein et al., 2017; Zimmermann et al., 2017). *H. pylori*, unlike *Shigella* and *Salmonella*, is an extracellular pathogen but is capable of injecting the effector CagA into the host cell via its T4SS, suggesting that a possible way that HBP enters the host cytosol is via this apparatus. However, due to the fundamental differences in the architecture, design and mechanism for the translocation of bacterial substrates between the T3SS and T4SS, whether this could be relevant for the latter is unclear.

Investigating this hypothesis would not be without its challenges. One possibility of testing whether *S. flexneri* could secrete HBP via its T3SS would be to use a *ΔipaB* or *ΔipaD* mutant, which secrete constitutively (Ménard et al., 1994; Roehrich et al., 2013), or to induce secretion using the dye Congo red, using a T3SS null mutant as a control. The supernatant could then be analyzed by liquid chromatography and mass spectrometry to test for the presence of HBP. However, this would only tell us if HBP could be secreted in a T3SS-dependent manner and not whether it is relevant during infection. Without being able to directly visualise HBP within the needle structure, it would be difficult to definitively prove that it was passing directly via the T3SS. One approach to get closer to elucidating this possibility would be to use a bacterial mutant which was capable of secretion into host cells via the T3SS without entering. Uncoupling the two processes in *S. flexneri* is an obvious challenge since the same effectors involved in secretion via the T3SS are also involved in the entry process. To simplify this question, we could use an extracellular pathogen such as EPEC, which is capable of secreting effectors into the host cell cytosol whilst remaining on the outside. We would also need to block endocytosis in this case to make sure that residual HBP was not entering via this mechanism. This would give us a firm idea whether HBP entry into the host cell cytosol was dependent on the T3SS in the context of infection.

1.5 HBP sensing?

In parallel to deciphering how HBP is delivered, defining how it is detected in the host cell cytosol is of particular importance since it could provide a potential target for therapeutic purposes. Lectins are well known to bind sugar residues. Most of the well-studied lectins involved in the sensing of microbial glycans, such as CLRs, are present on the cell surface (Dambuza and Brown, 2015). Intracellular lectins are mainly found in the luminal compartments of the secretory pathway and function in the trafficking, sorting and targeting of maturing glycoproteins (Yamamoto, 2014). One group of intracellular lectins, called intelectins, have been shown to recognize a number of monosaccharide residues in microbial glycans (Wesener et al., 2015). Two genes exist in humans; intelectin 1 and 2, which are highly expressed in IECs. Whether intelectins can recognize HBP and whether they could be the intracellular receptor is unknown. However, lectins to date have only been implicated in the recognition of monosaccharides as part of glycans and not as a single sugar moiety. In addition, they did not appear as hits in the RNAi genome wide screen that was performed in our laboratory. Nonetheless, it could be interesting to explore this avenue using additional sets of siRNA sequences.

Alternatively, it could be envisaged that HBP is not directly sensed by a known PRR in the classical sense of the term. Recently, Wolf et al. found that a metabolic enzyme, hexokinase was able to initiate an immune response following infection (Wolf et al., 2016). They found that N-

acetylglucosamine (NAG), a sugar subunit of the backbone of PGN, could compete with glucose to bind to hexokinases, leading to their dissociation from the mitochondrial membrane (Wolf et al., 2016). This dissociation was enough to activate the NLRP3 inflammasome in macrophages. Perhaps a similar mechanism is involved in HBP sensing, whereby HBP might disrupt the function of a metabolic enzyme or other. The downstream ALPK1-TIFA-TRAF6- NF-κB signaling cascade may therefore be induced in response to changes within the cell akin to DAMPs rather than direct activation by the PAMP itself *per se*.

In order to elucidate which molecules are involved in HBP recognition, we could take a systematic approach and re-screen the unexploited hits identified in the primary RNAi screen. In contrast to the primary screen, which used IL-8 production as the readout, we would use the oligomerization of TIFA as a readout, allowing us to identify the most upstream events following HBP recognition. Alternatively, we could take a more active approach and use a HBP-based trifunctional probe to perform a pull-down. This probe would consist of HBP on one end, a photoactivatable group that upon UV exposure could stabilize the interaction by cross-linkage, and a biotin-based molecule, or similar, for purification. The associated proteins would then be analyzed by mass spectrometry. This approach would allow us to identify any proteins which could interact with HBP. However, without knowing which structures of HBP are important for its recognition, linking HBP to the probe may present a problem.

To address the question of the specificity of HBP recognition we could test different analogues of the molecule and observe which confirmations induce TIFA oligomerization and which do not. These modifications could include modifying the carbon chain length by the addition of a carbon or by altering the position of the phosphate groups. Mammals have ten basic monosaccharide entities: glucose, galactose, mannose, sialic acid, *N*-acetyl-d-glucosamine, *N*-acetyl-d-galactosamine, fucose, xylose, glucuronic acid, and iduronic acid, with the first three representing 75% of monosaccharides (Werz et al 2007). Along with the ten mammalian monosaccharides, bacteria have more than 100. Heptoses are particularly present in Gram-negative bacteria but absent in mammals. In addition, secondary modifications differ between mammalian and bacterial monosaccharides. In mammals, the *N*-acetylamino group is the most common substituent, whereas it is less common in bacteria. Bacteria harbor modifications which are rare or absent in mammals such as *O*-methylation, *O*-acetylation or amino or phosphate substituents (Herget et al., 2008). We expect that only analogues of HBP which do not resemble mammalian monosaccharides would be recognized and able to trigger inflammation.

2 Bystander cell activation?

Since bystander cells are the main producers of inflammatory cytokines during *S. flexneri* infection, it is important to determine how they are activated. A previous study by our group showed that cell-cell communication was dependent on gap junctions but the mediator is not known (Kasper et al, 2010). One hypothesis is that HBP could be the mediator. Given its small 370 Da size, it is conceivable that it could freely pass through the gap junctions, which allow the passage of molecules smaller than 1–2 kDa (Yeager and Nicholson, 1996). To show this, we would need a method of detecting HBP. An obvious but challenging solution would be to synthesise a fluorescent HBP, which could be microinjected into cells. However, we would need to make sure that the resulting molecule did not interfere with HBP's ability to pass through gap junctions, which are thought to have a channel size of around 1.5 nm (Bennett, 2007). Even small nanoprobes, such as quantum dots and fluorescent nanodiamonds (Vlasov et al., 2014), may be too big to allow passage through gap junctions. Alternatively, smaller probes such as fluorescent dyes or boronic acid-based chemosensors, which have been shown to specifically bind monosaccharides (Wu et al., 2013), could be used. However, whether these molecules could be linked to or modified to specifically recognize HBP within the cell is not clear. Even if we were able to fluorescently trace HBP intracellularly, its physical ability to pass through gap junctions does not prove that this is what happens during infection. Introducing fluorescent HBP into the bacteria and being able to trace it during infection is a different challenge altogether. So whilst this presents a tempting hypothesis, the feasibility of proving it remains challenging.

An alternative hypothesis for bystander cell activation is that a second messenger produced following HBP recognition in the infected cell passes through gap junctions as Ablasser et al. observed during viral infection (Ablasser et al., 2013). They found that cGAMP, produced following viral DNA sensing in the infected cell, could pass through gap junctions to activate the antiviral interferon response in uninfected bystander cells. Whether the same mechanism, albeit with a different second messenger, is responsible for bystander cell activation in our model of infection remains to be explored.

Identifying the HBP receptor may give us a clue as to which of these two hypotheses is more likely. If HBP has a specific PRR, it would seem more logical that HBP itself was passing through the gap junctions and activating bystander cells since the same ALPK1-TIFA-TRAF6 pathway is activated in both cell types. On the other hand, if HBP activates a DAMP-like signal such as that observed with NAG and hexokinases, these changes may induce the production of second messengers, which could activate the ALPK1-TIFA-TRAF6 pathway both in the infected and bystander cells. The eventuality that the same pathway could be triggered through the recognition

of HBP itself in infected cells and a secondary messenger in bystander cells seems unlikely but remains to be determined.

3 The role of ALPK1

In addition to the questions surrounding HBP, the role of ALPK1 is still poorly understood. Here, we show that ALPK1 is necessary for the formation of TIFA oligomers and the ensuing cell signalling cascade, and that this is dependent on its kinase domain. Whilst this is an exciting starting point, it will be necessary to further characterize the protein interactions of ALPK1 in order to fully understand its function.

3.1 HBP receptor?

As previously described, it is unclear how HBP is recognized within the cell. Since ALPK1 acts upstream of TIFA, it is the closest candidate to the source. Whether ALPK1 could be the direct intracellular receptor of HBP remains to be determined, although nothing in the literature until now gives us any hint of this eventuality. Certain proteins, such as receptor tyrosine kinases, are known to have the dual roles of molecular recognition as well as kinase activity (Lemmon and Schlessinger, 2010). In addition, as previously mentioned, hexokinases have been recently shown to bind NAG of PGN. Most kinases, however, act in the signalling cascade downstream of receptors. In order to investigate whether ALPK1 could be implicated in the recognition process, we have started looking at its localization during *S. flexneri* infection. Although the localization and function of a protein are not necessarily linked, it provides a good starting point.

Whilst it is not clear where HBP recognition happens, given that it happens very early on suggests that it may be connected with bacterial entry or vacuolar lysis. Preliminary experiments into the localization of ALPK1 at 10–15 min post infection suggest that it may be present at the bacterial entry site. However, the observation that this localization is observed both with WT and *ΔhldE* bacteria implies that it is HBP-independent (Figure 16). ALPK1 has been shown to associate with the cytoskeleton (Heine et al., 2005), suggesting that its localization at the entry site may be a non-directed accumulation caused by membrane ruffling rather than specific recruitment. In addition, we observe some ALPK1 surrounding intracellular bacteria at 15 min post-infection. Again, it is unclear whether this is a specific recruitment or whether it is “residual” ALPK1 which had accumulated at the entry site and had not yet dispersed (unpublished data). High resolution live imaging will help us elucidate the spatiotemporal behaviour of ALPK1 at these early time-points of infection.

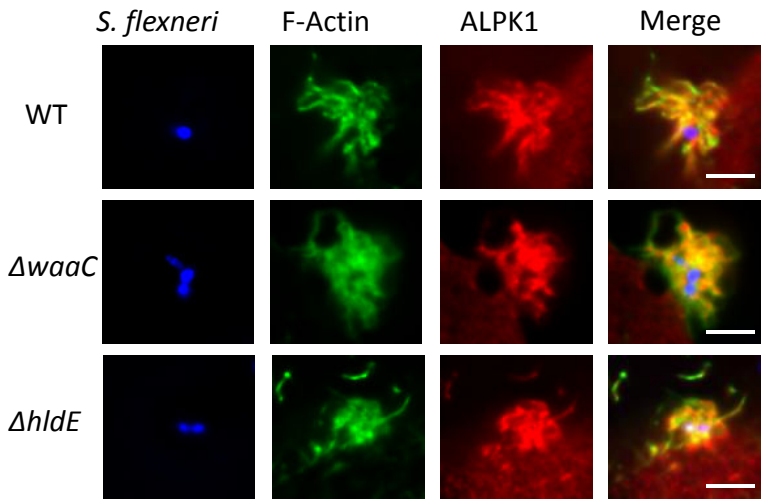

Figure 16. ALPK1 localization at the *S. flexneri* entry site. Actin foci (green) at the *S. flexneri* (blue) entry site 10 min post infection. Images show entry foci following infection with WT *S. flexneri* as well as the *ΔwaaC* and *ΔhldE* mutants. ALPK1 is shown in red. Scale bar; 5µm.

3.2 ALPK1 substrates and interaction partners?

In our work, we have shown that the kinase activity of ALPK1 is necessary for the oligomerization of TIFA; however, whether it is responsible for the direct phosphorylation of the threonine 9 is unknown. Alpha kinases were first so named since they recognize substrates in an alpha-helical formation yet this does not seem to be exclusive (Clark et al., 2008; Jørgensen et al., 2003). Therefore, although TIFA does not have an alpha-helical formation, this does not exclude the possibility that it is the substrate of ALPK1. In order to determine whether ALPK1 could phosphorylate TIFA, we would need to perform an *in vitro* kinase assay. Conversely, ALPK1 may be an intermediate that does not directly phosphorylate TIFA or that acts as part of a larger complex. To test this eventuality, we performed a pull-down of ALPK1 in the presence or absence of infection and characterized the associated proteins via mass spectrometry. We have generated a list of interaction partners, which will need to be further tested and verified. Amongst the interaction partners, we find moesin, filamin A and tubulin B (unpublished data). These proteins seem to be associated with ALPK1 constitutively and may promote its interaction with the actin cytoskeleton or microtubules. Interestingly, ALPK1 interacts with the proteins BAG2 (BCL2 associated athanogene 2), AHNAK (neuroblast differentiation-associated protein) and ANXA2 (annexin A2) (unpublished data). These proteins interact with each other and were found to be specifically recruited to the entry site during *Salmonella* infection (Jolly et al., 2014). Whether they are also recruited to the *S. flexneri* entry site and whether ALPK1 could be recruited with them is not known but may offer an explanation as to why we observe ALPK1 at the entry site and therefore should be explored further. Whilst this preliminary experiment has given us a first

indication of ALPK1's interaction partners, it does not provide an exhaustive list and further experiments will be needed to confirm the results.

3.3 Role of ALPK1 in immune cells?

Due to the central role of ALPK1 in inflammatory signalling in epithelial cells, it will be interesting to decipher its role in specialised immune cells such as macrophages, dendritic cells and T and B lymphocytes. Gaudet et al. found that THP1 macrophages produced IL-8 following HBP stimulation in a TIFA-dependent manner (Gaudet et al., 2015). In addition, they found that at least part of the IL-6 production following opsonized *E. coli* internalisation by THP1 macrophages was HBP- and TIFA-dependent. In accordance, our preliminary results show that myd88 KO THP1 macrophages respond to *S. flexneri* lysates in a HBP-dependent manner and that there is the formation of TIFA oligomers (unpublished data). The next step will be to determine whether, as in epithelial cells, ALPK1 is essential for this. How much HBP sensing contributes to the inflammatory response in immune cells during infection is questionable. Unlike epithelial cells, which generally have a low expression of cell surface PRRs, the expression of these molecules is very high in immune cells, as is the expression of other cytosolic receptors. It is possible that during infection the HBP signal is drowned out amongst all of the other PAMP-induced signalling pathways, particularly LPS induced TLR4 signalling. HBP recognition may, however, have a stronger significance against bacteria with a LPS which has been modified to avoid eliciting an immune response, such as *H. pylori* (Chmiela et al., 2014), or offer a distinct branch of signalling, which allows the fine tuning of the immune response.

Interestingly, TIFA has recently been shown to be implicated in the activation of the NLRP3 inflammasome following oxidative stress and resulting in the production of IL-1β and IL-18. Its phosphorylation was attributed to the kinase Akt (Lin et al., 2016). It would be interesting to determine whether TIFA is involved in inflammasome activation during bacterial infections, such as the *Shigella*-induced macrophage pyroptotic cell death. If it proves to be the case, determining whether ALPK1 is involved in this process or whether TIFA also acts independently of ALPK1 will be important.

3.4 ALPK1, a wider implication?

As previously mentioned, there is little literature available on the role of ALPK1. Of the most commonly reported associations, and for which some mechanistic explanation has been proposed, is its role in gout. ALPK1 was shown to be involved in the upregulation of TNFα, IL-1β and IL-8 production in a MAPK-dependent pathway following stimulation with MSU crystals (Wang et al., 2011). Whether this is in a TIFA-dependent manner or not is unknown but it is possible that

ALPK1 may be more largely involved in inflammatory pathways and possibly in a TIFA-independent manner. Whether there is a link between ALPK1's role in inflammation and the wide range of diseases with which it is associated, from heart and kidney disease to diabetes and cancers, such as breast and colorectal cancers, could be an interesting avenue to explore. The identification of the interaction partners of ALPK1 as mentioned above may provide an insight into this possibility, although this is going outside the scope of our work.

3.5 Therapeutic potential?

Whilst more work will be needed to characterise the exact role and function of ALPK1 and to attain confirmation in *in vivo* models, it is tempting to speculate that ALPK1 could present a potential therapeutic target given its central role in HBP-induced inflammation and low levels of shared homology with other kinases (Middelbeek et al., 2010). Considering the possible applications of ALPK1 as a therapeutic agent, two main scenarios can be envisaged in terms of bacterial infections. Firstly, blocking ALPK1 may help to decrease the HBP-dependent acute inflammation at the very early stages of Gram-negative bacterial infections. Whilst excessive inflammation is deleterious, retaining a certain level is necessary for bacterial clearance. Targeting ALPK1 could ensure that inflammation was only attenuated and not abrogated. However, in the case of acute inflammation, only a small window of opportunity exists where targeting ALPK1 may be beneficial. In practice, by the time the symptoms are already manifesting, this approach would probably offer limited advantages.

Alternatively, blocking ALPK1 may be advantageous in infections where chronic inflammation is the problem. For example, *H. pylori* infection may cause chronic inflammation of the gastric mucosa leading to complications such as peptic ulcers, gastric adenocarcinomas and lymphomas (White et al., 2015). TIFA has recently been shown to play a central role in HBP-dependent *H. pylori* induced inflammation (Gall et al., 2017; Stein et al., 2017). We and Zimmerman et al. have confirmed this result and in addition have found that ALPK1 is regulating this pathway as is observed during enteroinvasive bacterial infections (Unpublished data, Zimmermann et al., 2017). Further studies will be needed to determine the role of ALPK1-TIFA mediated activation in terms of *H. pylori* induced chronic inflammation. However, if a link is found, ALPK1 may offer a potential target to reduce chronic inflammation, which may decrease the risks of developing the associated diseases.

Whether ALPK1 could be a potential target in other chronic inflammatory disorders such as inflammatory bowel disease is unclear. IBD, at least in part, is caused or exacerbated by the intestinal microbiota and an abhorrent immune response (Abraham and Medzhitov, 2011). The chronic inflammation observed during IBD also pre-disposes patients to colitis associated cancers.

Whether ALPK1 may be implicated, given its links to inflammation, cancer and bacterial sensing, is all speculative for the moment; however, if there proves to be a link, the therapeutic potential of targeting ALPK1 could be very important.

4 Concluding remarks

The aim of this work was to characterise the signalling pathways involved in the immune response following enteroinvasive bacterial infections in epithelial cells. To this effect, we have identified a key and novel ALPK1-TIFA-TRAF6 signalling pathway. This pathway is specifically activated by the newly identified bacterial PAMP, HBP. Following HBP detection in the host cell cytosol, TIFA forms oligomers, which are dependent on the threonine at position 9 and the FHA domain. These structures interact with TRAF6 and are necessary for the downstream activation of NF-κB and the subsequent production of pro-inflammatory cytokines. The kinase activity of ALPK1 is indispensable for this process. We have shown that this pathway is activated in both infected and bystander cells, with the latter being necessary for IL-8 production. The identification of this novel pathway shows that epithelial cells are capable of detecting and responding to bacterial infections in response to different stimuli. The presence of multiple pathways most likely ensures the fine-tuning of the immune response to invading pathogens. Whilst many questions still remain surrounding the molecular mechanisms involved in the delivery, sensing of HBP and the activation of this pathway, the identification of the master regulator ALPK1 is an important first step. It is conceivable that ALPK1 could potentially be used as a therapeutic target to control inflammation both in acute and chronic Gram-negative bacterial infections and perhaps even beyond.

References

Aachoui, Y., Leaf, I.A., Hagar, J.A., Fontana, M.F., Campos, C.G., Zak, D.E., Tan, M.H., Cotter, P.A., Vance, R.E., Aderem, A., et al. (2013). Caspase-11 protects against bacteria that escape the vacuole. Science *339*, 975.

Abbott, D.W., Yang, Y., Hutti, J.E., Madhavarapu, S., Kelliher, M.A., and Cantley, L.C. (2007). Coordinated Regulation of Toll-Like Receptor and NOD2 Signaling by K63-Linked Polyubiquitin Chains. Mol. Cell. Biol. *27*, 6012.

Ablasser, A., Schmid-Burgk, J.L., Hemmerling, I., Horvath, G.L., Schmidt, T., Latz, E., and Hornung, V. (2013). Cell intrinsic immunity spreads to bystander cells via the intercellular transfer of cGAMP. Nature *503*, 530–534.

Abraham, C., and Medzhitov, R. (2011). Interactions Between the Host Innate Immune System and Microbes in Inflammatory Bowel Disease. Gastroenterology *140*, 1729.

Abreu, M.T. (2010). Toll-like receptor signalling in the intestinal epithelium: how bacterial recognition shapes intestinal function. Nat. Rev. Immunol. *10*, 131–144.

Abreu, M.T., Vora, P., Faure, E., Thomas, L.S., Arnold, E.T., and Arditi, M. (2001). Decreased expression of Toll-like receptor-4 and MD-2 correlates with intestinal epithelial cell protection against dysregulated proinflammatory gene expression in response to bacterial lipopolysaccharide. J. Immunol. Baltim. Md 1950 *167*, 1609–1616.

Abreu, M.T., Arnold, E.T., Thomas, L.S., Gonsky, R., Zhou, Y., Hu, B., and Arditi, M. (2002). TLR4 and MD-2 expression is regulated by immune-mediated signals in human intestinal epithelial cells. J. Biol. Chem. *277*, 20431–20437.

Aderem, A., and Ulevitch, R.J. (2000). Toll-like receptors in the induction of the innate immune response. Nature *406*, 782–787.

Akeda, Y., and Galán, J.E. (2005). Chaperone release and unfolding of substrates in type III secretion. Nature *437*, 911–915.

Akira, S., Uematsu, S., and Takeuchi, O. (2006). Pathogen Recognition and Innate Immunity. Cell *124*, 783–801.

Allaoui, A., Sansonetti, P.J., and Parsot, C. (1993). MxiD, an outer membrane protein necessary for the secretion of the Shigella flexneri Ipa invasins. Mol. Microbiol. *7*, 59–68.

Allen, I.C., Wilson, J.E., Schneider, M., Lich, J.D., Roberts, R.A., Arthur, J.C., Woodford, R.-M.T., Davis, B.K., Uronis, J.M., Herfarth, H.H., et al. (2012). NLRP12 Suppresses Colon Inflammation and Tumorigenesis through the Negative Regulation of Noncanonical NF-κB Signaling. Immunity *36*, 742–754.

Arbibe, L., Kim, D.W., Batsche, E., Pedron, T., Mateescu, B., Muchardt, C., Parsot, C., and Sansonetti, P.J. (2007). An injected bacterial effector targets chromatin access for transcription factor NF-κB to alter transcription of host genes involved in immune responses. Nat. Immunol. *8*, 47–56.

Arondel, J., Singer, M., Matsukawa, A., Zychlinsky, A., and Sansonetti, P.J. (1999). Increased Interleukin-1 (IL-1) and Imbalance between IL-1 and IL-1 Receptor Antagonist during Acute Inflammation in Experimental Shigellosis. Infect. Immun. *67*, 6056–6066.

Arthur, J.S.C. (2008). MSK activation and physiological roles. Front. Biosci. J. Virtual Libr. *13*, 5866–5879.

Ashida, H., and Sasakawa, C. (2016). Shigella IpaH Family Effectors as a Versatile Model for Studying Pathogenic Bacteria. Front. Cell. Infect. Microbiol. *5*.

Ashida, H., Kim, M., Schmidt-Supprian, M., Ma, A., Ogawa, M., and Sasakawa, C. (2010). A bacterial E3 ubiquitin ligase IpaH9.8 targets NEMO/IKKγ to dampen the host NF-κB-mediated inflammatory response. Nat. Cell Biol. *12*, 66–69.

Ashida, H., Ogawa, M., Mimuro, H., Kobayashi, T., Sanada, T., and Sasakawa, C. (2011). Shigella are versatile mucosal pathogens that circumvent the host innate immune system. Curr. Opin. Immunol. *23*, 448–455.

Ashida, H., Nakano, H., and Sasakawa, C. (2013). Shigella IpaH0722 E3 Ubiquitin Ligase Effector Targets TRAF2 to Inhibit PKC–NF-κB Activity in Invaded Epithelial Cells. PLOS Pathog. *9*, e1003409.

Ataie-Kachoie, P., Pourgholami, M.H., Richardson, D.R., and Morris, D.L. (2014). Gene of the month: Interleukin 6 (IL-6). J. Clin. Pathol. *67*, 932–937.

Ayabe, T., Satchell, D.P., Wilson, C.L., Parks, W.C., Selsted, M.E., and Ouellette, A.J. (2000). Secretion of microbicidal alpha-defensins by intestinal Paneth cells in response to bacteria. Nat. Immunol. *1*, 113–118.

Barman, S., Saha, D.R., Ramamurthy, T., and Koley, H. (2011). Development of a new guinea-pig model of shigellosis. FEMS Immunol. Med. Microbiol. *62*, 304–314.

Bauernfeind, F., Horvath, G., Stutz, A., Alnemri, E.S., MacDonald, K., Speert, D., Fernandes-Alnemri, T., Wu, J., Monks, B.G., Fitzgerald, K.A., et al. (2009). NF-kB activating pattern recognition and cytokine receptors license NLRP3 inflammasome activation by regulating NLRP3 expression. J. Immunol. Baltim. Md 1950 *183*, 787.

Beck-Schimmer, B., Schimmer, R.C., Warner, R.L., Schmal, H., Nordblom, G., Flory, C.M., Lesch, M.E., Friedl, H.P., Schrier, D.J., and Ward, P.A. (1997). Expression of Lung Vascular and Airway ICAM-1 after Exposure to Bacterial Lipopolysaccharide. Am. J. Respir. Cell Mol. Biol. *17*, 344–352.

Beinke, S., Robinson, M.J., Hugunin, M., and Ley, S.C. (2004). Lipopolysaccharide activation of the TPL-2/MEK/extracellular signal-regulated kinase mitogen-activated protein kinase cascade is regulated by IkappaB kinase-induced proteolysis of NF-kappaB1 p105. Mol. Cell. Biol. *24*, 9658–9667.

Bennett, M. (2007). Gap junctions. In New Encyclopedia of Neuroscience, L. Squire, ed. (Academic Press), p.

Bergsbaken, T., Fink, S.L., and Cookson, B.T. (2009). Pyroptosis: host cell death and inflammation. Nat. Rev. Microbiol. *7*, 99–109.

Bernardini, M.L., Mounier, J., d'Hauteville, H., Coquis-Rondon, M., and Sansonetti, P.J. (1989). Identification of icsA, a plasmid locus of Shigella flexneri that governs bacterial intra- and intercellular spread through interaction with F-actin. Proc. Natl. Acad. Sci. U. S. A. *86*, 3867–3871.

Bertin, J., Nir, W.-J., Fischer, C.M., Tayber, O.V., Errada, P.R., Grant, J.R., Keilty, J.J., Gosselin, M.L., Robison, K.E., Wong, G.H.W., et al. (1999). Human CARD4 Protein Is a Novel CED-4/Apaf-1 Cell Death Family Member That Activates NF-κB. J. Biol. Chem. *274*, 12955–12958.

Blocker, A., Gounon, P., Larquet, E., Niebuhr, K., Cabiaux, V., Parsot, C., and Sansonetti, P. (1999). The Tripartite Type III Secreton of Shigella flexneri Inserts Ipab and Ipac into Host Membranes. J. Cell Biol. *147*, 683.

Blocker, A., Jouihri, N., Larquet, E., Gounon, P., Ebel, F., Parsot, C., Sansonetti, P., and Allaoui, A. (2001). Structure and composition of the Shigella flexneri "needle complex", a part of its type III secreton. Mol. Microbiol. *39*, 652–663.

Blocker, A., Komoriya, K., and Aizawa, S.-I. (2003). Type III secretion systems and bacterial flagella: Insights into their function from structural similarities. Proc. Natl. Acad. Sci. *100*, 3027–3030.

Bowen, A. (2017). Chapter 3 - shigellosis. In CDC Yellow Book 2018: Health Information for International Travel, G. Brunette, ed. (Oxford, New York: Oxford University Press), p.

Branger, J., Knapp, S., Weijer, S., Leemans, J.C., Pater, J.M., Speelman, P., Florquin, S., and van der Poll, T. (2004). Role of Toll-like receptor 4 in gram-positive and gram-negative pneumonia in mice. Infect. Immun. *72*, 788–794.

Buchrieser, C., Glaser, P., Rusniok, C., Nedjari, H., D'Hauteville, H., Kunst, F., Sansonetti, P., and Parsot, C. (2000). The virulence plasmid pWR100 and the repertoire of proteins secreted by the type III secretion apparatus of Shigella flexneri. Mol. Microbiol. *38*, 760–771.

Cao, Z., Xiong, J., Takeuchi, M., Kurama, T., and Goeddel, D.V. (1996). TRAF6 is a signal transducer for interleukin-1. Nature *383*, 443–446.

Carayol, N., and Tran Van Nhieu, G. (2013). Tips and tricks about Shigella invasion of epithelial cells. Curr. Opin. Microbiol. *16*, 32–37.

Cario, E., and Podolsky, D.K. (2000). Differential Alteration in Intestinal Epithelial Cell Expression of Toll-Like Receptor 3 (TLR3) and TLR4 in Inflammatory Bowel Disease. Infect. Immun. *68*, 7010.

Caruso, R., Warner, N., Inohara, N., and Núñez, G. (2014). NOD1 and NOD2: Signaling, Host Defense, and Inflammatory Disease. Immunity *41*, 898–908.

Chamaillard, M., Hashimoto, M., Horie, Y., Masumoto, J., Qiu, S., Saab, L., Ogura, Y., Kawasaki, A., Fukase, K., Kusumoto, S., et al. (2003). An essential role for NOD1 in host recognition of bacterial peptidoglycan containing diaminopimelic acid. Nat. Immunol. *4*, 702–707.

Chassin, C., Picardeau, M., Goujon, J.-M., Bourhy, P., Quellard, N., Darche, S., Badell, E., d'Andon, M.F., Winter, N., Lacroix-Lamandé, S., et al. (2009). TLR4- and TLR2-mediated B cell responses control the clearance of the bacterial pathogen, Leptospira interrogans. J. Immunol. Baltim. Md 1950 *183*, 2669–2677.

Chen, G.Y. (2014). Role of Nlrp6 and Nlrp12 in the maintenance of intestinal homeostasis. Eur. J. Immunol. *44*, 321–327.

Chen, Z., Hagler, J., Palombella, V.J., Melandri, F., Scherer, D., Ballard, D., and Maniatis, T. (1995). Signal-induced site-specific phosphorylation targets I kappa B alpha to the ubiquitin-proteasome pathway. Genes Dev. *9*, 1586–1597.

Chiba, T., Matsuo, H., Sakiyama, M., Nakayama, A., Shimizu, S., Wakai, K., Suma, S., Nakashima, H., Sakurai, Y., Shimizu, T., et al. (2015). Common variant of ALPK1 is not associated with gout: a replication study. Hum. Cell *28*, 1–4.

Chmiela, M., Miszczyk, E., and Rudnicka, K. (2014). Structural modifications of Helicobacter pylori lipopolysaccharide: an idea for how to live in peace. World J. Gastroenterol. *20*, 9882–9897.

Ciacci-Woolwine, F., Blomfield, I.C., Richardson, S.H., and Mizel, S.B. (1998). Salmonella flagellin induces tumor necrosis factor alpha in a human promonocytic cell line. Infect. Immun. *66*, 1127–1134.

Clark, K., Middelbeek, J., Dorovkov, M.V., Figdor, C.G., Ryazanov, A.G., Lasonder, E., and van Leeuwen, F.N. (2008). The alpha-kinases TRPM6 and TRPM7, but not eEF-2 kinase, phosphorylate the assembly domain of myosin IIA, IIB and IIC. FEBS Lett. *582*, 2993–2997.

Conze, D.B., Wu, C.-J., Thomas, J.A., Landstrom, A., and Ashwell, J.D. (2008). Lys63-linked polyubiquitination of IRAK-1 is required for interleukin-1 receptor- and toll-like receptor-mediated NF-kappaB activation. Mol. Cell. Biol. *28*, 3538–3547.

Cordes, F.S., Komoriya, K., Larquet, E., Yang, S., Egelman, E.H., Blocker, A., and Lea, S.M. (2003). Helical structure of the needle of the type III secretion system of Shigella flexneri. J. Biol. Chem. *278*, 17103–17107.

Cornelis, G.R. (2006). The type III secretion injectisome. Nat. Rev. Microbiol. *4*, 811–825.

Cossart, P. (2011). Illuminating the landscape of host–pathogen interactions with the bacterium Listeria monocytogenes. Proc. Natl. Acad. Sci. U. S. A. *108*, 19484–19491.

Dambuza, I.M., and Brown, G.D. (2015). C-type lectins in immunity: recent developments. Curr. Opin. Immunol. *32*, 21–27.

Deng, L., Wang, C., Spencer, E., Yang, L., Braun, A., You, J., Slaughter, C., Pickart, C., and Chen, Z.J. (2000). Activation of the IkappaB kinase complex by TRAF6 requires a dimeric ubiquitin-conjugating enzyme complex and a unique polyubiquitin chain. Cell *103*, 351–361.

Desroy, N., Moreau, F., Briet, S., Fralliec, G.L., Floquet, S., Durant, L., Vongsouthi, V., Gerusz, V., Denis, A., and Escaich, S. (2009). Towards Gram-negative antivirulence drugs: New inhibitors of HldE kinase. Bioorg. Med. Chem. *17*, 1276–1289.

Desroy, N., Denis, A., Oliveira, C., Atamanyuk, D., Briet, S., Faivre, F., LeFralliec, G., Bonvin, Y., Oxoby, M., Escaich, S., et al. (2013). Novel HldE-K Inhibitors Leading to Attenuated Gram Negative Bacterial Virulence. J. Med. Chem. *56*, 1418–1430.

DiDonato, J.A., Hayakawa, M., Rothwarf, D.M., Zandi, E., and Karin, M. (1997). A cytokine-responsive IkappaB kinase that activates the transcription factor NF-kappaB. Nature *388*, 548–554.

Diepold, A., and Armitage, J.P. (2015). Type III secretion systems: the bacterial flagellum and the injectisome. Philos. Trans. R. Soc. Lond. B. Biol. Sci. *370*.

Dinarello, C.A. (1991). Interleukin-1 and interleukin-1 antagonism. Blood *77*, 1627–1652.

Dinarello, C.A. (2009). Immunological and Inflammatory Functions of the Interleukin-1 Family. Annu. Rev. Immunol. *27*, 519–550.

Dolowschiak, T., Chassin, C., Mkaddem, S.B., Fuchs, T.M., Weiss, S., Vandewalle, A., and Hornef, M.W. (2010). Potentiation of Epithelial Innate Host Responses by Intercellular Communication. PLOS Pathog. *6*, e1001194.

Dorsett, Y., and Tuschl, T. (2004). siRNAs: applications in functional genomics and potential as therapeutics. Nat. Rev. Drug Discov. *3*, 318–329.

DuPont, H.L., Levine, M.M., Hornick, R.B., and Formal, S.B. (1989). Inoculum size in shigellosis and implications for expected mode of transmission. J. Infect. Dis. *159*, 1126–1128.

Dupont, N., Lacas-Gervais, S., Bertout, J., Paz, I., Freche, B., Van Nhieu, G.T., van der Goot, F.G., Sansonetti, P.J., and Lafont, F. (2009). Shigella phagocytic vacuolar membrane remnants participate in the cellular response to pathogen invasion and are regulated by autophagy. Cell Host Microbe *6*, 137–149.

Dziarski, R. (2003). Recognition of bacterial peptidoglycan by the innate immune system. Cell. Mol. Life Sci. CMLS *60*, 1793–1804.

Ea, C.-K., Sun, L., Inoue, J.-I., and Chen, Z.J. (2004). TIFA activates IkappaB kinase (IKK) by promoting oligomerization and ubiquitination of TRAF6. Proc. Natl. Acad. Sci. U. S. A. *101*, 15318–15323.

Eckmann, L., Kagnoff, M.F., and Fierer, J. (1993). Epithelial cells secrete the chemokine interleukin-8 in response to bacterial entry. Infect. Immun. *61*, 4569.

Eferl, R., and Wagner, E.F. (2003). AP-1: a double-edged sword in tumorigenesis. Nat. Rev. Cancer *3*, 859–868.

Egile, C., Loisel, T.P., Laurent, V., Li, R., Pantaloni, D., Sansonetti, P.J., and Carlier, M.F. (1999). Activation of the CDC42 effector N-WASP by the Shigella flexneri IcsA protein promotes actin nucleation by Arp2/3 complex and bacterial actin-based motility. J. Cell Biol. *146*, 1319–1332.

Elinav, E., Strowig, T., Kau, A.L., Henao-Mejia, J., Thaiss, C.A., Booth, C.J., Peaper, D.R., Bertin, J., Eisenbarth, S.C., Gordon, J.I., et al. (2011). NLRP6 inflammasome regulates colonic microbial ecology and risk for colitis. Cell *145*, 745–757.

Epler, C.R., Dickenson, N.E., Olive, A.J., Picking, W.L., and Picking, W.D. (2009). Liposomes recruit IpaC to the Shigella flexneri type III secretion apparatus needle as a final step in secretion induction. Infect. Immun. *77*, 2754–2761.

Espina, M., Olive, A.J., Kenjale, R., Moore, D.S., Ausar, S.F., Kaminski, R.W., Oaks, E.V., Middaugh, C.R., Picking, W.D., and Picking, W.L. (2006). IpaD localizes to the tip of the type III secretion system needle of Shigella flexneri. Infect. Immun. *74*, 4391–4400.

Fernandez, M.I., Thuizat, A., Pedron, T., Neutra, M., Phalipon, A., and Sansonetti, P.J. (2003). A newborn mouse model for the study of intestinal pathogenesis of shigellosis. Cell. Microbiol. *5*, 481–491.

Fielding, C.A., McLoughlin, R.M., McLeod, L., Colmont, C.S., Najdovska, M., Grail, D., Ernst, M., Jones, S.A., Topley, N., and Jenkins, B.J. (2008). IL-6 Regulates Neutrophil Trafficking during Acute Inflammation via STAT3. J. Immunol. *181*, 2189–2195.

Franchi, L., Kamada, N., Nakamura, Y., Burberry, A., Kuffa, P., Suzuki, S., Shaw, M.H., Kim, Y.-G., and Núñez, G. (2012). NLRC4-driven production of IL-1β discriminates between pathogenic and commensal bacteria and promotes host intestinal defense. Nat. Immunol. *13*, 449–456.

Frey, H., Schroeder, N., Manon-Jensen, T., Iozzo, R.V., and Schaefer, L. (2013). Biological interplay between proteoglycans and their innate immune receptors in inflammation. FEBS J. *280*, 2165.

Fujimaki, T., Horibe, H., Oguri, M., Kato, K., and Yamada, Y. (2014). Association of genetic variants of the α-kinase 1 gene with myocardial infarction in community-dwelling individuals. Biomed. Rep. *2*, 127–131.

Fukazawa, A., Alonso, C., Kurachi, K., Gupta, S., Lesser, C.F., McCormick, B.A., and Reinecker, H.-C. (2008). GEF-H1 Mediated Control of NOD1 Dependent NF-κB Activation by Shigella Effectors. PLOS Pathog. *4*, e1000228.

Fukumatsu, M., Ogawa, M., Arakawa, S., Suzuki, M., Nakayama, K., Shimizu, S., Kim, M., Mimuro, H., and Sasakawa, C. (2012). Shigella targets epithelial tricellular junctions and uses a noncanonical clathrin-dependent endocytic pathway to spread between cells. Cell Host Microbe *11*, 325–336.

Fusunyan, R.D., Nanthakumar, N.N., Baldeon, M.E., and Walker, W.A. (2001). Evidence for an innate immune response in the immature human intestine: toll-like receptors on fetal enterocytes. Pediatr. Res. *49*, 589–593.

Gall, A., Gaudet, R.G., Gray-Owen, S.D., and Salama, N.R. (2017). TIFA Signaling in Gastric Epithelial Cells Initiates the cag Type 4 Secretion System-Dependent Innate Immune Response to Helicobacter pylori Infection. MBio *8*.

Gaudet, R.G., Sintsova, A., Buckwalter, C.M., Leung, N., Cochrane, A., Li, J., Cox, A.D., Moffat, J., and Gray-Owen, S.D. (2015). INNATE IMMUNITY. Cytosolic detection of the bacterial metabolite HBP activates TIFA-dependent innate immunity. Science *348*, 1251–1255.

Gaudet, R.G., Guo, C.X., Molinaro, R., Kottwitz, H., Rohde, J.R., Dangeard, A.-S., Arrieumerlou, C., Girardin, S.E., and Gray-Owen, S.D. (2017). Innate Recognition of Intracellular Bacterial Growth Is Driven by the TIFA-Dependent Cytosolic Surveillance Pathway. Cell Rep. *19*, 1418–1430.

Gay, N.J., Symmons, M.F., Gangloff, M., and Bryant, C.E. (2014). Assembly and localization of Toll-like receptor signalling complexes. Nat. Rev. Immunol. *14*, 546–558.

Gewirtz, A.T., Navas, T.A., Lyons, S., Godowski, P.J., and Madara, J.L. (2001). Cutting edge: bacterial flagellin activates basolaterally expressed TLR5 to induce epithelial proinflammatory gene expression. J. Immunol. Baltim. Md 1950 *167*, 1882–1885.

Ghosh, S., May, M.J., and Kopp, E.B. (1998). NF-kappa B and Rel proteins: evolutionarily conserved mediators of immune responses. Annu. Rev. Immunol. *16*, 225–260.

Girardin, S.E., Tournebize, R., Mavris, M., Page, A.-L., Li, X., Stark, G.R., Bertin, J., DiStefano, P.S., Yaniv, M., Sansonetti, P.J., et al. (2001). CARD4/Nod1 mediates NF-κB and JNK activation by invasive Shigella flexneri. EMBO Rep. *2*, 736–742.

Girardin, S.E., Travassos, L.H., Hervé, M., Blanot, D., Boneca, I.G., Philpott, D.J., Sansonetti, P.J., and Mengin-Lecreulx, D. (2003a). Peptidoglycan Molecular Requirements Allowing Detection by Nod1 and Nod2. J. Biol. Chem. *278*, 41702–41708.

Girardin, S.E., Boneca, I.G., Carneiro, L.A.M., Antignac, A., Jéhanno, M., Viala, J., Tedin, K., Taha, M.-K., Labigne, A., Zähringer, U., et al. (2003b). Nod1 detects a unique muropeptide from gram-negative bacterial peptidoglycan. Science *300*, 1584–1587.

Grimes, C.L., Ariyananda, L.D.Z., Melnyk, J.E., and O'Shea, E.K. (2012). The Innate Immune Protein Nod2 Binds Directly to MDP, a Bacterial Cell Wall Fragment. J. Am. Chem. Soc. *134*, 13535–13537.

Grishin, A.M., Condos, T.E.C., Barber, K.R., Campbell-Valois, F.-X., Parsot, C., Shaw, G.S., and Cygler, M. (2014). Structural basis for the inhibition of host protein ubiquitination by Shigella effector kinase OspG. Struct. Lond. Engl. 1993 *22*, 878–888.

Häcker, G., Redecke, V., and Häcker, H. (2002). Activation of the immune system by bacterial CpG-DNA. Immunology *105*, 245–251.

Hagar, J.A., Powell, D.A., Aachoui, Y., Ernst, R.K., and Miao, E.A. (2013). Cytoplasmic LPS activates caspase-11: implications in TLR4-independent endotoxic shock. Science *341*, 1250–1253.

Hao, L., Sakurai, A., Watanabe, T., Sorensen, E., Nidom, C.A., Newton, M.A., Ahlquist, P., and Kawaoka, Y. (2008). *Drosophila* RNAi screen identifies host genes important for influenza virus replication. Nature *454*, 890–893.

Harouz, H., Rachez, C., Meijer, B.M., Marteyn, B., Donnadieu, F., Cammas, F., Muchardt, C., Sansonetti, P., and Arbibe, L. (2014). Shigella flexneri targets the HP1γ subcode through the phosphothreonine lyase OspF. EMBO J. *33*, 2606–2622.

Hasegawa, M., Fujimoto, Y., Lucas, P.C., Nakano, H., Fukase, K., Núñez, G., and Inohara, N. (2008). A critical role of RICK/RIP2 polyubiquitination in Nod-induced NF-κB activation. EMBO J. *27*, 373.

Hayashi, F., Smith, K.D., Ozinsky, A., Hawn, T.R., Yi, E.C., Goodlett, D.R., Eng, J.K., Akira, S., Underhill, D.M., and Aderem, A. (2001). The innate immune response to bacterial flagellin is mediated by Toll-like receptor 5. Nature *410*, 1099–1103.

Heine, M., Cramm-Behrens, C.I., Ansari, A., Chu, H.-P., Ryazanov, A.G., Naim, H.Y., and Jacob, R. (2005). Alpha-kinase 1, a new component in apical protein transport. J. Biol. Chem. *280*, 25637–25643.

Henkel, T., Machleidt, T., Alkalay, I., Krönke, M., Ben-Neriah, Y., and Baeuerle, P.A. (1993). Rapid proteolysis of I kappa B-alpha is necessary for activation of transcription factor NF-kappa B. Nature *365*, 182–185.

Herget, S., Toukach, P.V., Ranzinger, R., Hull, W.E., Knirel, Y.A., and von der Lieth, C.-W. (2008). Statistical analysis of the Bacterial Carbohydrate Structure Data Base (BCSDB): characteristics and diversity of bacterial carbohydrates in comparison with mammalian glycans. BMC Struct. Biol. *8*, 35.

High, N., Mounier, J., Prévost, M.C., and Sansonetti, P.J. (1992). IpaB of Shigella flexneri causes entry into epithelial cells and escape from the phagocytic vacuole. EMBO J. *11*, 1991.

Hilbi, H., Moss, J.E., Hersh, D., Chen, Y., Arondel, J., Banerjee, S., Flavell, R.A., Yuan, J., Sansonetti, P.J., and Zychlinsky, A. (1998). Shigella-induced apoptosis is dependent on caspase-1 which binds to IpaB. J. Biol. Chem. *273*, 32895–32900.

Hillier, L.W., Graves, T.A., Fulton, R.S., Fulton, L.A., Pepin, K.H., Minx, P., Wagner-McPherson, C., Layman, D., Wylie, K., Sekhon, M., et al. (2005). Generation and annotation of the DNA sequences of human chromosomes 2 and 4. Nature *434*, 724–731.

Hoebe, K., Georgel, P., Rutschmann, S., Du, X., Mudd, S., Crozat, K., Sovath, S., Shamel, L., Hartung, T., Zähringer, U., et al. (2005). CD36 is a sensor of diacylglycerides. Nature *433*, 523–527.

Hofmann, K., and Bucher, P. (1995). The FHA domain: a putative nuclear signalling domain found in protein kinases and transcription factors. Trends Biochem. Sci. *20*, 347–349.

Holmgren, A.M., McConkey, C.A., and Shin, S. (2017). Outrunning the Red Queen: bystander activation as a means of outpacing innate immune subversion by intracellular pathogens. Cell. Mol. Immunol. *14*, 14–21.

Hornef, M.W., Normark, B.H., Vandewalle, A., and Normark, S. (2003). Intracellular Recognition of Lipopolysaccharide by Toll-like Receptor 4 in Intestinal Epithelial Cells. J. Exp. Med. *198*, 1225.

Hoshino, K., Takeuchi, O., Kawai, T., Sanjo, H., Ogawa, T., Takeda, Y., Takeda, K., and Akira, S. (1999). Cutting Edge: Toll-Like Receptor 4 (TLR4)-Deficient Mice Are Hyporesponsive to Lipopolysaccharide: Evidence for TLR4 as the Lps Gene Product. J. Immunol. *162*, 3749–3752.

Hosoyamada, M., Takiue, Y., Shibasaki, T., and Saito, H. (2010). The effect of testosterone upon the urate reabsorptive transport system in mouse kidney. Nucleosides Nucleotides Nucleic Acids *29*, 574–579.

Hu, H., and Sun, S.-C. (2016). Ubiquitin signaling in immune responses. Cell Res. *26*, 457–483.

Huang, C.-C.F., Weng, J.-H., Wei, T.-Y.W., Wu, P.-Y.G., Hsu, P.-H., Chen, Y.-H., Wang, S.-C., Qin, D., Hung, C.-C., Chen, S.-T., et al. (2012). Intermolecular binding between TIFA-FHA and TIFA-pT mediates tumor necrosis factor alpha stimulation and NF-κB activation. Mol. Cell. Biol. *32*, 2664–2673.

Huang, J., Xie, Y., Sun, X., Zeh, H.J., III, Kang, R., Lotze, M.T., and Tang, D. (2015). DAMPs, Ageing, and Cancer: The 'DAMP Hypothesis.' Ageing Res. Rev. *24*, 3.

Husnjak, K., and Dikic, I. (2012). Ubiquitin-binding proteins: decoders of ubiquitin-mediated cellular functions. Annu. Rev. Biochem. *81*, 291–322.

Inohara, N., Koseki, T., del Peso, L., Hu, Y., Yee, C., Chen, S., Carrio, R., Merino, J., Liu, D., Ni, J., et al. (1999). Nod1, an Apaf-1-like activator of caspase-9 and nuclear factor-kappaB. J. Biol. Chem. *274*, 14560–14567.

Inohara, N., Ogura, Y., Chen, F.F., Muto, A., and Nuñez, G. (2001). Human Nod1 Confers Responsiveness to Bacterial Lipopolysaccharides. J. Biol. Chem. *276*, 2551–2554.

Janeway, C.A. (1989). Approaching the asymptote? Evolution and revolution in immunology. Cold Spring Harb. Symp. Quant. Biol. *54 Pt 1*, 1–13.

Janot, L., Secher, T., Torres, D., Maillet, I., Pfeilschifter, J., Quesniaux, V.F.J., Landmann, R., Ryffel, B., and Erard, F. (2008). CD14 Works with Toll-Like Receptor 2 to Contribute to Recognition and Control of Listeria monocytogenes Infection. J. Infect. Dis. *198*, 115–124.

Jeong, K.-I., Zhang, Q., Nunnari, J., and Tzipori, S. (2010). A piglet model of acute gastroenteritis induced by Shigella dysenteriae Type 1. J. Infect. Dis. *201*, 903–911.

Jimenez-Dalmaroni, M.J., Xiao, N., Corper, A.L., Verdino, P., Ainge, G.D., Larsen, D.S., Painter, G.F., Rudd, P.M., Dwek, R.A., Hoebe, K., et al. (2009). Soluble CD36 Ectodomain Binds Negatively Charged Diacylglycerol Ligands and Acts as a Co-Receptor for TLR2. PLOS ONE *4*, e7411.

Jin, M.S., Kim, S.E., Heo, J.Y., Lee, M.E., Kim, H.M., Paik, S.-G., Lee, H., and Lee, J.-O. (2007). Crystal Structure of the TLR1-TLR2 Heterodimer Induced by Binding of a Tri-Acylated Lipopeptide. Cell *130*, 1071–1082.

Johnson, S., Roversi, P., Espina, M., Olive, A., Deane, J.E., Birket, S., Field, T., Picking, W.D., Blocker, A., Galyov, E.E., et al. (2007). Self-Chaperoning of the Type III Secretion System needle tip proteins IpaD and BipD. J. Biol. Chem. *282*, 4035–4044.

Johnston, A.C., Piro, A., Clough, B., Siew, M., Virreira Winter, S., Coers, J., and Frickel, E.-M. (2016). Human GBP1 does not localize to pathogen vacuoles but restricts Toxoplasma gondii. Cell. Microbiol. *18*, 1056–1064.

Jolly, C., Winfree, S., Hansen, B., and Steele-Mortimer, O. (2014). The Annexin A2/p11 complex is required for efficient invasion of Salmonella Typhimurium in epithelial cells. Cell. Microbiol. *16*, 64–77.

Jørgensen, R., Ortiz, P.A., Carr-Schmid, A., Nissen, P., Kinzy, T.G., and Andersen, G.R. (2003). Two crystal structures demonstrate large conformational changes in the eukaryotic ribosomal translocase. Nat. Struct. Biol. *10*, 379–385.

Jouihri, N., Sory, M.-P., Page, A.-L., Gounon, P., Parsot, C., and Allaoui, A. (2003). MxiK and MxiN interact with the Spa47 ATPase and are required for transit of the needle components MxiH and MxiI, but not of Ipa proteins, through the type III secretion apparatus of Shigella flexneri. Mol. Microbiol. *49*, 755–767.

Juliana, C., Fernandes-Alnemri, T., Kang, S., Farias, A., Qin, F., and Alnemri, E.S. (2012). Non-transcriptional Priming and Deubiquitination Regulate NLRP3 Inflammasome Activation. J. Biol. Chem. *287*, 36617.

Kanamori, M., Suzuki, H., Saito, R., Muramatsu, M., and Hayashizaki, Y. (2002). T2BP, a Novel TRAF2 Binding Protein, Can Activate NF-κB and AP-1 without TNF Stimulation. Biochem. Biophys. Res. Commun. *290*, 1108–1113.

Kanayama, A., Seth, R.B., Sun, L., Ea, C.-K., Hong, M., Shaito, A., Chiu, Y.-H., Deng, L., and Chen, Z.J. (2004). TAB2 and TAB3 activate the NF-kappaB pathway through binding to polyubiquitin chains. Mol. Cell *15*, 535–548.

Kang, J.Y., Nan, X., Jin, M.S., Youn, S.-J., Ryu, Y.H., Mah, S., Han, S.H., Lee, H., Paik, S.-G., and Lee, J.-O. (2009). Recognition of Lipopeptide Patterns by Toll-like Receptor 2-Toll-like Receptor 6 Heterodimer. Immunity *31*, 873–884.

Kanipes, M.I., Holder, L.C., Corcoran, A.T., Moran, A.P., and Guerry, P. (2004). A deep-rough mutant of Campylobacter jejuni 81-176 is noninvasive for intestinal epithelial cells. Infect. Immun. *72*, 2452–2455.

Kaparakis, M., Turnbull, L., Carneiro, L., Firth, S., Coleman, H.A., Parkington, H.C., Le Bourhis, L., Karrar, A., Viala, J., Mak, J., et al. (2010). Bacterial membrane vesicles deliver peptidoglycan to NOD1 in epithelial cells. Cell. Microbiol. *12*, 372–385.

Kasper, C.A., Sorg, I., Schmutz, C., Tschon, T., Wischnewski, H., Kim, M.L., and Arrieumerlou, C. (2010). Cell-cell propagation of NF-κB transcription factor and MAP kinase activation amplifies innate immunity against bacterial infection. Immunity *33*, 804–816.

Kaufmann, S.H.E. (2007). The contribution of immunology to the rational design of novel antibacterial vaccines. Nat. Rev. Microbiol. *5*, 491–504.

Kawai, T., and Akira, S. (2010). The role of pattern-recognition receptors in innate immunity: update on Toll-like receptors. Nat. Immunol. *11*, 373–384.

Kayagaki, N., Wong, M.T., Stowe, I.B., Ramani, S.R., Gonzalez, L.C., Akashi-Takamura, S., Miyake, K., Zhang, J., Lee, W.P., Muszyński, A., et al. (2013). Noncanonical Inflammasome Activation by Intracellular LPS Independent of TLR4. Science *341*, 1246–1249.

Killackey, S.A., Sorbara, M.T., and Girardin, S.E. (2016). Cellular Aspects of Shigella Pathogenesis: Focus on the Manipulation of Host Cell Processes. Front. Cell. Infect. Microbiol. *6*.

Kim, Y.S., and Ho, S.B. (2010). Intestinal Goblet Cells and Mucins in Health and Disease: Recent Insights and Progress. Curr. Gastroenterol. Rep. *12*, 319–330.

Kim, D.W., Lenzen, G., Page, A.-L., Legrain, P., Sansonetti, P.J., and Parsot, C. (2005). The Shigella flexneri effector OspG interferes with innate immune responses by targeting ubiquitin-conjugating enzymes. Proc. Natl. Acad. Sci. U. S. A. *102*, 14046–14051.

Kim, J.G., Lee, S.J., and Kagnoff, M.F. (2004). Nod1 is an essential signal transducer in intestinal epithelial cells infected with bacteria that avoid recognition by toll-like receptors. Infect. Immun. *72*, 1487–1495.

Kneidinger, B., Marolda, C., Graninger, M., Zamyatina, A., McArthur, F., Kosma, P., Valvano, M.A., and Messner, P. (2002). Biosynthesis Pathway of ADP-l-glycero-β-d-manno-Heptose in Escherichia coli. J. Bacteriol. *184*, 363.

Knodler, L.A., Crowley, S.M., Sham, H.P., Yang, H., Wrande, M., Ma, C., Ernst, R.K., Steele-Mortimer, O., Celli, J., and Vallance, B.A. (2014a). Noncanonical Inflammasome Activation of Caspase-4/Caspase-11 Mediates Epithelial Defenses against Enteric Bacterial Pathogens. Cell Host Microbe *16*, 249–256.

Knodler, L.A., Nair, V., and Steele-Mortimer, O. (2014b). Quantitative Assessment of Cytosolic Salmonella in Epithelial Cells. PLOS ONE *9*, e84681.

Kobayashi, T., Ogawa, M., Sanada, T., Mimuro, H., Kim, M., Ashida, H., Akakura, R., Yoshida, M., Kawalec, M., Reichhart, J.-M., et al. (2013). The Shigella OspC3 Effector Inhibits Caspase-4, Antagonizes Inflammatory Cell Death, and Promotes Epithelial Infection. Cell Host Microbe *13*, 570–583.

Kolios, G., Robertson, D.A., Jordan, N.J., Minty, A., Caput, D., Ferrara, P., and Westwick, J. (1996). Interleukin-8 production by the human colon epithelial cell line HT-29: modulation by interleukin-13. Br. J. Pharmacol. *119*, 351–359.

Kono, H., Chen, C.-J., Ontiveros, F., and Rock, K.L. (2010). Uric acid promotes an acute inflammatory response to sterile cell death in mice. J. Clin. Invest. *120*, 1939–1949.

Kortmann, J., Brubaker, S.W., and Monack, D.M. (2015). Cutting Edge: Inflammasome Activation in Primary Human Macrophages Is Dependent on Flagellin. J. Immunol. *195*, 815–819.

Kraehenbuhl, J.P., and Neutra, M.R. (2000). Epithelial M cells: differentiation and function. Annu. Rev. Cell Dev. Biol. *16*, 301–332.

Kreibich, S., Emmenlauer, M., Fredlund, J., Rämö, P., Münz, C., Dehio, C., Enninga, J., and Hardt, W.-D. (2015). Autophagy Proteins Promote Repair of Endosomal Membranes Damaged by the Salmonella Type Three Secretion System 1. Cell Host Microbe *18*, 527–537.

Kubori, T., Matsushima, Y., Nakamura, D., Uralil, J., Lara-Tejero, M., Sukhan, A., Galán, J.E., and Aizawa, S.-I. (1998). Supramolecular Structure of the Salmonella typhimurium Type III Protein Secretion System. Science *280*, 602–605.

Kufer, T.A., Kremmer, E., Adam, A.C., Philpott, D.J., and Sansonetti, P.J. (2008). The pattern-recognition molecule Nod1 is localized at the plasma membrane at sites of bacterial interaction. Cell. Microbiol. *10*, 477–486.

Kung, C.-T., Hsiao, S.-Y., Tsai, T.-C., Su, C.-M., Chang, W.-N., Huang, C.-R., Wang, H.-C., Lin, W.-C., Chang, H.-W., Lin, Y.-J., et al. (2012). Plasma nuclear and mitochondrial DNA levels as predictors of outcome in severe sepsis patients in the emergency room. J. Transl. Med. *10*, 130.

Kuo, T.-M., Huang, C.-M., Tu, H.-P., Min-Shan Ko, A., Wang, S.-J., Lee, C.-P., and Ko, Y.-C. (2017). URAT1 inhibition by ALPK1 is associated with uric acid homeostasis. Rheumatol. Oxf. Engl. *56*, 654–659.

Lamothe, B., Besse, A., Campos, A.D., Webster, W.K., Wu, H., and Darnay, B.G. (2007). Site-specific Lys-63-linked tumor necrosis factor receptor-associated factor 6 auto-ubiquitination is a critical determinant of I kappa B kinase activation. J. Biol. Chem. *282*, 4102–4112.

LaRock, D.L., Chaudhary, A., and Miller, S.I. (2015). Salmonellae interactions with host processes. Nat. Rev. Microbiol. *13*, 191–205.

Laroui, H., Yan, Y., Narui, Y., Ingersoll, S.A., Ayyadurai, S., Charania, M.A., Zhou, F., Wang, B., Salaita, K., Sitaraman, S.V., et al. (2011). L-Ala-γ-D-Glu-meso-diaminopimelic acid (DAP) interacts directly with leucine-rich region domain of nucleotide-binding oligomerization domain 1, increasing phosphorylation activity of receptor-interacting serine/threonine-protein kinase 2 and

its interaction with nucleotide-binding oligomerization domain 1. J. Biol. Chem. *286*, 31003–31013.

Le Gall, T., Mavris, M., Martino, M.C., Bernardini, M.L., Denamur, E., and Parsot, C. (2005). Analysis of virulence plasmid gene expression defines three classes of effectors in the type III secretion system of Shigella flexneri. Microbiol. Read. Engl. *151*, 951–962.

Le-Barillec, K., Magalhaes, J.G., Corcuff, E., Thuizat, A., Sansonetti, P.J., Phalipon, A., and Di Santo, J.P. (2005). Roles for T and NK cells in the innate immune response to Shigella flexneri. J. Immunol. Baltim. Md 1950 *175*, 1735–1740.

Lee, C.-P., Chiang, S.-L., Ko, A.M.-S., Liu, Y.-F., Ma, C., Lu, C.-Y., Huang, C.-M., Chang, J.-G., Kuo, T.-M., Chen, C.-L., et al. (2016). ALPK1 phosphorylates myosin IIA modulating TNF-α trafficking in gout flares. Sci. Rep. *6*, 25740.

Lee, J., Rachmilewitz, D., and Raz, E. (2006). Homeostatic effects of TLR9 signaling in experimental colitis. Ann. N. Y. Acad. Sci. *1072*, 351–355.

Lee, J., Tattoli, I., Wojtal, K.A., Vavricka, S.R., Philpott, D.J., and Girardin, S.E. (2009). pH-dependent Internalization of Muramyl Peptides from Early Endosomes Enables Nod1 and Nod2 Signaling. J. Biol. Chem. *284*, 23818–23829.

Lemaitre, B., Nicolas, E., Michaut, L., Reichhart, J.M., and Hoffmann, J.A. (1996). The dorsoventral regulatory gene cassette spätzle/Toll/cactus controls the potent antifungal response in *Drosophila* adults. Cell *86*, 973–983.

Lemmon, M.A., and Schlessinger, J. (2010). Cell signaling by receptor-tyrosine kinases. Cell *141*, 1117–1134.

Li, H., Xu, H., Zhou, Y., Zhang, J., Long, C., Li, S., Chen, S., Zhou, J.-M., and Shao, F. (2007). The phosphothreonine lyase activity of a bacterial type III effector family. Science *315*, 1000–1003.

Liao, H.-F., Lee, H.-H., Chang, Y.-S., Lin, C.-L., Liu, T.-Y., Chen, Y.-C., Yen, J.-C., Lee, Y.-T., Lin, C.-Y., Wu, S.-H., et al. (2016). Down-regulated and Commonly mutated ALPK1 in Lung and Colorectal Cancers. Sci. Rep. *6*, 27350.

Lieschke, G.J., and Currie, P.D. (2007). Animal models of human disease: zebrafish swim into view. Nat. Rev. Genet. *8*, 353–367.

Liew, F.Y., Xu, D., Brint, E.K., and O'Neill, L.A.J. (2005). Negative regulation of Toll-like receptor-mediated immune responses. Nat. Rev. Immunol. *5*, 446–458.

Lin, S.-C., Lo, Y.-C., and Wu, H. (2010). Helical assembly in the MyD88:IRAK4:IRAK2 complex in TLR/IL-1R signaling. Nature *465*, 885.

Lin, T.-Y., Wei, T.-Y.W., Li, S., Wang, S.-C., He, M., Martin, M., Zhang, J., Shentu, T.-P., Xiao, H., Kang, J., et al. (2016). TIFA as a crucial mediator for NLRP3 inflammasome. Proc. Natl. Acad. Sci. U. S. A. *113*, 15078–15083.

Lindberg, A.A., Kärnell, A., and Weintraub, A. (1991). The Lipopolysaccharide of Shigella Bacteria as a Virulence Factor. Rev. Infect. Dis. *13*, S279–S284.

Lindgren, H., Shen, H., Zingmark, C., Golovliov, I., Conlan, W., and Sjöstedt, A. (2007). Resistance of Francisella tularensis strains against reactive nitrogen and oxygen species with special reference to the role of KatG. Infect. Immun. *75*, 1303–1309.

Magdalena, J., Hachani, A., Chamekh, M., Jouihri, N., Gounon, P., Blocker, A., and Allaoui, A. (2002). Spa32 Regulates a Switch in Substrate Specificity of the Type III Secreton of Shigella flexneri from Needle Components to Ipa Proteins. J. Bacteriol. *184*, 3433–3441.

Mahajan, A., Yuan, C., Lee, H., Chen, E.S.-W., Wu, P.-Y., and Tsai, M.-D. (2008). Structure and function of the phosphothreonine-specific FHA domain. Sci. Signal. *1*, re12.

Maier, J.K.X., Balabanian, S., Coffill, C.R., Stewart, A., Pelletier, L., Franks, D.J., Gendron, N.H., and MacKenzie, A.E. (2007). Distribution of neuronal apoptosis inhibitory protein in human tissues. J. Histochem. Cytochem. Off. J. Histochem. Soc. *55*, 911–923.

Malott, R.J., Keller, B.O., Gaudet, R.G., McCaw, S.E., Lai, C.C.L., Dobson-Belaire, W.N., Hobbs, J.L., St Michael, F., Cox, A.D., Moraes, T.F., et al. (2013). Neisseria gonorrhoeae-derived heptose elicits an innate immune response and drives HIV-1 expression. Proc. Natl. Acad. Sci. U. S. A. *110*, 10234–10239.

Man, S.M., Karki, R., Malireddi, R.K.S., Neale, G., Vogel, P., Yamamoto, M., Lamkanfi, M., and Kanneganti, T.-D. (2015). The transcription factor IRF1 and guanylate-binding proteins target activation of the AIM2 inflammasome by Francisella infection. Nat. Immunol. *16*, 467–475.

Mani, S., Wierzba, T., and Walker, R.I. (2016). Status of vaccine research and development for Shigella. Vaccine *34*, 2887–2894.

Marina-García, N., Franchi, L., Kim, Y.-G., Hu, Y., Smith, D.E., Boons, G.-J., and Núñez, G. (2009). Clathrin- and Dynamin-Dependent Endocytic Pathway Regulates Muramyl Dipeptide Internalization and NOD2 Activation. J. Immunol. *182*, 4321–4327.

Martinon, F., Burns, K., and Tschopp, J. (2002). The Inflammasome. Mol. Cell *10*, 417–426.

Mattock, E., and Blocker, A.J. (2017). How Do the Virulence Factors of Shigella Work Together to Cause Disease? Front. Cell. Infect. Microbiol. *7*.

Matzinger, P. (1994). Tolerance, danger, and the extended family. Annu. Rev. Immunol. *12*, 991–1045.

Matzinger, P. (2002). The danger model: a renewed sense of self. Science *296*, 301–305.

Maurelli, A.T., Baudry, B., d'Hauteville, H., Hale, T.L., and Sansonetti, P.J. (1985). Cloning of plasmid DNA sequences involved in invasion of HeLa cells by Shigella flexneri. Infect. Immun. *49*, 164–171.

Mavris, M., Page, A.-L., Tournebize, R., Demers, B., Sansonetti, P., and Parsot, C. (2002). Regulation of transcription by the activity of the Shigella flexneri type III secretion apparatus. Mol. Microbiol. *43*, 1543–1553.

McDonald, B., Pittman, K., Menezes, G.B., Hirota, S.A., Slaba, I., Waterhouse, C.C.M., Beck, P.L., Muruve, D.A., and Kubes, P. (2010). Intravascular Danger Signals Guide Neutrophils to Sites of Sterile Inflammation. Science *330*, 362–366.

Medzhitov, R., and Janeway, C.A. (1997). Innate Immunity: The Virtues of a Nonclonal System of Recognition. Cell *91*, 295–298.

Medzhitov, R., Preston-Hurlburt, P., and Janeway, C.A. (1997). A human homologue of the *Drosophila* Toll protein signals activation of adaptive immunity. Nature *388*, 394–397.

Mellouk, N., Weiner, A., Aulner, N., Schmitt, C., Elbaum, M., Shorte, S.L., Danckaert, A., and Enninga, J. (2014). Shigella Subverts the Host Recycling Compartment to Rupture Its Vacuole. Cell Host Microbe *16*, 517–530.

Mempin, R., Tran, H., Chen, C., Gong, H., Kim Ho, K., and Lu, S. (2013). Release of extracellular ATP by bacteria during growth. BMC Microbiol. *13*, 301.

Ménard, R., Sansonetti, P.J., and Parsot, C. (1993). Nonpolar mutagenesis of the ipa genes defines IpaB, IpaC, and IpaD as effectors of Shigella flexneri entry into epithelial cells. J. Bacteriol. *175*, 5899–5906.

Ménard, R., Sansonetti, P., and Parsot, C. (1994). The secretion of the Shigella flexneri Ipa invasins is activated by epithelial cells and controlled by IpaB and IpaD. EMBO J. *13*, 5293–5302.

Menu, P., and Vince, J.E. (2011). The NLRP3 inflammasome in health and disease: the good, the bad and the ugly. Clin. Exp. Immunol. *166*, 1–15.

Mercurio, F., Zhu, H., Murray, B.W., Shevchenko, A., Bennett, B.L., Li, J., Young, D.B., Barbosa, M., Mann, M., Manning, A., et al. (1997). IKK-1 and IKK-2: cytokine-activated IkappaB kinases essential for NF-kappaB activation. Science *278*, 860–866.

Meunier, E., Dick, M.S., Dreier, R.F., Schürmann, N., Broz, D.K., Warming, S., Roose-Girma, M., Bumann, D., Kayagaki, N., Takeda, K., et al. (2014). Caspase-11 activation requires lysis of pathogen-containing vacuoles by IFN-induced GTPases. Nature *509*, 366–370.

Meunier, E., Wallet, P., Dreier, R.F., Costanzo, S., Anton, L., Rühl, S., Dussurgey, S., Dick, M.S., Kistner, A., Rigard, M., et al. (2015). Guanylate-binding proteins promote activation of the AIM2 inflammasome during infection with Francisella novicida. Nat. Immunol. *16*, 476–484.

Miao, E.A., Alpuche-Aranda, C.M., Dors, M., Clark, A.E., Bader, M.W., Miller, S.I., and Aderem, A. (2006). Cytoplasmic flagellin activates caspase-1 and secretion of interleukin 1β via Ipaf. Nat. Immunol. *7*, 569–575.

Miao, E.A., Mao, D.P., Yudkovsky, N., Bonneau, R., Lorang, C.G., Warren, S.E., Leaf, I.A., and Aderem, A. (2010). Innate immune detection of the type III secretion apparatus through the NLRC4 inflammasome. Proc. Natl. Acad. Sci. U. S. A. *107*, 3076.

Middelbeek, J., Clark, K., Venselaar, H., Huynen, M.A., and van Leeuwen, F.N. (2010). The alpha-kinase family: an exceptional branch on the protein kinase tree. Cell. Mol. Life Sci. *67*, 875–890.

Milivojevic, M., Dangeard, A.-S., Kasper, C.A., Tschon, T., Emmenlauer, M., Pique, C., Schnupf, P., Guignot, J., and Arrieumerlou, C. (2017). ALPK1 controls TIFA/TRAF6-dependent innate immunity against heptose-1,7-bisphosphate of gram-negative bacteria. PLoS Pathog. *13*, e1006224.

Mohr, S.E., Smith, J.A., Shamu, C.E., Neumüller, R.A., and Perrimon, N. (2014). RNAi screening comes of age: improved techniques and complementary approaches. Nat. Rev. Mol. Cell Biol. *15*, 591–600.

Monack, D.M., and Theriot, J.A. (2001). Actin-based motility is sufficient for bacterial membrane protrusion formation and host cell uptake. Cell. Microbiol. *3*, 633–647.

Morita-Ishihara, T., Ogawa, M., Sagara, H., Yoshida, M., Katayama, E., and Sasakawa, C. (2006). Shigella Spa33 Is an Essential C-ring Component of Type III Secretion Machinery. J. Biol. Chem. *281*, 599–607.

Mostowy, S., Boucontet, L., Moya, M.J.M., Sirianni, A., Boudinot, P., Hollinshead, M., Cossart, P., Herbomel, P., Levraud, J.-P., and Colucci-Guyon, E. (2013). The Zebrafish as a New Model for the In Vivo Study of Shigella flexneri Interaction with Phagocytes and Bacterial Autophagy. PLoS Pathog. *9*.

Motshwene, P.G., Moncrieffe, M.C., Grossmann, J.G., Kao, C., Ayaluru, M., Sandercock, A.M., Robinson, C.V., Latz, E., and Gay, N.J. (2009). An Oligomeric Signaling Platform Formed by the Toll-like Receptor Signal Transducers MyD88 and IRAK-4. J. Biol. Chem. *284*, 25404.

Motta, V., Soares, F., Sun, T., and Philpott, D.J. (2015). NOD-like receptors: versatile cytosolic sentinels. Physiol. Rev. *95*, 149–178.

Mounier, J., Vasselon, T., Hellio, R., Lesourd, M., and Sansonetti, P.J. (1992). Shigella flexneri enters human colonic Caco-2 epithelial cells through the basolateral pole. Infect. Immun. *60*, 237–248.

Müller, A.A., Dolowschiak, T., Sellin, M.E., Felmy, B., Verbree, C., Gadient, S., Westermann, A.J., Vogel, J., LeibundGut-Landmann, S., and Hardt, W.-D. (2016). An NK Cell Perforin Response Elicited via IL-18 Controls Mucosal Inflammation Kinetics during Salmonella Gut Infection. PLOS Pathog. *12*, e1005723.

Muñoz-Planillo, R., Kuffa, P., Martínez-Colón, G., Smith, B.L., Rajendiran, T.M., and Núñez, G. (2013). K+ efflux is the Common Trigger of NLRP3 inflammasome Activation by Bacterial Toxins and Particulate Matter. Immunity *38*, 1142–1153.

Nagai, Y., Akashi, S., Nagafuku, M., Ogata, M., Iwakura, Y., Akira, S., Kitamura, T., Kosugi, A., Kimoto, M., and Miyake, K. (2002). Essential role of MD-2 in LPS responsiveness and TLR4 distribution. Nat. Immunol. *3*, 667–672.

Newton, H.J., Pearson, J.S., Badea, L., Kelly, M., Lucas, M., Holloway, G., Wagstaff, K.M., Dunstone, M.A., Sloan, J., Whisstock, J.C., et al. (2010). The type III effectors NleE and NleB from enteropathogenic E. coli and OspZ from Shigella block nuclear translocation of NF-kappaB p65. PLoS Pathog. *6*, e1000898.

Niebuhr, K., Giuriato, S., Pedron, T., Philpott, D.J., Gaits, F., Sable, J., Sheetz, M.P., Parsot, C., Sansonetti, P.J., and Payrastre, B. (2002). Conversion of PtdIns(4,5)P(2) into PtdIns(5)P by the S.flexneri effector IpgD reorganizes host cell morphology. EMBO J. *21*, 5069–5078.

Nordlander, S., Pott, J., and Maloy, K.J. (2014). NLRC4 expression in intestinal epithelial cells mediates protection against an enteric pathogen. Mucosal Immunol. *7*, 775–785.

Ogura, Y., Inohara, N., Benito, A., Chen, F.F., Yamaoka, S., and Núñez, G. (2001). Nod2, a Nod1/Apaf-1 Family Member That Is Restricted to Monocytes and Activates NF-κB. J. Biol. Chem. *276*, 4812–4818.

Olive, A.J., Kenjale, R., Espina, M., Moore, D.S., Picking, W.L., and Picking, W.D. (2007). Bile salts stimulate recruitment of IpaB to the Shigella flexneri surface, where it colocalizes with IpaD at the tip of the type III secretion needle. Infect. Immun. *75*, 2626–2629.

Oliveira-Nascimento, L., Massari, P., and Wetzler, L.M. (2012). The Role of TLR2 in Infection and Immunity. Front. Immunol. *3*.

O'Neill, L.A.J., and Bowie, A.G. (2007). The family of five: TIR-domain-containing adaptors in Toll-like receptor signalling. Nat. Rev. Immunol. *7*, 353–364.

Opitz, B., Püschel, A., Beermann, W., Hocke, A.C., Förster, S., Schmeck, B., van Laak, V., Chakraborty, T., Suttorp, N., and Hippenstiel, S. (2006). Listeria monocytogenes activated p38 MAPK and induced IL-8 secretion in a nucleotide-binding oligomerization domain 1-dependent manner in endothelial cells. J. Immunol. Baltim. Md 1950 *176*, 484–490.

Papenfort, K., and Bassler, B.L. (2016). Quorum sensing signal-response systems in Gram-negative bacteria. Nat. Rev. Microbiol. *14*, 576–588.

Park, B.S., Song, D.H., Kim, H.M., Choi, B.-S., Lee, H., and Lee, J.-O. (2009). The structural basis of lipopolysaccharide recognition by the TLR4–MD-2 complex. Nature *458*, 1191–1195.

Parsot, C., Ménard, R., Gounon, P., and Sansonetti, P.J. (1995). Enhanced secretion through the Shigella flexneri Mxi-Spa translocon leads to assembly of extracellular proteins into macromolecular structures. Mol. Microbiol. *16*, 291–300.

Pastorelli, L., De Salvo, C., Cominelli, M.A., Vecchi, M., and Pizarro, T.T. (2011). Novel cytokine signaling pathways in inflammatory bowel disease: insight into the dichotomous functions of IL-33 during chronic intestinal inflammation. Ther. Adv. Gastroenterol. *4*, 311–323.

Patel, S.J., King, K.R., Casali, M., and Yarmush, M.L. (2009). DNA-triggered innate immune responses are propagated by gap junction communication. Proc. Natl. Acad. Sci. U. S. A. *106*, 12867–12872.

Paz, I., Sachse, M., Dupont, N., Mounier, J., Cederfur, C., Enninga, J., Leffler, H., Poirier, F., Prevost, M.-C., Lafont, F., et al. (2010). Galectin-3, a marker for vacuole lysis by invasive pathogens. Cell. Microbiol. *12*, 530–544.

Pennell, S., Westcott, S., Ortiz-Lombardía, M., Patel, D., Li, J., Nott, T.J., Mohammed, D., Buxton, R.S., Yaffe, M.B., Verma, C., et al. (2010). Structural and functional analysis of phosphothreonine-dependent FHA domain interactions. Struct. Lond. Engl. 1993 *18*, 1587–1595.

Phalipon, A., and Sansonetti, P.J. (2007). Shigella's ways of manipulating the host intestinal innate and adaptive immune system: a tool box for survival? Immunol. Cell Biol. *85*, 119–129.

Philip, R., and Epstein, L.B. (1986). Tumour necrosis factor as immunomodulator and mediator of monocyte cytotoxicity induced by itself, gamma-interferon and interleukin-1. Nature *323*, 86–89.

Philpott, D.J., and Girardin, S.E. (2004). The role of Toll-like receptors and Nod proteins in bacterial infection. Mol. Immunol. *41*, 1099–1108.

Philpott, D.J., Yamaoka, S., Israël, A., and Sansonetti, P.J. (2000). Invasive Shigella flexneri activates NF-kappa B through a lipopolysaccharide-dependent innate intracellular response and leads to IL-8 expression in epithelial cells. J. Immunol. Baltim. Md 1950 *165*, 903–914.

Philpott, D.J., Sorbara, M.T., Robertson, S.J., Croitoru, K., and Girardin, S.E. (2014). NOD proteins: regulators of inflammation in health and disease. Nat. Rev. Immunol. *14*, 9–23.

Picking, W.L., Nishioka, H., Hearn, P.D., Baxter, M.A., Harrington, A.T., Blocker, A., and Picking, W.D. (2005). IpaD of Shigella flexneri is independently required for regulation of Ipa protein secretion and efficient insertion of IpaB and IpaC into host membranes. Infect. Immun. *73*, 1432–1440.

Poltorak, A., He, X., Smirnova, I., Liu, M.Y., Van Huffel, C., Du, X., Birdwell, D., Alejos, E., Silva, M., Galanos, C., et al. (1998). Defective LPS signaling in C3H/HeJ and C57BL/10ScCr mice: mutations in Tlr4 gene. Science *282*, 2085–2088.

Pott, J., and Hornef, M. (2012). Innate immune signalling at the intestinal epithelium in homeostasis and disease. EMBO Rep. *13*, 684–698.

Pruneda, J.N., Smith, F.D., Daurie, A., Swaney, D.L., Villén, J., Scott, J.D., Stadnyk, A.W., Le Trong, I., Stenkamp, R.E., Klevit, R.E., et al. (2014). E2~Ub conjugates regulate the kinase activity of Shigella effector OspG during pathogenesis. EMBO J. *33*, 437–449.

Puhar, A., Tronchère, H., Payrastre, B., Tran Van Nhieu, G., and Sansonetti, P.J. (2013). A Shigella Effector Dampens Inflammation by Regulating Epithelial Release of Danger Signal ATP through Production of the Lipid Mediator PtdIns5P. Immunity *39*, 1121–1131.

Qureshi, S.T., Larivière, L., Leveque, G., Clermont, S., Moore, K.J., Gros, P., and Malo, D. (1999). Endotoxin-tolerant Mice Have Mutations in Toll-like Receptor 4 (Tlr4). J. Exp. Med. *189*, 615–625.

Raetz, C.R.H., and Whitfield, C. (2002). Lipopolysaccharide Endotoxins. Annu. Rev. Biochem. *71*, 635–700.

Rämö, P., Drewek, A., Arrieumerlou, C., Beerenwinkel, N., Ben-Tekaya, H., Cardel, B., Casanova, A., Conde-Alvarez, R., Cossart, P., Csúcs, G., et al. (2014). Simultaneous analysis of large-scale RNAi screens for pathogen entry. BMC Genomics *15*.

Ray, K., Bobard, A., Danckaert, A., Paz-Haftel, I., Clair, C., Ehsani, S., Tang, C., Sansonetti, P., Van Nhieu, G.T., and Enninga, J. (2010). Tracking the dynamic interplay between bacterial and host factors during pathogen-induced vacuole rupture in real time. Cell. Microbiol. *12*, 545–556.

Reiterer, V., Grossniklaus, L., Tschon, T., Kasper, C.A., Sorg, I., and Arrieumerlou, C. (2011). Shigella flexneri type III secreted effector OspF reveals new crosstalks of proinflammatory signaling pathways during bacterial infection. Cell. Signal. *23*, 1188–1196.

Roebuck, K.A. (1999). Regulation of interleukin-8 gene expression. J. Interferon Cytokine Res. Off. J. Int. Soc. Interferon Cytokine Res. *19*, 429–438.

Roehrich, A.D., Guillossou, E., Blocker, A.J., and Martinez-Argudo, I. (2013). Shigella IpaD has a dual role: signal transduction from the type III secretion system needle tip and intracellular secretion regulation. Mol. Microbiol. *87*, 690–706.

Roger, T., Froidevaux, C., Roy, D.L., Reymond, M.K., Chanson, A.-L., Mauri, D., Burns, K., Riederer, B.M., Akira, S., and Calandra, T. (2009). Protection from lethal Gram-negative bacterial sepsis by targeting Toll-like receptor 4. Proc. Natl. Acad. Sci. *106*, 2348–2352.

Rohde, J.R., Breitkreutz, A., Chenal, A., Sansonetti, P.J., and Parsot, C. (2007). Type III secretion effectors of the IpaH family are E3 ubiquitin ligases. Cell Host Microbe *1*, 77–83.

Romero, S., Grompone, G., Carayol, N., Mounier, J., Guadagnini, S., Prevost, M.-C., Sansonetti, P.J., and Van Nhieu, G.T. (2011). ATP-mediated Erk1/2 activation stimulates bacterial capture by filopodia, which precedes Shigella invasion of epithelial cells. Cell Host Microbe *9*, 508–519.

Rothwarf, D.M., Zandi, E., Natoli, G., and Karin, M. (1998). IKK-gamma is an essential regulatory subunit of the IkappaB kinase complex. Nature *395*, 297–300.

Ryazanov, A.G., Pavur, K.S., and Dorovkov, M.V. (1999). Alpha-kinases: a new class of protein kinases with a novel catalytic domain. Curr. Biol. *9*, R43–R45.

Sakaguchi, T., Köhler, H., Gu, X., McCormick, B.A., and Reinecker, H.-C. (2002). Shigella flexneri regulates tight junction-associated proteins in human intestinal epithelial cells. Cell. Microbiol. *4*, 367–381.

Sanada, T., Kim, M., Mimuro, H., Suzuki, M., Ogawa, M., Oyama, A., Ashida, H., Kobayashi, T., Koyama, T., Nagai, S., et al. (2012). The Shigella flexneri effector OspI deamidates UBC13 to dampen the inflammatory response. Nature *483*, 623–626.

Sani, M., Allaoui, A., Fusetti, F., Oostergetel, G.T., Keegstra, W., and Boekema, E.J. (2007). Structural organization of the needle complex of the type III secretion apparatus of Shigella flexneri. Micron *38*, 291–301.

Sansonetti, P.J. (2004). War and peace at mucosal surfaces. Nat. Rev. Immunol. *4*, 953–964.

Sansonetti, P.J., Ryter, A., Clerc, P., Maurelli, A.T., and Mounier, J. (1986). Multiplication of Shigella flexneri within HeLa cells: lysis of the phagocytic vacuole and plasmid-mediated contact hemolysis. Infect. Immun. *51*, 461–469.

Sansonetti, P.J., Arondel, J., Huerre, M., Harada, A., and Matsushima, K. (1999). Interleukin-8 Controls Bacterial Transepithelial Translocation at the Cost of Epithelial Destruction in Experimental Shigellosis. Infect. Immun. *67*, 1471–1480.

Sansonetti, P.J., Phalipon, A., Arondel, J., Thirumalai, K., Banerjee, S., Akira, S., Takeda, K., and Zychlinsky, A. (2000). Caspase-1 activation of IL-1beta and IL-18 are essential for Shigella flexneri-induced inflammation. Immunity *12*, 581–590.

Sasakawa, C., Adler, B., Tobe, T., Okada, N., Nagai, S., Komatsu, K., and Yoshikawa, M. (1989). Functional organization and nucleotide sequence of virulence Region-2 on the large virulence plasmid in Shigella flexneri 2a. Mol. Microbiol. *3*, 1191–1201.

Schaefer, L. (2014). Complexity of Danger: The Diverse Nature of Damage-associated Molecular Patterns. J. Biol. Chem. *289*, 35237–35245.

Schroeder, G.N., and Hilbi, H. (2008). Molecular Pathogenesis of Shigella spp.: Controlling Host Cell Signaling, Invasion, and Death by Type III Secretion. Clin. Microbiol. Rev. *21*, 134–156.

Schroeder, G.N., Jann, N.J., and Hilbi, H. (2007). Intracellular type III secretion by cytoplasmic Shigella flexneri promotes caspase-1-dependent macrophage cell death. Microbiol. Read. Engl. *153*, 2862–2876.

Schuch, R., and Maurelli, A.T. (2001). MxiM and MxiJ, base elements of the Mxi-Spa type III secretion system of Shigella, interact with and stabilize the MxiD secretin in the cell envelope. J. Bacteriol. *183*, 6991–6998.

Seibert, S.A., Mex, P., Köhler, A., Kaufmann, S.H.E., and Mittrücker, H.-W. (2010). TLR2-, TLR4- and Myd88-independent acquired humoral and cellular immunity against Salmonella enterica serovar Typhimurium. Immunol. Lett. *127*, 126–134.

Sellin, M.E., Müller, A.A., and Hardt, W.-D. (2014). Consequences of Epithelial Inflammasome Activation by Bacterial Pathogens. J. Mol. Biol.

Sellin, M.E., Maslowski, K.M., Maloy, K.J., and Hardt, W.-D. (2015). Inflammasomes of the intestinal epithelium. Trends Immunol. *36*, 442–450.

Sen, R., and Baltimore, D. (1986). Inducibility of kappa immunoglobulin enhancer-binding protein Nf-kappa B by a posttranslational mechanism. Cell *47*, 921–928.

Senerovic, L., Tsunoda, S.P., Goosmann, C., Brinkmann, V., Zychlinsky, A., Meissner, F., and Kolbe, M. (2012). Spontaneous formation of IpaB ion channels in host cell membranes reveals how Shigella induces pyroptosis in macrophages. Cell Death Dis. *3*, e384.

Shalaby, M.R., Waage, A., Aarden, L., and Espevik, T. (1989). Endotoxin, tumor necrosis factor-α and interleukin 1 induce interleukin 6 production in vivo. Clin. Immunol. Immunopathol. *53*, 488–498.

Shen, W., Chang, A., Wang, J., Zhou, W., Gao, R., Li, J., Xu, Y., Luo, X., Xiang, R., Luo, N., et al. (2015). TIFA, an inflammatory signaling adaptor, is tumor suppressive for liver cancer. Oncogenesis *4*, e173.

Shi, J., Zhao, Y., Wang, Y., Gao, W., Ding, J., Li, P., Hu, L., and Shao, F. (2014). Inflammatory caspases are innate immune receptors for intracellular LPS. Nature *514*, 187–192.

Shibuya, H., Yamaguchi, K., Shirakabe, K., Tonegawa, A., Gotoh, Y., Ueno, N., Irie, K., Nishida, E., and Matsumoto, K. (1996). TAB1: an activator of the TAK1 MAPKKK in TGF-beta signal transduction. Science *272*, 1179–1182.

Shim, D.-H., Suzuki, T., Chang, S.-Y., Park, S.-M., Sansonetti, P.J., Sasakawa, C., and Kweon, M.-N. (2007). New animal model of shigellosis in the Guinea pig: its usefulness for protective efficacy studies. J. Immunol. Baltim. Md 1950 *178*, 2476–2482.

Shimazu, R., Akashi, S., Ogata, H., Nagai, Y., Fukudome, K., Miyake, K., and Kimoto, M. (1999). MD-2, a Molecule that Confers Lipopolysaccharide Responsiveness on Toll-like Receptor 4. J. Exp. Med. *189*, 1777.

Shimokata, S., Oguri, M., Fujimaki, T., Horibe, H., Kato, K., and Yamada, Y. (2013). Association between polymorphisms of the α-kinase 1 gene and type 2 diabetes mellitus in community-dwelling individuals. Biomed. Rep. *1*, 940–944.

Sisti, F., Fernández, J., Rodríguez, M.E., Lagares, A., Guiso, N., and Hozbor, D.F. (2002). In vitro and in vivo characterization of a Bordetella bronchiseptica mutant strain with a deep rough lipopolysaccharide structure. Infect. Immun. *70*, 1791–1798.

Skoudy, A., Mounier, J., Aruffo, A., Ohayon, H., Gounon, P., Sansonetti, P., and Tran Van Nhieu, G. (2000). CD44 binds to the Shigella IpaB protein and participates in bacterial invasion of epithelial cells. Cell. Microbiol. *2*, 19–33.

Smith, C.W., Rothlein, R., Hughes, B.J., Mariscalco, M.M., Rudloff, H.E., Schmalstieg, F.C., and Anderson, D.C. (1988). Recognition of an endothelial determinant for CD 18-dependent human neutrophil adherence and transendothelial migration. J. Clin. Invest. *82*, 1746–1756.

Song, N., Liu, Z.-S., Xue, W., Bai, Z.-F., Wang, Q.-Y., Dai, J., Liu, X., Huang, Y.-J., Cai, H., Zhan, X.-Y., et al. (2017). NLRP3 Phosphorylation Is an Essential Priming Event for Inflammasome Activation. Mol. Cell.

Song-Zhao, G.X., Srinivasan, N., Pott, J., Baban, D., Frankel, G., and Maloy, K.J. (2014). Nlrp3 activation in the intestinal epithelium protects against a mucosal pathogen. Mucosal Immunol. *7*, 763–774.

Spiller, S., Dreher, S., Meng, G., Grabiec, A., Thomas, W., Hartung, T., Pfeffer, K., Hochrein, H., Brade, H., Bessler, W., et al. (2007). Cellular recognition of trimyristoylated peptide or enterobacterial lipopolysaccharide via both TLR2 and TLR4. J. Biol. Chem. *282*, 13190–13198.

Spiller, S., Elson, G., Ferstl, R., Dreher, S., Mueller, T., Freudenberg, M., Daubeuf, B., Wagner, H., and Kirschning, C.J. (2008). TLR4-induced IFN-γ production increases TLR2 sensitivity and drives Gram-negative sepsis in mice. J. Exp. Med. *205*, 1747.

Sridharan, G.V., Choi, K., Klemashevich, C., Wu, C., Prabakaran, D., Pan, L.B., Steinmeyer, S., Mueller, C., Yousofshahi, M., Alaniz, R.C., et al. (2014). Prediction and quantification of bioactive microbiota metabolites in the mouse gut. Nat. Commun. *5*, ncomms6492.

Stein, S.C., Faber, E., Bats, S.H., Murillo, T., Speidel, Y., Coombs, N., and Josenhans, C. (2017). Helicobacter pylori modulates host cell responses by CagT4SS-dependent translocation of an intermediate metabolite of LPS inner core heptose biosynthesis. PLoS Pathog. *13*, e1006514.

Stojiljkovic, I., Hwa, V., Larson, J., Lin, L., So, M., and Nassif, X. (1997). Cloning and characterization of the Neisseria meningitidis rfaC gene encoding α-1,5 heptosyltransferase I. FEMS Microbiol. Lett. *151*, 41–49.

Strietz, J., Stepputtis, S.S., Preca, B.-T., Vannier, C., Kim, M.M., Castro, D.J., Au, Q., Boerries, M., Busch, H., Aza-Blanc, P., et al. (2016). ERN1 and ALPK1 inhibit differentiation of bi-potential tumor-initiating cells in human breast cancer. Oncotarget *7*, 83278–83293.

Suzuki, M., Hisamatsu, T., and Podolsky, D.K. (2003). Gamma interferon augments the intracellular pathway for lipopolysaccharide (LPS) recognition in human intestinal epithelial cells through coordinated up-regulation of LPS uptake and expression of the intracellular Toll-like receptor 4-MD-2 complex. Infect. Immun. *71*, 3503–3511.

Suzuki, S., Mimuro, H., Kim, M., Ogawa, M., Ashida, H., Toyotome, T., Franchi, L., Suzuki, M., Sanada, T., Suzuki, T., et al. (2014). Shigella IpaH7.8 E3 ubiquitin ligase targets glomulin and activates inflammasomes to demolish macrophages. Proc. Natl. Acad. Sci. U. S. A. *111*, E4254-4263.

Suzuki, T., Franchi, L., Toma, C., Ashida, H., Ogawa, M., Yoshikawa, Y., Mimuro, H., Inohara, N., Sasakawa, C., and Nuñez, G. (2007). Differential regulation of caspase-1 activation, pyroptosis, and autophagy via Ipaf and ASC in Shigella-infected macrophages. PLoS Pathog. *3*, e111.

Takaesu, G., Kishida, S., Hiyama, A., Yamaguchi, K., Shibuya, H., Irie, K., Ninomiya-Tsuji, J., and Matsumoto, K. (2000). TAB2, a novel adaptor protein, mediates activation of TAK1 MAPKKK by linking TAK1 to TRAF6 in the IL-1 signal transduction pathway. Mol. Cell *5*, 649–658.

Takatsuna, H., Kato, H., Gohda, J., Akiyama, T., Moriya, A., Okamoto, Y., Yamagata, Y., Otsuka, M., Umezawa, K., Semba, K., et al. (2003). Identification of TIFA as an adapter protein that links tumor necrosis factor receptor-associated factor 6 (TRAF6) to interleukin-1 (IL-1) receptor-associated kinase-1 (IRAK-1) in IL-1 receptor signaling. J. Biol. Chem. *278*, 12144–12150.

Takeuchi, O., Hoshino, K., and Akira, S. (2000). Cutting edge: TLR2-deficient and MyD88-deficient mice are highly susceptible to Staphylococcus aureus infection. J. Immunol. Baltim. Md 1950 *165*, 5392–5396.

Takeuchi, O., Kawai, T., Mühlradt, P.F., Morr, M., Radolf, J.D., Zychlinsky, A., Takeda, K., and Akira, S. (2001). Discrimination of bacterial lipoproteins by Toll-like receptor 6. Int. Immunol. *13*, 933–940.

Takeuchi, O., Sato, S., Horiuchi, T., Hoshino, K., Takeda, K., Dong, Z., Modlin, R.L., and Akira, S. (2002). Cutting edge: role of Toll-like receptor 1 in mediating immune response to microbial lipoproteins. J. Immunol. Baltim. Md 1950 *169*, 10–14.

Tamano, K., Aizawa, S., Katayama, E., Nonaka, T., Imajoh-Ohmi, S., Kuwae, A., Nagai, S., and Sasakawa, C. (2000). Supramolecular structure of the Shigella type III secretion machinery: the needle part is changeable in length and essential for delivery of effectors. EMBO J. *19*, 3876–3887.

Tattoli, I., Lembo-Fazio, L., Nigro, G., Carneiro, L.A.M., Ferraro, E., Rossi, G., Martino, M.C., de Stefano, M.E., Cecconi, F., Girardin, S.E., et al. (2008). Intracellular bacteriolysis triggers a massive apoptotic cell death in Shigella-infected epithelial cells. Microbes Infect. *10*, 1114–1123.

Ting, J.P.-Y., Lovering, R.C., Alnemri, E.S., Bertin, J., Boss, J.M., Davis, B.K., Flavell, R.A., Girardin, S.E., Godzik, A., Harton, J.A., et al. (2008). The NLR gene family: a standard nomenclature. Immunity *28*, 285–287.

Tobe, T., Nagai, S., Okada, N., Adler, B., Yoshikawa, M., and Sasakawa, C. (1991). Temperature-regulated expression of invasion genes in Shigella flexneri is controlled through the transcriptional activation of the virB gene on the large plasmid. Mol. Microbiol. *5*, 887–893.

Tobe, T., Yoshikawa, M., Mizuno, T., and Sasakawa, C. (1993). Transcriptional control of the invasion regulatory gene virB of Shigella flexneri: activation by virF and repression by H-NS. J. Bacteriol. *175*, 6142–6149.

Tominaga, K., Yoshimoto, T., Torigoe, K., Kurimoto, M., Matsui, K., Hada, T., Okamura, H., and Nakanishi, K. (2000). IL-12 synergizes with IL-18 or IL-1beta for IFN-gamma production from human T cells. Int. Immunol. *12*, 151–160.

Torres, D., Barrier, M., Bihl, F., Quesniaux, V.J.F., Maillet, I., Akira, S., Ryffel, B., and Erard, F. (2004). Toll-like receptor 2 is required for optimal control of Listeria monocytogenes infection. Infect. Immun. *72*, 2131–2139.

Uhlén, M., Fagerberg, L., Hallström, B.M., Lindskog, C., Oksvold, P., Mardinoglu, A., Sivertsson, Å., Kampf, C., Sjöstedt, E., Asplund, A., et al. (2015). Proteomics. Tissue-based map of the human proteome. Science *347*, 1260419.

Ulevitch, R.J., and Tobias, P.S. (1995). Receptor-dependent mechanisms of cell stimulation by bacterial endotoxin. Annu. Rev. Immunol. *13*, 437–457.

Urbonaviciute, V., Fürnrohr, B.G., Meister, S., Munoz, L., Heyder, P., De Marchis, F., Bianchi, M.E., Kirschning, C., Wagner, H., Manfredi, A.A., et al. (2008). Induction of inflammatory and immune responses by HMGB1-nucleosome complexes: implications for the pathogenesis of SLE. J. Exp. Med. *205*, 3007–3018.

Vallabhapurapu, S., and Karin, M. (2009). Regulation and function of NF-kappaB transcription factors in the immune system. Annu. Rev. Immunol. *27*, 693–733.

Vamadevan, A.S., Fukata, M., Arnold, E.T., Thomas, L.S., Hsu, D., and Abreu, M.T. (2010). Regulation of TLR4-associated MD-2 in intestinal epithelial cells: a comprehensive analysis. Innate Immun. *16*, 93.

Van Nhieu, G.T., Clair, C., Bruzzone, R., Mesnil, M., Sansonetti, P., and Combettes, L. (2003). Connexin-dependent inter-cellular communication increases invasion and dissemination of Shigella in epithelial cells. Nat. Cell Biol. *5*, 720–726.

Varga, M.G., Shaffer, C.L., Sierra, J.C., Suarez, G., Piazuelo, M.B., Whitaker, M.E., Romero-Gallo, J., Krishna, U.S., Delgado, A., Gomez, M.A., et al. (2016). Pathogenic Helicobacter pylori Strains Translocate DNA and Activate TLR9 via the Cancer-Associated cag Type IV Secretion System. Oncogene *35*, 6262–6269.

Veenendaal, A.K.J., Hodgkinson, J.L., Schwarzer, L., Stabat, D., Zenk, S.F., and Blocker, A.J. (2007). The type III secretion system needle tip complex mediates host cell sensing and translocon insertion. Mol. Microbiol. *63*, 1719–1730.

van de Verg, L.L., Mallett, C.P., Collins, H.H., Larsen, T., Hammack, C., and Hale, T.L. (1995). Antibody and cytokine responses in a mouse pulmonary model of Shigella flexneri serotype 2a infection. Infect. Immun. *63*, 1947–1954.

Verma, I.M., Stevenson, J.K., Schwarz, E.M., Van Antwerp, D., and Miyamoto, S. (1995). Rel/NF-kappa B/I kappa B family: intimate tales of association and dissociation. Genes Dev. *9*, 2723–2735.

Viala, J. a, Sansonetti, P., and Philpott, D.J. (2004). Nods and “intracellular” innate immunity. C. R. Biol. *327*, 551–555.

Vlasov, I.I., Shiryaev, A.A., Rendler, T., Steinert, S., Lee, S.-Y., Antonov, D., Vörös, M., Jelezko, F., Fisenko, A.V., Semjonova, L.F., et al. (2014). Molecular-sized fluorescent nanodiamonds. Nat. Nanotechnol. *9*, 54–58.

Wajant, H., Henkler, F., and Scheurich, P. (2001). The TNF-receptor-associated factor family. Cell. Signal. *13*, 389–400.

Walsh, M.C., Lee, J., and Choi, Y. (2015). Tumor necrosis factor receptor- associated factor 6 (TRAF6) regulation of development, function, and homeostasis of the immune system. Immunol. Rev. *266*, 72–92.

Wang, X., and Quinn, P.J. (2010). Lipopolysaccharide: Biosynthetic pathway and structure modification. Prog. Lipid Res. *49*, 97–107.

Wang, C., Deng, L., Hong, M., Akkaraju, G.R., Inoue, J., and Chen, Z.J. (2001). TAK1 is a ubiquitin-dependent kinase of MKK and IKK. Nature *412*, 346–351.

Wang, F., Jiang, Z., Li, Y., He, X., Zhao, J., Yang, X., Zhu, L., Yin, Z., Li, X., Wang, X., et al. (2013). Shigella flexneriT3SS effector IpaH4.5 modulates the host inflammatory response via interaction with NF-κB p65 protein. Cell. Microbiol. *15*, 474–485.

Wang, S.-J., Tu, H.-P., Ko, A.M.-S., Chiang, S.-L., Chiou, S.-J., Lee, S.-S., Tsai, Y.-S., Lee, C.-P., and Ko, Y.-C. (2011). Lymphocyte α-kinase is a gout-susceptible gene involved in monosodium urate monohydrate-induced inflammatory responses. J. Mol. Med. Berl. Ger. *89*, 1241–1251.

Wang, X., Moser, C., Louboutin, J.-P., Lysenko, E.S., Weiner, D.J., Weiser, J.N., and Wilson, J.M. (2002). Toll-like receptor 4 mediates innate immune responses to Haemophilus influenzae infection in mouse lung. J. Immunol. Baltim. Md 1950 *168*, 810–815.

Wassef, J.S., Keren, D.F., and Mailloux, J.L. (1989). Role of M cells in initial antigen uptake and in ulcer formation in the rabbit intestinal loop model of shigellosis. Infect. Immun. *57*, 858–863.

Watarai, M., Funato, S., and Sasakawa, C. (1996). Interaction of Ipa proteins of Shigella flexneri with alpha5beta1 integrin promotes entry of the bacteria into mammalian cells. J. Exp. Med. *183*, 991–999.

Way, S.S., Borczuk, A.C., Dominitz, R., and Goldberg, M.B. (1998). An essential role for gamma interferon in innate resistance to Shigella flexneri infection. Infect. Immun. *66*, 1342–1348.

Webster, S.J., Brode, S., Ellis, L., Fitzmaurice, T.J., Elder, M.J., Gekara, N.O., Tourlomousis, P., Bryant, C., Clare, S., Chee, R., et al. (2017). Detection of a microbial metabolite by STING regulates inflammasome activation in response to Chlamydia trachomatis infection. PLOS Pathog. *13*, e1006383.

Wei, T.-Y.W., Wu, P.-Y., Wu, T.-J., Hou, H.-A., Chou, W.-C., Teng, C.-L.J., Lin, C.-R., Chen, J.-M.M., Lin, T.-Y., Su, H.-C., et al. (2017). Aurora A and NF-κB Survival Pathway Drive Chemoresistance in Acute Myeloid Leukemia via the TRAF-Interacting Protein TIFA. Cancer Res. *77*, 494–508.

Weiner, A., Mellouk, N., Lopez-Montero, N., Chang, Y.-Y., Souque, C., Schmitt, C., and Enninga, J. (2016). Macropinosomes are Key Players in Early Shigella Invasion and Vacuolar Escape in Epithelial Cells. PLOS Pathog. *12*, e1005602.

Wesener, D.A., Wangkanont, K., McBride, R., Song, X., Kraft, M.B., Hodges, H.L., Zarling, L.C., Splain, R.A., Smith, D.F., Cummings, R.D., et al. (2015). Recognition of microbial glycans by human intelectin-1. Nat. Struct. Mol. Biol. *22*, 603–610.

Wheeler, D.S., Chase, M.A., Senft, A.P., Poynter, S.E., Wong, H.R., and Page, K. (2009). Extracellular Hsp72, an endogenous DAMP, is released by virally infected airway epithelial cells and activates neutrophils via Toll-like receptor (TLR)-4. Respir. Res. *10*, 31.

White, J.R., Winter, J.A., and Robinson, K. (2015). Differential inflammatory response to Helicobacter pylori infection: etiology and clinical outcomes. J. Inflamm. Res. *8*, 137–147.

Whitmarsh, A.J. (2007). Regulation of gene transcription by mitogen-activated protein kinase signaling pathways. Biochim. Biophys. Acta BBA - Mol. Cell Res. *1773*, 1285–1298.

Williams, T.M., Leeth, R.A., Rothschild, D.E., Coutermarsh-Ott, S.L., McDaniel, D.K., Simmons, A.E., Heid, B., Cecere, T.E., and Allen, I.C. (2015). The NLRP1 inflammasome attenuates colitis and colitis-associated tumorigenesis. J. Immunol. Baltim. Md 1950 *194*, 3369–3380.

Wlodarska, M., Thaiss, C.A., Nowarski, R., Henao-Mejia, J., Zhang, J.-P., Brown, E.M., Frankel, G., Levy, M., Katz, M.N., Philbrick, W.M., et al. (2014). NLRP6 inflammasome orchestrates the colonic host-microbial interface by regulating goblet cell mucus secretion. Cell *156*, 1045.

Wolf, A.J., Reyes, C.N., Liang, W., Becker, C., Shimada, K., Wheeler, M.L., Cho, H.C., Popescu, N.I., Coggeshall, K.M., Arditi, M., et al. (2016). Hexokinase Is an Innate Immune Receptor for the Detection of Bacterial Peptidoglycan. Cell *166*, 624–636.

Worthington, J.J., Reimann, F., and Gribble, F.M. (2017). Enteroendocrine cells-sensory sentinels of the intestinal environment and orchestrators of mucosal immunity. Mucosal Immunol.

Wu, C.-J., Conze, D.B., Li, T., Srinivasula, S.M., and Ashwell, J.D. (2006). Sensing of Lys 63-linked polyubiquitination by NEMO is a key event in NF-kappaB activation [corrected]. Nat. Cell Biol. *8*, 398–406.

Wu, X., Li, Z., Chen, X.-X., S. Fossey, J., D. James, T., and Jiang, Y.-B. (2013). Selective sensing of saccharides using simple boronic acids and their aggregates. Chem. Soc. Rev. *42*, 8032–8048.

Xia, Z.-P., Sun, L., Chen, X., Pineda, G., Jiang, X., Adhikari, A., Zeng, W., and Chen, Z.J. (2009). Direct activation of protein kinases by unanchored polyubiquitin chains. Nature *461*, 114–119.

Xie, P. (2013). TRAF molecules in cell signaling and in human diseases. J. Mol. Signal. *8*, 7.

Xue, H.-Y., Ji, L.-J., Gao, A.-M., Liu, P., He, J.-D., and Lu, X.-J. (2016). CRISPR-Cas9 for medical genetic screens: applications and future perspectives. J. Med. Genet. *53*, 91–97.

Yamada, Y., Nishida, T., Ichihara, S., Kato, K., Fujimaki, T., Oguri, M., Horibe, H., Yoshida, T., Watanabe, S., Satoh, K., et al. (2013). Identification of chromosome 3q28 and ALPK1 as susceptibility loci for chronic kidney disease in Japanese individuals by a genome-wide association study. J. Med. Genet. *50*, 410–418.

Yamada, Y., Matsui, K., Takeuchi, I., and Fujimaki, T. (2015a). Association of genetic variants with coronary artery disease and ischemic stroke in a longitudinal population-based genetic epidemiological study. Biomed. Rep. *3*, 413–419.

Yamada, Y., Matsui, K., Takeuchi, I., Oguri, M., and Fujimaki, T. (2015b). Association of genetic variants of the α-kinase 1 gene with type 2 diabetes mellitus in a longitudinal population-based genetic epidemiological study. Biomed. Rep. *3*, 347–354.

Yamada, Y., Matsui, K., Takeuchi, I., and Fujimaki, T. (2015c). Association of genetic variants with dyslipidemia and chronic kidney disease in a longitudinal population-based genetic epidemiological study. Int. J. Mol. Med. *35*, 1290–1300.

Yamamoto, K. (2014). Intracellular lectins are involved in quality control of glycoproteins. Proc. Jpn. Acad. Ser. B Phys. Biol. Sci. *90*, 67–82.

Yamaoka, S., Courtois, G., Bessia, C., Whiteside, S.T., Weil, R., Agou, F., Kirk, H.E., Kay, R.J., and Israël, A. (1998). Complementation cloning of NEMO, a component of the IkappaB kinase complex essential for NF-kappaB activation. Cell *93*, 1231–1240.

Yang, J., Zhao, Y., Shi, J., and Shao, F. (2013). Human NAIP and mouse NAIP1 recognize bacterial type III secretion needle protein for inflammasome activation. Proc. Natl. Acad. Sci. U. S. A. *110*, 14408–14413.

Yang, S.-H., Sharrocks, A.D., and Whitmarsh, A.J. (2003). Transcriptional regulation by the MAP kinase signaling cascades. Gene *320*, 3–21.

Ye, H., Arron, J.R., Lamothe, B., Cirilli, M., Kobayashi, T., Shevde, N.K., Segal, D., Dzivenu, O.K., Vologodskaia, M., Yim, M., et al. (2002). Distinct molecular mechanism for initiating TRAF6 signalling. Nature *418*, 443–447.

Yeager, M., and Nicholson, B.J. (1996). Structure of gap junction intercellular channels. Curr. Opin. Struct. Biol. *6*, 183–192.

Zhang, Q., Raoof, M., Chen, Y., Sumi, Y., Sursal, T., Junger, W., Brohi, K., Itagaki, K., and Hauser, C.J. (2010). Circulating Mitochondrial DAMPs Cause Inflammatory Responses to Injury. Nature *464*, 104–107.

Zhao, Y., Yang, J., Shi, J., Gong, Y.-N., Lu, Q., Xu, H., Liu, L., and Shao, F. (2011). The NLRC4 inflammasome receptors for bacterial flagellin and type III secretion apparatus. Nature *477*, 596–600.

Zhou, R., Yazdi, A.S., Menu, P., and Tschopp, J. (2011). A role for mitochondria in NLRP3 inflammasome activation. Nature *469*, 221–225.

Zhou, Y., Dong, N., Hu, L., and Shao, F. (2013). The Shigella type three secretion system effector OspG directly and specifically binds to host ubiquitin for activation. PloS One *8*, e57558.

Zimmermann, S., Wagner, C., Müller, W., Brenner-Weiss, G., Hug, F., Prior, B., Obst, U., and Hänsch, G.M. (2006). Induction of Neutrophil Chemotaxis by the Quorum-Sensing Molecule N-(3-Oxododecanoyl)-l-Homoserine Lactone. Infect. Immun. *74*, 5687.

Zimmermann, S., Pfannkuch, L., Al-Zeer, M.A., Bartfeld, S., Koch, M., Liu, J., Rechner, C., Soerensen, M., Sokolova, O., Zamyatina, A., et al. (2017). ALPK1- and TIFA-Dependent Innate Immune Response Triggered by the Helicobacter pylori Type IV Secretion System. Cell Rep. *20*, 2384–2395.

Zychlinsky, A., Prevost, M.C., and Sansonetti, P.J. (1992). Shigella flexneri induces apoptosis in infected macrophages. Nature *358*, 167–169.